Preventing DNA over-replication by precise cell cycle regulation of origin firing factors

Dissertation der Fakultät für Biologie

der Ludwig-Maximilians-Universität München

vorgelegt von

Diplom-Biochemiker

Karl-Uwe Johannes Reußwig

Mai 2019

EIDESSTATTLICHE VERSICHERUNG

Hiermit erkläre ich an Eides statt, dass ich die vorliegende Dissertation selbstständig und ohne unerlaubte Hilfe angefertigt habe. Ich habe weder anderweitig versucht, eine Dissertation einzureichen oder eine Doktorprüfung durchzuführen, noch habe ich diese Dissertation oder Teile derselben einer anderen Prüfungskommission vorgelegt.

_____

Karl-Uwe Johannes Reußwig

München, den 28. Mai 2019

Promotionsgesuch eingereicht:	28. Mai 2019
Tag der mündlichen Prüfung:	24. Juli 2019
Erstgutachter:	Prof. Dr. Heinrich Leonhardt
Zweitgutachter:	Prof. Dr. Peter Becker

Die vorliegende Arbeit wurde zwischen August 2013 und Mai 2019 unter der Anleitung von Dr. Boris Pfander am Max-Planck-Institut für Biochemie in Martinsried durchgeführt.

Wesentliche Teile dieser Arbeit sind in den folgenden Publikationen veröffentlicht und zusammengefasst:

Reusswig KU, Boos D, & Pfander B. Roles of Sld2, Sld3, and Dpb11 in replication initiation. *The initiation of DNA Replication in Eukaryotes.* Springer. 297-318 (2016).

Reusswig KU, Zimmermann F, Galanti L, & Pfander B. Robust replication control is generated by temporal gaps between licensing and firing phases and depends on degradation of firing factor Sld2. *Cell Rep* 17, 556-569 (2016).

Reusswig KU, & Pfander B. Control of eukaryotic DNA replication initiation – mechanisms to ensure smooth transitions. *Genes* 10, 99 (2019).

Table of contents

Summary

Eukaryotic DNA replication relies on a tight two-step regulation to maintain genome stability and ensure that the genome is copied precisely once during each cell cycle. The first step – origin licensing – is restricted to late M and G1 phase of the cell cycle, whereas the second step – origin firing – is restricted to S, G2 and early M phase. This strict temporal separation of licensing and firing prevents uncontrolled over-replication, which is associated with hallmarks of genome instability such as gene amplifications or gross chromosomal rearrangements that are often observed during early stages of tumorigenesis. However, it is unclear how strict control is achieved on the molecular level at the transitions between licensing and firing. While the regulation of licensing factors has been studied in detail, much less is known about the regulation of firing factors. Particularly, it is unclear how firing factors are inactivated in M phase and how deregulation of firing factors causes genome instability.

To address these gaps in our knowledge, we have established an experimental setup to monitor the dynamic regulation of replication proteins throughout the cell cycle in budding yeast cells. Our data demonstrate that at the transition in M phase firing is inactivated before licensing is re-activated, thereby generating an intermittent gap phase. Early inactivation of origin firing is mediated by precisely timed degradation of firing factor Sld2. We decipher the underlying degradation pathway involving four kinases and two ubiquitin ligases and demonstrate that preventing rapid degradation of Sld2 in M phase shortens the gap phase between firing and licensing. Importantly, such shortening of the gap in M phase results in significant levels of genome instability when combined with other replication mutants.

Moreover, we investigate the cellular consequences of deregulated origin firing. In particular, we study deregulated origin firing in G1 phase and find that cellular DNA surveillance mechanisms such as the DNA damage checkpoint appear to be blind to this type of problem. Even after deregulated replication initiation in G1 phase, cells commit to another full round of DNA replication in S phase. Consequently, we observe strong induction of DNA damage in late S phase, which ultimately activates DNA damage signaling after bulk replication is finished. We identify factors required for this checkpoint response and characterize replisomes under over-replication conditions using mass spectrometry and next-generation sequencing.

Taken together, our work reveals new regulatory controls of DNA replication and establishes gap phases as integral elements of replication control, which allow safe transitions between origin licensing and origin firing.

Introduction

Each cell needs to replicate its DNA in order to pass on the genetic information to its progeny. Preserving the integrity of the genetic information is of utmost importance and therefore many regulatory mechanisms are in place to ensure that replication proceeds correctly. In this regard, a critical and highly regulated step in all domains of life is the assembly of replisomes, which are the protein complexes that replicate DNA.

1. DNA replication and the cell cycle

The regulated assembly of replisomes occurs at distinct locations on chromosomes which are called origins of replication. For bacteria and many lower eukaryotes such as *Saccharomyces cerevisiae* or *Schizosaccharomyces pombe*, these DNA sequences have been mapped to specific sequence elements [1,2]. It has however proven difficult to define specific DNA sequences that promote DNA replication in other organisms. One common characteristic of origins of replication is their high A/T-content, which facilitates initial unwinding of the DNA double helix.

Prokaryotic cells typically harbor small, circular genomes, which are replicated from a single origin. In contrast, archaeal cells and eukaryotic cells rely on multiple origins to copy their genomes that are typically distributed on multiple chromosomes [3,4]. The usage of multiple origins allows efficient and fast replication of increasingly larger and more complex genomes. For example, a haploid budding yeast cell initiates replication from about 400 origins that are located on 16 different chromosomes [5]. Interestingly, eukaryotes only use a subset of all origins that would be available. Origins that do not initiate replication are named “dormant origins” and constitute back-up initiation sites in case of replication stress [6].

While using multiple origins greatly benefits cells by reducing the time needed for replication of the genome and by providing a back-up mechanism in case of replication stalling, this system of organizing DNA replication requires a tight regulation to ensure that each part of the genome is replicated precisely once. Therefore, DNA replication occurs in two distinct steps that are coupled to different phases of the cell division cycle (Figure 1). Origins of replication can be licensed while cells are in late M phase and G1 phase. Conversely, origins of replication can be fired from S phase until M phase. Importantly, passive replication of an origin by a replication fork that emerged from a neighboring origin removes the license and thereby ensures that no segment of the genome is copied more than once.

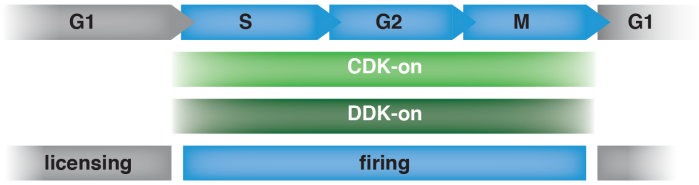

Figure 1 – DNA replication control during the cell cycle.
Origin licensing and origin firing are strictly separated throughout the cell cycle. Origin licensing occurs in cell cycle phases without cyclin-dependent kinase (CDK) activity, whereas origin firing is restricted to cell cycle phases where CDK and Dbf4-dependent kinase (DDK) are active.

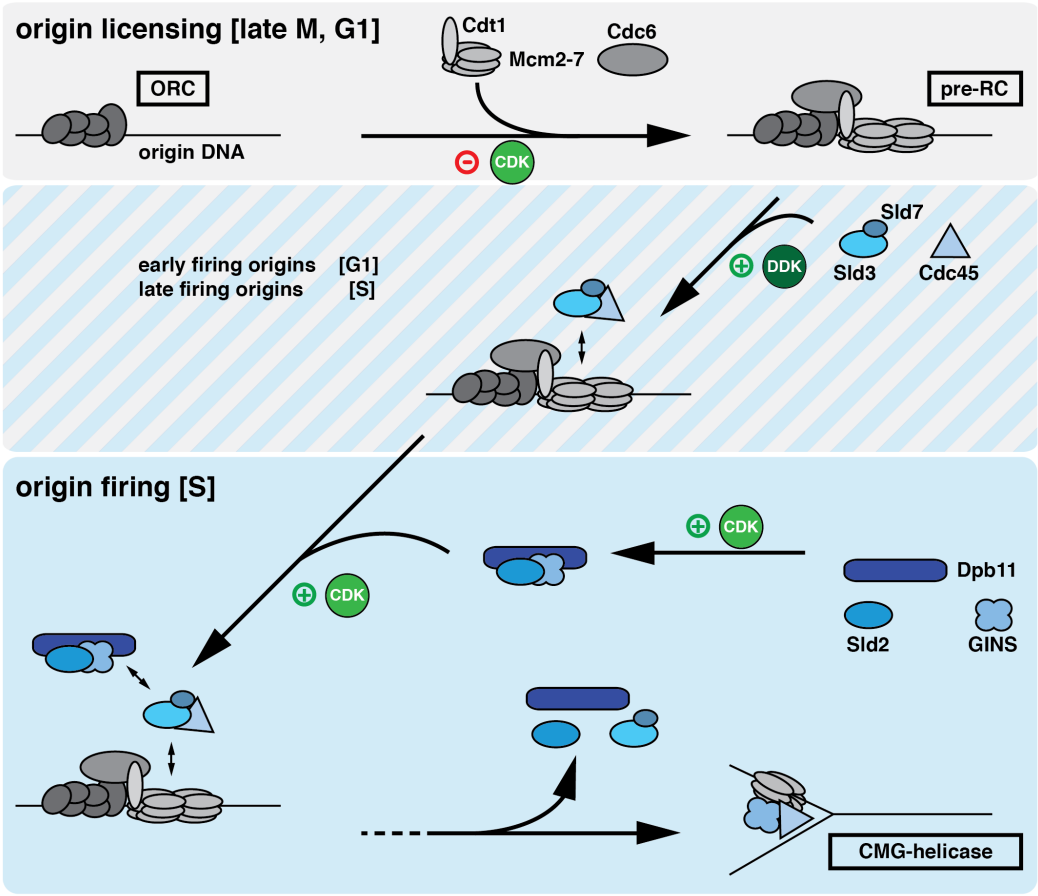

Figure 2 – Key intermediates during origin licensing and origin firing.
In order to license a replication origin for DNA replication, the origin recognition complex (ORC) together with the licensing factors Cdt1 and Cdc6 mediates the recruitment of two Mcm2-7 hexamers to form a pre-replicative complex (pre-RC). The Dbf4-dependent kinase (DDK) promotes the association of firing factor Sld3-Sld7 together with the helicase activator Cdc45 to early firing origins and also alleviates an inhibitory interaction within the Mcm2-7 double hexamer. Cyclin-dependent kinase (CDK) facilitates the association of firing factor Sld2 and helicase activator GINS (Sld5, Psf1-3) with the scaffold protein Dpb11 and their recruitment to the pre-RC via interaction with CDK-phosphorylated Sld3. While CDK drives origin firing, it also inhibits origin licensing through multiple molecular mechanisms (see main text). In subsequent steps, the helicase activators Cdc45 and GINS are integrated into the Mcm2-7 complex to form active Cdc45/Mcm2-7/GINS (CMG) helicases, which is the committed step in the initiation of DNA replication. Additional replication factors were omitted from this scheme for clarity.

2. The molecular mechanism of DNA replication in eukaryotes

The molecular mechanism of DNA replication has been studied in several eukaryotic model organisms. Particularly, the budding yeast *Saccharomyces cerevisiae* has been instrumental in the study of DNA replication due to the availability of defined origin sequences. Combining this knowledge with the powerful genetic and biochemical tools available for this model organism allowed researchers to elucidate and reconstitute the key steps of eukaryotic DNA replication [7], which are also highly conserved.

As mentioned before, DNA replication initiates at distinct sites within the genome, which are called origins of replication. In an ATP-dependent process, the hexameric origin recognition complex (ORC) binds to these sites and serves as a platform for the assembly of further replication proteins [8]. In budding yeast, ORC remains bound to the DNA throughout the cell cycle [9]. In other organisms, ORC binding to DNA appears to be controlled so that ORC only associates with DNA in G1 phase of the cell cycle [10-13].

DNA-bound ORC orchestrates the assembly and recruitment of replication proteins at the origin (Figure 2, top panel). In another ATP-dependent process, ORC together with the licensing factors Cdc6 and Cdt1 facilitates the loading of the core helicase proteins Mcm2-7 onto DNA [14-16]. Subsequently, a second Mcm2-7 hexamer is loaded in opposite orientation to form a head-to-head Mcm2-7 double hexamer, which is inactive and encircles double-stranded DNA [17,18]. How the second hexamer is loaded with the correct orientation has been a long-standing question in the field. While one ORC molecule can in principle already mediate the loading of double-hexamers [16], a recent study demonstrated that specific sequence motifs with opposite directionality at the origin of replication promote the loading of two Mcm2-7 hexamers with the correct orientation by two distinct ORC molecules [19]. The protein complexes present at this stage at the origin of replication are commonly also referred to as pre-replicative complexes (pre-RCs). While all interactions between the licensing factors are rather transient and driven by ATP-hydrolysis, double-hexamers remain bound to DNA as relatively stable complexes and constitute the basis for subsequent steps of origin firing [20,21].

To trigger origin firing, additional accessory subunits need to be recruited to the double-hexameric helicase precursor in order to activate the helicase and initiate unwinding of the DNA (Figure 2, middle and bottom panel). The helicase-activating protein Cdc45 [22,23], that can already associate with pre-RCs at origins that fire early during S phase [24,25], as well as the tetrameric GINS complex consisting of Sld5 and Psf1-3 [26] need to be recruited to and integrated into the double-hexamer in order to form the active replicative CMG (Cdc45/Mcm2-7/GINS) helicase [27-29]. This committed step in origin firing is mediated by a ternary protein complex between the scaffold protein Dpb11 and the two firing factors Sld2 and Sld3. Sld2 and Sld3 in turn interact with the

GINS complex and with Cdc45. Importantly, formation of this complex requires phosphorylation of both Sld2 and Sld3 by CDK [30-32]. In addition to Cdc45 and GINS, several other replication factors such as e.g. Mcm10, DNA polymerase ε, replication protein A (RPA), and DNA polymerase α are recruited to the CMG helicase to form the replisome, also referred to as replisome progression complex (RPC) [28]. The components of replisomes are summarized in Table 1. In contrast to the double-hexamers, the CMG helicase encircles single-stranded DNA [33,34], hence initial unwinding of the DNA double helix at the origin and strand extrusion from the Mcm2-7 ring must occur during the activation of double-hexamers to CMG helicases. How all these steps in the assembly of the replisome are coordinated and executed is a matter of ongoing investigation.

During S phase, origins do not fire all at once but follow a specific timing (Figure 3). The firing time of origins in budding yeast has been determined [35,36] and it was found that a specific set of origins reproducibly fired early in S phase whereas other origins only fired late. The precise cellular function of replication timing is not known but it is assumed to facilitate smooth S phase progression by limiting the number of active replisomes at a given time. On the molecular level, this phenomenon can be explained by competition between origins for limiting firing factors. Two independent studies revealed that the protein levels of firing factors constitute a bottle-neck to replication initiation [37,38]. Consistent with this notion, over-expression of Dbf4 and Sld3 either together with Dpb11/Sld2 or with Cdc45/Sld7 promoted early firing of otherwise late firing origins. Since Sld3 and Cdc45 are recruited to origins already during G1 phase in a DDK-dependent manner, these proteins therefore prime origins for early replication in S phase [38-41]. Similarly, the high affinity for Dbf4 of some genomic regions such as for example centromeres seems to promote the early firing of origins [41,42].

Table 1 – Summary of replisome components in *S. cerevisiae*.

protein	function
Mcm2-7	core helicase subunits
Sld5 / Psf1-3	helicase activator (GINS complex)
Cdc45	helicase activator
Mrc1 / Tof1-Csm3	fork protection complex
Ctf4	hub for connecting accessory factors
Mcm10	helicase activator
Pob3 / Spt16	histone chaperone (FACT complex)
Top1	topoisomerase
Pri1 / Pri2	primase
Pol1 / Pol12	DNA polymerase α
Pol2 / Dpb2-4	DNA polymerase ε
Pol3 / Pole31 / Pol32	DNA polymerase δ
Pol30	sliding clamp for DNA polymerase δ
Fen1	endonuclease (lagging strand processing)
Rfa1-3	ssDNA-binding protein RPA

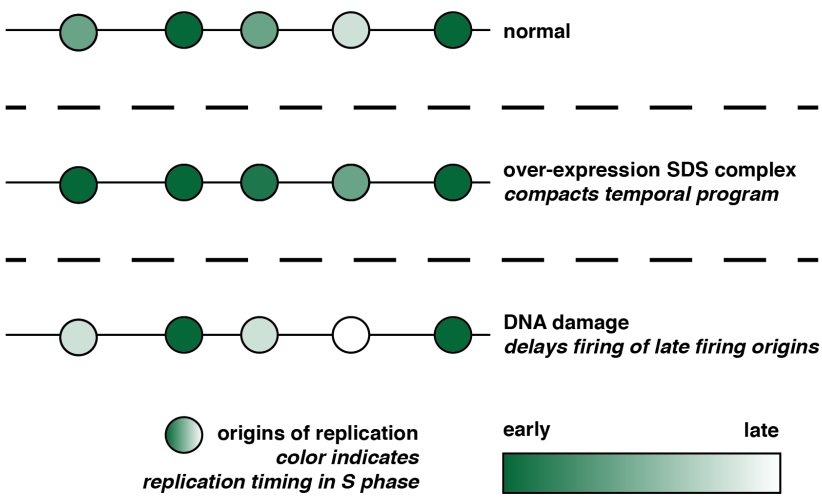

Figure 3 – Replication timing and its control.
Replication origins fire with a different timing during S phase (indicated by shading). The normal pattern of the temporal program of DNA replication can be compacted by over-expressing the Sld2, Dpb11 and Sld3 proteins together with the DDK activator Dbf4, since these proteins are limiting for origin firing. Conversely, the firing of late origins is delayed in response to DNA damage.

Recently, it has become evident that not only the assembly but also the disassembly of replisomes is a highly regulated process. In budding yeast, the E3 ubiquitin ligase Dia2 targets Mcm7 for ubiquitination and thereby drives disassembly of the CMG helicase [43]. A similar pathway has also been described in higher eukaryotes [44-48] and mitotic CDK is a key regulator of this process [49]. However, the molecular mechanisms behind the disassembly are still being investigated.

Since DNA replication is such a central cellular process, it has proven to be challenging to study all of its aspects *in vivo*. Therefore, the biochemical reconstitution of origin-dependent eukaryotic DNA replication has been a long-standing goal in the field. Building on initial milestones such as the assembly of double-hexamers on origin DNA [18] and their conversion into replisomes using S phase extracts [50], a recent landmark study ultimately demonstrated the full reconstitution of eukaryotic DNA replication *in vitro* using purified proteins from budding yeast [51]. Quickly, this *in vitro* system has been further refined and yielded detailed insights into how replication is affected by chromatin [52,53] and by non-essential replisome components [54]. Subsequent studies have revealed how the helicase becomes activated [55], how the replisome deals with DNA damage or helicase-polymerase uncoupling [56,57], and how replisomes converge during replication termination [58]. Single-molecule assays provided further mechanistic insight into origin licensing and its intricate regulation [16,59,60]. Taken together, these data comprehensively outline the molecular mechanism and the proteins involved in eukaryotic DNA replication. Nonetheless, key questions concerning the transition from double-hexamer to fully assembled replisome, the termination of replisomes, and the regulation of replication proteins remain to be answered.

3. The regulation of DNA replication

DNA replication proteins are regulated by the two cell cycle kinases CDK and DDK to ensure that each part of the genome is replicated precisely once. Both of these kinases are activated at the transition from G1 to S phase and inactivated during M phase. Thus, both of them are intimately linked with origin licensing and origin firing phases and, in budding yeast, they are the major regulators of replication proteins (Figure 4).

Origin licensing is inhibited by CDK phosphorylation and thereby restricted to late M phase and G1 phase. Ectopic expression of CDK in G1 phase can fully inhibit origin licensing [61]. Importantly, CDK not just targets a single licensing factor but rather affects all licensing factors to synergistically inhibit licensing via different mechanisms. First, direct binding of CDK to the ORC-subunit Orc6 blocks initial recruitment of Cdt1-Mcm2-7 and leads to phosphorylation of Orc2 and Orc6, which additionally impairs their ability to recruit Cdt1-Mcm2-7 [62-64]. Second, the Cdt1-Mcm2-7 complex itself is exported from the nucleus upon phosphorylation by CDK [65-67]. Third, the protein levels of Cdc6 are tightly regulated throughout the cell cycle [68-70] and binding of CDK to Cdc6 in mitosis is thought to inhibit Cdc6 activity [71].

On the other hand, CDK phosphorylation is strictly required for origin firing. In particular, CDK drives CMG formation by phosphorylating firing factors Sld2 and Sld3 and thus facilitating their interaction with the scaffold protein Dpb11 [30-32]. Importantly, Sld2 and Sld3 constitute the minimal set of CDK targets required for origin firing. DNA replication can be triggered in the absence of CDK activity by mimicking phosphorylation through an acidic amino acid substitution on Sld2 [72], by covalently fusing the Sld3 to Dpb11 [31], or by introducing mutations in Sld3's binding partner Cdc45 [32]. In higher eukaryotes, phosphorylation of homologs of Sld2 and Sld3 by CDK has also been reported [73-75]. However, the minimal set of CDK targets to trigger origin firing in cells besides budding yeast still remains to be determined.

Origin firing also requires the activity of DDK [76,77]. Even though DDK activity is low in late mitosis and G1 phase due to the degradation of its regulatory subunit Dbf4 [78], Dbf4 can still be detected at low levels at early firing origins of replication in G1 phase [42]. The essential function of DDK in replication control is to alleviate an inhibitory interaction within the Mcm2-7 double-hexamer. Thus, specific mutants in the Mcm2-7 complex can bypass the requirement for functional DDK [79-81]. Importantly, DDK facilitates association of Cdc45 and Sld3 with replication origins [38] as Sld3 binds to DDK-phosphorylated Mcm-proteins [82]. While DDK clearly promotes origin firing, it is currently unclear if this kinase also has any inhibitory effect on origin licensing.

As DDK activity in G1 is decreased but not completely absent, a counteracting mechanism is important to allow cells to correctly respond to a rise in DDK activity. The protein phosphatase

PP1-Rif1 has recently been shown to counteract DDK-phosphorylation of Mcm2-7 and Sld3 in budding yeast [83-85] and to contribute to the establishment of the timing of origin firing [86,87]. This function of PP1-Rif1 is evolutionarily conserved [88,89] and, in human cells, PP1-Rif1 also protects Orc1 from phosphorylation and thereby supports origin licensing in G1 phase [89]. Whether this negative regulation of Orc1 in G1 phase is brought about by DDK or by another kinase has however not been addressed yet. Interestingly, SUMOylation of Mcm2-7 seems to facilitate the recruitment of PP1-Rif1 in budding yeast cells [90]. This modification was only found on a subset of Mcm2-7 complexes under physiological conditions, but artificially enforcing SUMOylation of Mcm6 strongly impaired replication initiation, consistent with a more local regulatory role for this modification. Therefore, it will be interesting to determine in which genomic context this modification occurs.

Previous studies have also investigated the removal of CDK-phosphorylation marks from replication factors. In contrast to kinases, protein phosphatases have generally a broader and often overlapping substrate specificity thus acting redundantly with other phosphatases. Instead of recognizing specific amino acid sequence motifs, changes in protein localization rather appear to determine the activity of phosphatases towards certain sets of substrates. For example, the phosphatase Cdc14, which is central to mitotic exit in budding yeast, is sequestered in the nucleolus throughout most of the cell cycle and only released in anaphase [91,92]. Importantly, Cdc14 has been shown to dephosphorylate replication proteins [93] and particularly licensing factors appear to be good substrates [94]. Large-scale genetic screens have also reported a genetic interaction between the phosphatase PP2A-Rts1 and ORC [95] but could not be confirmed [96]. Yet, abrogation of PP2A-Rts1 in cells with compromised replication control results in synthetic lethality [97]. Since PP2A-Rts1 also is a key factor in the regulation of chromosome segregation, this genetic interaction is difficult to interpret. A role for PP2A in combination with its other regulatory subunit Cdc55 in controlling replication proteins has so far not been reported.

On top of the regulation by CDK- and DDK-mediated phosphorylation, metazoan cells have evolved additional means to regulate DNA replication. Specifically, the small protein geminin inhibits licensing by binding to Cdt1 and thereby preventing Mcm2-7 loading [98-100]. The protein levels of geminin are strictly cell cycle-controlled via degradation by the anaphase-promoting complex (APC) [98]. Consequently, geminin restricts Cdt1 availability for origin licensing to late M phase and G1 phase [98-100]. Furthermore, Cdt1 is targeted for degradation during S phase by the ubiquitin ligase Cul4-Cdt2 [101-104]. The degradation of Cdt1 is coupled to ongoing DNA replication as Cul4-Cdt2 requires association with replication sliding clamp PCNA to target Cdt1 [105-107]. Together, these synergistic mechanisms targeting licensing factor Cdt1 ensure that origin licensing is effectively inhibited as soon as origin firing has started.

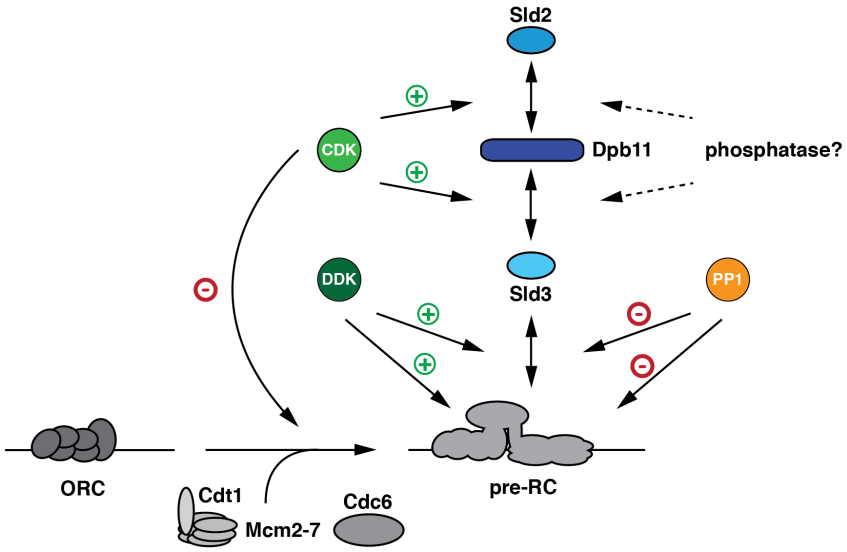

Figure 4 – Cell cycle regulation of licensing and firing factors.
Phosphorylation of licensing factors by cyclin-dependent kinase (CDK) inhibits the formation of pre-replicative complexes (pre-RCs). Additionally, CDK drives origin firing by facilitating the association of firing factors Sld2 and Sld3 with the scaffold protein Dpb11. Dbf4-dependent kinase (DDK) drives origin firing by promoting the recruitment of Sld3 to pre-RCs and by alleviating an inhibitory interaction within the pre-RC. Protein phosphatase 1 (PP1) in complex with its targeting subunit Rif1 counteracts DDK at a subset of origins and thereby contributes to the temporal replication program in S phase.

4. Origin firing in the presence of DNA damage

In the presence of DNA damage, eukaryotic cells activate the DNA damage checkpoint to stop cell cycle progression and coordinate an appropriate response to the DNA damage [108]. In budding yeast, the DNA damage checkpoint can arrest cells in principle at three stages: First, cells can transiently (10-20 min) arrest at the transition from G1 to S phase [109-111] in response to severe DNA damage such as multiple DNA double-strand breaks (DSB). Second, the intra-S phase checkpoint safeguards impeded replisomes by blocking further origin firing, stabilizing replisomes and initiating adequate repair mechanisms [112-116]. Third, the G2/M checkpoint arrests budding yeast cells at the transition from metaphase to anaphase and thereby prevents cells from segregating damaged DNA to their daughter cells [117].

Signaling of the DNA damage checkpoint involves a cascade of phosphorylation events. The so-called apical kinases Mec1 (homolog of ATR) or Tel1 (homolog of ATM) act as sensors and are recruited to the DNA lesion, e.g. by binding to RPA that coats exposed single-stranded DNA. The apical kinases also phosphorylate the carboxy-terminal tail of histone H2A and thereby generate a DNA damage signal that is referred to as γH2A [118,119]. Depending on the type of the encountered lesion, the mediator proteins Mrc1 or Rad9 facilitate the activation of effector kinases such as Rad53 (homolog of CHK2) [120-124]. Rad53 achieves full activity by auto-phosphorylation [125-127] and, due to its position within the DNA damage checkpoint signaling pathway, the presence of hyper-phosphorylated Rad53 is a prime indicator for an activated DNA damage checkpoint (Figure 5).

Firing of late origins is delayed by the DNA damage checkpoint [128-130]. Intriguingly, it has been shown that the checkpoint effector kinase Rad53 effectively inhibits further origin firing by targeting both DDK- as well as CDK-mediated replication controls. Rad53 hyper-phosphorylates Dbf4 and thereby inhibits DDK directly by a currently elusive mechanism [131,132]. Similarly, Rad53 hyper-phosphorylates firing factor Sld3 and prevents its interaction with the scaffold protein Dpb11 thereby interfering with the CDK-mediated branch of origin firing [131,132]. Hyper-phosphorylation of Dbf4 occurs via a direct binding of Rad53 to Dbf4 [133-135], whereas hyper-phosphorylation of Sld3 is mediated by binding of Rad53 to the helicase-activator Cdc45, which itself is also a Rad53 target [136]. Importantly, the interaction of Rad53 with Cdc45 provides a model for how Rad53 can be recruited to and stabilize stalled replication forks [137,138].

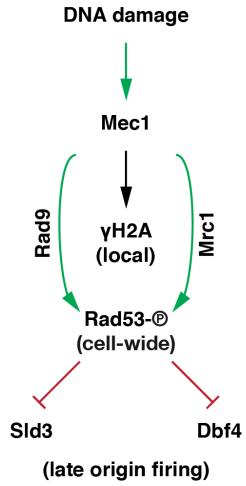

Figure 5 – Control of DNA replication by the DNA damage checkpoint. The apical checkpoint kinase Mec1 is activated in response to DNA damage and recruited to the site of DNA damage. It introduces the γH2A mark (phosphorylation of H2A S129) in chromatin close to the DNA damage site. To trigger a cell-wide response, Mec1 also activates the checkpoint effector kinase Rad53 by hyper-phosphorylation. This activation can occur via two different pathways: The mediator protein Rad9 is used in response to lesions of the DNA, whereas the mediator protein Mrc1 signals at stalled replication forks. Among other targets, hyper-phosphorylated Rad53 blocks further origin firing by phosphorylating Sld3 and Dbf4 and thereby affecting CDK- and DDK-dependent regulation of origin firing.

5. The physiological impact of DNA over-replication

Loss of DNA replication control can result in over-replication of specific parts of the genome within a single cell cycle. Over-replication is possible when both origin licensing and firing occur at the same time and, due to the cyclic nature of the replication phases, can either result from deregulated origin firing during the origin licensing phase or from deregulated origin licensing during the origin firing phase. In budding yeast, one experimental strategy has yielded many important insights into the underlying mechanisms of over-replication. In this strategy, CDK-regulation of licensing factors is abolished by mutation of the CDK-phosphorylation sites on ORC and by fusing a nuclear localization sequence to Mcm7. Cells are arrested in M phase and over-replication can then be induced by the expression of a Cdc6 variant that lacks its N-terminal degron and CDK-binding motifs [63]. The efficiency of re-licensing in this system can be boosted by additionally removing a binding site for CDK on Orc6 [62]. By utilizing microarrays of the budding yeast genome, it was shown that over-replication occurs at regular replication origins but affects chromosomes unevenly with a bias for sub-telomeric regions and even specific origins [139,140]. The preferential re-licensing of some origins appears to be mediated by local sequences [141].

Importantly, overt DNA over-replication is accompanied by hallmarks of DNA damage such as foci of the apical checkpoint kinase Mec1-Ddc2 and hyper-phosphorylated Rad53 [142]. By using a Southern blot-based assay, it was furthermore shown that over-replication generates sub-chromosomal fragments. Over-replication also induces gene amplifications [143], which can be sensitively detected in a reporter-based assay [144]. Particularly, over-replication of a centromere sequence results in aneuploidy [145]. Besides these severe forms of genomic instability, over-replication can also induce nucleotide level mutations due to attenuated mismatch repair [146]. Interestingly, while overt uncontrolled over-replication is highly toxic [63], cells tolerate going through a full round of regulated replication thus indicating that the loss of coordination between origins and not the additional round of replication *per se* is detrimental [147,148].

An alternative way to induce over-replication involves triggering premature origin firing already in G1 phase. Currently, such a system is only available in budding yeast [31,32,149] since the minimal sets of CDK targets required for origin firing have not been identified in other organisms yet. Replication in G1 occurs semi-conservatively and some origins that fire early in S phase were shown to fire under these deregulated conditions [32]. Moreover, over-replication in G1 critically requires DDK activity since a temperature-sensitive *cdc7* kinase mutant suppresses origin firing in G1, whereas overexpression of the regulatory DDK-subunit Dbf4 strongly increases it [31,32]. Similar to over-replication in M phase, over-replication in G1 is also toxic and generates genomic instability: Aberrant numbers of fully duplicated chromosomes as well as gross chromosomal rearrangements such as truncated chromosome arms were detected in survivors after a pulse of

origin firing in G1 [149]. DNA damage as detected by Ddc1 foci and Rad53 hyperphosphorylation was only observed when cells were released from the G1 arrest into the cell cycle [149]. Yet, it remains to be elucidated how cells cope with over-replication structures during S phase, how the DNA damage is generated, and which DNA structures activate the DNA damage checkpoint.

Other systems to induce over-replication have been reported for higher eukaryotic cells. In contrast to budding yeast, Cdt1 is a regulatory hub for origin licensing control in vertebrates [150]. As mentioned before, this protein is bound by the licensing inhibitor geminin and also targeted for degradation in a replication-coupled manner [98-104]. Abolishing these pathways can induce over-replication in *Xenopus* egg extracts as well as human cell lines [101,105,151-154]. Similarly, depletion of the APC-inhibitor Emi1, which is thought to cause premature degradation of geminin and cyclin A, has been shown to drive over-replication in human cells [155]. In these systems, over-replication is also associated with extensive DNA damage and a loss in cellular viability. Over-replication in *Xenopus* egg extracts gives rise to DNA fragments, which display characteristics of head-to-tail replication fork collisions [156]. Consistent with this model, a study in human cells suggested that the first round of DNA replication could leave gaps behind in the newly replicated DNA, which could pose a problem for subsequent over-replicating forks and ultimately lead to fork breakage [157]. Over-replication also occurs as a developmentally programmed process in Drosophila follicle cells [158]. This system demonstrates that collision of replication forks generates DNA double-strand breaks and it has been instrumental to address specific aspects of the activation of the DNA damage checkpoint as well as the roles of different repair pathways after over-replication [159-161], particularly in conjunction with the studies carried out in budding yeast.

One commonality between all these over-replication systems is the induction of genomic instability. All these systems generate overt over-replication, i.e. over-replication from multiple origins or even multiple times at single origins, which is highly toxic to cells. However, even if over-replication occurs more sporadically, e.g. if it is caused by less severe mutations, it is expected to give rise to DNA damage, mutations and overall genome instability. Deregulation of the G1/S transition is often observed in cancer cells and could induce such sporadic over-replication that would ultimately result in genomic instability [162-166]. Other hallmarks of tumorigenesis are gene amplifications and gross chromosomal rearrangements, which have been observed in over-replicating budding yeast cells [143]. It is therefore an open question whether sporadic over-replication could be a driving early event in the formation of cancerous cells.

Systems to study over-replication in M phase have yielded many important insights. Yet, it is not known if over-replication forks differ from regular replication forks and identifying such a marker for over-replication would facilitate the detection and investigation of early stages of cancer development. Most studies of over-replication have utilized systems to deregulate origin

licensing, particularly during G2 and M phase. Yet, premature origin firing in G1 phase might be a more common scenario and it is unclear if cells respond to this deregulation in the same way. Specifically, it needs to be determined if and how premature origin firing affects replication in S phase and how the DNA damage checkpoint is activated under these conditions. While many studies have investigated the regulation of licensing factors, the regulation of firing factors remains understudied. Furthermore, despite the clear importance of correctly regulating DNA replication, little is known about the molecular mechanisms that ensure a safe transition from licensing to firing and vice versa and, therefore, safeguard cells against sporadic over-replication.

Aims of the study

Seminal studies in budding yeast as well as *Xenopus* egg extracts have identified the key proteins involved in DNA replication and outlined how these proteins cooperate to produce one exact copy of the genome during each cell cycle. Central to this process is the separation of DNA replication initiation into mutually exclusive origin licensing and origin firing phases, which are tightly coupled to the cell cycle. Impairing this temporal separation of licensing and firing can culminate in uncontrolled over-replication, which generates genomic instability in the form of gene amplifications or gross chromosomal rearrangements. Therefore, licensing and firing factors are tightly regulated throughout the cell cycle. While many different regulatory mechanisms for licensing factors have been characterized, the regulation of firing factors is understudied. Furthermore, even though the two-step licensing/firing regulation of DNA replication is critical for maintaining genome stability, it remains unclear how transitions between the two phases are regulated.

We therefore pursued three synergizing lines of research to investigate these key aspects of replication control: First, we aimed to understand the molecular mechanisms of how cells transit between replication phases by monitoring the activity of licensing and firing factors in synchronously cycling cells. Second, we aimed to identify regulatory mechanisms that inactivate firing factors and thereby allow a regulated transition between origin firing and origin licensing during M phase. Third, we aimed to elucidate how cells respond to a deregulated transition from firing to licensing, which yields over-replication.

In summary, our research aimed at providing a new angle at DNA replication control by focusing on firing factors, their temporal regulation during the cell cycle, and the consequences of their deregulation.

Results

1. Gap phases separate origin licensing and origin firing

DNA replication in eukaryotes occurs in two distinct steps – origin licensing and firing – which are coupled to different cell cycle phases. In budding yeast, the regulation of these two steps depends on the cyclin-dependent kinase CDK. Licensing can occur from late M to G1 phase while CDK is inactive, whereas firing is triggered by active CDK that is present in cells from S until M phase. Previous studies have demonstrated the detrimental consequences of losing this two-step control [143,167]. However, it has not been addressed how cells achieve the strict temporal separation at the transitions between licensing and firing.

1.1. Phosphorylation-dependent mobility shifts serve as read-outs for replication protein activities

We first sought to establish a simple assay for monitoring the cellular capacity of licensing or firing origins of replication throughout the cell cycle. As CDK phosphorylation is central to the regulation of origin licensing and firing in budding yeast, we aimed to resolve these phosphorylation events by electrophoretic mobility shifts in acrylamide gels. These shifts would then serve as read-outs to determine if the replication factors of interest would be active (hypo-phosphorylated licensing factors, hyper-phosphorylated firing factors) or inactive (hyper-phosphorylated licensing factor, hypo-phosphorylated firing factors). Therefore, we focused on the licensing factors Mcm3 and Orc6 as well as the firing factors Sld2 and Sld3, which are all well-known CDK targets.

To easily resolve CDK-dependent phosphorylation, we made use of an engineered allele of *CDC28* (the single CDK gene in budding yeast), which is called *cdc28-as1* and can be specifically inhibited by the nucleoside-analogous chemical 1NM-PP1 [168]. We first arrested these *cdc28-as1* cells in M phase by the addition of the microtubule-depolymerizing drug nocodazole and then added 1NM-PP1 while taking samples. These samples were used to find gel conditions that would resolve the phosphorylation-dependent electrophoretic mobility shifts and thus allow us to assess the activity of replication factors by western blot (Figure 6). Such shifts were readily detectable for the licensing factor Orc6 and the firing factor Sld2 in 10% and 12% acrylamide gels, respectively. Supplementing 6% acrylamide gels with 15 µM phos-tag chemical enhanced the retention of phosphorylated proteins in the acrylamide gels and allowed us to resolve hyper-phosphorylated licensing factor Mcm3 and firing factor Sld3 in this western blot-based assay. In all four cases, the slower-migrating, hyper-phosphorylated bands shifted to faster-migrating, hypo-phosphorylated species upon CDK inhibition. While the hyper-phosphorylated isoforms of the firing factors Sld2 and Sld3 reacted similarly and were completely lost within the first minutes of the experiment, hyper-phosphorylated licensing factors Mcm3 and Orc6 were only reset with slower kinetics.

These data thus indicate that there is a difference in the regulation of licensing factors and firing factors even though these two sets of replication proteins are both CDK-regulated. Taken together, we have established a western blot-based assay to monitor the activity of replication factors using their phosphorylation state as a proxy.

1.2. Licensing inactivation and firing activation are temporally separated at the G1/S-transition

Next, we asked how licensing and firing factors are regulated at the transition from G1 to S phase. It had previously been shown that CDK in complex with G1 phase cyclins (G1-CDK) already phosphorylates and thereby inhibits the licensing factors Mcm3 and Cdc6 [65,68], whereas only CDK in complex with S phase cyclins (S-CDK) could efficiently activate Sld2 and Sld3 or inhibit Orc6 [31,32,72,169,170]. Nevertheless, it was unclear if these different requirements for CDK would translate into a specific temporal order of inactivation/activation of replication factors at the transition from G1 to S phase.

In an initial experiment, we arrested cells in G1 phase with the mating pheromone α-factor and then released them to the cell cycle while taking samples for subsequent analysis by western blot. In addition to the four factors that we used previously, we also monitored Cdc6 levels since phosphorylation of Cdc6 by CDK activates a phosphorylation-dependent degron on this protein and triggers its degradation. Licensing as well as firing factors shifted to their respective hyper-phosphorylated species at about the same time post release (data not shown). Since the literature suggested that licensing and firing factors should in principle be targeted by different CDK complexes, which should also be active at slightly different times, we continued to scrutinize these data by modulating CDK activity.

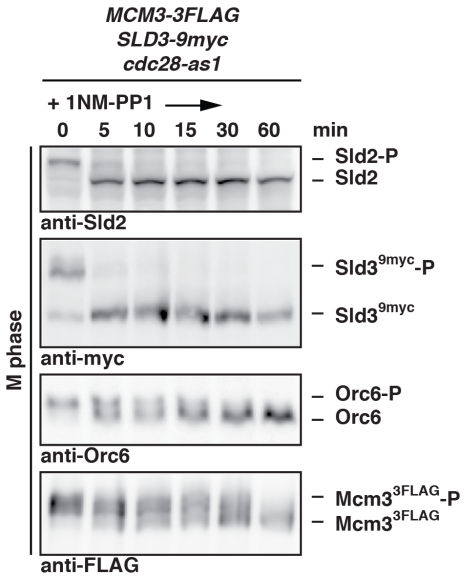

Figure 6 – Licensing and firing factors are reset with different kinetics.
Western blots resolving phosphorylated isoforms of the firing factors Sld2 and Sld3 as well as of the licensing factors Orc6 and Mcm3. Cells were arrested in M phase and treated with the chemical 1NM-PP1 to selectively inhibit the CDK-allele *cdc28-as1*.

To this end, we repeated the experiment and released the cells to a block at the border between G1 and S phase by over-expressing sic1ΔN, which is a non-degradable inhibitor of S-CDK [171]. Under these conditions, only G1-CDK but not S-CDK is active. Indeed, we observed that hyper-phosphorylation of Mcm3 as well as phosphorylation-dependent degradation of Cdc6 could be induced under these conditions whereas Orc6, Sld2 and Sld3 were detected only in their hypo-phosphorylated states (Figure 7).

Additionally, we prolonged G1 phase by deleting the genes coding for the two S phase cyclins *CLB5* and *CLB6* and assessed the CDK-regulation of licensing and firing factors after releasing cells from an arrest in G1. Again, we observed that hyper-phosphorylation of Mcm3 and phosphorylation-dependent degradation of Cdc6 occurred earlier than activation of firing factors Sld2 and Sld3 by hyper-phosphorylation (Figure 8).

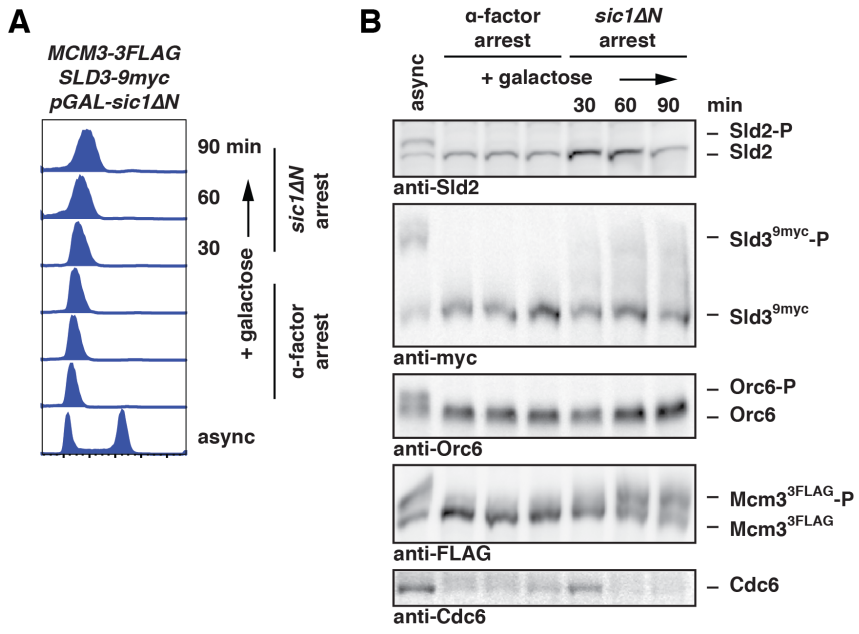

Figure 7 – G1-CDK targets licensing factors but not firing factors.
(A) Cell cycle phase analysis by flow cytometry measuring total DNA content with SYTOX green. Cells were first arrested in G1 phase using mating pheromone α-factor and then released to a sic1ΔN arrest, where G1-CDK is active but S-CDK is inhibited. (B) Western blots resolving phosphorylated isoforms of the firing factors Sld2 and Sld3, the licensing factors Orc6 and Mcm4 as well as total protein levels of licensing factor Cdc6. Samples as in (A).

For the interpretation of these findings, it should be considered that the mating pheromone α-factor triggers a cellular pathway inducing the production of the G1-CDK inhibitor Far1 [172-174]. Consequently, G1-CDK activity is strongly inhibited in experiments using α-factor resulting in an imbalance between the specific activities of G1-CDK and S-CDK. Most likely, it is owed to this imbalance that we could not resolve differences in the phosphorylation kinetics of G1-CDK- and S-CDK-specific sets of target proteins in the initial experiment. In contrast, the differential regulation of licensing and firing factors at the border between G1 and S phase became evident when we precisely manipulated S-CDK activity: By either deleting the S phase cyclins *CLB5* and *CLB6* (Figure 8) or by expressing of S-CDK inhibitor sic1ΔN (Figure 7) we were able to show that licensing factors are inactivated before firing factors are activated. Taken together, our data indicate the need for an optimized experimental approach to synchronize cells in G1 phase in order to resolve activation/inactivation kinetics of replication factors in *wild-type* cells. Nevertheless, our data confirm that there is differential regulation of licensing and firing factors at the border between G1 and S phase.

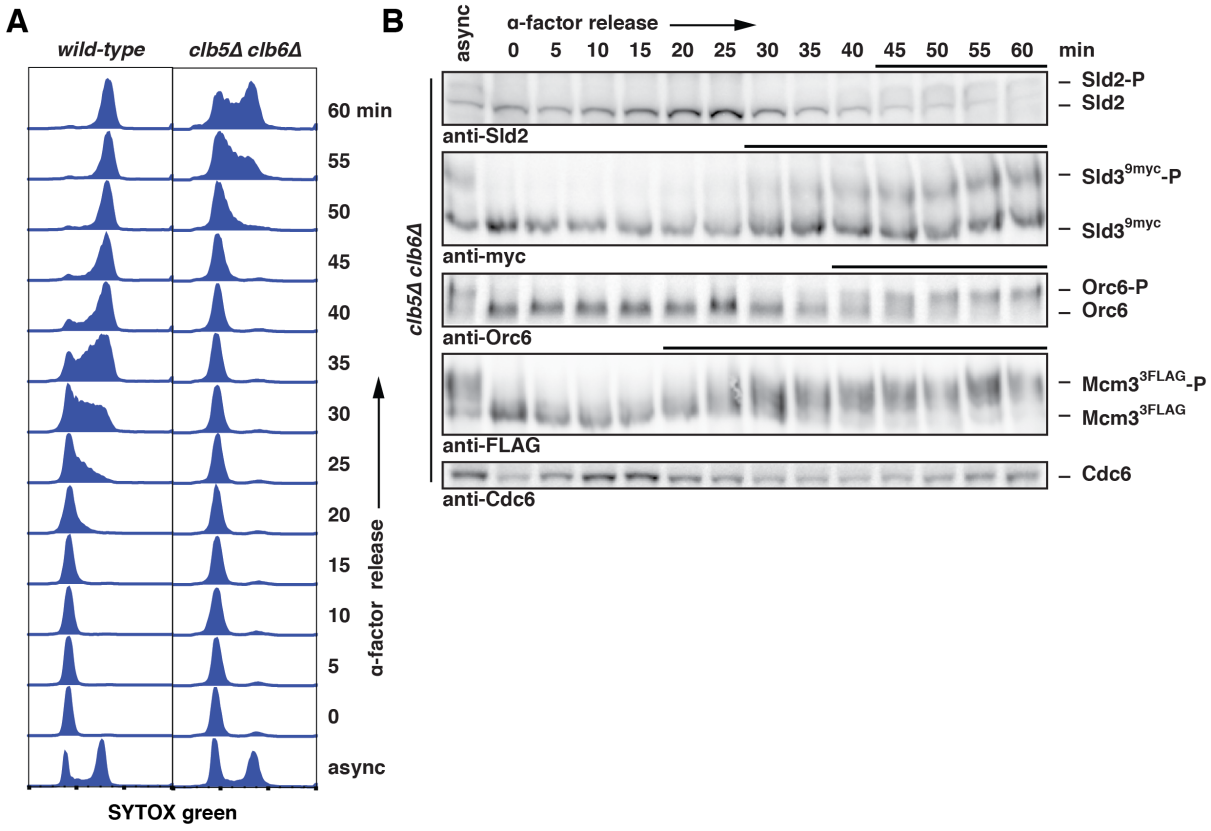

Figure 8 – Inactivation of licensing factors precedes activation of firing factors at the G1-S-transition.
(A) Cell cycle analysis by flow cytometry measuring total DNA content with SYTOX green. Cells were arrested in G1 phase using mating pheromone α-factor and then released to fresh medium. (B) Western blots resolving phosphorylated isoforms of firing factors Sld2 and Sld3, licensing factors Orc6 and Mcm3 as well as total protein levels of licensing factor Cdc6. Horizontal lines above the blots indicate the presence of a phosphorylated isoform. Samples as in (A) from *clb5Δ clb6Δ* cells, which lack S phase cyclins.

1.3. Firing inactivation and licensing activation are temporally separated in M phase

Since cells need to switch between high CDK activity and low CDK activity during M phase, we next investigated how replication factors are regulated at this transition. Cells were arrested in G1 phase with α-factor and subsequently released to fresh medium (Figure 9). We observed that phosphorylation marks on the licensing factors Mcm3 and Orc6 were lost with a similar timing at around 70 min post release. Interestingly, the signal from hyper-phosphorylated, active firing factor Sld3 was lost about 10 min earlier. For the firing factor Sld2, we observed an even earlier shift from hyper-phosphorylated to hypo-phosphorylated species as compared to the licensing factors Mcm3 and Orc6. In addition, the protein levels of hyper-phosphorylated Sld2 decreased specifically during M phase thus inactivating Sld2 even earlier than Sld3. These data demonstrate a clear temporal order in the control of replication factors in M phase such that firing factors are inactivated before licensing factors are re-activated.

To further improve the temporal resolution in our experiments, we introduced a second synchronization step by adding hydroxyurea to the medium, which reversibly inhibits the enzyme ribonucleotide reductase and thus blocks cells in early S phase. When we released the cells from this arrest, we observed again that inactivation of firing factors preceded the re-activation of licensing factors (Figure 10). Importantly, the loss of active, hyper-phosphorylated Sld2 occurred even earlier, thus increasing the length of the gap between firing factor inactivation and licensing factor re-activation. Taken together our data demonstrate that cells ensure that origin firing and origin licensing never occur simultaneously. In M phase, this is achieved by inactivating origin firing first and only later reactivating origin licensing, thereby generating a temporal gap, during which no replication factor is active.

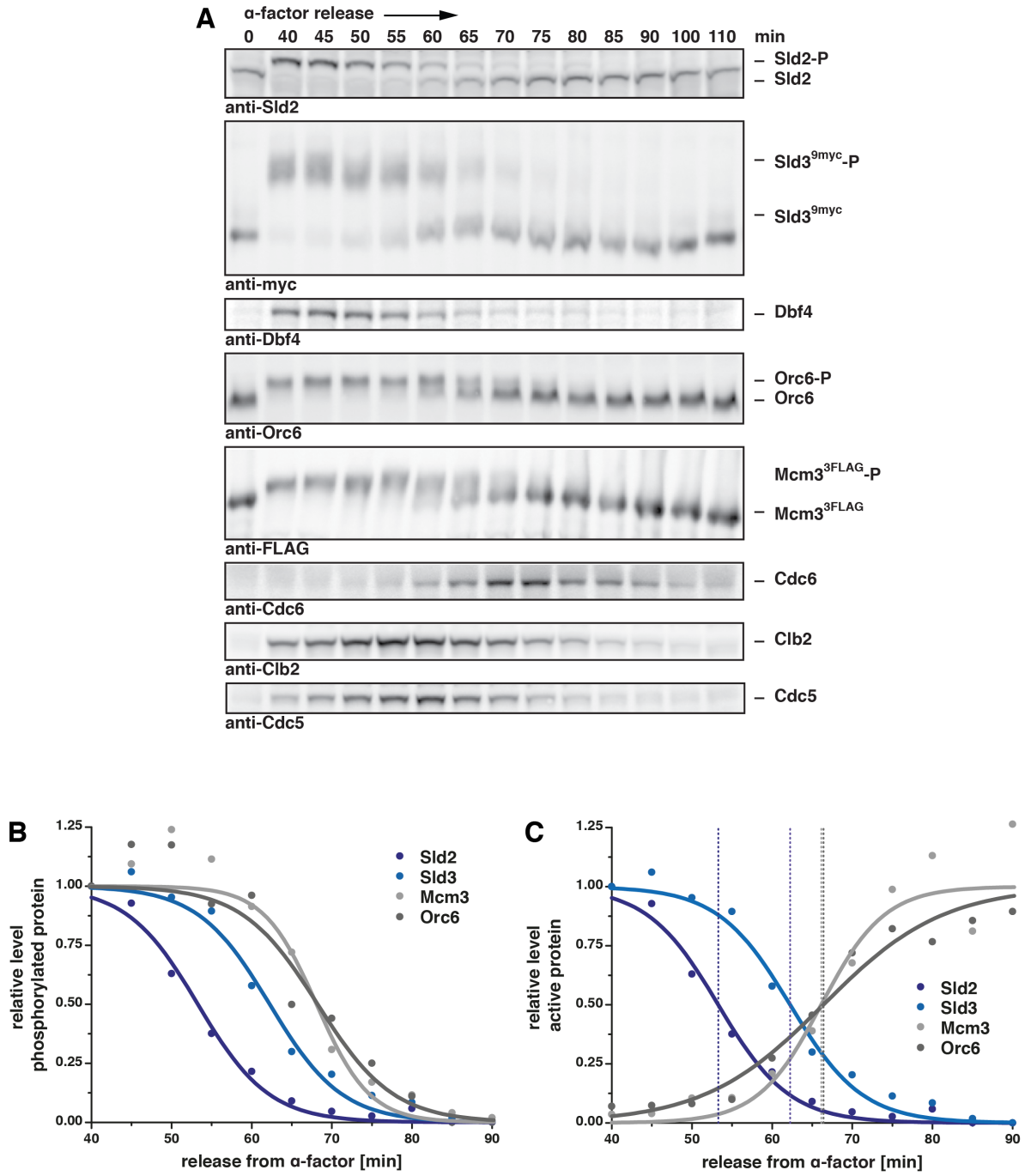

Figure 9 – Inactivation of firing factors precedes re-activation of licensing factors in M phase.
Cells were released from an α-factor arrest into fresh medium and samples were taken at the indicated timepoints. To prevent entry into a second cell cycle, α-factor was added back after 45 min of release. (A) Western blots resolving phosphorylated isoforms of the firing factors Sld2 and Sld3, licensing factors Orc6 and Mcm3 as well as total protein levels of licensing factor Cdc6. Total protein levels of M phase cyclin Clb2 and the yeast Polo-kinase homolog Cdc5 were measured as indicators for cell cycle stage. (B) Quantification of the phosphorylated bands from western blots shown in (A). Band intensities were normalized to the value at 40 min post release. (C) Quantification of the active protein species (hypo-phosphorylated licensing factors Mcm3 and Orc6; hyper-phosphorylated firing factors Sld2 and Sld3) from western blots shown in (A). Band intensities were normalized to the value at 40 min post release.

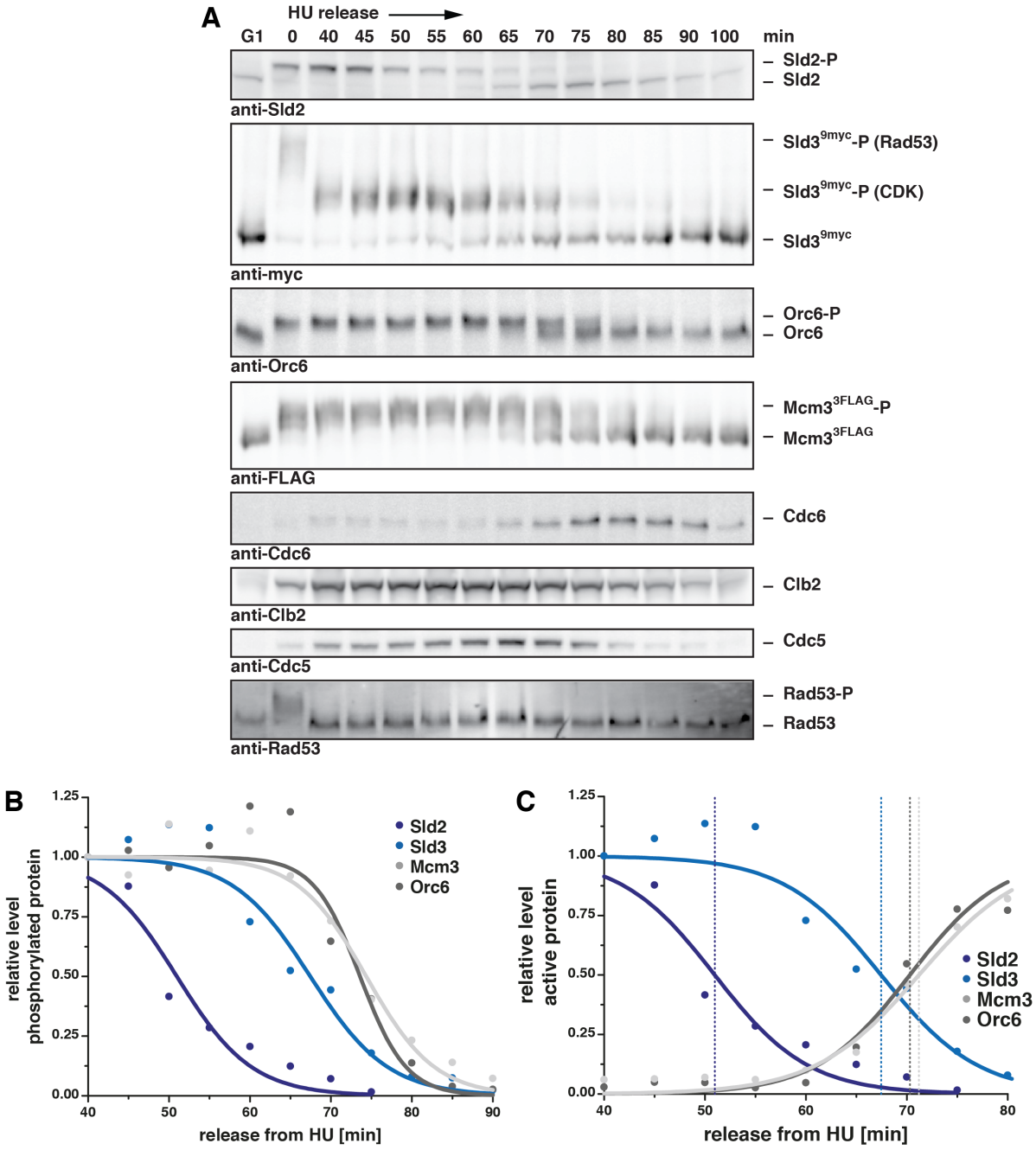

Figure 10 – Releasing cells from HU leads to earlier inactivation of Sld2 in M phase in comparison to all other replication proteins.
Cells were released from an α-factor arrest into medium containing 200 mM hydroxyurea (HU). Afterwards, cells were released to fresh medium and samples were taken at the indicated timepoints. To prevent entry into a second cell cycle, α-factor was added to the medium after the release. (A) Western blots resolving phosphorylated isoforms of the firing factors Sld2 and Sld3, the licensing factors Orc6 and Mcm3 as well as total protein levels of the licensing factor Cdc6. Total protein levels of M phase cyclin Clb2 and the yeast Polo-kinase homolog Cdc5 were measured as indicators for cell cycle stage. (B) Quantification of the phosphorylated bands from western blots shown in (A). Band intensities were normalized to the value at the 0 min timepoint. (C) Quantification of the active protein species (hypo-phosphorylated licensing factors Mcm3 and Orc6; hyper-phosphorylated firing factors Sld2 and Sld3) from western blots shown in (A). Band intensities were normalized to the value at 0 min.

2. Degradation of firing factor Sld2 generates a gap in M phase

2.1. Four kinases trigger Sld2 degradation in M phase

The M phase-specific decrease in the protein levels of Sld2 prompted us to investigate the stability of this protein. To this end, we inhibited protein translation by adding cycloheximide (CHX) and followed the stability of Sld2 in western blots (Figure 11). When we performed these experiments in cell cycle-arrested cells, we could observe a striking difference: Sld2 was turned over with a half-life time of approximately 40 min in G1-arrested cells whereas its half-life time was decreased to approximately 10 min in M-arrested cells.

This rapid degradation was also observed when cells were released from a G1 arrest and Sld2 stability was assessed at different timepoints after the release (Figure 12). In this case, Sld2 was stable throughout S phase and its degradation was specifically triggered approximately 60 min post release. Thus, we conclude that Sld2 is degraded in a M phase-specific and drug-independent manner.

Since Sld2 was particularly unstable in mitotic cells, we reasoned that this might be mediated by a phosphorylation-dependent degron and investigated kinases that have been associated with such degrons before. Indeed, we were able to identify four distinct kinases that were required for the rapid degradation of Sld2 in M phase (Figure 13). Abrogating their activity by either direct inhibition (as in the case of CDK via *cdc28-as1* and the specific inhibitor 1NM-PP1), deletion (as with *MCK1* or DDK by using the bypass mutation *bob1-1*) or transcriptional repression (as with *CDC5* by using a glucose-repressible *pGALL* promoter) strongly stabilized Sld2 in mitotic cells.

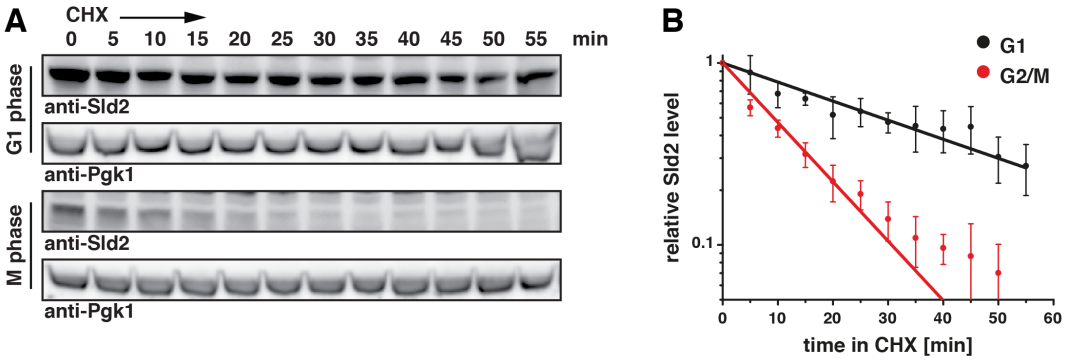

Figure 11 – Sld2 is rapidly degraded in M phase.
Cells were arrested in G1 phase with α-factor and in M phase with nocodazole. Protein translation inhibitor cycloheximide (CHX) was added and samples were taken at the indicated timepoints. (A) Representative western blots detecting total Sld2 levels in G1 and M phase after CHX addition. Western blots against Pgk1 serve as control. (B) Quantification of Sld2 protein levels as in (A), normalized to 0 min timepoint. Data represent means of three (M phase) and two (G1 phase) independent experiments; error bars represent standard deviation.

We hypothesized that the kinases could control the timing of Sld2 degradation. Since the yeast Polo kinase homolog Cdc5's activity and protein levels peak in M phase [175], the availability of this kinase could determine the timing of rapid Sld2 degradation. To experimentally test this hypothesis, we coupled a G1-release experiment with cycloheximide-mediated protein translation shut-offs and induced expression of Cdc5 already during the G1 arrest (Figure 14). In control cells, we observed that Sld2 was stable during S phase, but became rapidly degraded when cells entered M phase. In contrast, cells that over-expressed Cdc5 were already delayed in their cell cycle progression. These cells entered S phase later than the control cells and also appeared to progress slower through S phase. Intriguingly, Sld2 levels were generally decreased and rapid degradation of Sld2 could already be detected in S phase. These data thus suggest that Cdc5 controls the timing of Sld2 degradation. Taken together, we have discovered a rapid degradation process targeting Sld2 specifically in M phase, that requires the activity of the kinases CDK, DDK, Mck1 and particularly Cdc5.

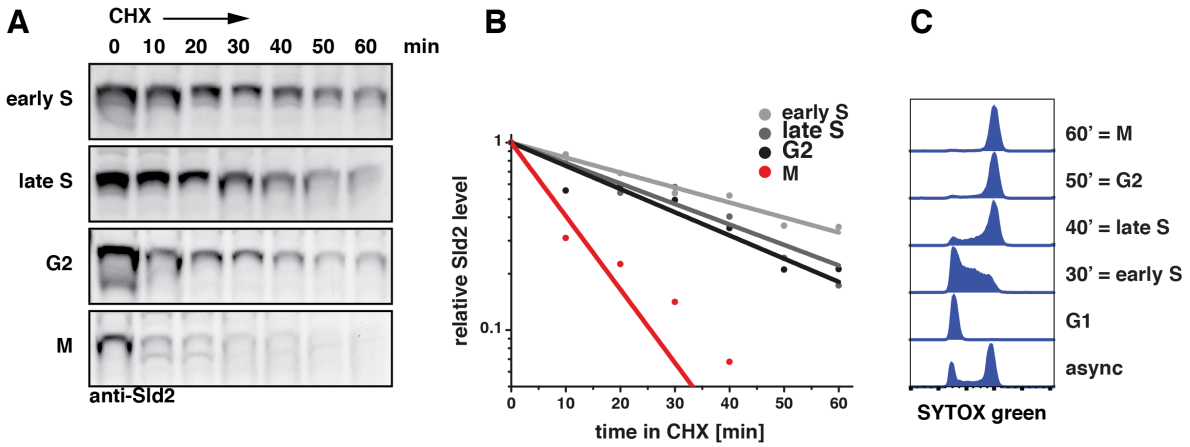

Figure 12 – Rapid Sld2 degradation is restricted to M phase.
Cells were released from G1 arrest and treated with cycloheximide (CHX) to inhibit protein translation at early S phase, late S phase, G2 phase and M phase. Samples were taken at the indicated timepoints after CHX addition. (A) Western blots against Sld2. (B) Quantification of Sld2 protein levels in (A). Data are normalized to the 0 min timepoint. (C) Cell cycle analysis by flow cytometry measuring total DNA content with SYTOX green. Samples correspond to the 0 min timepoints in (A) and (B).

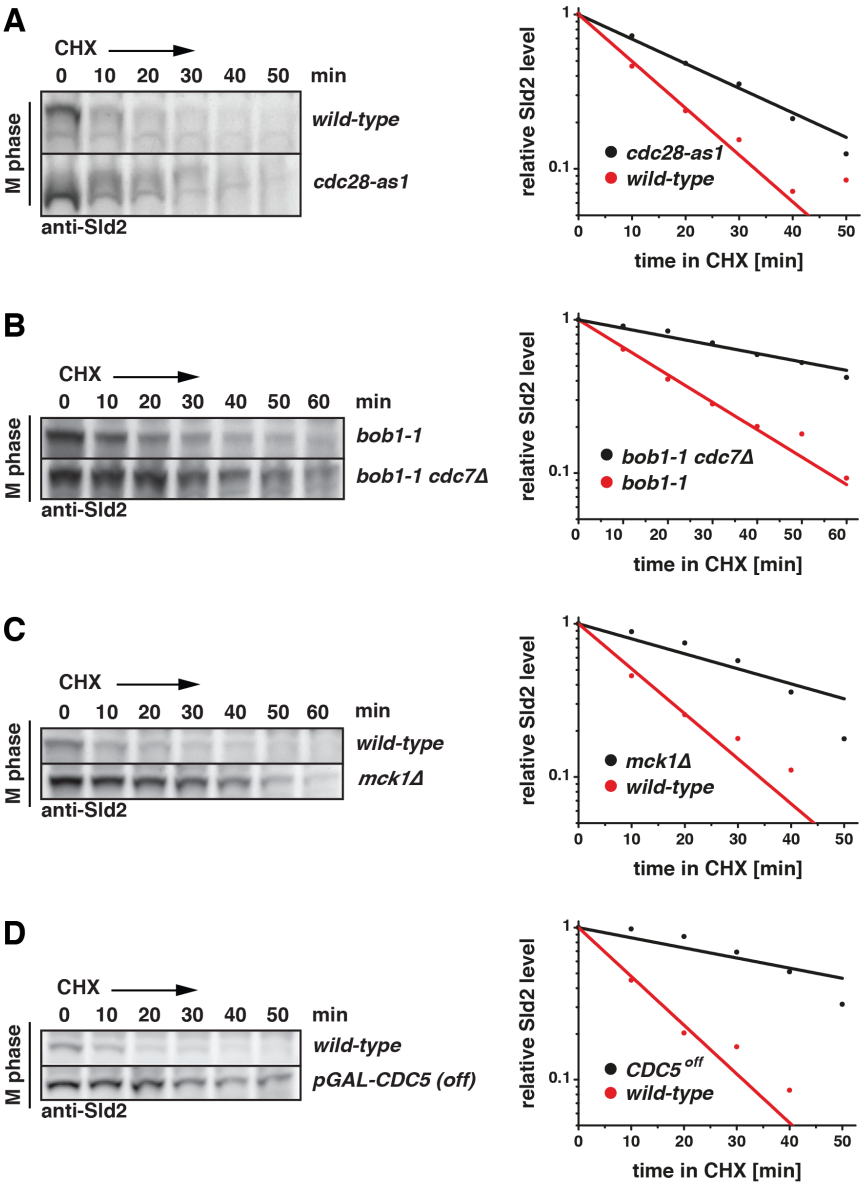

Figure 13 – Four distinct kinases mediate rapid Sld2 degradation in M phase.
Cells from wild-type and kinase-mutant cells were arrested in M phase using nocodazole and treated with the protein translation inhibitor cycloheximide (CHX). Samples were taken at the indicated timepoints after CHX addition. (A) Western blots against Sld2 from *wild-type* and CDK-mutant *cdc28-as1* cells. CHX was added concomitantly with the CDK inhibitor 1NM-PP1. Right inlet shows quantification of Sld2 protein levels, normalized to the 0 min timepoint. (B) Western blots against Sld2 from *bob1-1* and DDK-deficient *bob1-1 cdc7Δ* cells. Right inlet shows quantification of Sld2 protein levels, normalized to the 0 min timepoint. (C) Western blots against Sld2 from *wild-type* and kinase-deficient *mck1Δ* cells. Right inlet shows quantification of Sld2 protein levels, normalized to the 0 min timepoint. (D) Western blots against Sld2 from *wild-type* cells and cells depleted of Polo-kinase Cdc5 activity by transcriptional repression. Right inlet shows quantification of Sld2 protein levels, normalized to the 0 min timepoint.

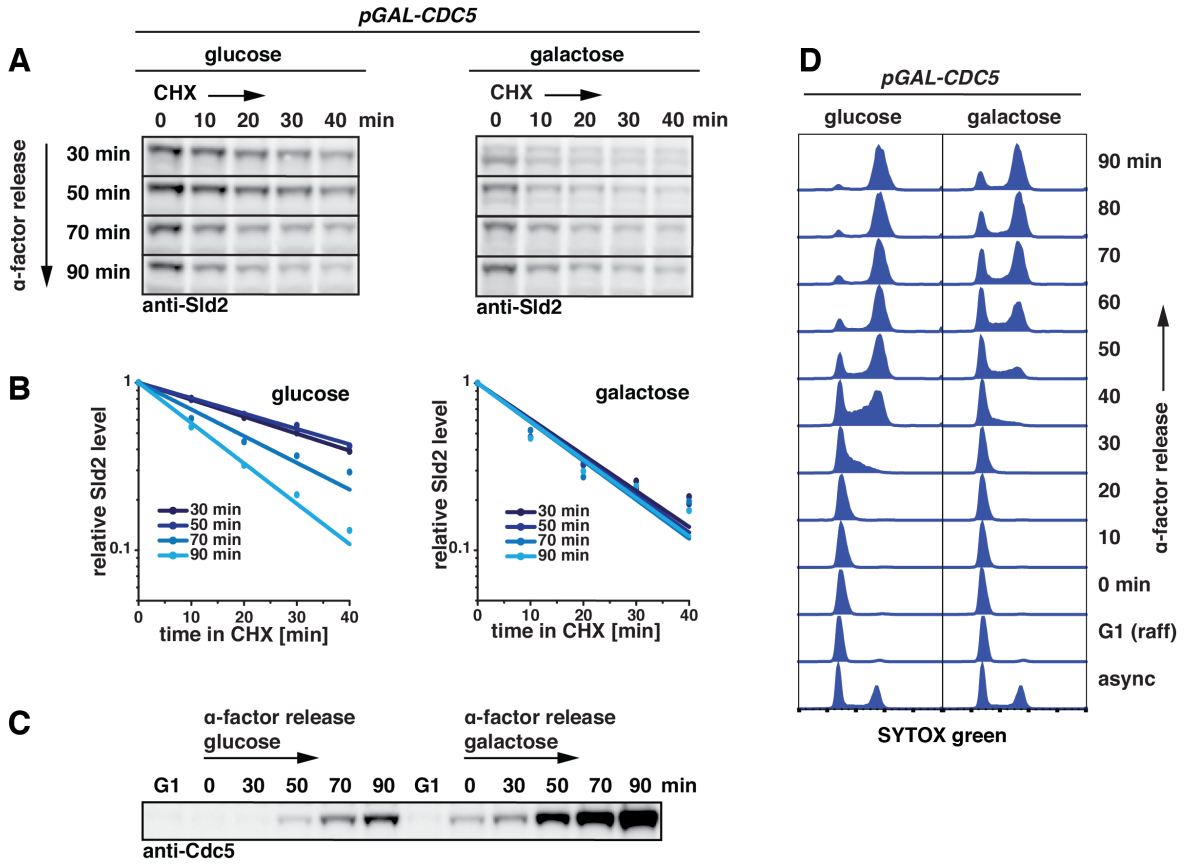

Figure 14 – Yeast Polo-kinase Cdc5 determines the timing of rapid Sld2 degradation.
Cells harboring an ectopic galactose-inducible copy of polo kinase *CDC5* were arrested in G1 phase. In the G1 arrest, *CDC5* was repressed (glucose) or induced (galactose) for 2 h before release to the cell cycle in fresh medium containing glucose or galactose. The protein translation inhibitor cycloheximide (CHX) was added after 30 / 50 / 70 / 90 min of release to measure the stability of Sld2. (A) Western blots against Sld2 after CHX addition at different timepoints post release. (B) Quantifications of Sld2 protein levels in (A). Data are normalized to the 0 min timepoints. (C) Western blots against Cdc5 at different timepoints before CHX addition. (D) Cell cycle analysis by flow cytometry measuring total DNA content with SYTOX green. Samples as in (A) and (C).

2.2. Phosphorylation of Sld2 within a short degron region mediates its degradation

Since the four kinases CDK, DDK, Mck1 and Cdc5 were required for rapid Sld2 degradation, we asked if they were targeting Sld2 directly. To this end, we first determined the degron region in Sld2 by performing CHX-mediated translation shut-offs in M phase-arrested cells that harbored a truncated copy of the *SLD2* gene (Figure 15). This approach allowed us to narrow down the degron to the N-terminus of Sld2 in a region spanning amino acids 120 to 150.

We next purified all four kinases as well as the Sld2 N-terminus (amino acids 1-150, fused to GST) to perform *in vitro* kinase assays. The kinases DDK, Mck1 and Cdc5 were purified from budding yeast cultures; the Sld2 N-terminus and a model CDK (Cdk2/cycAΔN170) were purified from *E. coli* cells. CDK and Cdc5 were able to directly phosphorylate Sld2 using radio-labelled ATP, whereas Mck1 and DDK targeted the Sld2 N-terminus only after it had been pre-phosphorylated by CDK (Figure 16 A and C). Analysis of these samples by mass spectrometry allowed us to correlate the phosphorylation of specific sites with distinct kinases and directed our attention to a region spanning amino acids 122 to 143 that was particularly rich in phosphorylation sites (Figure 16 B).

To analyze the interdependencies of the kinases in detail, we utilized phosphorylated peptides spanning the degron region of Sld2 (amino acids 118 to 143) and incubated them with the purified kinases and radio-labelled ATP (Figure 17). The kinases would only be able to incorporate the radio-labelled phosphate at a specific site if this site was not blocked by a cold phosphate group during peptide synthesis and thus allow us to map the target sites of each kinase within this region. Using this approach, we identified serine 128 and 138 as target sites for CDK phosphorylation and threonine 122 and 143 as targets sites for Cdc5 phosphorylation. Moreover, we could show that Mck1 phosphorylates serine 124 and DDK phosphorylates serine 137, and that both required pre-phosphorylation of the downstream CDK sites serine 128 (Mck1) and serine 138 (DDK). In summary, these experiments firmly established that Sld2 is directly phosphorylated by the kinases CDK, DDK, Mck1 and Cdc5. Furthermore, these experiments allowed us to assign phosphorylation sites on Sld2 to specific kinases as summarized in Figure 18.

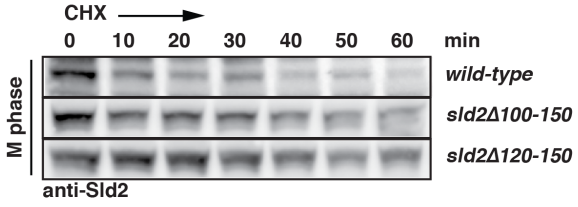

Figure 15 – Rapid Sld2 degradation signals are present within a short region of Sld2.
Cells expressing either wild-type Sld2 or truncated versions lacking amino acids 100-150 (*sld2Δ100-150*) or 120-150 (*sld2Δ120-150*) were arrested in M phase and treated with protein translation inhibitor cycloheximide (CHX). Western blot against Sld2 from samples taken at the indicated timepoints after CHX addition.

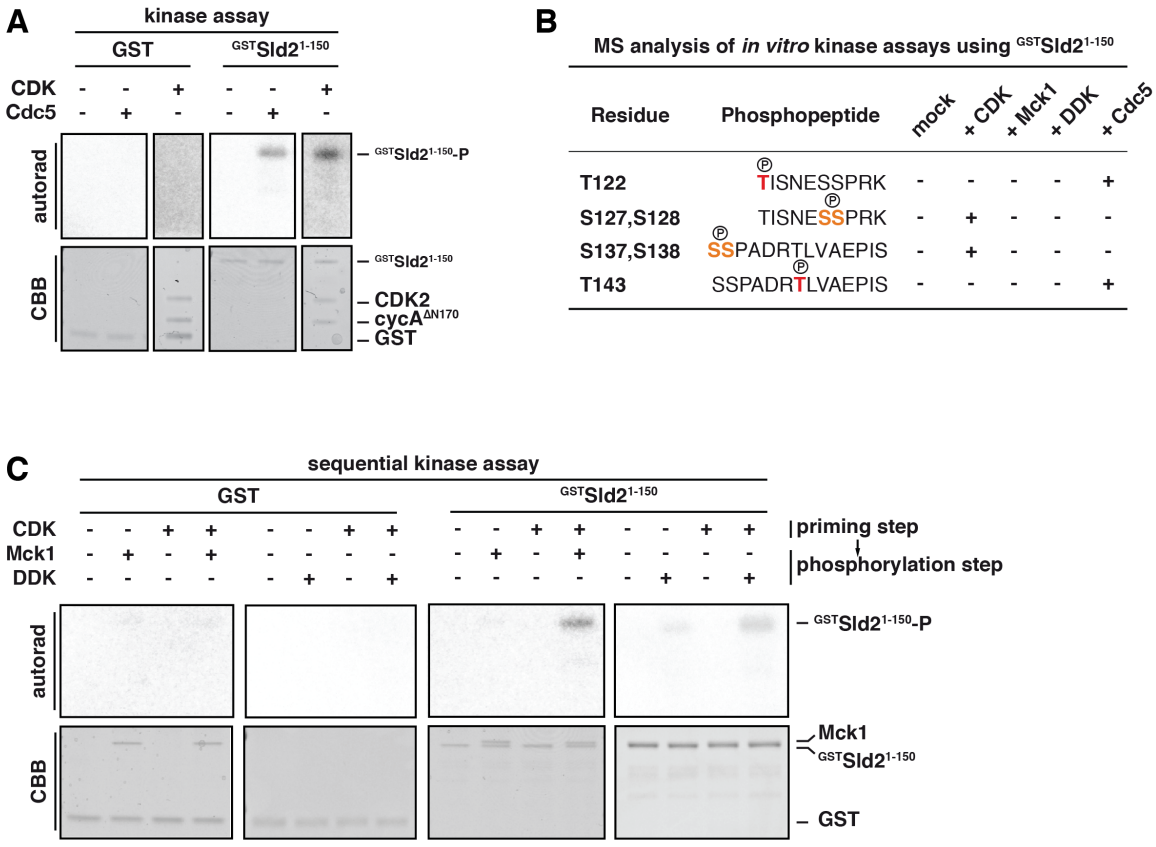

Figure 16 – The N-terminus of Sld2 is phosphorylated by CDK, DDK, Mck1 and Cdc5.
(A) Autoradiogram and Coomassie brilliant blue stain (CBB) of purified GST or GST-Sld2$^{1-150}$ after incubation with CDK or Cdc5 in the presence of [γ^{32}P]-ATP. (B) Experiment as in (A) but in addition to CDK and Cdc5 also using the kinases DDK and Mck1. Samples were subjected to analysis by mass spectrometry. The table summarizes the detected phosphorylated peptides and the position (red = exact position, orange = ambiguous positions) of the phosphate group on the peptides. (C) Autoradiogram and Coomassie brilliant blue stain (CBB) of purified GST or GST-Sld2$^{1-150}$ after incubation with CDK in the presence of cold ATP and subsequent incubation with either Mck1 or DDK in the presence of [γ^{32}P]-ATP.

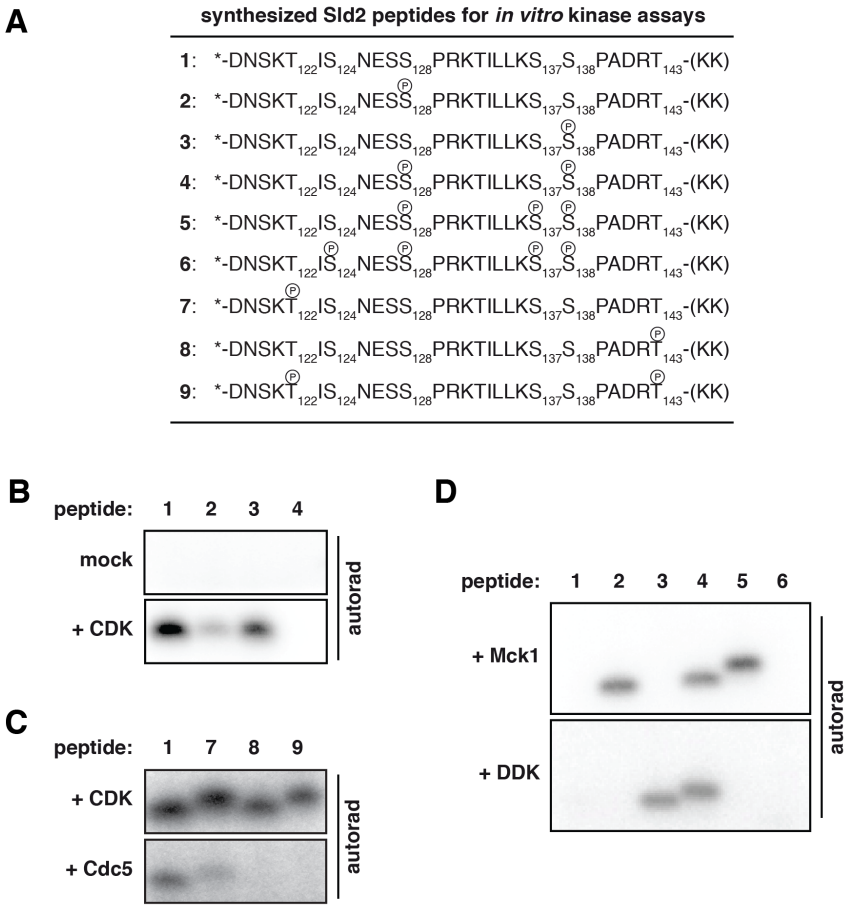

Figure 17 – CDK, DDK, Mck1 and Cdc5 phosphorylate Sld2 within the degron region.
(A) Summary of the Sld2 peptides spanning amino acids 118-143 reconstituting different phosphorylated states. (B) Autoradiograms of peptides as in (A) after incubation with CDK in the presence of [γ^{32}P]-ATP. (C) Autoradiograms of peptides as in (A) after incubation with either CDK or Cdc5 in the presence of [γ^{32}P]-ATP. (D) Autoradiograms of peptides as in (A) after incubation with either Mck1 or DDK in the presence of [γ^{32}P]-ATP.

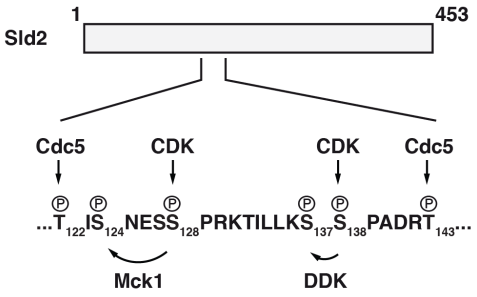

Figure 18 – Summary of phosphorylation sites within the Sld2 degron.
The Sld2 degron is phosphorylated on six distinct sites within the degron region. Phosphorylation by Mck1 and by DDK requires pre-phosphorylation of the degron region by CDK.

2.3. Mutation of the phospho-degron stabilizes Sld2 specifically in M phase

Having established that Sld2 is a direct target of all four kinases, we hypothesized that mutating these phosphorylation sites might prevent rapid degradation of Sld2 in M phase. Hence, we performed CHX shut-off experiments in M phase with cells that harbored *SLD2* alleles with mutations in either the CDK-targeted sites (*sld2-2SA*), the Cdc5-targeted sites (*sld2-2TA*), the CDK- and the Cdc5-targeted sites (*sld2-4A*), or all six identified phosphorylation sites (*sld2-6A*). All four mutant *sld2* alleles led to the same extent of stabilization of the Sld2 protein in M phase in CHX shut-off experiments (Figure 19). Importantly, these mutations did not generate an otherwise hypomorphic *sld2* allele: The interaction between Sld2 and Dpb11 was not impaired as judged by a yeast-two hybrid experiment and cells harboring our mutant *sld2* alleles as their only copy of *SLD2* progressed through the cell cycle as *wild-type* cells (Figure 20). In addition, plasmid loss rates, which when elevated indicate impaired replication initiation, from yeast strains with mutant *sld2* were indistinguishable from those with wild-type *SLD2*. Taken together, these data demonstrate that mutation of the phosphorylation-dependent degron specifically impairs degradation of Sld2 in M phase while not affecting Sld2's essential functions.

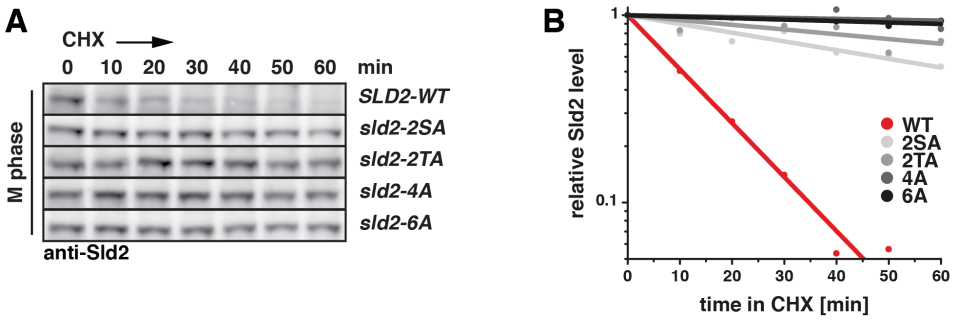

Figure 19 – Mutation of the phosphorylation sites within the degron region stabilizes Sld2 in M phase.
Cells were arrested in M phase and treated with cycloheximide (CHX). Samples were taken at the indicated timepoints after CHX addition. Mutations in SLD2 either abrogate CDK-phosphorylation sites (*sld2-2SA*), Cdc5-phosphorylation sites (*sld2-2TA*), CDK-/Cdc5-phosphorylation sites (*sld2-4A*), or all phosphorylation sites (*sld2-6A*) within the degron region. (A) Western blots against Sld2 at different timepoints after CHX addition. (B) Quantification of Sld2 protein levels in (A), normalized to 0 min timepoints.

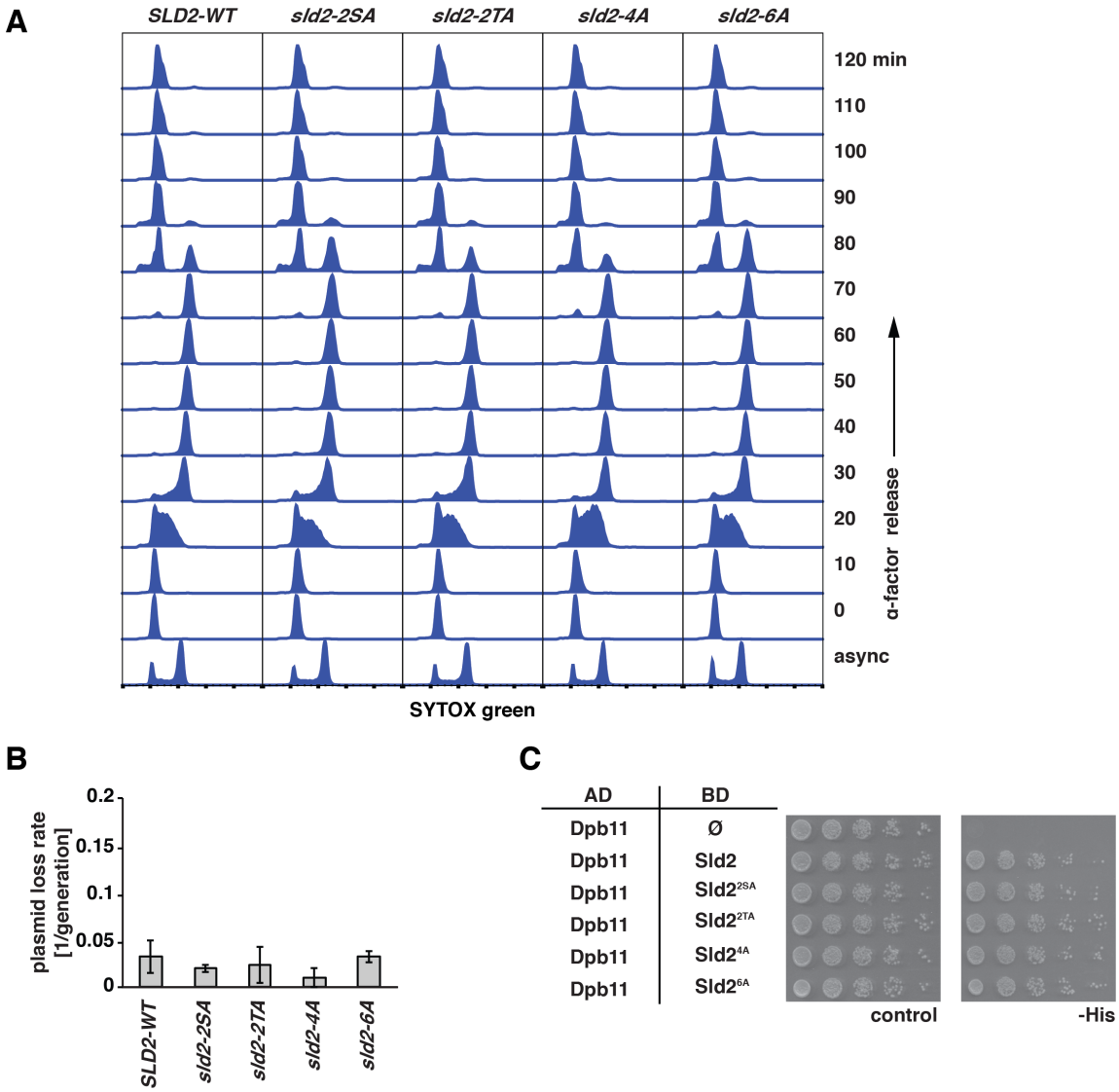

Figure 20 – Mutation of the Sld2 degron region does not impair Sld2's function.
(A) DNA replication analysis by flow cytometry measuring total DNA content with SYTOX green. Cells were arrested in G1 phase using α-factor and released to fresh medium. Samples were taken at the indicated timepoints. To prevent entry into a second cell cycle, α-factor was added back after 45 min of release. Mutations in *SLD2* either abrogate CDK-phosphorylation sites (*sld2-2SA*), Cdc5-phosphorylation sites (*sld2-2TA*), CDK-/Cdc5-phosphorylation sites (*sld2-4A*), or all phosphorylation sites (*sld2-6A*) within the degron region. (B) Plasmid loss rates of *wild-type* cells and degron mutants of *SLD2* as in (A) determined using the *ARS/CEN* plasmid YCplac33. The mean and standard deviation of three independent experiments are shown. (C) Yeast two-hybrid analysis of the interaction between the scaffold protein Dpb11 and wild-type Sld2 as well as degron mutants of Sld2 as in (A).

2.4. The E3 ubiquitin ligases Dma1/2 recognize the Sld2 phospho-degron

In order to trigger degradation of Sld2, the complex phospho-degron must be recognized by a E3 ubiquitin ligase. To this end, we screened a set of ubiquitin ligase candidates, which were selected either because of their role in cell cycle regulation or because of their propensity for binding to phosphorylated target proteins. Neither the anaphase-promoting complex APC (tested by activator mutant *cdh1Δ* and transcriptional repression of the second activator *CDC20*) nor temperature-sensitive mutants of the SCF-Cdc4 complex were involved in targeting Sld2 for degradation in M phase (data not shown), even though these complexes play major roles in the regulation of the cell cycle. Instead, we observed that deletion of the genes *DMA1* and *DMA2*, which encode two closely-related E3 ubiquitin ligases, abolished the rapid degradation of Sld2 in M phase as assayed in a CHX shut-off experiment (Figure 21). Dma1 and Dma2 both contain the characteristic RING domain of E3 ubiquitin ligases and in addition an FHA domain, which has been described to preferentially bind to phosphorylated threonine residues [176-179]. These data suggest that Dma1 and Dma2 mediate the rapid degradation of Sld2.

We observed that Dma1 and Dma2 interacted with Sld2 in a yeast-two hybrid assay (Figure 22 A). Notably, we could facilitate the detection of the interaction by generating a substrate trap through mutation of the RING domain of Dma1 (Figure 22 B). This finding supports our interpretation that the interaction between Dma1 and Sld2 targets Sld2 for degradation. Importantly, mutations in either the FHA domain of Dma1 or in the previously mapped phosphorylation sites on Sld2 abolished the interaction (Figure 22 C). Peptide pulldowns, fluorescence anisotropy measurements and micro-scale thermophoresis experiments incubating phosphorylated peptides with the purified FHA-domain of Dma1 further supported these findings and pointed to a critical role for phosphorylation of Sld2 residues threonine 122 and threonine 143 (Figure 23). Thus, we conclude that Dma1's and most likely also Dma2's FHA domain recognize the phosphorylation marks on Sld2 – particularly phosphorylated threonine 122 and 143.

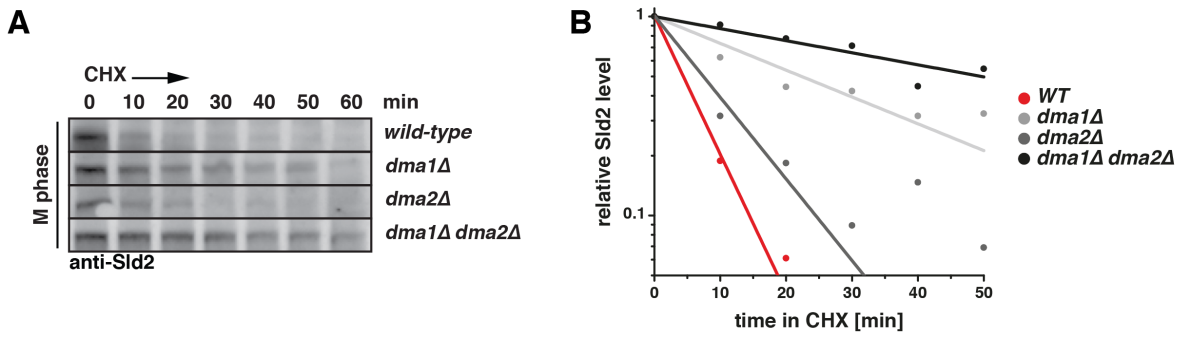

Figure 21 – The ubiquitin ligases Dma1/2 mediate rapid Sld2 degradation in M phase.
Wild-type cells and cells lacking *DMA1* and/or *DMA2* were arrested in M phase and treated with cycloheximide (CHX). Samples were taken at the indicated timepoints after CHX addition. (A) Western blots against Sld2 at different timepoints after CHX addition. (B) Quantification of Sld2 protein levels in (A), normalized to 0 min timepoints.

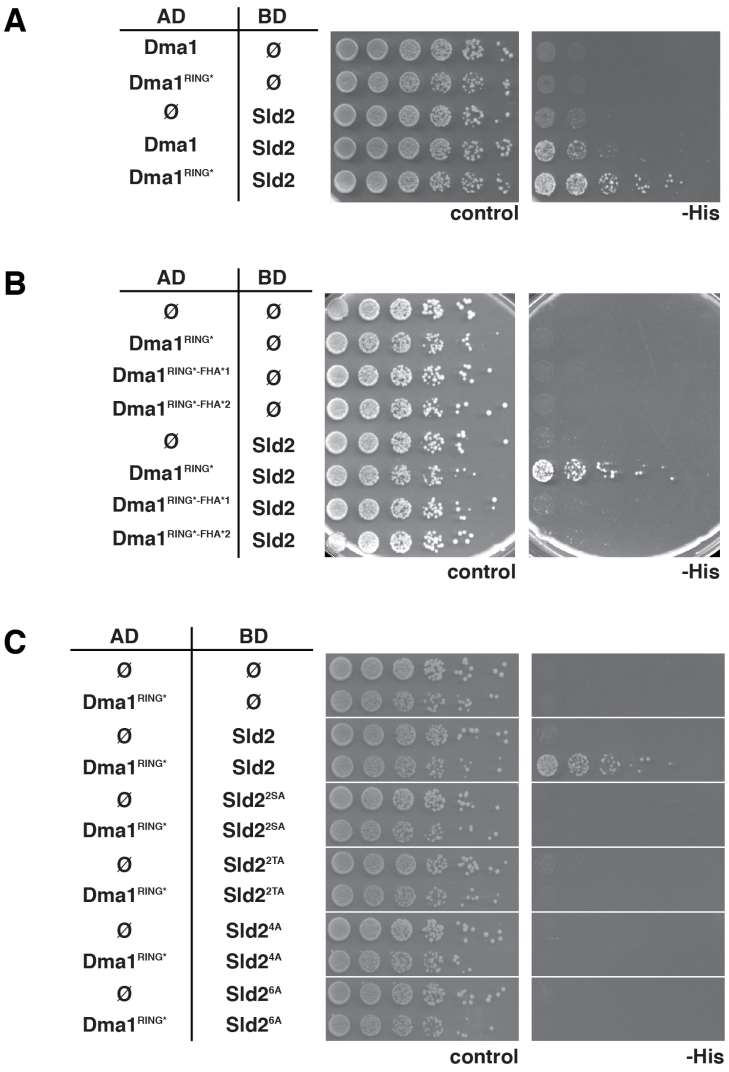

Figure 22 – The FHA-domain of Dma1/2 recognizes the phospho-degron on Sld2.
Yeast two-hybrid analyses of the interaction between Dma1 and Sld2 using (A) a mutant in the RING-domain of Dma1 (C345S H350A) to avoid Sld2 degradation and thereby stabilize the interaction with Sld2, (B) combined mutants in the RING domain and the FHA domain of Dma1 (G192E or S220A H223L), and (C) mutants in the phosphorylation sites within the degron region (2SA – CDK sites; 2TA – Cdc5 sites; 4A – CDK-/Cdc5-sites; 6A – all six sites).

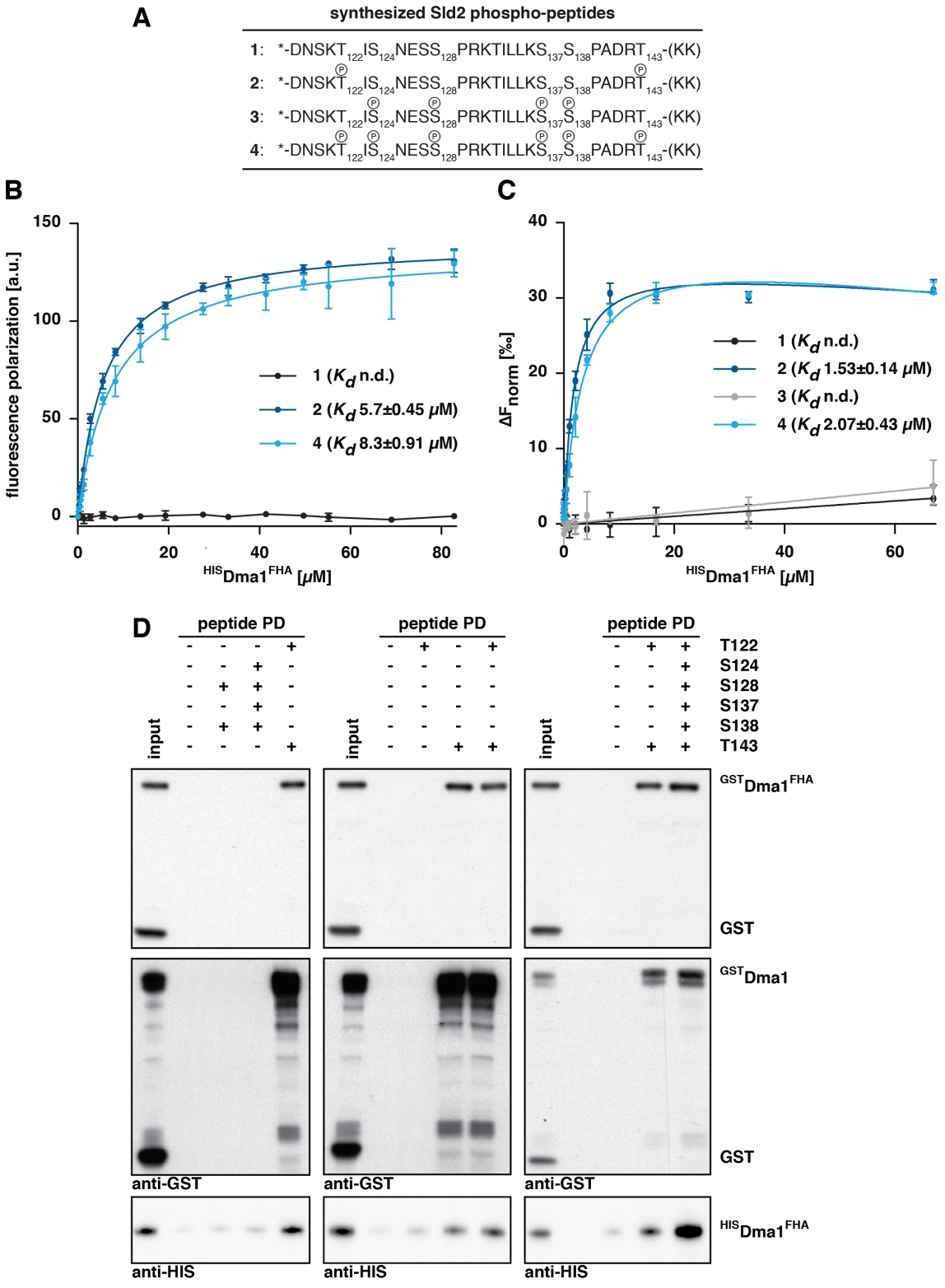

Figure 23 – Phosphorylation of threonine residues is critical for binding of the Dma1 FHA domain to Sld2.
(A) Summary of the used phospho-peptides, labeled with fluorescein. (B) Fluorescence anisotropy measurements with phospho-peptides as in (A) and purified FHA domain of Dma1. Binding affinities are given in the inset. Data from three independent experiments are displayed as mean with standard deviation. (C) Micro-scale thermophoresis measurements with phospho-peptides as in (A) and purified FHA domain of Dma1. Binding affinities are given in the inset. Data from three independent experiments are displayed as mean with standard deviation. (D) Peptide pulldown experiments with the indicated phospho-peptides. Using their desthiobiotin-label, the peptides were bound to streptavidin beads and incubated with GST, GST-Dma1, GST-Dma1-FHA, and HIS-Dma1-FHA. Input and eluate samples were analyzed by western blotting against GST- and HIS-tags.

3. A shortened gap in M phase leads to increased genomic instability

3.1. Stable Sld2 shortens the gap phase in M phase

Our initial experiments indicated that the timely inactivation of Sld2 correlated well with the temporal separation of firing factor inactivation from licensing factor re-activation in M phase. Hence, we investigated whether stable *sld2* mutants would affect this element of replication control and potentially also lead to genome instability. We arrested cells expressing either wild-type or stable Sld2 in G1 phase, released them first to early S phase (HU-containing medium) and subsequently to fresh medium and took samples in 5 min intervals (Figure 24). In the case of *wild-type* cells, the signal for the hyper-phosphorylated, active Sld2 was lost at around 50 min post release, as observed before. Hyper-phosphorylated, inactive Orc6 was reset at around 65 min post release. Strikingly, the signal for active Sld2 persisted in cells expressing stable Sld2 until about 60 min post release while the reset of Orc6 occurred with normal kinetics, thereby abolishing the early loss of active Sld2 in comparison to active Sld3. We observed similar results when we skipped the block in early S phase and released cells directly from G1 into the cell cycle (Figure 25). Thus, we conclude that preventing Sld2 degradation in M phase allows to specifically shorten the gap phase between firing inactivation and licensing re-activation.

3.2. Stable Sld2 causes increased genomic instability

A shorter gap as caused by stabilization of Sld2 in M phase might increase the probability that origin firing and licensing could occur at the same time. Such an overlap could lead to deregulated replication initiation and consequently induce genomic instability. Since gross chromosomal rearrangements (GCRs) could occur as a consequence of deregulated replication initiation, we utilized a highly sensitive assay to measure this type of genomic instability [149,180,181].

In this assay, the two counter-selectable marker genes *URA3* and *CAN1* are inserted approximately 25 kb distal to the telomere of budding yeast chromosome V [182]. Since there are no essential genes located between *URA3*/*CAN1* and the telomere, a cell can lose this region of chromosome V during a GCR event and still proliferate. While mutations in either *URA3* or *CAN1* will occur with higher rates, it is unlikely that both genes acquire independent mutations at both loci. Thus, by selecting against *URA3* with the anti-metabolite 5'-fluoroorotic acid (FOA) and at the same time against *CAN1* with the non-proteinogenic, toxic amino acid L-canavanine, it is possible to detect rare GCR events that occur with a frequency of e.g. 3.5 $x10^{-10}$ events per cell per division in *wild-type* cells.

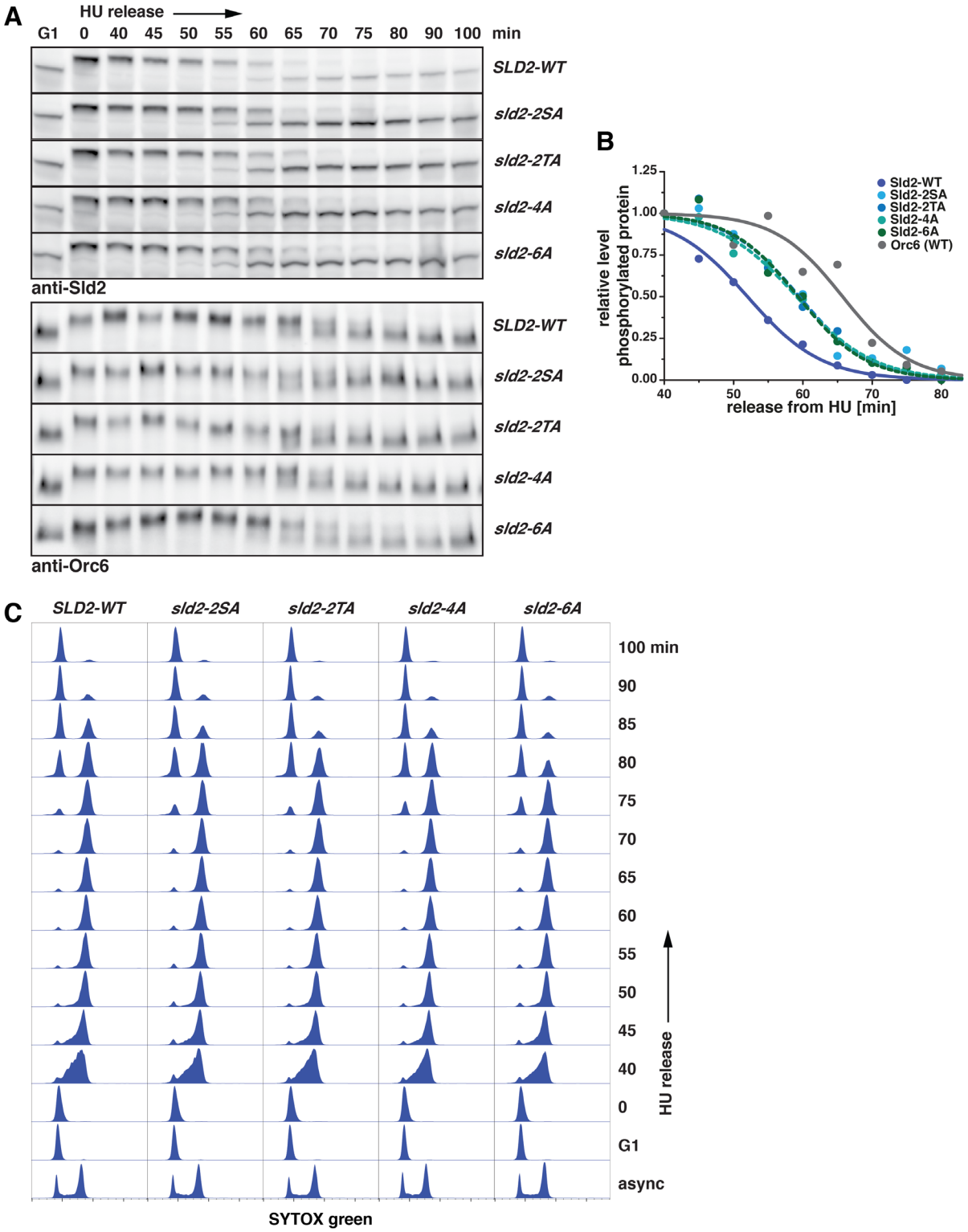

Figure 24 – Stable Sld2 degron mutants shorten the gap between firing inactivation and licensing re-activation after release from HU.
Cells expressing either *SLD2-WT* or *sld2*-degron mutants (*2SA* – CDK sites; *2TA* – Cdc5 sites; *4A* – CDK-/Cdc5-sites; *6A* – all six sites) as the only copy of *SLD2* were arrested in G1 phase using α-factor, released to 200 mM HU and subsequently released to fresh medium taking samples at the indicated timepoints. After 45 min of release from HU, α-factor was added back to prevent cells from entering a second cell cycle. (A) Western blots resolving phosphorylated isoforms of the firing factor Sld2 and the licensing factor Orc6. (B) Quantification of the phosphorylated Sld2 bands in (A). Data are normalized to the intensity of the phosphorylated band at the 0 min timepoint. (C) Replication analysis by flow cytometry measuring total DNA content with SYTOX green. Samples as in (A).

We utilized this GCR assay to address if stable *sld2* mutants affected genomic stability. As judged by our release experiments, origin firing and licensing are still readily separated during M phase in these cells and replication control should therefore be largely intact. However, the shorter gap between firing inactivation and licensing re-activation could increase the probability for co-occurring licensing and firing phases and ultimately lead to higher GCR rates.

In otherwise *wild-type* cells, we detected normal GCR rates of about 2 x 10^{-10} GCR events per cell per division and no differences between *SLD2* and stable *sld2* mutants (Figure 26 A). However, when we abrogated the DNA damage checkpoint (*sml1Δ mec1Δ* cells) and thus sensitized cells to genomic instability, we observed that the GCR rate was already elevated by two orders of magnitude in *SLD2 sml1Δ mec1Δ* cells and additionally increased to about two-fold of that in *sld2-6A sml1Δ mec1Δ* cells (Figure 26 B). Therefore, stable *sld2* mutants can induce genome instability even when all other mechanisms of DNA replication control are intact.

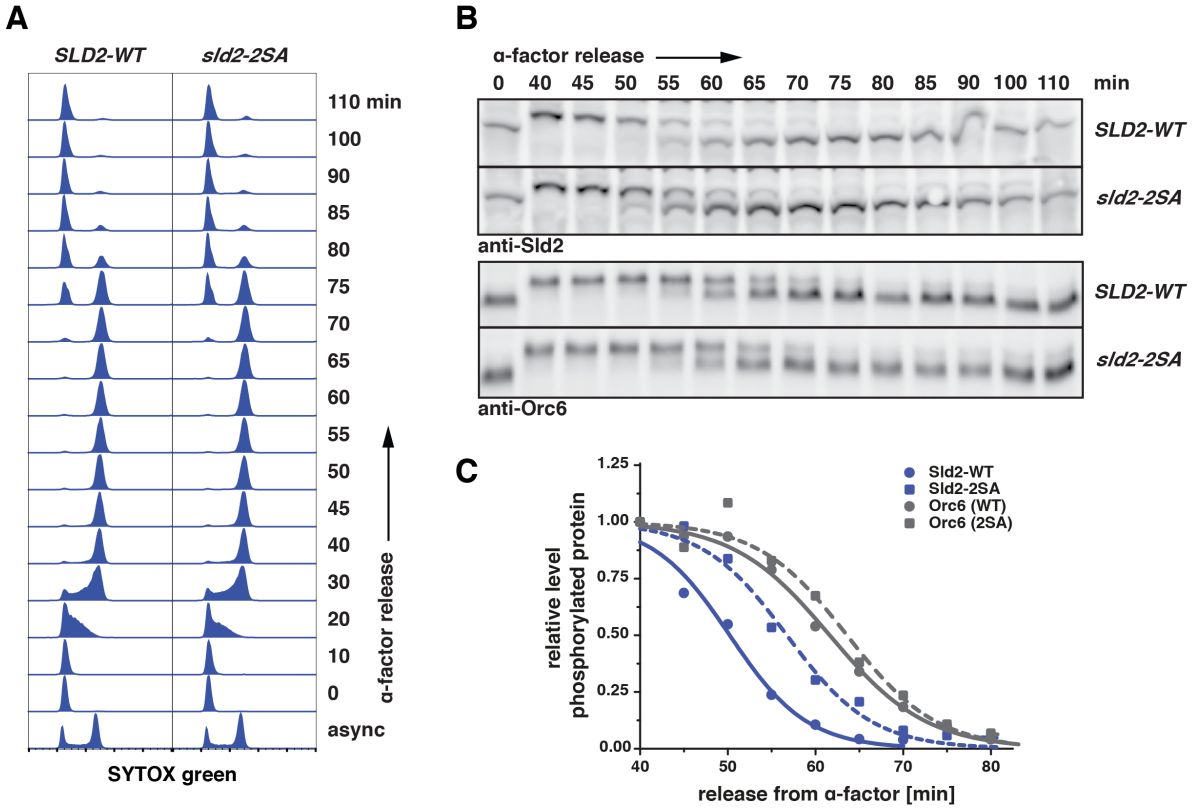

Figure 25 – Stable Sld2 degron mutants shorten the gap between firing inactivation and licensing re-activation after release from G1.
Cells expressing either *SLD2-WT* or *sld2-2SA* degron mutants (mutation of CDK sites) as the only copy of *SLD2* were arrested in G1 phase using α-factor and released to fresh medium taking samples at the indicated timepoints. After 45 min of release, α-factor was added back to prevent cells from entering a second cell cycle. (A) Cell cycle analysis by flow cytometry measuring total DNA content with SYTOX green. (B) Western blots resolving phosphorylated isoforms of firing factor Sld2 and licensing factor Orc6 at the indicated timepoints. Samples as in (A). (C) Quantification of the phosphorylated Sld2 bands in (B). Data are normalized to the intensity of the phosphorylated band at the 40 min timepoint.

We also addressed if stable *sld2* mutants would lead to further increased GCR rates in combination with deregulation of other DNA replication factors (Figure 27). First, we combined stable *sld2* mutants with a genetic fusion of *SLD3* and *DPB11* (*SLD3-DPB11ΔN-fusion*, *SD-fusion*), which bypasses the requirement for CDK phosphorylation of Sld3 for origin firing and thereby renders Sld2 the only critical target of CDK for triggering origin firing [31]. Under these conditions, we already observed highly elevated GCR rates with *SLD2 SD-fusion*, which increased further in combination with stable *sld2* mutants. Second, we assessed the influence of deregulated DDK activity in a strain with a stable *sld2* mutant by introducing a galactose-inducible copy of the regulatory DDK subunit *DBF4*. Here, we observed that the stable *sld2* mutant increased the GCR rate by about two-fold when combined with deregulated DDK. Third, we combined the stable *sld2* mutant with a partial deregulation of origin licensing by using the *cdc6ΔNT* allele, which lacks the CDK-regulated degron sequences in the N-terminus of Cdc6 [183]. Again, we could observe an increased GCR rate for stable *sld2* as compared to *SLD2* in combination with *cdc6ΔNT*.

Taken together, these results emphasize that many regulatory mechanisms synergize to control DNA replication during the cell cycle control. Cells can normally tolerate limited deregulation, e.g. stable *sld2* mutant or galactose-induced expression of *DBF4* alone, but show signs of increased genomic instability if several regulatory mechanisms are affected. Our stable *sld2* mutants manipulate DNA replication control more specifically than e.g. the constitutive *SD-fusion* and thus provide an experimental tool to precisely study the regulation of the transitions between replication phases.

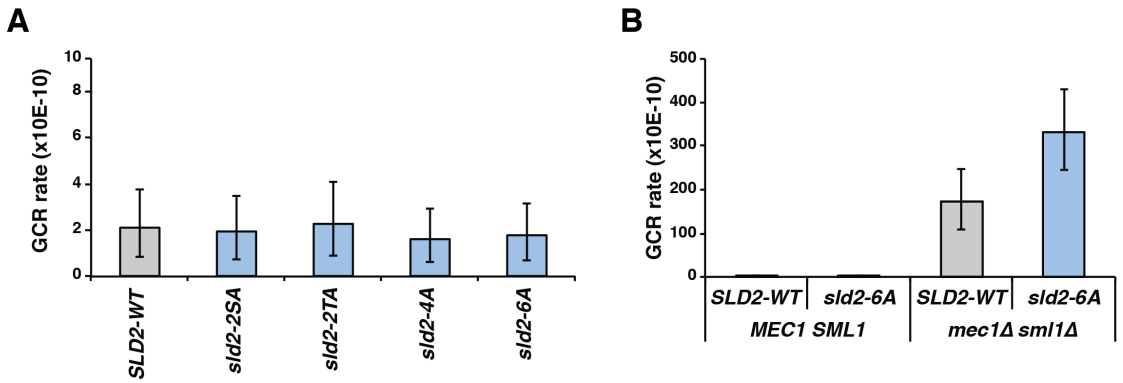

Figure 26 – Stable Sld2 increases GCR rates in DNA damage checkpoint-deficient cells.
Gross chromosomal rearrangements (GCR) rates were measured using a *CAN1::URA3* reporter on chromosome V. Fluctuation analysis with eight fluctuations per condition was used to calculate GCR rates per cell per division; error bars indicate a 95% confidence interval. (A) GCR rates of *wild-type* (gray) and stable *sld2* mutants (blue, *2SA* – CDK sites; *2TA* – Cdc5 sites; *4A* – CDK-/Cdc5-sites; *6A* – all six sites). (B) GCR rate of *wild-type* (gray) and stable *sld2-6A* mutant (blue) in the presence (*MEC1 SML1*) or absence (*mec1Δ sml1Δ*) of the DNA damage checkpoint. Note the different scale of the y-axis compared to (A).

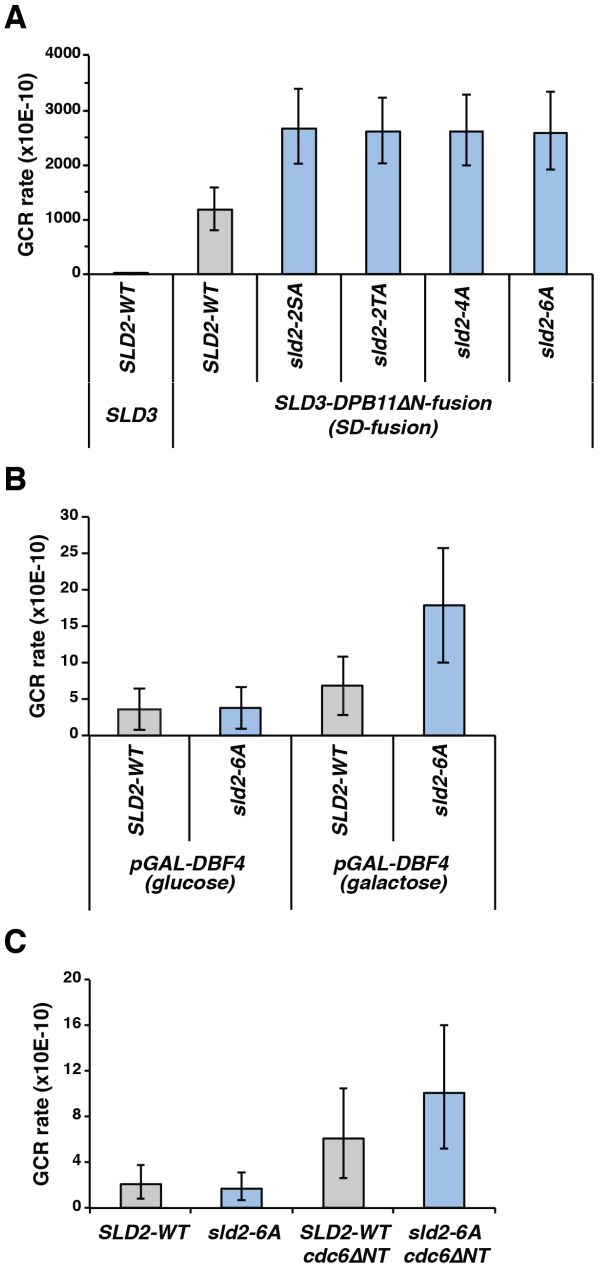

Figure 27 – Stable Sld2 increases GCR rates in combination with other mutants affecting replication control. Gross chromosomal rearrangements (GCR) rates were measured using a *CAN1::URA3* reporter on chromosome V. Fluctuation analysis with eight fluctuations per condition was used to calculate GCR rates per cell per division; error bars indicate a 95% confidence interval. Note different y-axis scales. (A) GCR rates of *wild-type* (gray) and stable *sld2* mutants (blue, *2SA* – CDK sites; *2TA* – Cdc5 sites; *4A* – CDK-/Cdc5-sites; *6A* – all six sites) in combination with the constitutively active *SLD3*-allele *SD-fusion* (*SLD3-DPB11ΔN-fusion*). (B) GCR rate in *wild-type* (gray) and stable *sld2-6A* mutant (blue) cells harboring a second, galactose-inducible copy of *DBF4*. This copy is repressed by the presence of glucose and is induced by the presence of galactose. (C) GCR rate of *wild-type* (gray) and stable *sld2-6A* mutant (blue) combined with the mutant licensing factor allele *cdc6ΔNT* that is refractory to CDK inhibition.

4. Phosphatases affect the length of the gap in M phase

Having established that stable *sld2* mutants shorten the gap between firing inactivation and licensing re-activation in M phase, we hypothesized that phosphatases most likely generate the remaining separation. Throughout eukaryotes, phosphatases of the Cdc14, PP1 and PP2A families regulate key events in M phase by dephosphorylating serine and threonine residues, particularly during mitotic exit [184,185]. We therefore focused on these three classes of phosphatases and investigated if interfering with their activity would affect the length of the gap.

4.1. Cdc14 targets replication factors redundantly with other phosphatases in M phase

In budding yeast, Cdc14 is the central phosphatase during late M phase [91,186]. This monomeric phosphatase broadly counteracts CDK phosphorylation [187,188] and is activated sequentially by the FEAR network (Fourteen Early Anaphase Release) and the MEN (Mitotic Exit Network). Earlier studies have already provided evidence that Cdc14 might dephosphorylate replication proteins such as Sld2 and Orc6 [93,94]. We therefore used a yeast strain carrying the temperature-sensitive *cdc14-3* allele to address if Cdc14 is responsible for generating the temporal separation between inactivation of firing factors and re-activation of licensing factors when CDK is inhibited in cells that are arrested in M phase (Figure 28). We performed the experiment as before (see Figure 6), but shifted the cells to 37 °C for one hour before adding the CDK inhibitor 1NM-PP1 and taking samples for analysis by western blot in short intervals. In *CDC14* control cells, hyper-phosphorylated Sld2 was lost already after one minute of treatment with the inhibitor. The band corresponding to hyper-phosphorylated Orc6 persisted for longer but was also strongly decreased after 10 min, indicating that dephosphorylation of Sld2 and Orc6 occur with different kinetics. In *cdc14-3* cells, however, we observed that hyper-phosphorylated Sld2 as well as hyper-phosphorylated Orc6 could be detected at later time points. While dephosphorylation of Sld2 was only delayed by a few minutes, Orc6 phosphorylation appeared to be only minorly affected. These data thus indicate that Cdc14 is indeed involved in regulating replication factors but at the same time demonstrate that there are also other phosphatases next to Cdc14, which reverse CDK-phosphorylation marks particularly on firing factors.

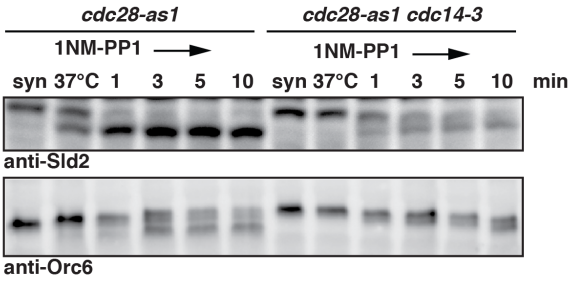

Figure 28 – The phosphatase Cdc14 dephosphorylates replication proteins in M phase.
Western blots resolving phosphorylated isoforms of Sld2 and Orc6. *Wild-type* cells and *cdc14-3* mutant cells were arrested in M phase, shifted to 37 °C for 1 h and treated with 1NM-PP1 to selectively inhibit the CDK-allele *cdc28-as1*. Samples were taken at the indicated timepoints after addition of 1NM-PP1.

4.2. PP1 targets both licensing and firing factors in M phase

To elucidate a possible role of PP1 in dephosphorylating replication factors in M phase, we decided to first test temperature-sensitive mutants of *GLC7* [189-191], which is the catalytic subunit of PP1 and associates with various targeting subunits to achieve substrate specificity. We therefore introduced temperature-sensitive *glc7-10* or *glc7-12* alleles into our *cdc28-as1* strains, arrested the cells in M phase using nocodazole and shifted them to 37 °C for two hours before adding the CDK inhibitor 1NM-PP1 (Figure 29). As previously, we observed in control cells that Sld2 and Sld3 were quickly dephosphorylated whereas Orc6 dephosphorylation occurred later and more slowly. In *glc7* mutants, Orc6 phosphorylation barely decreased during the time course. Furthermore, phosphorylated Sld3 withstood dephosphorylation for longer time in *glc7-12* but not in *glc7-10* cells, which is consistent with the finding that *glc7-12* retains less phosphatase activity at the restrictive temperature than *glc7-10* [192]. Unexpectedly, total levels of Sld2 decreased substantially in *glc7-10* as well as *glc7-12* cells but not in the control cells. Hence, we could not analyze Sld2 dephosphorylation kinetics in this experiment. As the strains used in this experiment only harbored *wild-type SLD2*, this decrease in response to Glc7 inactivation could hint at an accelerated degradation of Sld2. It is for example possible that Glc7 directly counteracts phosphorylation of the degron region of Sld2, particularly when considering the antagonism between PP1 and DDK. For this reason, this experiment should be repeated with a strain expressing one of the stable *sld2* alleles, which we have characterized before. Taken together, this experiment demonstrates that PP1 contributes to the regulation of replication proteins in M phase. Our data also indicate that Sld3 might be among the preferential targets of PP1 since a change in dephosphorylation kinetics could only be observed with the very tight temperature-sensitive allele *glc7-12* but not with the slightly less tight *glc7-10* allele.

Recently, the phosphatase PP1 in complex with its targeting subunit Rif1 has been implicated in the regulation of DNA replication at the transition from G1 to S phase [83-85] by counteracting DDK-phosphorylation of the Mcm2-7 complex and also affecting the phosphorylation state of Sld3 in G1-arrested cells [84]. We thus hypothesized that PP1-Rif1 might also target replication factors in M phase. Since the rapid degradation of hyper-phosphorylated Sld2 potentially concurs with its dephosphorylation, we decided to conduct our experiments in a genetic background harboring the stable *sld2-6A* allele as the only copy of *SLD2* to facilitate our studies on potential phosphatases. We deleted *RIF1* in a *cdc28-as1* strain and performed a CDK inhibition experiment in cells that were arrested in M phase (Figure 30). In control cells, hyper-phosphorylated Sld2 and Sld3 were dephosphorylated quickly and could not be detected after 10 min of treatment with the CDK inhibitor 1NM-PP1. Dephosphorylation of Orc6, on the other hand, only started 10-15 min after adding the inhibitor and proceeded relatively slowly. Deletion of *RIF1* did not alter the dephosphorylation kinetics in M phase. Sld2 and Sld3 were still dephosphorylated quickly within

the first 10 min of the experiment, whereas Orc6 was slowly dephosphorylated only later. To scrutinize the role of PP1-Rif1 in regulating the phosphorylation state of Sld3, we also monitored phosphorylation of Sld2, Sld3 and Orc6 through a single cell cycle from G1 to the next G1 phase in *wild-type* and *rif1Δ* cells (Figure 31). In this experiment, we observed that the M phase dephosphorylation kinetics of all three proteins remained unchanged independent of the presence of *RIF1*. However, *rif1Δ* cells accumulated a semi-phosphorylated Sld3 isoform when they stayed arrested in G1 phase. Therefore, Rif1-targeting of PP1 seems to be dispensable for the proper regulation of replication factors in M phase and appears to affect phosphorylation of Sld3 only in G1 phase. We thus conclude that a currently elusive targeting subunit directs PP1 activity towards replication factors in M phase.

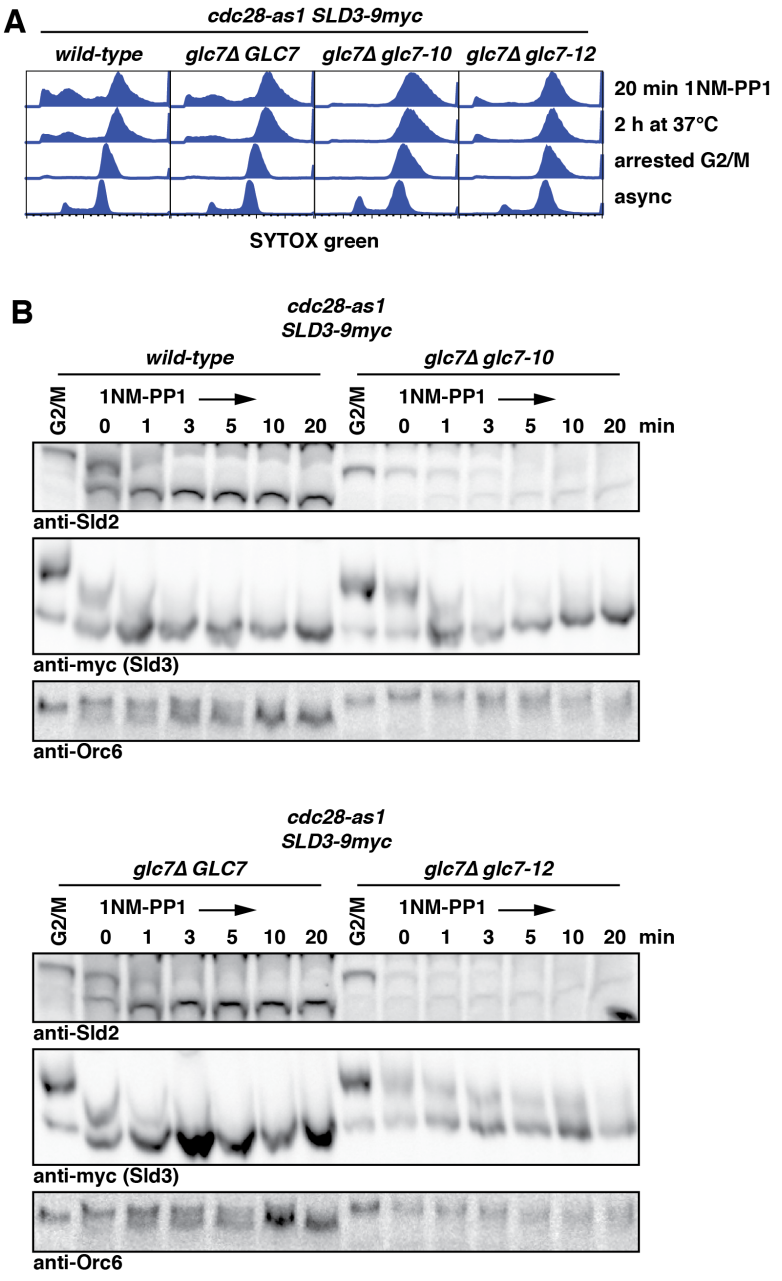

Figure 29 – The phosphatase PP1 regulates replication proteins in M phase.
(A) Cell cycle phase analysis by flow cytometry measuring total DNA content with SYTOX green. Cells harboring the catalytic PP1 subunit as either *wild-type GLC7* or temperature-sensitive *glc7-10* or *glc7-12* alleles were arrested in M phase, shifted to 37 °C for 2 h and then treated with 1NM-PP1, which selectively inhibits the CDK-allele *cdc28-as1*. (B) Western blots resolving phosphorylated isoforms of the firing factors Sld2 and Sld3 as well as licensing factor Orc6. Samples from experiment in (A), taken at the indicated timepoints after 1NM-PP1 addition.

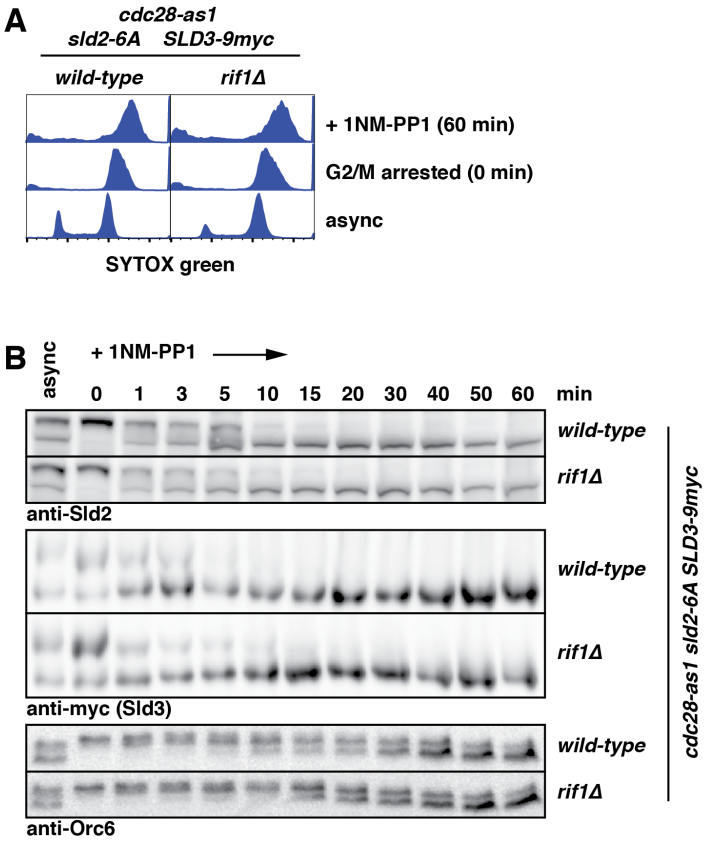

Figure 30 – Regulation of replication proteins by PP1 does not involve its targeting subunit Rif1.
(A) Cell cycle phase analysis by flow cytometry measuring total DNA content with SYTOX green. *Wild-type* and *rif1Δ* cells were arrested in M phase and then treated with 1NM-PP1, which selectively inhibits the CDK-allele *cdc28-as1*. Samples were taken at the indicated timepoints. (B) Western blots resolving phosphorylated isoforms of the firing factors Sld2 and Sld3 as well as licensing factor Orc6. Samples from same experiment as in (A).

4.3. PP2A-Cdc55 regulates the phosphorylation state of Orc6

Finally, we also investigated how manipulation of PP2A activity affects the dephosphorylation kinetics of replication factors in M phase. The phosphatase PP2A is a heterotrimeric complex consisting of the essential A-type regulatory subunit Tpd3, one of the two B-type regulatory subunits Cdc55 or Rts1, and one of the two catalytic subunits Pph21 or Pph22. The composition of the complex, particularly the B-type regulatory subunit, determines the subcellular localization and the substrate specificity [184,185]. We first focused on these regulatory subunits and asked if they are required to quickly dephosphorylate firing factors in mitosis. Unfortunately, we were not able to generate a *cdc28-as1 rts1Δ* strain, which might be owed to the about 20% reduced kinase activity of the *cdc28-as1* allele [168] that could result in synthetic lethality when combined with *rts1Δ*. Such a negative genetic interaction has been reported previously for *rts1Δ* together with other mutant *cdc28* alleles [193]. Nonetheless, we were able to test the effect of *CDC55* deletion in a CDK inhibition experiment in M phase (Figure 32). In the *CDC55* cells, we again observed quick dephosphorylation of Sld2 and slow dephosphorylation of Orc6 as before. In *cdc55Δ* cells, these dephosphorylation events occurred with very similar or even accelerated kinetics, which might be due to a premature release of Cdc14 [194-196]. Ideally, the *cdc55Δ* mutant should be studied in a *cdc14-3* background to exclude these effects of Cdc14, but we were not able to generate such a yeast strain.

To circumvent these technical difficulties, we decided to study *cdc55Δ* and *rts1Δ* mutants in a release experiment. We arrested cells in G1 phase and released them to the next G1 phase while taking samples for western blot analysis (Figure 33). Considering the slight delay in cell cycle progression that is caused by *cdc55Δ* and by *rts1Δ*, the dephosphorylation of Sld2 occurred with a very similar timing in all strains. Dephosphorylation of Orc6 was also similar in control cells and *rts1Δ* cells. We however observed that phosphorylated Orc6 persisted in *cdc55Δ* cells. Since these cells were not arrested in M phase, Cdc14 (even though presumably released prematurely) was only released from the nucleolus for a relatively short period of time. Therefore, in contrast to the previous CDK inhibition experiment, Orc6 was probably not targeted efficiently by Cdc14 and could retain its phosphorylation when cells entered G1 phase. These data thus suggest that PP2A-Cdc55 contributes to the regulation of Orc6. It remains to be determined if and how other licensing factors are affected.

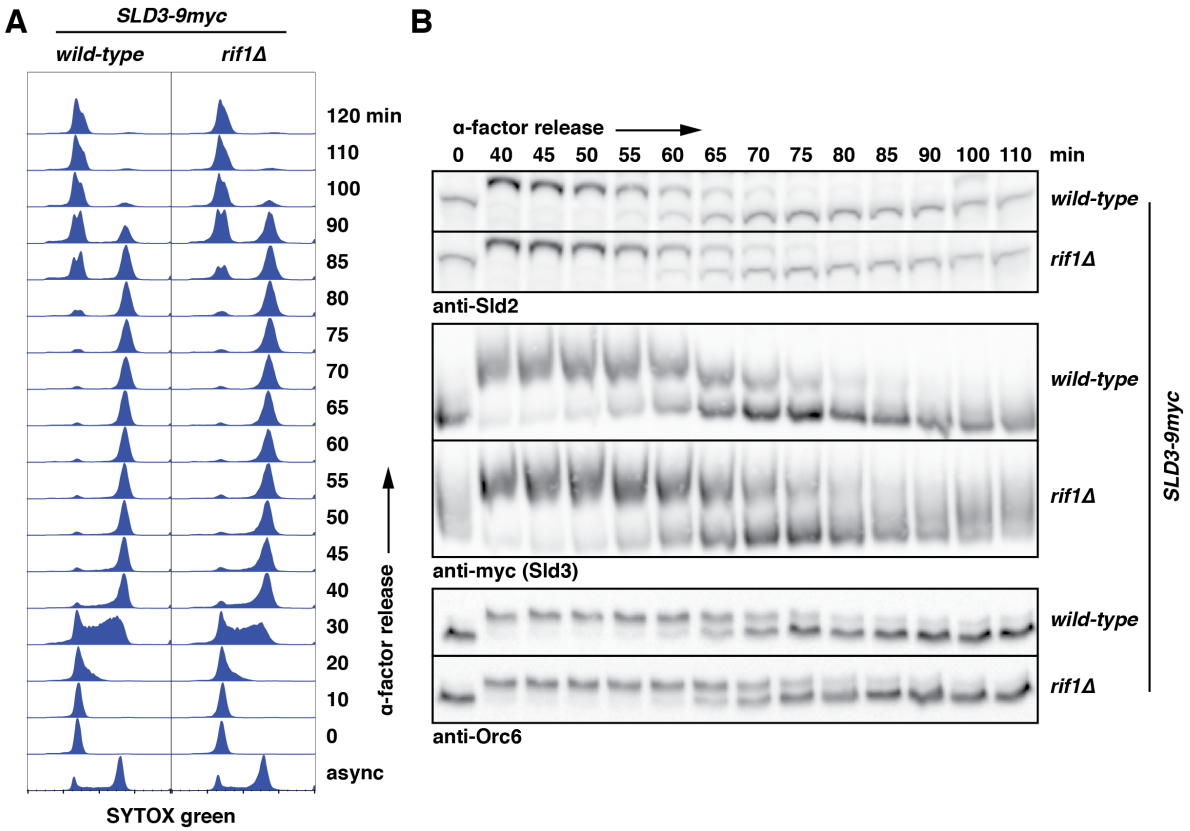

Figure 31 – PP1-Rif1 regulates firing factor Sld3 rather in G1 phase.
(A) Cell cycle analysis by flow cytometry measuring total DNA content with SYTOX green. *Wild-type* and *rif1Δ* cells were arrested in G1 phase using α-factor and then released to fresh medium. Samples were taken at the indicated timepoints. To prevent cells from entering a second cell cycle, α-factor was added back 45 min after the release. (B) Western blots resolving phosphorylated isoforms of the firing factors Sld2 and Sld3 as well as licensing factor Orc6. Samples from same experiment as in (A).

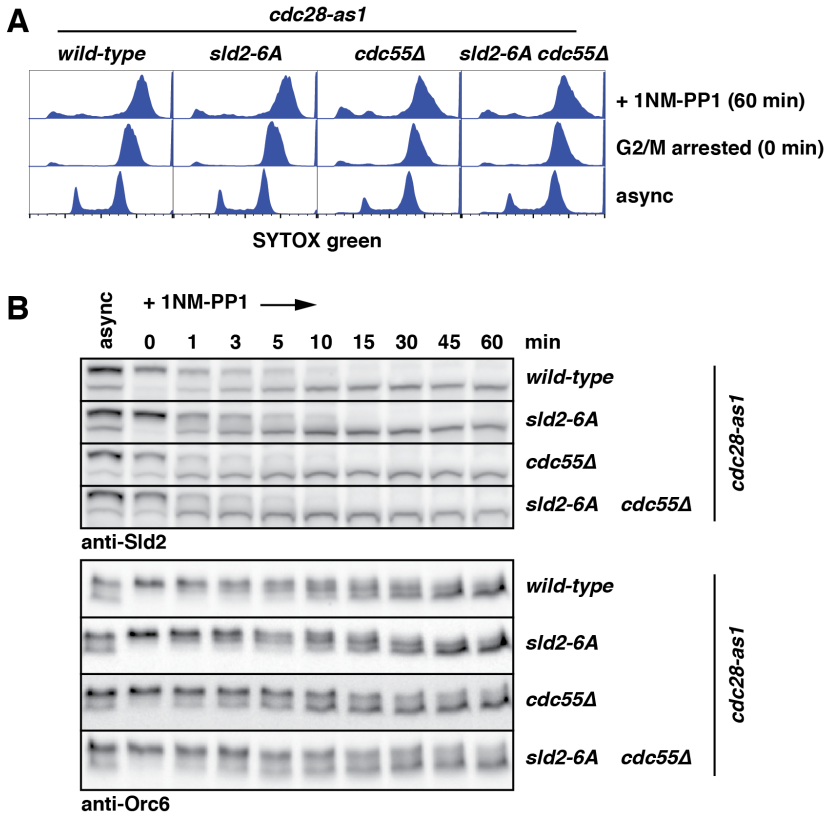

Figure 32 – The phosphatase PP2A-Cdc55 does not dephosphorylate firing factor Sld2 in M phase.
(A) Cell cycle phase analysis by flow cytometry measuring total DNA content with SYTOX green. *Wild-type* and *cdc55Δ* cells either harboring *SLD2* or stable *sld2-6A* were arrested in M phase and then treated with 1NM-PP1, which selectively inhibits the CDK-allele *cdc28-as1*. Samples were taken at the indicated timepoints after addition of 1NM-PP1. (B) Western blots resolving phosphorylated isoforms of the firing factor Sld2 as well as licensing factor Orc6. Samples from same experiment as in (A).

In summary, our study of phosphatases has revealed additional layers of complexity in the regulation of replication factors in M phase. Inactivation of the central M phase phosphatase Cdc14 only had minor effects on the dephosphorylation of replication factors thus indicating that other effective phosphatases are involved and also hinting at functional overlap. On the one hand, Cells lacking the regulatory B-type subunit Cdc55 of PP2A had defects in dephosphorylating Orc6 whereas Sld2 was not impaired, thus implicating a specific role for PP2A-Cdc55 in regulating Orc6 phosphorylation. Importantly, our experiments identify PP1 as a very good candidate for a phosphatase that acts more broadly. Reduced PP1 activity led to slower dephosphorylation of Sld3 and Orc6 and also affected the regulation of Sld2. As PP1 is predominantly regulated via its association with targeting subunits, it will be most instructive to identify the subunit that promotes dephosphorylation of replication factors in mitosis. However, firing factors are still more efficiently dephosphorylated than licensing factors in PP1 mutants. To this end, the redundancy and synergy between phosphatases should also be addressed and it needs to be determined how the preferential dephosphorylation of firing factors is achieved. Our data argue against a model were one specific phosphatase targets them preferentially but rather suggest that multiple phosphatases accomplish this task together. It is remarkable that so many different regulatory mechanisms are in place to ensure the correct timing of inactivation and activation of replication factors during M phase and this complexity highlights how crucial it is for eukaryotic cells to robustly control DNA replication.

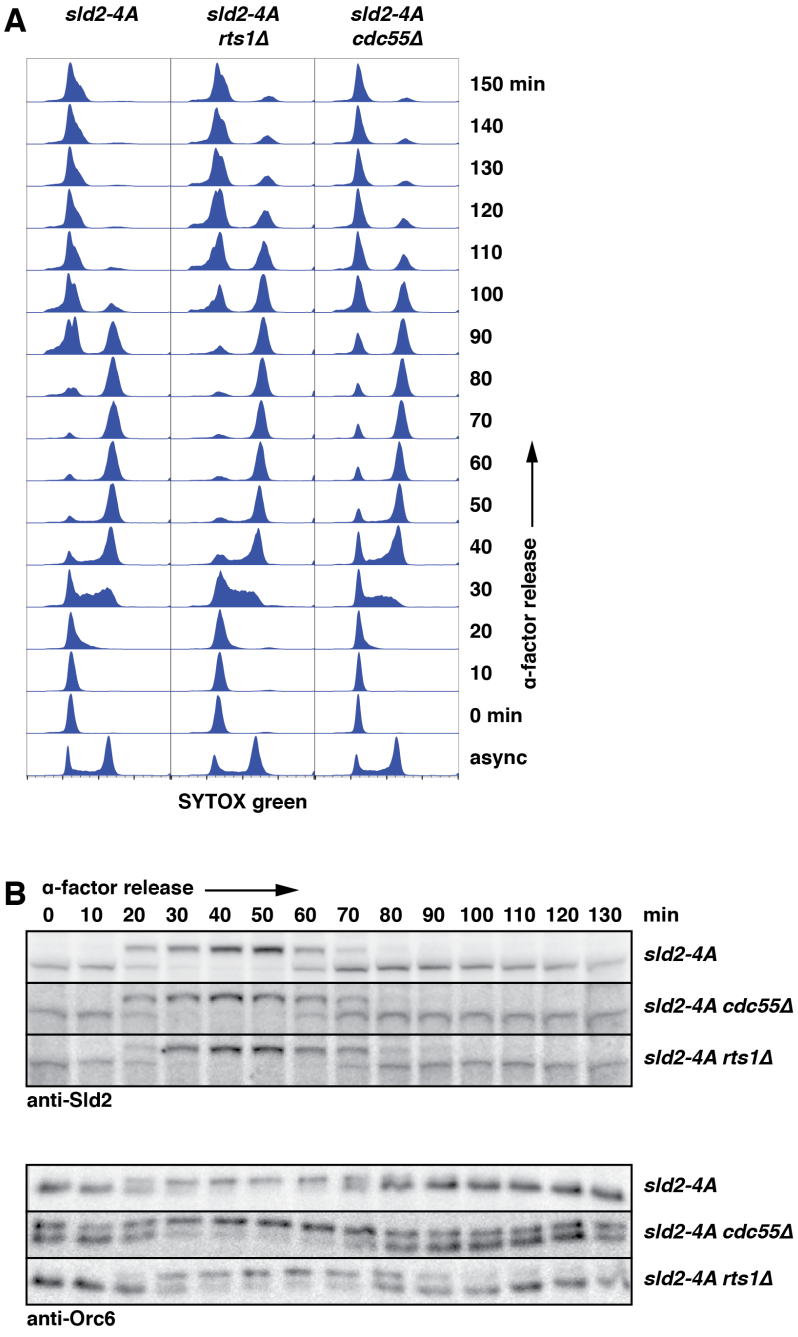

Figure 33 – The phosphatase PP2A-Cdc55 mediates dephosphorylation of Orc6 but not Sld2.
(A) Cell cycle analysis by flow cytometry measuring total DNA content with SYTOX green. Cells expressing *sld2-4A* and lacking the PP2A regulatory subunits *CDC55* or *RTS1* were arrested in G1 phase using α-factor and then released to fresh medium. After 50 min of release, α-factor was added back to arrest the cells in the next G1 phase. Samples were taken at the indicated timepoints after release. (B) Western blots resolving phosphorylated isoforms of firing factor Sld2 and licensing factor Orc6. Samples as in (A).

5. Detection and consequences of deregulated origin firing

By just considering the sheer number of molecular mechanisms that ensure the correct regulation of DNA replication throughout the cell cycle, it becomes evident that origin licensing and origin firing should never occur at the same time within a cell cycle. Most of our current knowledge about deregulated DNA replication has been obtained from experimental systems that manipulate the regulation of licensing factors [63,139,140]. In these systems, replication origins could be re-licensed during S, G2 or M phase and thus re-used for a second round of replication. In addition, it cannot be ensured that all parts of the genome are copied precisely once within one cell cycle. It has been shown that such over-replication leads to the generation of DNA damage and cells with over-replicated DNA will be arrested by the DNA damage checkpoint [142]. How this damage is generated is still a matter of active research.

On the other hand, over-replication can also be induced by premature, uncontrolled origin firing in G1 phase when cells still have the capacity to license origins. From a cellular perspective this scenario appears to be even more interesting as many oncogenes act by deregulating replication at the border between G1 and S phase [162-166]. However, there have only been very few attempts to study how cells respond to over-replication in G1 mainly owing to the lack of experimental systems to induce it. So far, *S. cerevisiae* is the only model organisms in which the essential sets of targets for CDK and DDK to trigger DNA replication in G1 phase have been identified [31,32,79,197] and thus this organism gives us the unique opportunity to study premature origin firing and over-replication in G1 phase.

5.1. Establishing an experimental setup to induce and measure origin firing in G1

During our study of over-replication control we realized that the cellular consequences of and responses to over-replication at the G1/S transition were largely unknown. We thus set out to investigate the cellular consequences and responses by establishing an experimental system that allowed us to (i) conditionally induce over-replication and (ii) label newly synthesized DNA with the synthetic thymidine analog EdU.

Previous studies have identified Sld2 and Sld3 as the critical targets of CDK for triggering origin firing [30-32]. More importantly, these studies also described ways to uncouple Sld2 and Sld3 from CDK regulation. Even though there are eleven sites for CDK phosphorylation on Sld2, threonine 84 is the critical target of CDK [72]. Phosphorylation of this residue facilitates Sld2's interaction with Dpb11 and is key for Sld2 to fulfill its essential function to drive origin firing. This phosphorylation mark can be mimicked by mutating threonine 84 to aspartic acid (*sld2-T84D*), which renders Sld2 constitutively active throughout the cell cycle. An even more active allele of *SLD2* can be generated by mutating all eleven CDK sites to aspartic acid (*sld2-11D*) [72].

CDK phosphorylation of three residues in the C-terminus of Sld3 facilitates the interaction of Sld3 with Dpb11 [31,32]. However, mutating these residues to phosphorylation-mimicking, acidic amino acids has not been a successful approach to bypass the requirement for CDK phosphorylation of Sld3 to induce origin firing. Yet, there are three alternative strategies available to abolish the regulation of Sld3 by CDK: The need for CDK phosphorylation of Sld3 can be bypassed by (i) a covalent fusion between Sld3 and Dpb11 (called *SD-fusion*, as mentioned above), (ii) the *jet1-1* mutation in the Sld3-interactor Cdc45, which is thought to foster the interaction between Sld3 and Dpb11, or (iii) high levels of Dpb11 and Sld2, which compensate for a lack of Sld3 phosphorylation[31,32].

Since our study focused on the effects of deregulation, we wanted to introduce as few mutations as possible to avoid artefacts that could come along with mutated proteins. We thus decided to use galactose-inducible alleles of *DPB11* and *sld2-T84D* to bypass the CDK-mediated control of origin firing and facilitate origin firing already in the absence of CDK activity in G1. To further increase the efficiency of origin firing, we also constructed a yeast strain that uncoupled DDK from its cell cycle regulation via a galactose-inducible allele of *DBF4* and thereby bypasses the DDK-mediated control of origin firing (Figure 34).

The incorporation of thymidine analogs such as e.g. bromo-deoxyuridine (BrdU) or ethinyl-deoxyuridine (EdU) is routinely used to label newly synthesized DNA when studying cells from higher eukaryotes [198]. These cells rely on specific metabolic pathways, the nucleotide salvage pathways, to convert free nucleobases from the growth medium into nucleosides. The enzymes of these pathways are not limited to the natural occurring nucleobases but also accept the above mentioned, synthetic nucleobases and thus enable their incorporation into DNA. Later on, such synthetic nucleosides can be detected by specific antibodies or, as in the case of EdU, serve as a versatile platform for attaching e.g. fluorophores or affinity tags via a click chemistry reaction involving a Cu(I)-catalyzed azide-alkyne cycloaddition. In contrast to many higher eukaryotes, budding yeast cells lack the nucleotide salvage pathway for pyrimidines and thus require genetic modifications to readily incorporate synthetic pyrimidine-nucleosides such as EdU. Previous studies found that expression of the human nucleoside transporter ENT1 together with expression of thymidine kinase (TK) from *Herpes simplex* virus enable yeast cells to effectively utilize BrdU or EdU supplied in their growth medium [199-205]. The levels of TK seem to be limiting, since a yeast strain harboring multiple copies of the thymidine kinase gene can utilize synthetic nucleosides more efficiently (i.e. at lower concentrations in the medium) than a yeast strain with just one copy of it [205,206].

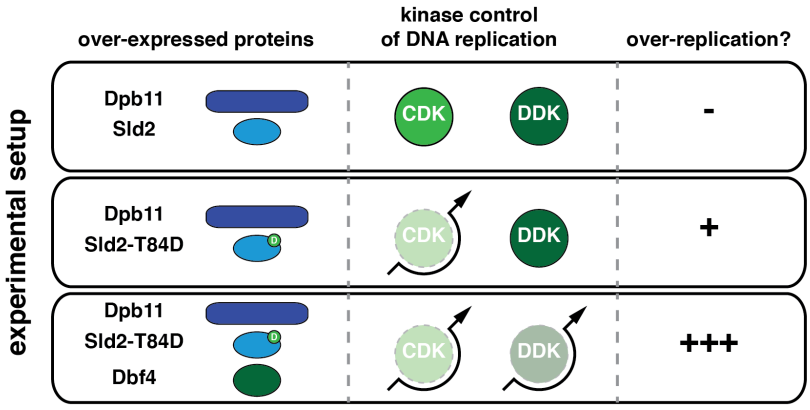

Figure 34 – Systems used to induce origin firing in G1 phase.
Summary of the genetic system to bypass CDK- and DDK-regulation of origin firing. Over-expression is achieved by putting the genes of interest under the control of a galactose-inducible *GAL1-10* promoter. Induction of origin firing in G1 can give rise to over-replication, particularly when both CDK- and DDK-dependent regulation are bypassed (see Figure 35).

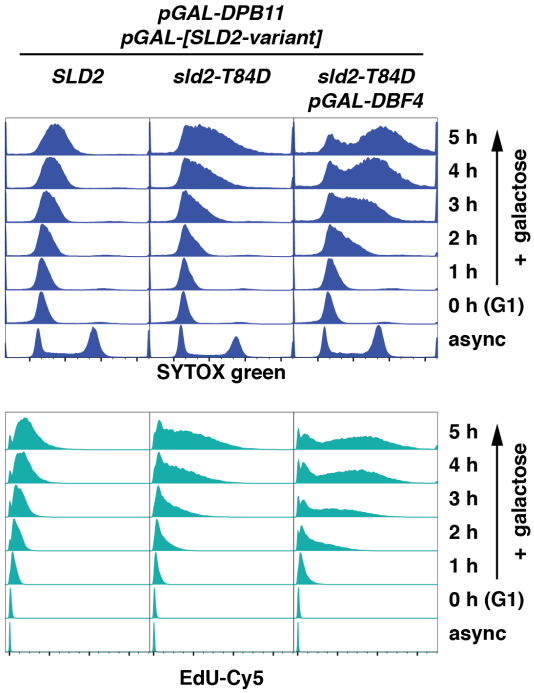

Figure 35 – EdU incorporation is a sensitive measure for DNA synthesis in G1 phase.
Analysis of DNA synthesis triggered by over-replication setups in G1 phase by flow cytometry, either measuring total DNA content with SYTOX green or labeling newly synthesized DNA with EdU and coupling the fluorescent dye Cy5 to EdU. Cells lacking the α-factor-degrading protease *BAR1* were kept arrested in G1 phase and CDK and/or DDK regulation of origin firing were bypassed by overexpression of the indicated firing factors in the presence of EdU while cells were kept arrested. Samples for flow cytometry were taken at the indicated timepoints.

To validate this system, we arrested cells in G1 and added EdU together with galactose to bypass CDK-/DDK-mediated control of origin firing as outlined above (Figure 35). At different times after addition of galactose, we took samples to measure the DNA content of these cells by flow cytometry using the DNA-intercalating dye SYTOX green. A slight increase in DNA content was detectable in wild-type cells and control cells over-expressing *DPB11* and *SLD2*, where replication control by CDK and DDK was intact. This increase can be attributed to ongoing replication of mitochondrial DNA which is not cell cycle-regulated. More interestingly, we observed a stronger increase in DNA content, when we bypassed CDK-mediated control of origin firing. Consistent with the literature, additional bypass of DDK-mediated control led to an even further increase in DNA content.

In order to confirm that the increase in DNA content was due to synthesis of new DNA, we applied click chemistry to label and measure the EdU that was incorporated into newly synthesized DNA in different ways [198]. We attached the fluorescent dye Cy5 to EdU and measured the Cy5 signal by flow cytometry. Intriguingly, the intensity of the Cy5 signal correlated well with the DNA content measurement. The low background, as judged by the Cy5 signal in the control cells, allowed us to readily quantify DNA synthesis under the different experimental conditions. We performed a control experiment (data not shown) to measure the amount of EdU incorporated during a normal S phase and used these data to put amounts of DNA synthesized in G1 into perspective: Bypassing CDK-mediated control of origin firing allows for replication of 0.60 S phase equivalents of DNA; bypassing of CDK- and DDK-mediated control together increases this to 1.15 S phase equivalents of DNA after 5 hours of origin firing in G1 phase.

Next, we attached biotin to EdU and utilized it as an affinity tag to purify the newly synthesized DNA for analysis by next-generation sequencing (Figure 36 A). We aligned the obtained reads to the budding yeast genome (version sacCer3) and observed that they mainly mapped to mitochondrial DNA in control cells, which corroborates our initial notion that the minor increase in DNA content is due to cell cycle-independent mitochondrial DNA replication. In contrast, reads mapped to the yeast chromosomes when CDK- and/or DDK-mediated regulation of origin firing was bypassed. While the reads where relatively evenly distributed over all chromosomes when we bypassed both CDK- and DDK-mediated regulation of origin firing, we observed that some regions of the genome did not replicate efficiently when just CDK-mediated regulation was bypassed. Under this condition, regions close to the centromeres seemed to fire more efficiently and signals from telomeres were absent on several chromosomes. These data are in line with previous studies which showed that Dbf4 is enriched around centromeres and that DDK activity controls when a specific origin of replication will fire during S phase [41,42]. Unfortunately, owing to the long induction time and the inherent stochasticity of origin firing, we were not able to determine which specific origins were activated in this experiment.

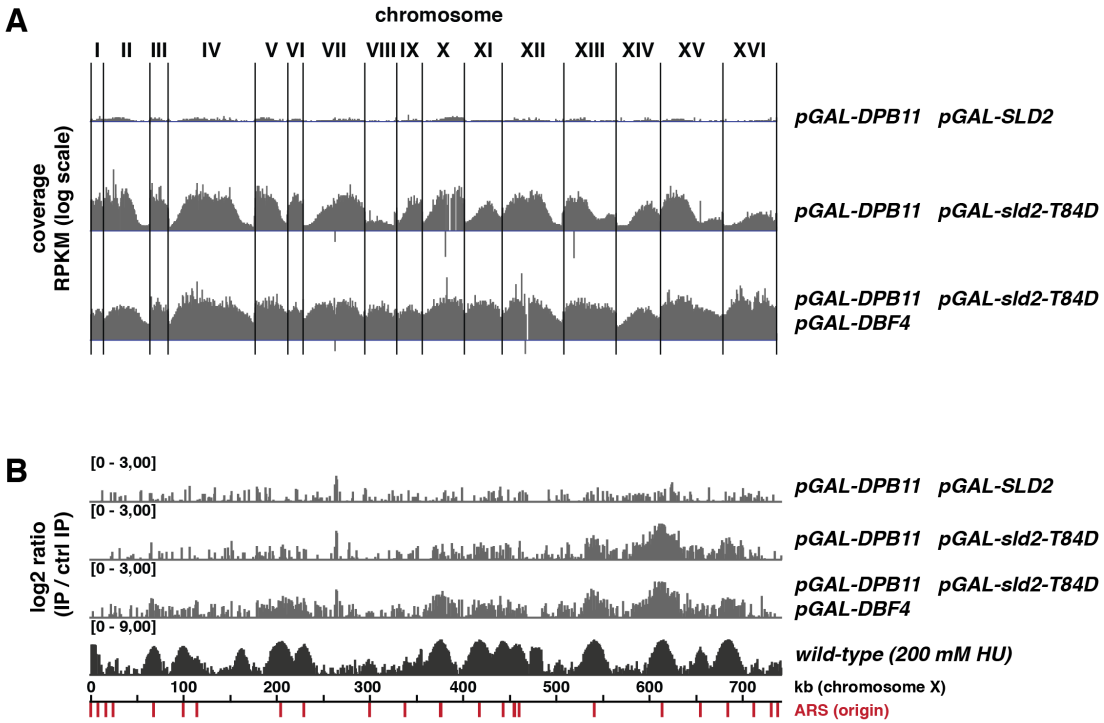

Figure 36 – Origin firing in G1 affects all chromosomes and uses canonical origins of replication.
(A) Analysis of immunoprecipitated DNA labeled with EdU. Cells were arrested in G1 and origin firing was induced by adding galactose for 3 h without releasing the cells from the arrest. The nucleoside analog EdU was added together with galactose to label newly synthesized DNA. A biotin label was attached to EdU-labeled DNA and used for immunoprecipitation and subsequent analysis by next-generation sequencing. Reads were mapped to the budding yeast genome and adjusted for sequencing depth to calculate the coverage of the different chromosomes. (B) Analysis of immunoprecipitated DNA labeled with EdU. Experiment as in (A) with induction in the presence of 200 mM hydroxyurea (HU) to block replication elongation. In addition, a sample from cells arrested in early S phase with 200 mM HU for 90 min is also shown (in black, different scaling). Data were first adjusted for sequencing depth and afterwards normalized to a wild-type control, which did not over-express any replication proteins. Chromosome X is shown as a representative of all chromosomes in the data set.

To scrutinize these data and test which replication origins were responsible for replication in G1, we adjusted the experiment and blocked replication elongation by adding the replication elongation inhibitor hydroxyurea (HU) together with EdU and galactose (Figure 36 B). Under these experimental conditions, origin firing is still possible but replication forks are confined to regions surrounding the origin due to a lack of dNTPs. We included a sample from cells arrested in early S phase by HU treatment as a control, which allowed us to visualize known replication origins. As seen in the previous experiment, reads from cells with normal regulation of origin firing mapped almost exclusively to mitochondrial DNA. When CDK- and/or DDK-mediated regulation was bypassed, we observed that only around 10% of the total reads aligned to the yeast chromosomes. These data indicate that nuclear and mitochondrial DNA replication compete for reads with a strong bias for mitochondria under our experimental conditions. Nonetheless, the aligned reads piled up symmetrically around well-defined origins of replication which is a characteristic of canonical bi-directional replication initiation. Furthermore, most of the detected origins were also fired in cells arrested in early S phase by HU. Thus, our experimental system allows us to induce and quantitatively measure origin-dependent replication in G1 phase.

Third, to further characterize this system and identify potential differences to replication in S phase, we affinity-purified replisomes that were induced in G1 and compared them to replisomes in S phase using mass spectrometry (Figure 37 A). We purified replisomes via GFP-tagged Psf2, which is a component of the GINS complex and therefore constitutes an integral part of the Cdc45-Mcm2-6-GINS (CMG) replicative helicase. Indeed, we purified all ten other components of the CMG helicase (green) together with Psf2. In addition, we detected DNA polymerase α/primase (cyan), the leading strand DNA polymerase ε (blue), and replisome-associated factors (magenta) such as the fork protection complex Mrc1-Tof1-Csm3, topoisomerase Top1, single-stranded DNA-binding protein RPA, as well as Mcm10, Ctf4 and Dia2. Replisomes purified from cells in early S phase contained the same set of proteins, which has previously also been named as replisome progression complexes (RPC) [207]. These data demonstrate that replisomes in G1 phase are highly similar to those in S phase.

We compared replisomes from G1 and S phase directly to resolve cell cycle-related differences in replisome composition (Figure 37 B). While there was no difference detectable for Psf2 and associated members of the GINS complex, the S phase sample was slightly enriched in other RPC components suggesting a higher number of replisomes active in this condition. Interestingly, we also found a cell cycle-specific replisome interactor: The cohesin complex co-purified only with replisomes in S phase but not in G1 phase. Normally, establishment of cohesion between sister chromatids is tightly linked to DNA replication and S phase to ensure the proper alignment and segregation of sister chromatids on the mitotic spindle [208,209]. These data indicate that cohesion establishment might be impaired in cells that undergo premature origin firing in G1 and therefore it could be one source of genomic instability.

In summary, we have established and characterized an experimental system that allows us to effectively induce origin firing in G1 phase, to efficiently label the newly synthesized DNA, and to sensitively measure it.

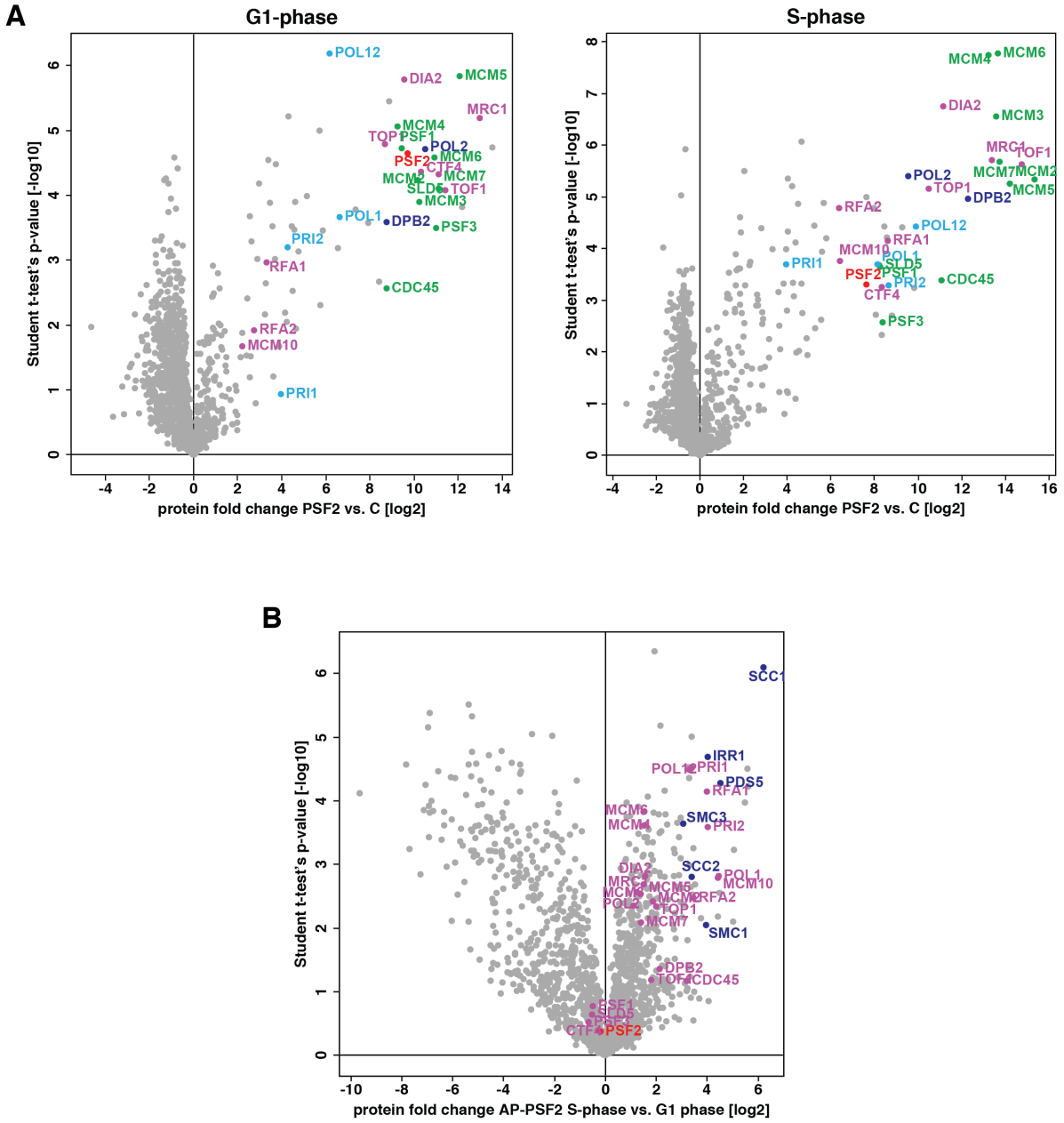

Figure 37 – Replisomes in G1 are highly similar to replisomes in S phase but lack cohesin.
(A) Analysis of replisome composition by quantitative mass spectrometry. Replisomes were isolated from cells in G1 phase (3 h induction of origin firing in G1-arrest) or S phase (90 min release from G1 to 200 mM hydroxyurea) by affinity-purifying Psf2-GFP (red). Components of the CMG helicase (green), DNA polymerase α (light blue), DNA polymerase ε (dark blue) and replisome-associated factors (magenta) are highlighted. Three independent biological replicates were measured for strains expressing Psf2-GFP or untagged Psf2 to allow for label-free quantification. (B) Data sets as in (A), comparing affinity-purified replisomes in G1 phase and S phase. Replisome components (magenta) as detected in (A) and cohesin complex (dark blue) are highlighted.

5.2. Over-replication is not detected by the DNA damage checkpoint during G1 phase

Next, we were interested to determine the cellular consequences of origin firing in G1. Our system allowed us to already induce over-replication under these conditions, which has been associated with the generation of DNA damage and the activation of the DNA damage checkpoint in response to that. The DNA damage checkpoint is a signaling pathway that is mediated by protein phosphorylation. One of its key components is the kinase Rad53, which is activated by hyper-phosphorylation and can subsequently phosphorylate many target proteins to enforce the checkpoint response. The activity of the DNA damage checkpoint as judged by the phosphorylation state of Rad53 can be viewed as a read-out for the general state of the cells. In addition, we also decided to look at the DNA damage-induced phosphorylation of H2A – so-called γH2A – as a direct and sensitive read-out for local DNA damage.

To address if origin firing in G1 generates DNA damage and triggers the DNA damage checkpoint, we analyzed samples from the experiment shown in Figure 35 in western blots for Rad53 and γH2A (Figure 38). Unexpectedly, we did not detect hyper-phosphorylated Rad53 even after five hours of origin firing in G1 by bypassing both CDK- and DDK-dependent control mechanisms even though these cells had over-replicated their DNA at this point. On the other hand, we detected a weak signal for γH2A under the same conditions. Taken together, this experiment suggests that only limited DNA damage was generated when DNA was over-replicated in G1. However, this DNA damage did not activate the DNA damage checkpoint and therefore cells should be able to enter the cell cycle.

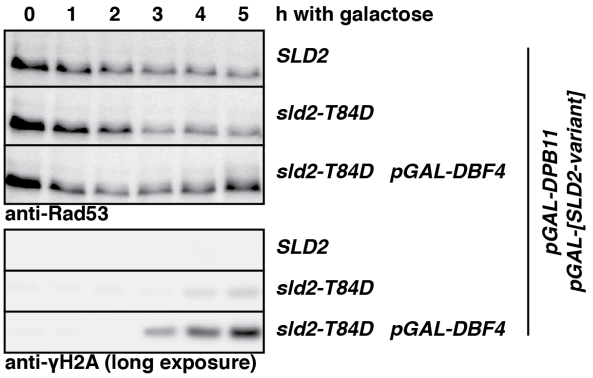

Figure 38 – Origin firing in G1 generates limited amounts of DNA damage but does not activate the DNA damage checkpoint.
Western blots resolving phosphorylated Rad53 and detecting γH2A as markers of DNA damage checkpoint signaling. Samples from experiment in Figure 35. Origin firing was induced in G1-arrested cells by adding galactose.

To corroborate these findings, we aimed to establish conditions to further boost replication in G1 phase. First, we reasoned that Dbf4 levels might be limiting in our conditions since Dbf4 is actively degraded in G1 phase by the APC [78,210-212]. We thus introduced mutations in the destruction boxes of *DBF4* to achieve expression at higher levels (Figure 39). Indeed, these mutations allowed us to express twice as much Dbf4 in G1 phase as with the *wild-type* allele, but this only resulted in a minor increase in DNA synthesis. Most prominently, the DNA content of the cells increased more quickly at early timepoints. This difference, however, was balanced out in the course of the experiment. This experiment therefore indicates that Dbf4 levels affect the initial efficiency of origin firing but overall there are other factors limiting the extent of over-replication in G1 phase.

Second, we considered that the extent of over-replication might be limited by the licensing capacity of cells. It has been previously reported that licensing factor Cdc6 is degraded when cells are arrested in G1 phase [68,213]. We thus introduced a galactose-inducible copy of *CDC6* into our system and tested if it can increase the amount of DNA that is replicated during the G1 arrest (Figure 40). As assayed by western blot, Cdc6 as well as all other factors were efficiently expressed under these conditions. Yet, the increased Cdc6 level hardly affected the extent of over-replication as judged by total DNA content and EdU-incorporation in flow cytometry. Thus, there are either additional blocks to re-license origins during a prolonged G1 arrest or re-licensing is not limiting over-replication in G1 phase.

Third, we hypothesized that deoxyribonucleotide (dNTP) levels might be too low in G1 phase to allow for more efficient replication. To this end, we over-expressed the *RNR1* gene to drive production of dNTPs in G1 phase [214,215] and assessed total DNA content and EdU uptake by flow cytometry (Figure 41). Again, we were not able to observe striking changes in the extent of over-replication. The most noteworthy difference was that cells over-expressing *RNR1* synthesized DNA more efficiently at earlier time points (1.5 and 2 h after induction), but this difference was balanced out later in the experiment. Thus, we conclude that dNTP levels are most likely not limiting the extent of over-replication in G1 phase.

Taken together, we have explored multiple options to boost origin firing in G1 phase in order to generate more over-replicated DNA. Increasing the levels of dNTPs or of limiting proteins such as Dbf4 appear to be the most promising approaches despite yielding only slightly increased amounts of DNA. Thus, it appears not unlikely that there are other mechanisms active in G1 phase to limit origin firing.

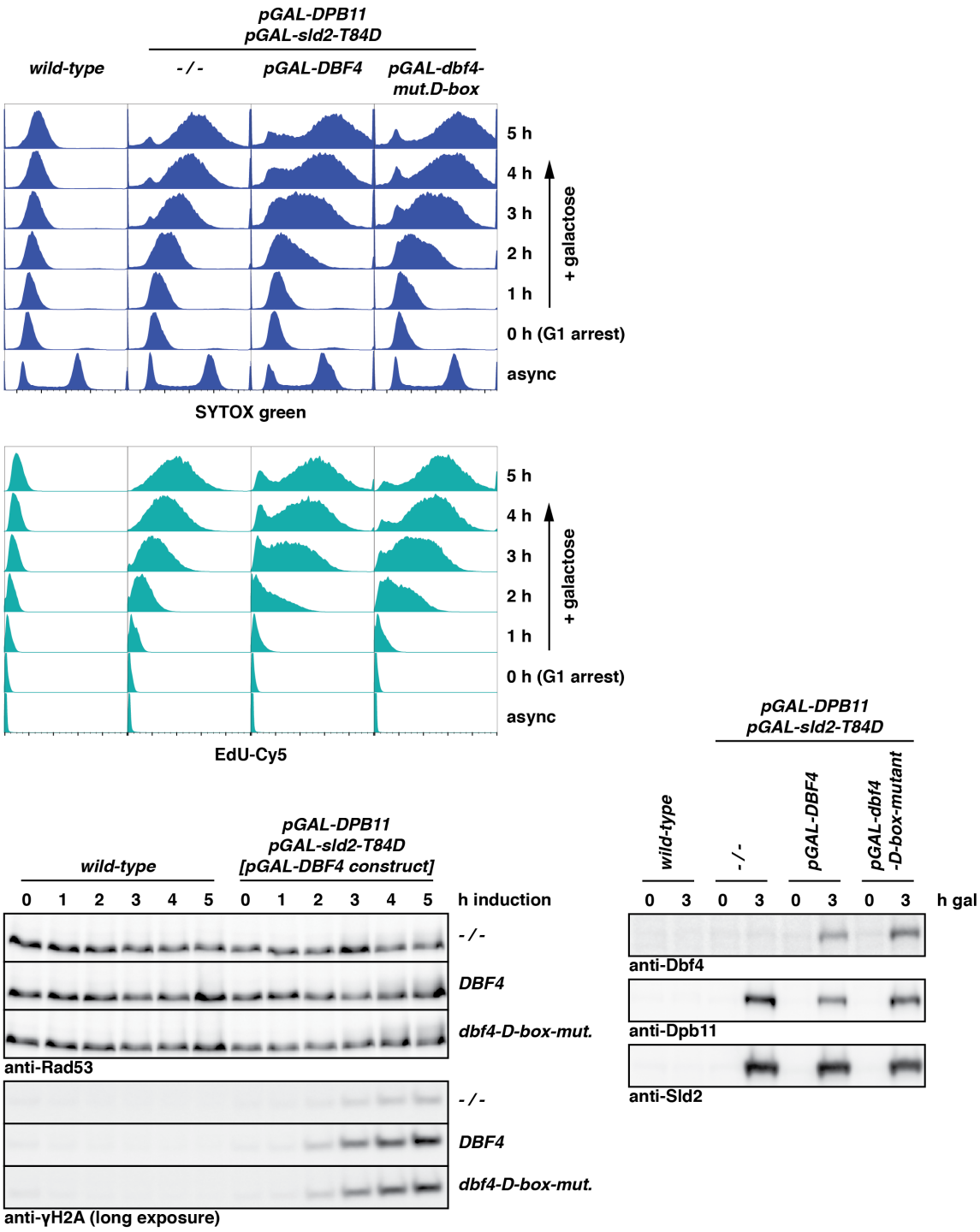

Figure 39 – Stabilization of Dbf4 accelerates replication in G1 phase initially, but does not increase the total amount of over-replication.
Cells were arrested in G1 phase and CDK and/or DDK regulation of origin firing were bypassed by overexpression of the indicated firing factors. EdU was kept in the cell medium to visualize DNA synthesis while cells were kept in the G1-arrest. Samples were taken at the indicated timepoints. The Dbf4 D-box mutant (R10A L13A R62A L65A) prevents degradation of Dbf4 in G1 phase by the ubiquitin ligase APC-Cdh1. (A) Analysis of DNA synthesis by flow cytometry, either measuring total DNA content with SYTOX green or labeling newly synthesized DNA with EdU and later attaching the fluorescent dye Cy5. (B) Western blots resolving phosphorylated Rad53 and detecting γH2A as markers of DNA damage checkpoint signaling. Samples as in (A). (C) Western blots against Dbf4, Dpb11 and Sld2 measuring total protein levels before and after induction with galactose. Samples as in (A).

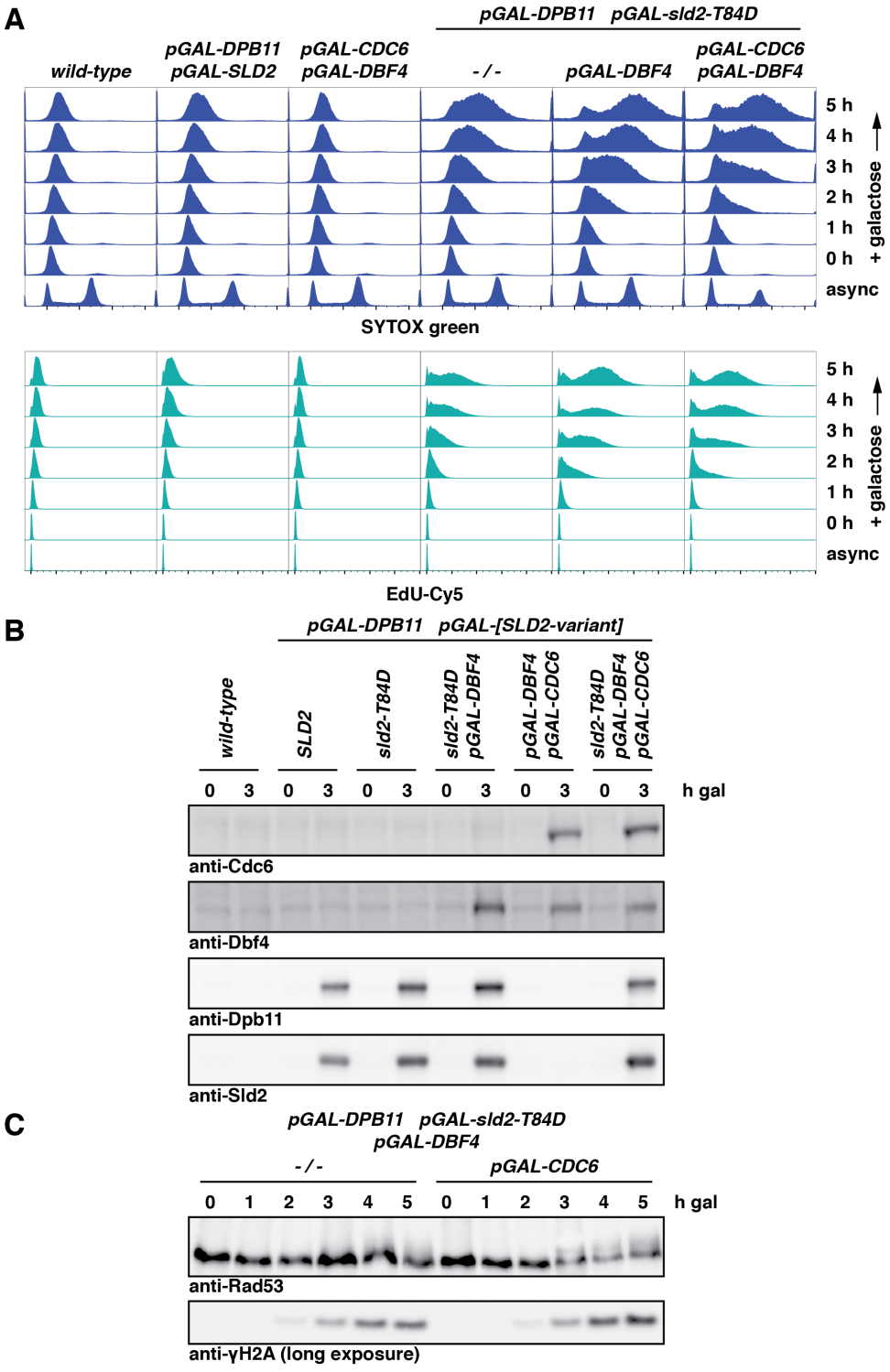

Figure 40 – Licensing factor Cdc6 does not limit the total amount of over-replicated DNA in G1 phase.
Cells were arrested in G1 phase and CDK and/or DDK regulation of origin firing were bypassed by overexpression of the indicated firing factors. EdU was kept in the cell medium to visualize DNA synthesis while cells were kept in the G1-arrest. Licensing factor Cdc6, which becomes degraded in the G1 arrest, was also over-expressed. Samples were taken at the indicated timepoints. (A) Analysis of DNA synthesis by flow cytometry, either measuring total DNA content with SYTOX green or labeling newly synthesized DNA with EdU and later attaching the fluorescent dye Cy5. (B) Western blots against Cdc6, Dbf4, Dpb11 and Sld2 measuring total protein levels before and after induction with galactose. Samples as in (A). (C) Western blots resolving phosphorylated Rad53 and detecting γH2A as markers of DNA damage checkpoint signaling. Samples as in (A).

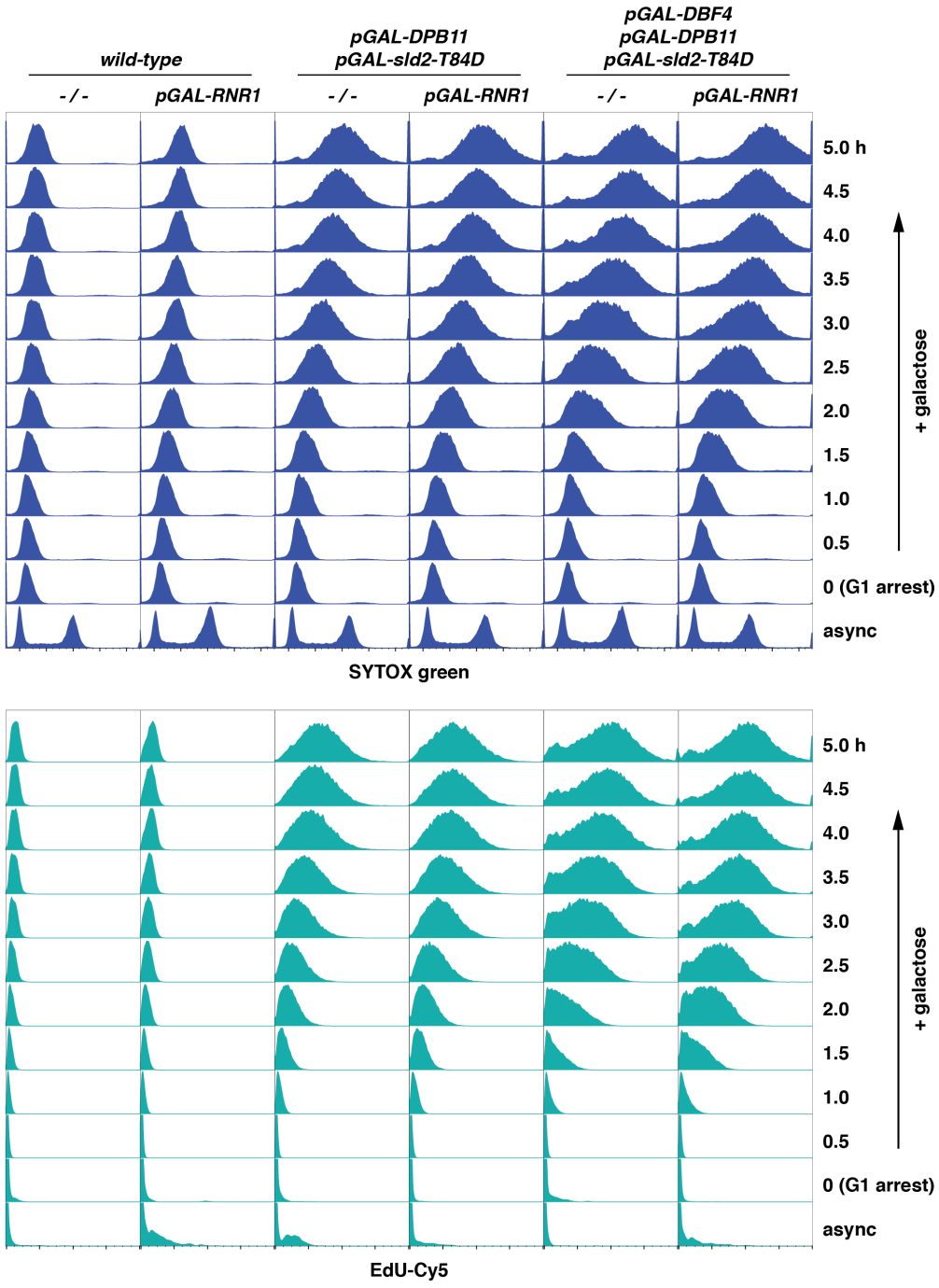

Figure 41 – Ribonucleotide reductase does not limit the total amount of over-replicated DNA in G1 phase.
Cells were arrested in G1 phase and CDK and/or DDK regulation of origin firing were bypassed by overexpression of the indicated firing factors. EdU was kept in the cell medium to visualize DNA synthesis while cells were kept in the G1-arrest. In addition to the firing factors, the large subunit Rnr1 of ribonucleotide reductase was also over-expressed to increase dNTP levels. Analysis of DNA synthesis by flow cytometry, either measuring total DNA content with SYTOX green or labeling newly synthesized DNA with EdU and later attaching the fluorescent dye Cy5.

5.3. DNA damage checkpoint activation occurs in subsequent M phase

Since the DNA damage checkpoint was not activated in direct response to origin firing in G1 phase, we investigated how cells deal with the prematurely replicated DNA in the following phases of the cell cycle, particularly in S phase when additional replisomes are formed and might encounter over-replicated DNA. We thus performed an "arrest-induction-release" experiment, where we arrested cells in G1 phase, induced origin firing while keeping the G1-arrest for three more hours, and then released the cells to fresh medium and thereby to the cell cycle. To ensure that all cells just go through a single S and M phase, we added the drug nocodazole to the medium to stop cells in early M phase. Samples were taken at regular intervals after the release and analyzed by flow cytometry for DNA content and western blot for Rad53 phosphorylation and γH2A (Figure 42). Control cells progressed through the cell cycle normally and neither Rad53 phosphorylation nor substantial γH2A signal could be detected. Cells that fired origins already during the G1-arrest progressed through S phase with kinetics that were similar to the control cells as measured by flow cytometry. Yet, Rad53 activation and therefore an activated DNA damage checkpoint could be observed in these cells 60 min after release from the G1-arrest – a timepoint where cells have normally entered M phase. A signal for γH2A was already detectable 20 min earlier. Taken together, these data suggest that cells progress through S phase normally and are not affected by premature origin firing. However, when origins are fired in G1 phase, substantial DNA damage is generated presumably in late S phase, but activation of the DNA damage checkpoint only occurs later in M phase.

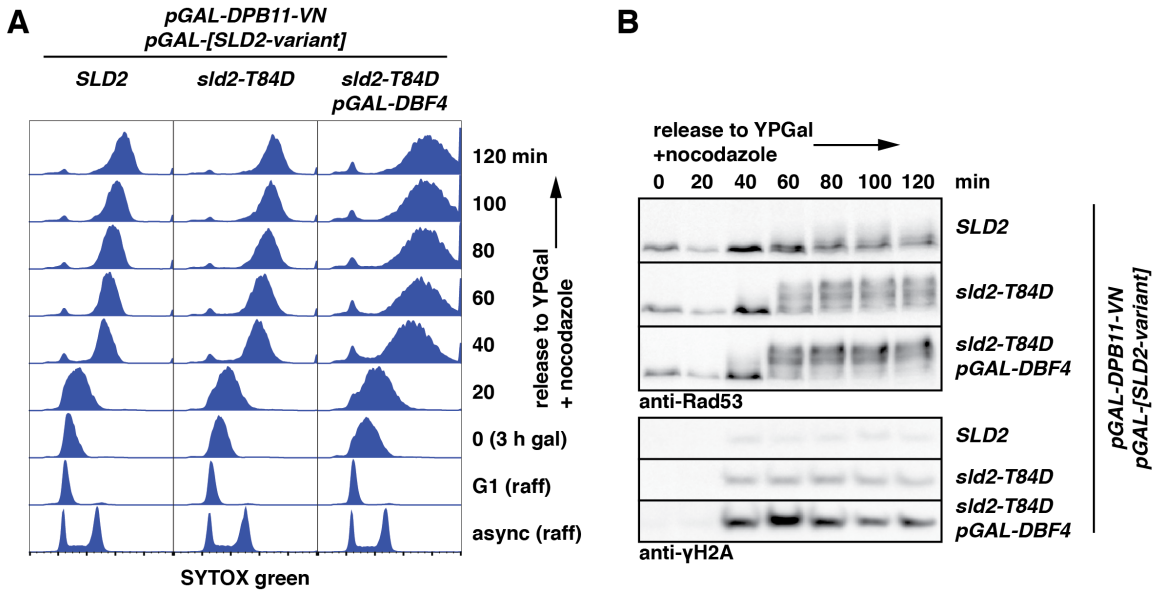

Figure 42 – Bulk replication during S phase is finished before the over-replication-induced DNA damage checkpoint is triggered.
(A) Cell cycle analysis by flow cytometry measuring total DNA content with SYTOX green. Cells were arrested in G1 phase and CDK and/or DDK regulation of origin firing were bypassed by overexpression of the indicated firing factors while cells were kept arrested for 3 h. Thereafter, the cells were released to fresh medium containing nocodazole to arrest all cells in M phase. (B) Western blots resolving phosphorylated Rad53 and detecting γH2A as markers of DNA damage checkpoint signaling. Samples as in (A).

The activation of the DNA damage checkpoint could in principle occur via two different pathways that involve specific mediator proteins to achieve phosphorylation of the effector kinase Rad53. While checkpoint signaling via Mrc1 responds to problems of the DNA replication machinery, the mediator protein Rad9 signals that the integrity of the DNA itself is impaired [112-114]. To distinguish which of the two signaling pathways is involved, we generated yeast strains either lacking *MRC1* or *RAD9* and performed an arrest-induction-release experiment (Figure 43). Consistent with its role in helping the replisome achieve speed and efficiency [54], origin firing was less efficient in *mrc1Δ* cells as judged by flow cytometry data staining for total DNA. Despite this reduced amount of synthesized DNA during the G1-arrest, *mrc1Δ* cells still arrested in M phase with hyper-phosphorylated Rad53. Contrary to this, origin firing could be readily induced in G1 phase in *rad9Δ* cells, but these cells did not respond with hyper-phosphorylated Rad53. These data therefore suggest that DNA damage checkpoint activation in response to deregulated origin firing involves the Rad9-dependent checkpoint signaling pathway.

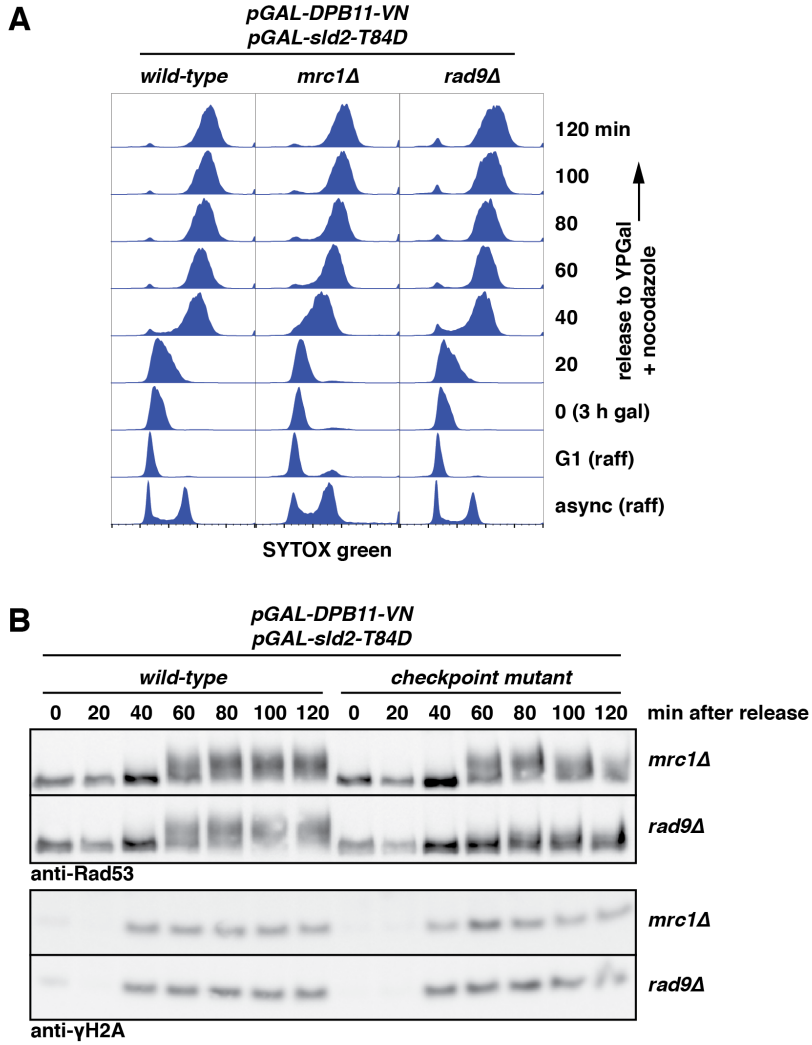

Figure 43 – Rad9 mediates the DNA damage checkpoint signaling in response to over-replication.
(A) Cell cycle analysis by flow cytometry measuring total DNA content with SYTOX green. *Wild-type* cells and *mrc1Δ* / *rad9Δ* cells lacking the DNA damage checkpoint mediators Mrc1 or Rad9 were arrested in G1 phase and CDK regulation of origin firing was bypassed by overexpression of the indicated firing factors while cells were kept arrested for 3 h. Subsequently, the cells were released to fresh medium containing nocodazole to arrest all cells in M phase. (B) Western blots resolving phosphorylated Rad53 and detecting γH2A as markers of DNA damage checkpoint signaling. Samples as in (A).

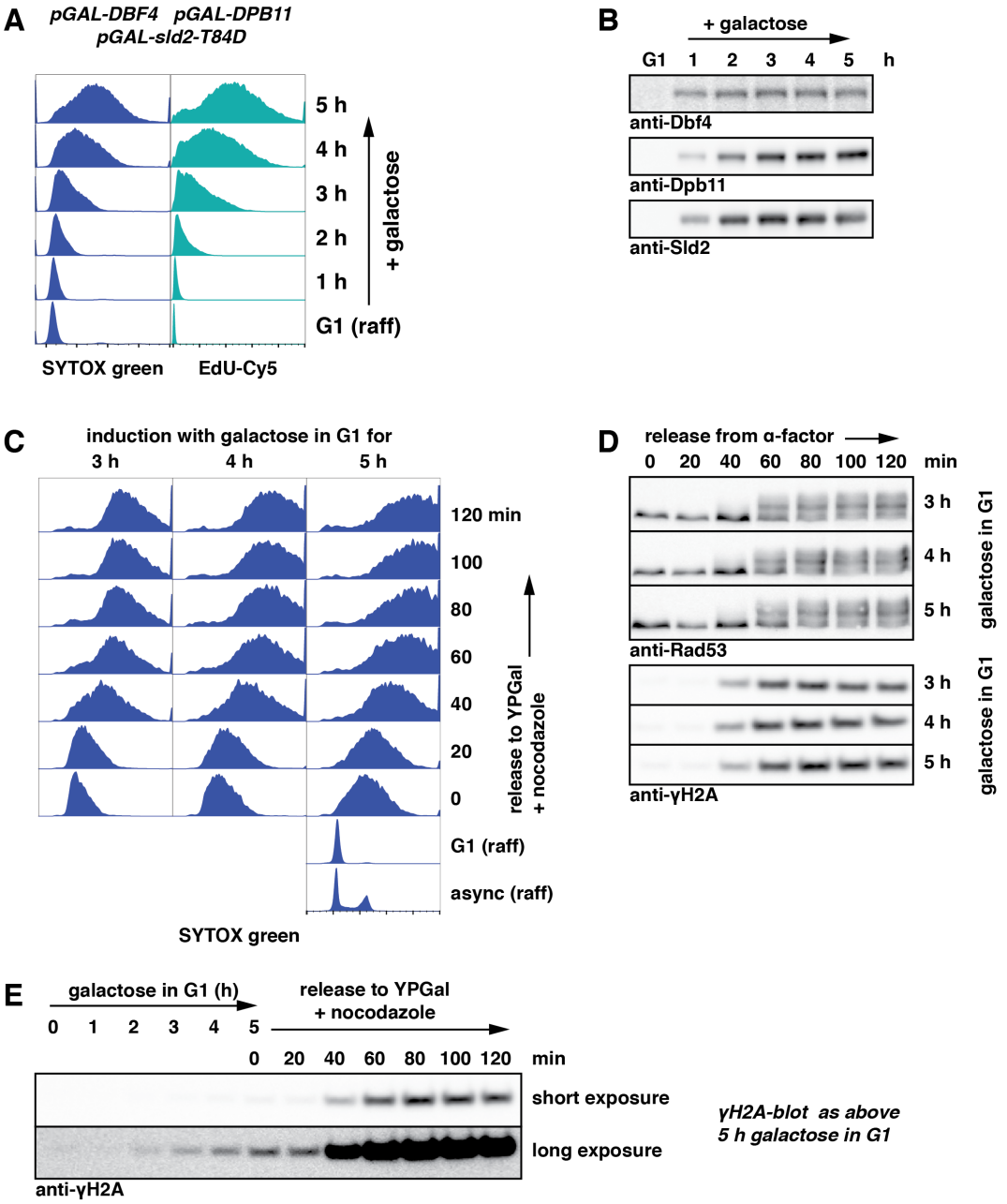

Figure 44 – Following over-replication in G1 phase, DNA damage is strongly induced in late S and M phase.
(A) Analysis of DNA synthesis by flow cytometry, either measuring total DNA content with SYTOX green or labeling newly synthesized DNA with EdU and later attaching the fluorescent dye Cy5. Cells were arrested in G1 phase and CDK as well as DDK regulation of origin firing were bypassed in the presence of EdU by overexpression of the indicated firing factors while cells were kept arrested for indicated times. (B) Western blots against Dbf4, Dpb11 and Sld2 measuring total protein levels during the induction period with galactose. Samples as in (A). (C) Cell cycle analysis by flow cytometry measuring total DNA content with SYTOX green. Cells from (A) were released as indicated to fresh medium containing nocodazole to arrest all cells in M phase. Samples were taken at the indicated timepoints. (D) Western blots resolving phosphorylated Rad53 and detecting γH2A as markers of DNA damage checkpoint signaling. Samples as in (C). (E) Western blot against γH2A with samples after 5 h induction from (D) is shown again in short and long exposure next to samples from (A) during the induction period.

This result led us to focus again on the γH2A signal. To re-evaluate if our detection of the γH2A signal 40 min after release was not influenced by the shorter induction period of three hours, we repeated the experiment and induced origin firing in the G1-arrest for five hours before releasing the cells to fresh medium containing nocodazole (Figure 44). Here, we could clearly observe that a weak γH2A signal was accumulating during the induction period while the cells were still in the G1-arrest. This signal only increased strongly once cells went through S phase (40 min after release). Thus, the majority of the DNA damage is generated after cells have finished or are close to the end of S phase.

The late activation of the DNA damage checkpoint prompted us to investigate if cells activate post-replicative repair mechanisms when they encounter DNA damage caused by over-replication in G1 phase. During normal S phase, PCNA (Pol30 in budding yeast) is modified by SUMO and this modification recruits the anti-recombinase Srs2 to protect replication forks against unwanted recombination events [216,217]. In response to DNA damage, PCNA can also be modified by ubiquitin or by a poly-ubiquitin chain and thereby enable post-replicative repair mechanisms [218]. To this end, we performed an arrest-induction-release experiment and analyzed the post-translational modification state of Pol30 as well as Rad53 phosphorylation and γH2A accumulation in western blots (Figure 45). When we induced origin firing in G1 phase, a signal for γH2A could already be detected 30 min post release whereas Rad53 phosphorylation was only detected around 40 min to 50 min post release. We did not detect ubiquitin-modified PCNA. Instead, we observed SUMOylated PCNA indicative of cells in S phase at 20 min and 30 min post release in control cells. Interestingly, we did not detect SUMOylation of PCNA when replication was induced in G1 phase cells. This might either be due to low numbers of replisomes present at this timepoint and consequently a signal below the detection threshold or it might also hint at a difference between replisomes in G1 and S phases that could not be accessed in our mass spectrometry experiments. In addition, SUMOylated PCNA was present in over-replicating cells also at 40 min post release indicating that S phase might be slightly slower in these cells. Taken together, these data exclude a contribution of post-replicative repair processes and support the notion that, even in the presence of over-replicated DNA, replication in S phase is hardly impaired.

To elucidate if deregulated origin firing in our setup affects cellular viability, we also performed survival assays by plating cells out after arresting them in G1 phase and inducing origin firing for different amounts of time (Figure 46). In these assays, we also assessed if abrogation of checkpoint signaling by either deleting *RAD9* or *MRC1* influences the survival after premature origin firing in G1 phase. Control cells tolerated an arrest in G1 phase for seven hours without a decrease in viability. However, when origin firing was induced, cellular viability dropped to about 50% after three hours and 25% after five hours of induction. Furthermore, colonies became irregularly shaped and/or relatively small after these longer incubation times. Interestingly, deletion of *RAD9*

did not influence cellular viability. On the other hand, *mrc1Δ* cells were not as strongly affected during the first time points but also started to give rise to smaller and irregularly shaped colonies after five hours of induction. Therefore, this experiment supports the view that over-replication is toxic to cells regardless of their ability to detect it through the DNA damage checkpoint. Combined with the data presented above (Figure 43), this experiment also suggests that the toxicity of premature origin firing depends on the actual amount of DNA that is replicated in G1.

As abrogating DNA damage checkpoint signaling did not affect cellular viability, we performed an arrest-induction-release experiment with *rad9Δ* cells to fresh medium without nocodazole after inducing origin firing in G1 phase for three hours (Figure 47). As judged by our flow cytometry data, control cells went through the cell cycle regardless of the presence of *RAD9*. Despite going through S phase similarly, cells that fired origins during the G1-arrest started to differ from the control cells during late M phase: Control cells started mitotic exit at around 100 min after release. In contrast, over-replicating *RAD9* cells arrested in M phase when origins were fired during the G1 arrest. The over-replicating *rad9Δ* cells progressed through M phase and eventually started mitotic exit, but with relatively slow and delayed kinetics. These data suggest that, if undetected, over-replicated DNA severely challenges mitotic progression.

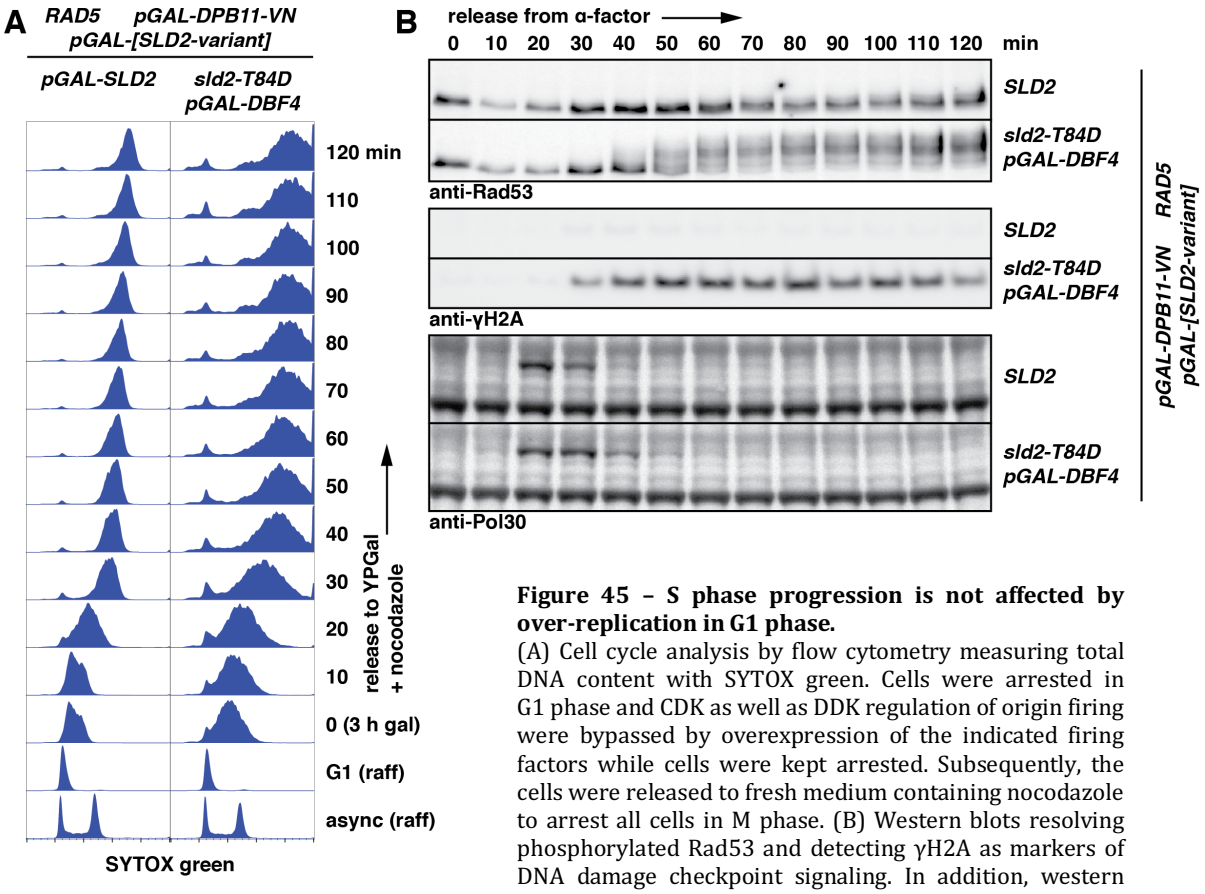

Figure 45 – S phase progression is not affected by over-replication in G1 phase.
(A) Cell cycle analysis by flow cytometry measuring total DNA content with SYTOX green. Cells were arrested in G1 phase and CDK as well as DDK regulation of origin firing were bypassed by overexpression of the indicated firing factors while cells were kept arrested. Subsequently, the cells were released to fresh medium containing nocodazole to arrest all cells in M phase. (B) Western blots resolving phosphorylated Rad53 and detecting γH2A as markers of DNA damage checkpoint signaling. In addition, western blots resolving SUMOylated PCNA (Pol30, upper band) from unmodified PCNA (lower band) to monitor S phase progression. Samples as in (A).

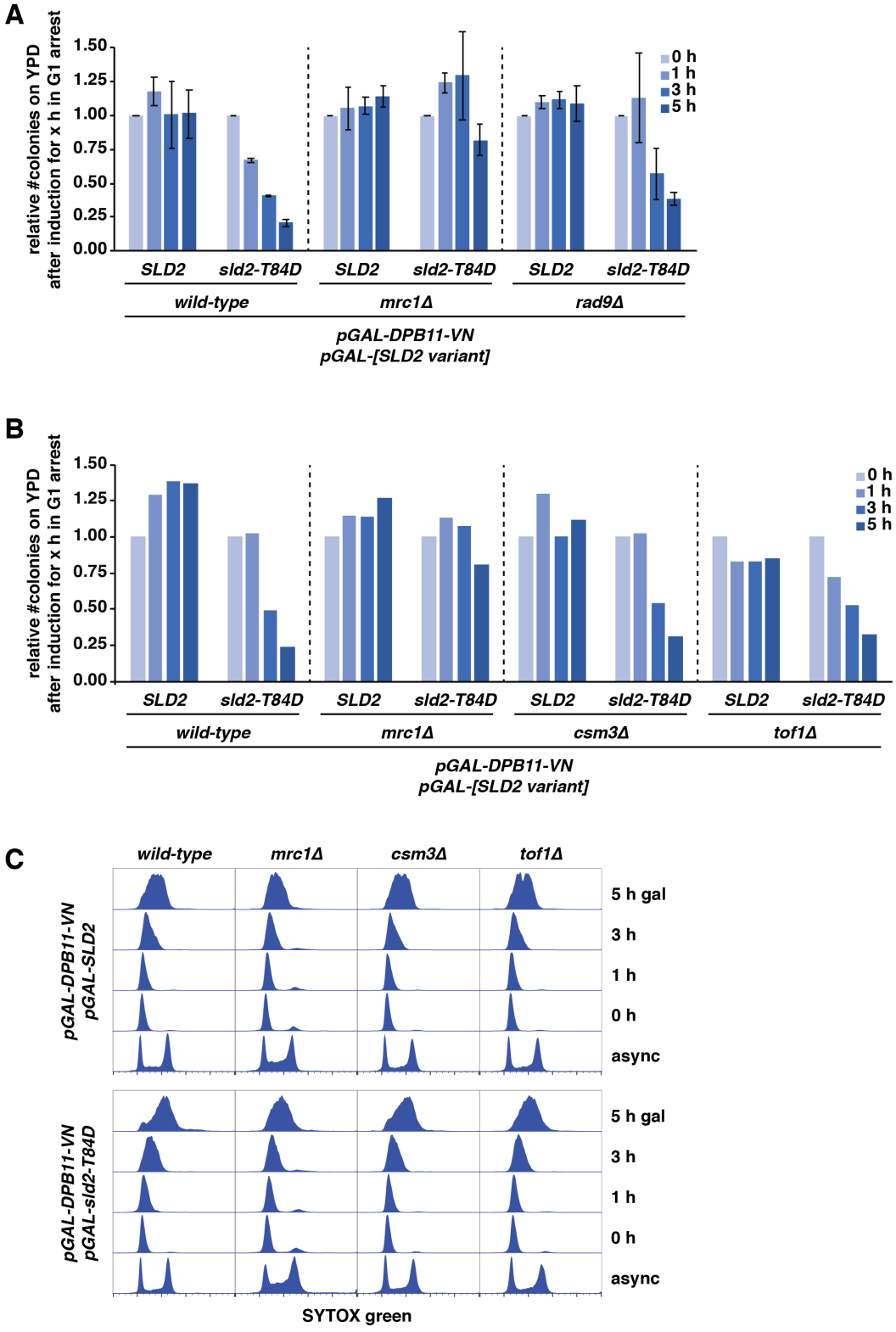

Figure 46 – Over-replication in G1 is toxic regardless of whether it is recognized by the DNA damage checkpoint. (A) Survival assay with over-replicating *wild-type* and *mrc1Δ* / *rad9Δ* cells lacking the DNA damage checkpoint mediators Mrc1 or Rad9. CDK-regulation of origin firing was bypassed in G1-arrested cells for 0 / 1 / 3 / 5 h and the cells were subsequently plated on non-selective medium in duplicates to score colony forming units of survivors. Number of colonies relative to the starting timepoint are plotted as mean and standard deviation from three independent experiments. (B) As in (A) but with mutants in the fork protection complex consisting of Mrc1 and Tof1-Csm3. Data from a single experiment. (C) Induction of origin firing during the G1 arrest in (B) was measured by staining total DNA with SYTOX green and analyzing cells by flow cytometry.

In summary, our experiments provide clear evidence that, even though we induced over-replication in G1 phase, it is not detected by the Rad9-dependent DNA damage checkpoint before M phase. DNA damage as measured by γH2A accumulation occurs already in late S phase but apparently has little influence on S phase progression. In contrast, the actual amount of over-replicated DNA seems to affect cellular viability probably due to processes that occur during M phase and cannot be ameliorated by a prolonged checkpoint arrest.

5.4. DNA damage is only generated upon replication in S phase

Our previous experiments suggested that the DNA damage was mainly generated in late S phase. Consequently, we asked if induction of DNA damage requires additional replication during S phase. To block replication initiation in S phase, we introduced an auxin-inducible degron [219-221] on either the helicase activator Cdc45 or on the firing factor Sld3. Since Sld3 is exclusively involved in origin firing but does not travel with replisomes, depletion of Sld3 will not affect already assembled replisomes but prevent further origin firing. In contrast, depletion of Cdc45 will potentially affect both assembled replisomes as well as further origin firing and thereby block replication entirely.

We performed a slightly modified arrest-induction-release experiment: After induction of origin firing in G1 phase, cells were depleted of either Cdc45 (Figure 48) or Sld3 (Figure 49) via the auxin-inducible degron system and afterwards released to fresh medium in the presence of auxin. As judged by the cell cycle flow cytometry data, both degron systems worked effectively. While control cells replicated their DNA after being released to fresh medium, depletion of Cdc45 or Sld3 completely blocked this increase in DNA content. Auxin-induced depletion of Cdc45 imposed a tight block for the duration of the experiment whereas cells depleted of Sld3 were slightly leaky and showed some increased DNA content at late timepoints. This leakiness is most likely owed to the continuous over-expression of *DPB11* and *sld2-T84D* in these cells which can bypass the requirement for functional Sld3 during origin firing to a certain degree. Hyper-phosphorylation of Rad53 and accumulation of γH2A were detected with the same kinetics as previously in the presence of Cdc45 and Sld3. Importantly, however, when replication in S phase was blocked, we neither detected hyper-phosphorylation of Rad53 nor a substantial increase in the γH2A signal. Therefore, our data suggest that the DNA damage is generated during S phase.

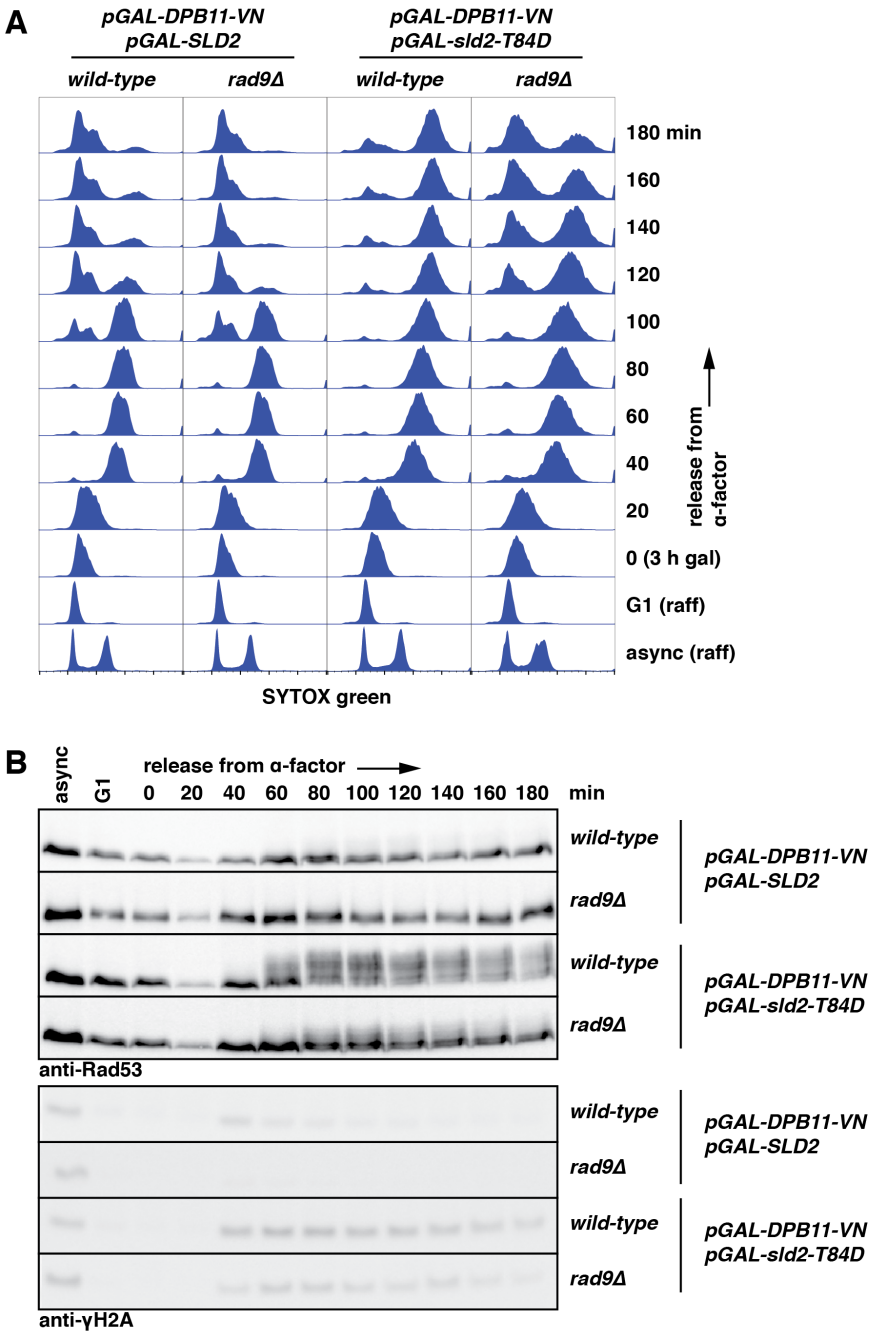

Figure 47 – Undetected over-replication impairs progression through M phase even in the absence of a functional checkpoint.
(A) Cell cycle analysis by flow cytometry measuring total DNA content with SYTOX green. *Wild-type* cells and *rad9Δ* cells lacking DNA damage checkpoint mediator Rad9 were arrested in G1 phase and CDK regulation of origin firing was bypassed by overexpression of the indicated firing factors while cells were kept arrested. Subsequently, the cells were released to fresh medium. To prevent cells from entering a second cell cycle, α-factor was added back to the medium 60 min after release. (B) Western blots resolving phosphorylated Rad53 and detecting γH2A as markers of DNA damage checkpoint signaling. Samples as in (A).

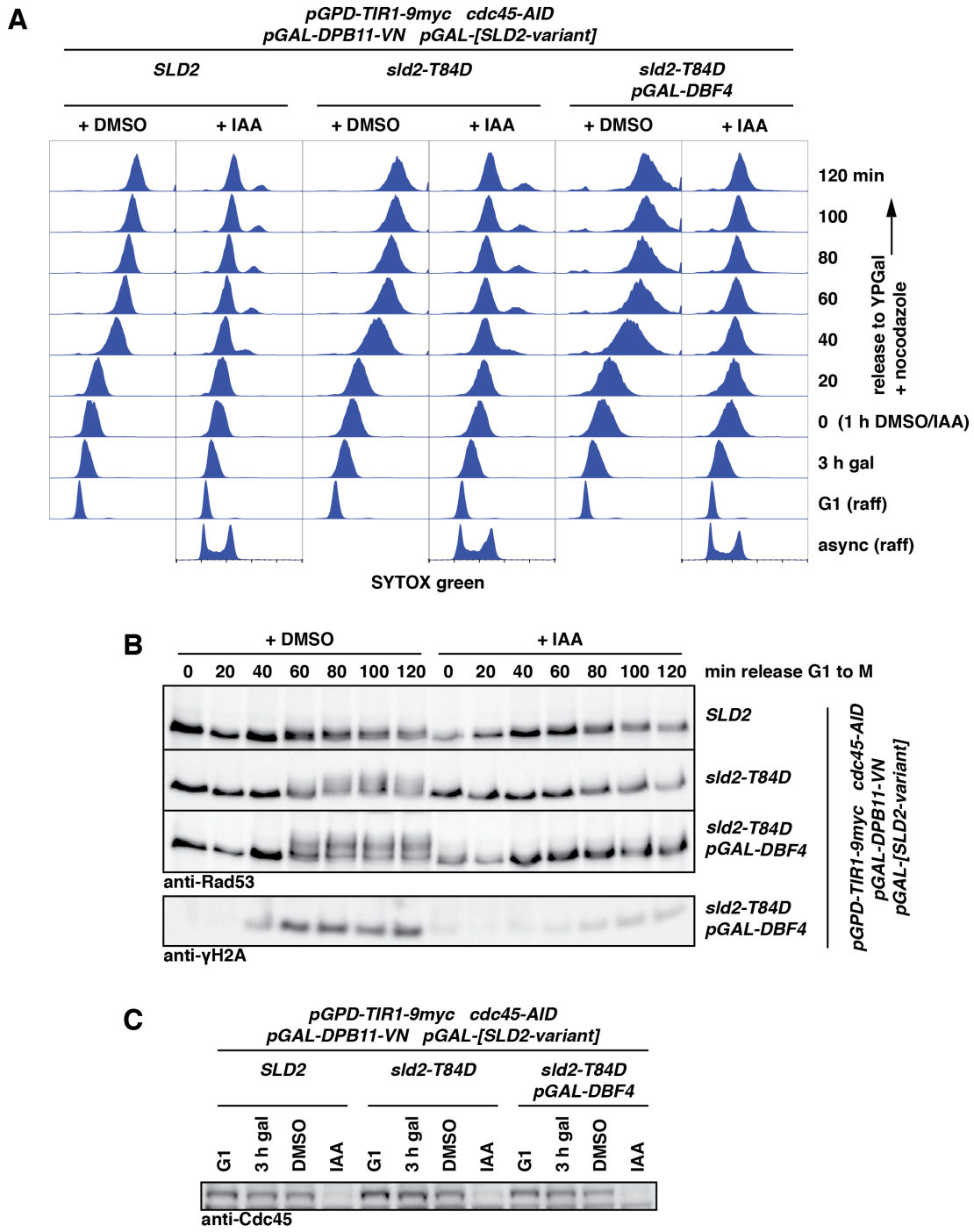

Figure 48 – Activation of the DNA damage checkpoint requires DNA replication in S phase.
(A) Cell cycle analysis by flow cytometry measuring total DNA content with SYTOX green. Cells with an auxin-inducible degron (AID) tag on the helicase activator Cdc45 were arrested in G1 phase and CDK and/or DDK regulation of origin firing were bypassed by overexpression of the indicated firing factors while cells were kept arrested. Subsequently, cells were incubated with either DMSO or the auxin IAA for 1 h and then released to fresh medium containing nocodazole to prevent cells from exiting M phase. In addition, the fresh medium was supplemented with either DMSO or IAA to ensure continuous depletion of Cdc45. (B) Western blots resolving phosphorylated Rad53 and detecting γH2A as markers of DNA damage checkpoint signaling. Samples as in (A). (C) Western blots detecting the total protein levels of Cdc45 at the indicated timepoints. Samples as in (A) and (B).

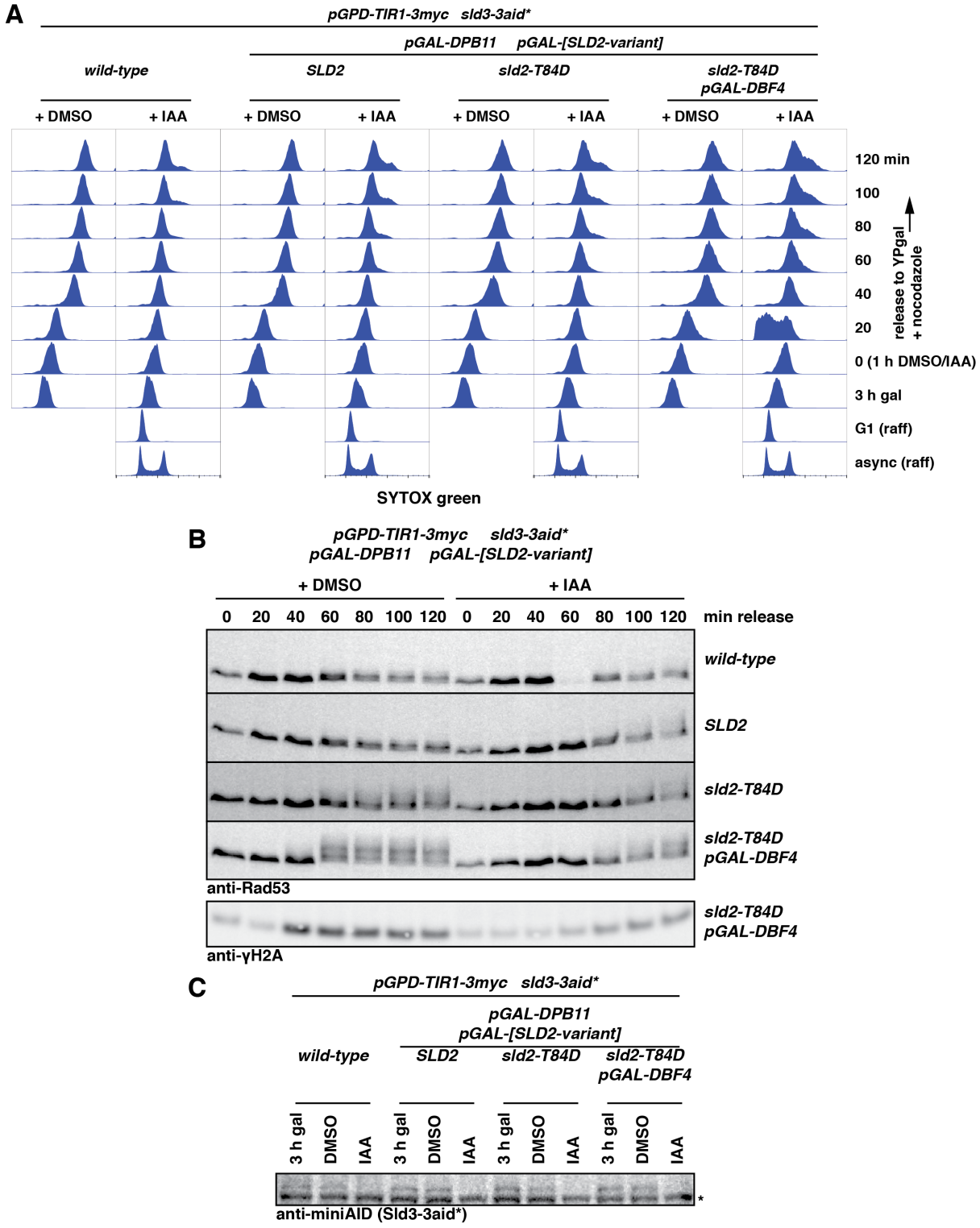

Figure 49 – Activation of the DNA damage checkpoint requires DNA replication initiation in S phase.
(A) Cell cycle analysis by flow cytometry measuring total DNA content with SYTOX green. Cells expressing firing factor Sld3 tagged with three copies of a truncated version of the auxin inducible degron tag (*sld3-3aid**) were arrested in G1 phase and CDK and/or DDK regulation of origin firing were bypassed by overexpression of the indicated firing factors, while cells were kept arrested. Subsequently, cells were incubated with either DMSO or the auxin IAA for 1 h and then released to fresh medium containing nocodazole to prevent cells from exiting M phase. In addition, the fresh medium was supplemented with either DMSO or IAA to ensure continuous depletion of Sld3. (B) Western blots resolving phosphorylated Rad53 and detecting γH2A as markers of DNA damage checkpoint signaling. Samples as in (A). (C) Western blots detecting the total protein levels of Sld3-3aid* at the indicated timepoints. Samples as in (A) and (B). The asterisk indicates an unspecific band.

5.5. Mitotic processing contributes to DNA damage checkpoint activation

We also aimed to understand how the specific timing of the DNA damage checkpoint activation was achieved. In our initial arrest-induction-release experiments, we observed that the hyper-phosphorylation of Rad53 temporally correlated with the accumulation of the mitotic cyclin Clb2 and the budding yeast Polo-kinase homolog Cdc5, thus raising the possibility that these kinases could affect the timing of the DNA damage checkpoint activation by activating other M phase-specific processes. For example, structure-specific endonucleases such as Mus81-Mms4 or Yen1 are under tight cell cycle control and mitotic CDK and Cdc5 have been shown to activate Mus81-Mms4 [222-226]. An attractive model would hence be that over-replication generates aberrant DNA structures, which are recognized and processed by structure-specific endonucleases exclusively in M phase and thereby activate the DNA damage checkpoint. Alternatively, processes that are associated with the termination of replisomes, e.g. unloading of terminated helicases, might influence the DNA damage checkpoint signaling as well.

Following this general line of thought, we focused on decreasing the activity of mitotic CDK and its effects on the timing of DNA damage checkpoint activation. We deleted the *CLB2* gene, which encodes the major mitotic cyclin in budding yeast, and performed an arrest-induction-release experiment (Figure 50). As judged by our analysis of EdU-incorporation, deletion of *CLB2* did not affect the efficiency of inducing origin firing in G1. In contrast, hyper-phosphorylation of Rad53 was reduced in *clb2Δ* cells. This experiment therefore suggests a role for mitotic CDK in promoting activation of the DNA damage checkpoint potentially by facilitating M phase-specific processing.

As outlined above, one attractive hypothesis would be that such M phase-specific processing is mediated by Mus81-Mms4. Hyper-phosphorylation of the regulatory subunit Mms4 by both CDK and Cdc5 is necessary for the activation of this structure-specific endonuclease [222,224,227]. Mms4 hyper-phosphorylation can be monitored by electrophoretic mobility shifts in acrylamide gels and provides a simple read-out for the activity of the Mus81-Msm4 endonuclease. We thus performed another arrest-induction-release experiment and followed the phosphorylation state of Mms4 (Figure 51). In *wild-type* cells, hyper-phosphorylated Mms4 is readily detected after 60 min release from the G1 arrest. However, in cells that fired origins in G1, this hyper-phosphorylation was largely absent and we only detected a minor shift in electrophoretic mobility. Since Cdc5 was expressed under these conditions, these data support the interpretation that the DNA damage checkpoint prevents the activation of Mus81-Mms4 thereby excluding a role for Mus81-Mms4 in M phase-specific processing. Taken together, we observed that an activated DNA damage checkpoint due to over-replication results in downregulation of mitotic genes such as *CLB2* and *CDC5*. These data indicate that the cells arrest at a very early stage of mitosis and argue strongly against a role for Mus81-Mms4 in processing aberrant DNA structures under these conditions.

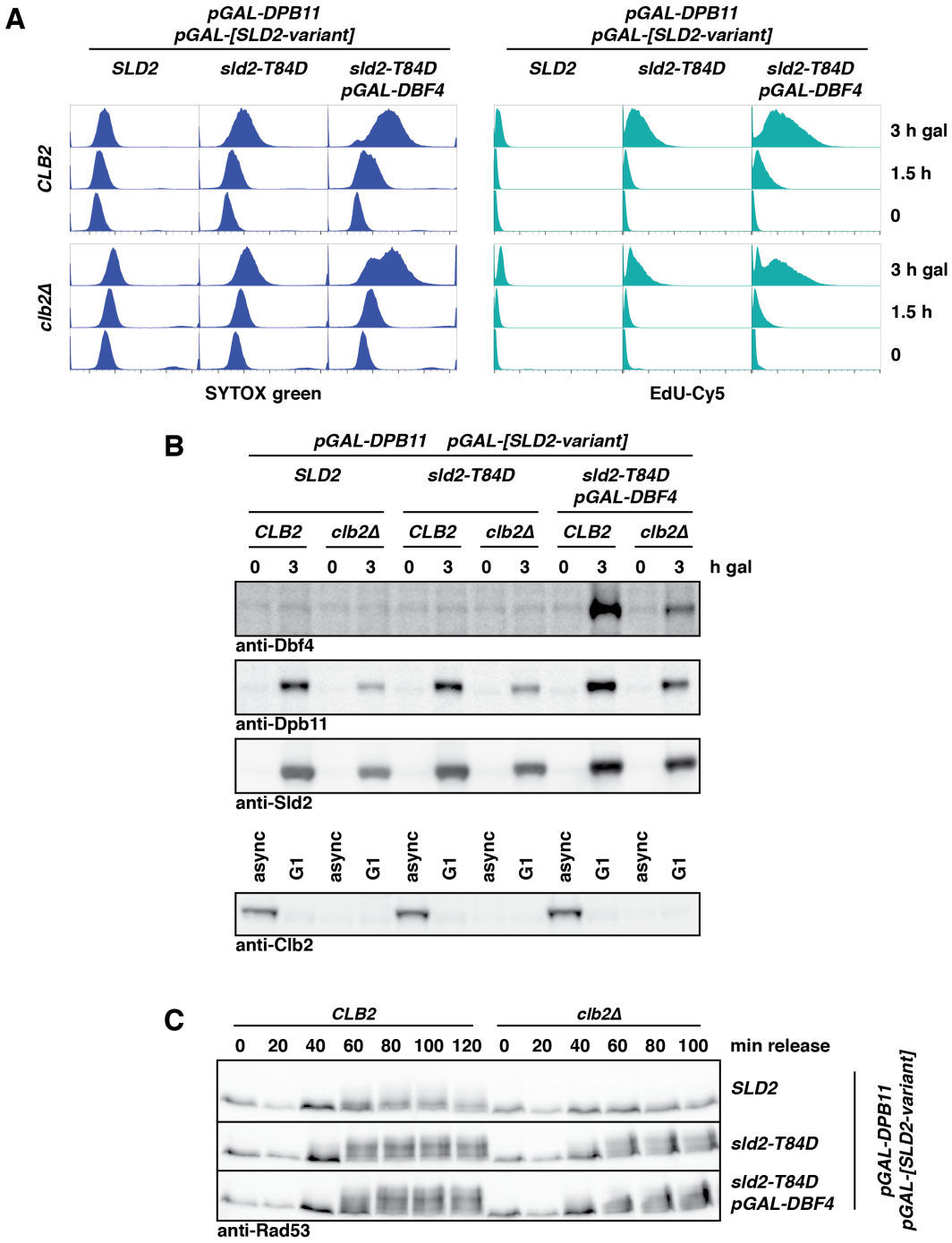

Figure 50 – Over-replication-induced DNA damage checkpoint activation is reduced in mutants lacking M phase cyclin *CLB2*.
(A) Analysis of DNA synthesis by flow cytometry, either measuring total DNA content with SYTOX green or labeling newly synthesized DNA with EdU and later attaching the fluorescent dye Cy5. *Wild-type CLB2* cells and *clb2Δ* cells lacking the M phase cyclin Clb2 were arrested in G1 phase and CDK and/or DDK regulation of origin firing were bypassed in the presence of EdU by overexpression of the indicated firing factors for 3 h while cells were kept arrested. (B) Western blots against Dbf4, Dpb11, Sld2 and Clb2 measuring total protein levels during the induction period with galactose. Samples as in (A). (C) Western blots resolving phosphorylated Rad53 as a marker of DNA damage checkpoint signaling. Samples from experiment in (A) but after release to fresh medium containing nocodazole.

We also considered that termination of replication forks could influence the timing of the DNA damage checkpoint activation. Normally, terminated replisomes are disassembled after S phase in a process that is driven by the ATPase Cdc48 and the ubiquitin-ligase SCF-Dia2 [43]. It seemed plausible that the presence of replisomes on DNA could mask potential sites of DNA damage and that checkpoint signaling proteins would only gain access to these sites once the replisomes were disassembled. To test this hypothesis, we performed an arrest-induction-release experiment with cells lacking *DIA2* (Figure 52). Intriguingly, we observed a decrease in hyper-phosphorylation of Rad53 in *dia2Δ* cells. When we compared the amount of replicated DNA during the G1-arrest, it became apparent, however, that *dia2Δ* cells had a defect in inducing origin firing in G1 phase. On average, these cells were synthesizing less than 50% DNA during the G1-arrest compared to congenic *DIA2* cells and this discrepancy complicates the interpretation of this experiment. As the relationship between amount of replicated DNA in G1 and resulting activation of the DNA damage checkpoint is currently not defined well enough, we aim to circumvent this issue by using an allele of *DIA2* that can be conditionally inactivated in future experiments.

Another hypothesis was that proteins with nucleolytic activity that would normally function at replisomes could be mis-regulated and erroneously cut DNA when encountering over-replication structures. One attractive candidate in this regard was topoisomerase *TOP1*, since we also observed its association with replisomes in our mass spectrometry data. To evaluate if *TOP1* affects the activation of the DNA damage checkpoint in response to origin firing in G1 phase, we performed an arrest-induction-release experiment with *top1Δ* cells (Figure 53). As judged by the analysis of total DNA content in the cells, we observed that *top1Δ* cells replicated DNA less efficiently in G1 phase and their progression through S phase was also slightly delayed, consistent with previous studies showing that replisomes move with reduced speed in the absence of *TOP1* [228,229]. Interestingly, we observed that phosphorylation of Rad53 was decreased in over-replicating cells lacking *TOP1*. Since *mrc1Δ* cells were also less efficient at replicating DNA in G1 phase but did not show decreased Rad53 phosphorylation, these data suggest that Top1 contributes to checkpoint activation and this mutant condition should be studied further. Top1 has been linked to the removal of mis-incorporated ribonucleotides from DNA [230-234], which might occur frequently during replication in G1 phase owing to the low levels of dNTPs at this stage of the cell cycle. Therefore, we conclude that deletion of *TOP1* reduces checkpoint activation in response to over-replication. The mechanistic details however remain to be determined.

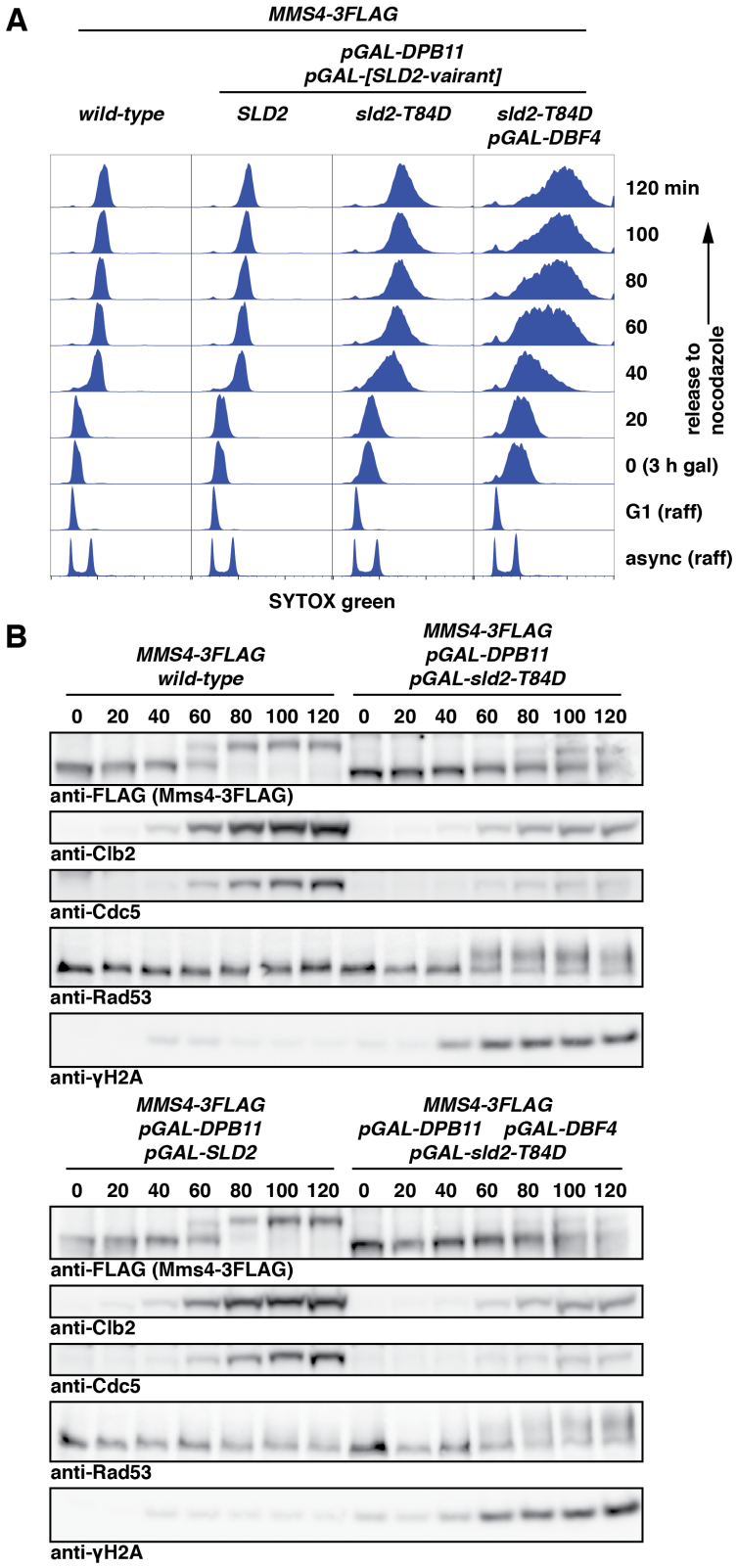

Figure 51 – Cells arrest with reduced Cdc5 and M-CDK levels and activity in response to over-replication.
(A) Cell cycle analysis by flow cytometry measuring total DNA content with SYTOX green. Cells were arrested in G1 phase and CDK and/or DDK regulation of origin firing were bypassed by overexpression of the indicated firing factors while cells were kept arrested. Subsequently, the cells were released to fresh medium containing nocodazole to arrest all cells in M phase. (B) Western blots resolving phosphorylated endonuclease Mms4 as an indicator for the activity of M phase kinases and western blots detecting total levels of Polo-kinase Cdc5 and M-CDK cyclin Clb2. In addition, also western blots resolving phosphorylated Rad53 and detecting γH2A as markers of DNA damage checkpoint signaling. Samples as in (A).

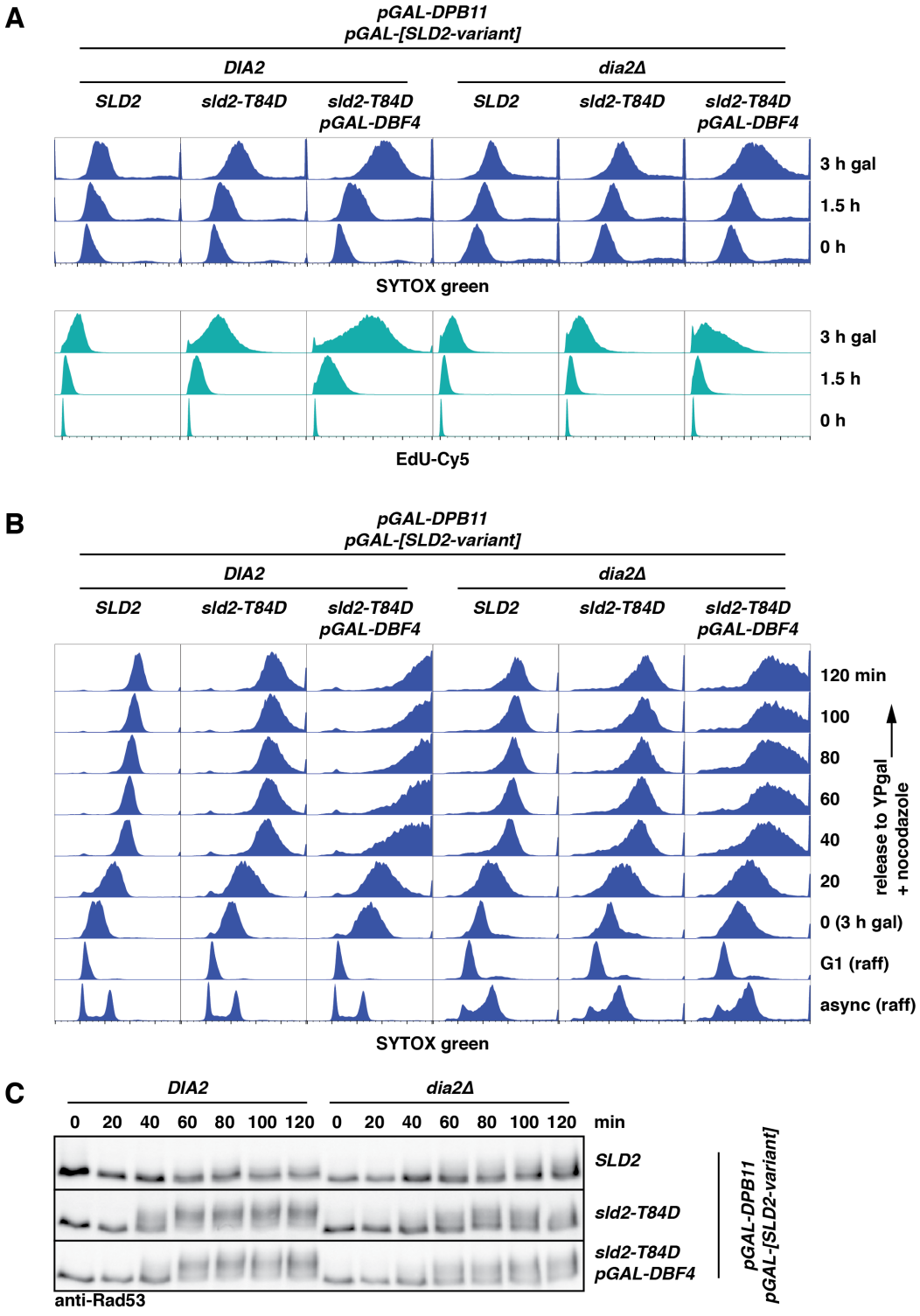

Figure 52 – Reduced over-replication-induced DNA damage checkpoint in *dia2Δ* cells correlates with reduced DNA synthesis in G1 phase.
(A) Analysis of DNA synthesis by flow cytometry, either measuring total DNA content with SYTOX green or labeling newly synthesized DNA with EdU and later attaching the fluorescent dye Cy5. *Wild-type DIA2* cells or *dia2Δ* cells lacking ubiquitin ligase Dia2, which mediates replisome disassembly, were arrested in G1 phase and CDK and/or DDK regulation of origin firing were bypassed in the presence of EdU by overexpression of the indicated firing factors while cells were kept arrested. (B) Cell cycle analysis by flow cytometry measuring total DNA content with SYTOX green. Cells from (A) were released to fresh medium containing nocodazole to arrest all cells in M phase. Samples were taken at the indicated timepoints. (C) Western blots resolving phosphorylated Rad53 as a marker of DNA damage checkpoint signaling. Samples as in (B).

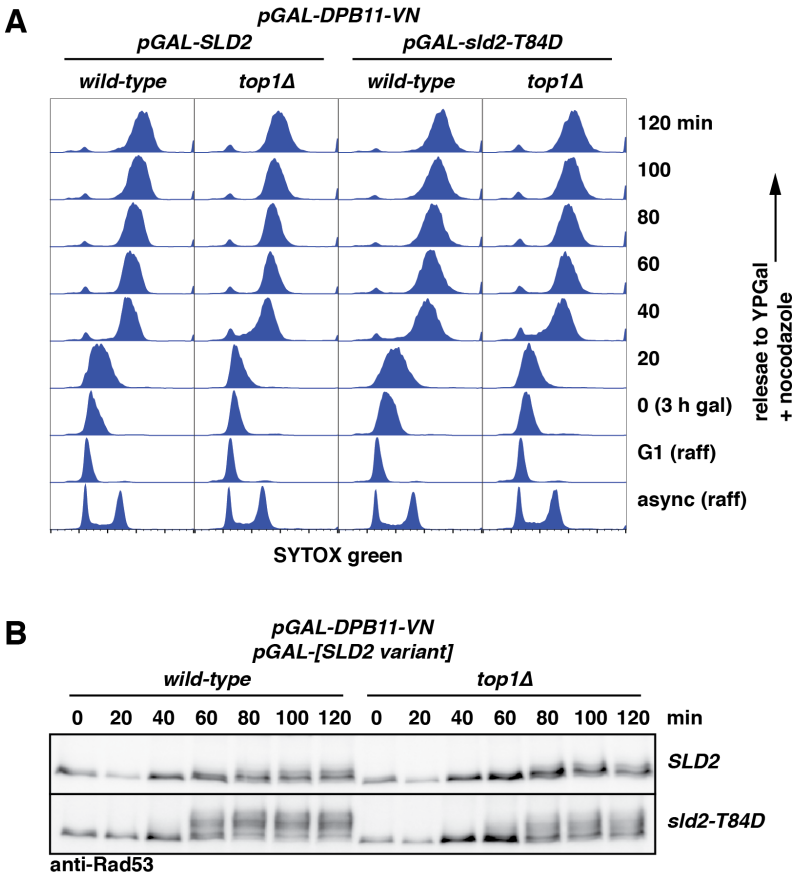

Figure 53 – Cells lacking topoisomerase *TOP1* show reduced over-replication-induced DNA damage checkpoint. (A) Cell cycle analysis by flow cytometry measuring total DNA content with SYTOX green. *Wild-type TOP1* cells and *top1Δ* cells lacking topoisomerase Top1 were arrested in G1 phase and CDK regulation of origin firing was bypassed by overexpression of the indicated firing factors while cells were kept arrested for 3 h. Subsequently, the cells were released to fresh medium containing nocodazole to arrest all cells in M phase. (B) Western blots resolving phosphorylated Rad53 as a marker of DNA damage checkpoint signaling. Samples as in (A).

In summary, we have investigated alternatives models to explain the late activation of the DNA damage checkpoint. While we can exclude M phase-specific processing by endonucleases such as Mus81-Mms4 due to reduced activity of Cdc5, we obtained evidence that mitotic CDK is required for the full activation of Rad53 in response to over-replication. Furthermore, interfering with helicase unloading via the SCF-Dia2 complex as well as manipulating replisomes by removing Top1 are additional conditions that lead to reduced DNA damage checkpoint activation and merit further investigation.

5.6. Hyper-sensitized checkpoint signaling allows for earlier detection and delays S phase entry

In parallel to investigating how the specific timing of DNA damage checkpoint activation is determined, we also tried to manipulate it. To this end, we utilized a fusion protein consisting of Ddc1 and Rad9, which has been shown to hyper-sensitize DNA damage checkpoint signaling [235]. We hypothesized that this fusion protein might allow cells to detect and react to origin firing already in G1 phase and to counteract the accompanying DNA damage.

First, we induced origin firing while keeping the cells tightly arrested in G1 and analyzed samples at regular intervals for DNA content and EdU-incorporation by flow cytometry as well as for γH2A accumulation and Rad53 phosphorylation in western blots (Figure 54). The presence of *DDC1-RAD9-fusion* led to hyper-phosphorylation of Rad53 in G1-arrested cells when origin firing was induced for three to four hours, while no such effect was visible in control cells. Interestingly, this activation of the DNA damage checkpoint prevented the accumulation of γH2A during the course of the experiment. In addition, the activated DNA damage checkpoint apparently restricted further origin firing and led to reduced total cellular DNA levels after inducing origin firing in G1 phase for five hours. Similar results (data not shown) were also obtained, when we used a different construct that hypersensitizes DNA damage checkpoint signaling via a covalent fusion of checkpoint mediator Rad9 to scaffold protein Dpb11 [236,237]. Thus, we conclude that hyper-sensitive checkpoint signaling could prevent the accumulation of DNA damage already during G1 phase by blocking further DNA replication.

This finding motivated us to examine the consequences of hyper-sensitive DNA damage checkpoint signaling in an arrest-induction-release experiments (Figure 55 and Figure 56). As previously, we induced de-regulated origin firing in G1 for three hours. *Wild-type* cells progressed relatively normal through the cell cycle regardless of the presence of *DDC1-RAD9-fusion*. A transient hyper-phosphorylation of Rad53 was detectable in *DDC1-RAD9-fusion* cells progressing through S phase. When we bypassed the CDK-dependent regulation of origin firing in G1 phase, we observed that *DDC1-RAD9-fusion* cells progressed through S phase slowly, consistent with an earlier detection of hyper-phosphorylated Rad53. This behavior became even more pronounced when we also bypassed DDK-dependent regulation of origin firing in G1 phase: As we observed previously, hyper-phosphorylated Rad53 was already present during the G1-arrest and the amount of newly synthesized DNA in G1 phase was reduced as compared to cells without *DDC1-RAD9-fusion* (Figure 55). The activated checkpoint also blocked further origin firing as judged by DNA content analysis in flow cytometry. Furthermore, levels of γH2A were strongly reduced in *DDC1-RAD9-fusion* cells, even when released from the G1-arrest (Figure 56). These data support the notion that hyper-sensitive checkpoint signaling can modulate the amount of DNA damage that cells encounter after premature origin firing in G1 phase.

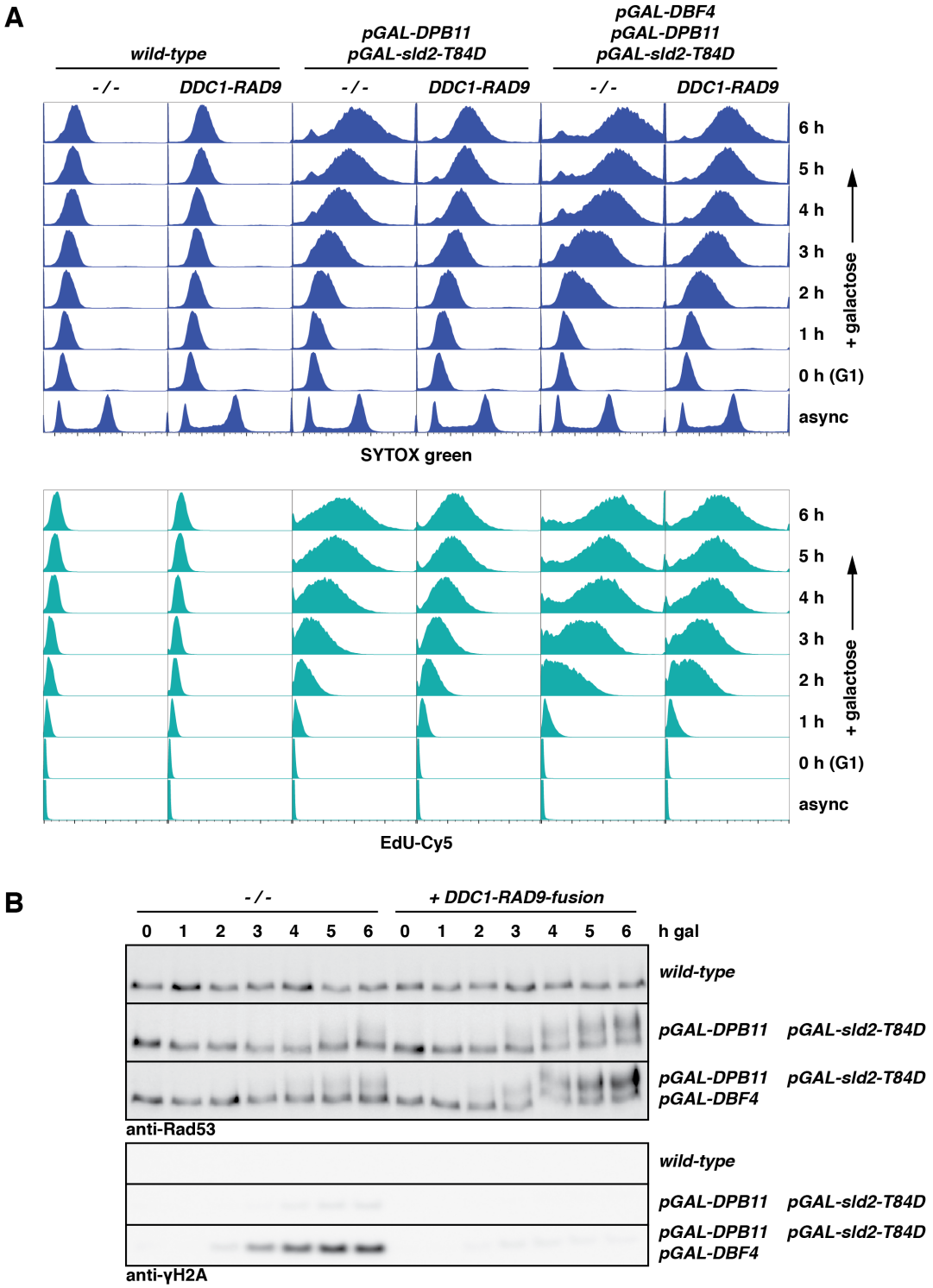

Figure 54 – Hyper-sensitized DNA damage checkpoint signaling in G1 prevents accumulation of over-replication-induced DNA damage.
(A) Analysis of DNA synthesis by flow cytometry, either measuring total DNA content with SYTOX green or labeling newly synthesized DNA with EdU and later attaching the fluorescent dye Cy5. *Wild-type* cells and cells expressing a chimeric *DDC1-RAD9-fusion* gene, which hyper-sensitizes signaling by the DNA damage checkpoint, were arrested in G1 phase and CDK and/or DDK regulation of origin firing were bypassed by overexpression of the indicated firing factors in the presence of EdU while cells were kept arrested. (B) Western blots resolving phosphorylated Rad53 and detecting γH2A as markers of DNA damage checkpoint signaling. Samples as in (A).

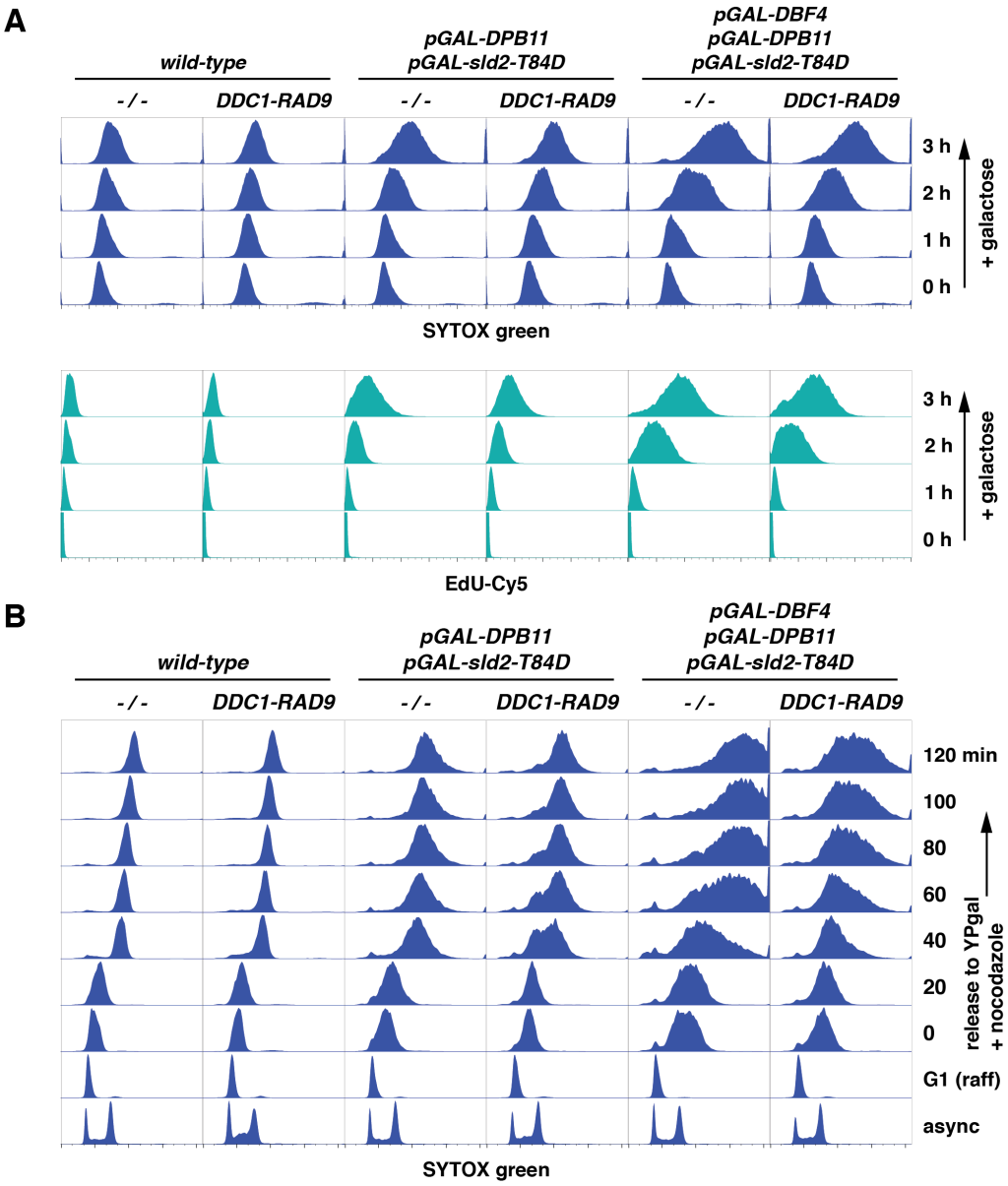

Figure 55 – Hyper-sensitized DNA damage checkpoint signaling allows for entry into S phase even after induction of over-replication.
(A) Analysis of DNA synthesis by flow cytometry, either measuring total DNA content with SYTOX green or labeling newly synthesized DNA with EdU and later attaching the fluorescent dye Cy5. *Wild-type* cells and cells expressing a chimeric *DDC1-RAD9-fusion* gene, which hyper-sensitizes signaling by the DNA damage checkpoint, were arrested in G1 phase and CDK and/or DDK regulation of origin firing were bypassed by overexpression of the indicated firing factors in the presence of EdU while cells were kept arrested. (B) Cell cycle analysis by flow cytometry measuring total DNA content with SYTOX green. Cells from (A) were released to fresh medium containing nocodazole to arrest all cells in M phase.

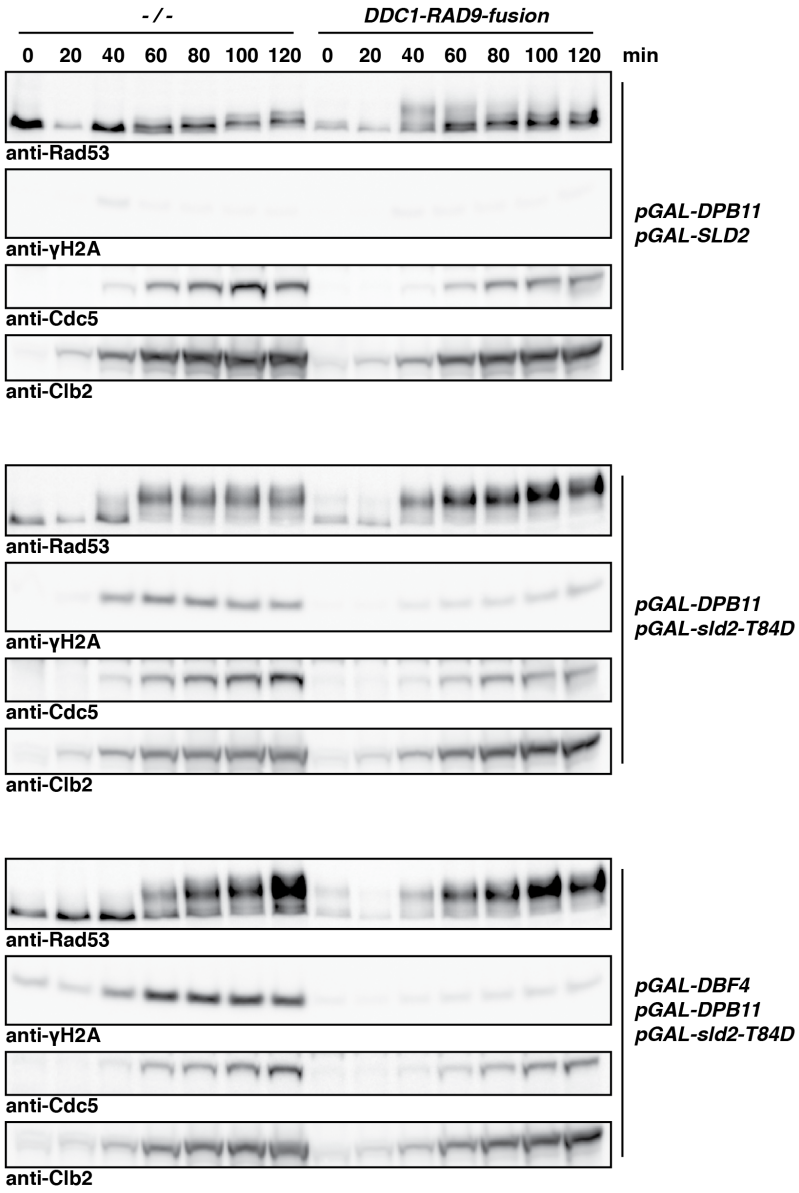

Figure 56 – Hyper-sensitized DNA damage checkpoint signaling in G1 phase prevents accumulation of over-replication induced DNA damage also late in the cell cycle.
Western blots resolving phosphorylated Rad53 and detecting γH2A as markers of DNA damage checkpoint signaling as well as detecting total levels of Cdc5 and Clb2 as indicators for cell cycle progression. Samples as in Figure 55.

In summary, our studies have revealed that deregulated origin firing in G1 phase generates replisomes, which are highly similar to those in S phase in terms of protein composition and origin usage. Depending on the amount of copied DNA, these prematurely activated replisomes become toxic for the cells. However, the presence of over-replicated DNA in G1 phase just generates a weak DNA damage signal in the form of γH2A but does not elicit a cellular response by the DNA damage checkpoint. Cells experiencing over-replication in G1 phase start and proceed through S phase highly similar to *wild-type* cells but accumulate additional DNA damage towards the end of S phase. When cells are about to enter M phase, this high level of DNA damage ultimately activates the Rad9-dependent DNA damage checkpoint and reduced mitotic CDK activity also

decreases total DNA damage checkpoint activation. By manipulating progression of replisomes or by interfering with termination of replisomes trough deletion of *TOP1* or *DIA2*, respectively, we have identified cellular factors that decrease DNA damage checkpoint activation in response to over-replication and should be investigated further. Importantly, hyper-sensitized DNA damage checkpoint signaling allows for earlier detection of over-replicated DNA and thereby prevents the accumulation of DNA damage. Whether hyper-sensitized checkpoint signaling positively affects viability remains to be determined. Taken together, our data provide a systematic and comprehensive analysis of over-replication in G1 phase and put us now in the position to elucidate cell cycle-specific responses to over-replication.

6. Results obtained in collaboration

This thesis built on results of my own Diploma thesis "Rapid degradation of phosphorylated Sld2 is a novel mechanism to regulate origin firing" at the Eberhard Karls University Tuebingen in July 2013, which comprises the initial cycloheximide shut-off experiments with *wild-type* cells and kinase mutants presented in Figure 11, Figure 12, and Figure 13.

In vitro kinase experiments in Figure 16 and Figure 17 were performed and analyzed by Fabian Zimmermann (Pfander laboratory, Max Planck Institute of Biochemistry, Martinsried) as part of his Diploma thesis "Phosphorylation controls rapid turnover of a replication initiation protein" at the Eberhard Karls University Tuebingen in August 2014. Mass spectrometry samples were measured in collaboration with Dr. Nagarjuna Nagaraj (mass spectrometry core facility, Max Planck Institute of Biochemistry, Martinsried).

The plasmid loss assay in Figure 20 B as well as the initial peptide-pulldown experiments using GST-tagged constructs in Figure 23 D were contributed by Dr. Boris Pfander (Pfander laboratory, Max Planck Institute of Biochemistry, Martinsried).

The fluorescence anisotropy measurements, the micro-scale thermophoresis experiments, and the peptide-pulldown experiments using ^{HIS}Dma1^{FHA} in Figure 23 were performed and analyzed by Lorenzo Galanti (Pfander laboratory, Max Planck Institute of Biochemistry, Martinsried).

Preparation and sequencing of libraries for both experiments in Figure 36 were carried out by Dr. Marja Driessen (NGS core facility, Max Planck Institute of Biochemistry, Martinsried).

Trypsin-digested samples of the experiments in Figure 37 were measured and analyzed by Dr. Michael Wierer (Mann laboratory, Max Planck Institute of Biochemistry).

Discussion

Eukaryotic cells utilize many different molecular mechanisms to ensure that their genomes are copied precisely once during each cell cycle. Most importantly, DNA replication in eukaryotes is carried out as a two-step process with origin licensing occurring from late M to late G1 phase and origin firing occurring from S to M phase. The regulation of licensing factors has been intensively studied over the last two decades in several model organisms. These studies revealed that each of the participating protein complexes is targeted by at least one if not more molecular mechanisms [238]. Yet, we know comparatively little about the regulation of firing factors, particularly when it comes to higher eukaryotes. The best understanding has been attained in budding yeast, where three main regulators of firing factors have been characterized: CDK activates firing factors [30-32] and Rad53 as part of an activated DNA damage checkpoint response inhibits them [131,132]. Further research suggested a role for Cdc14 in the inactivation [93], however mechanistic details remained to be determined. We thus set out to investigate the regulatory mechanisms inactivating firing factors in M phase in more detail.

1. Gap phases and the cell cycle

While general cell cycle transitions behave like unidirectional, ultrasensitive switches [239,240], it is currently unclear how principal cell cycle regulation mechanisms are linked to the control of DNA replication. In general, transitions between replication phases could occur highly similar to transitions between cell cycle phases (Figure 57 A). However, such ultrasensitive switches would require the presence of feedback loops [241] and supporting experimental evidence for their existence has not been obtained so far. Thus, in the absence of feedback loops, transitions will occur more gradually (Figure 57 B). In such a scenario, it becomes difficult to keep the two molecular processes completely separate and cells might risk an overlap of licensing and firing phases that could give rise to genomic instability by sporadic over-replication (as discussed below). Yet, no matter if the transition occurs switch-like or gradually, cells could also avoid any potential overlap between licensing and firing phases by introducing a temporal order in the transition so that first one phase is inactivated before the next phase is activated (Figure 57 C). Even though still limited, there is mounting evidence that the regulation of replication phases could occur via ordered sequences of inactivation and activation. Our study now provided a comprehensive analysis of the inactivation and activation of replication factors in M phase.

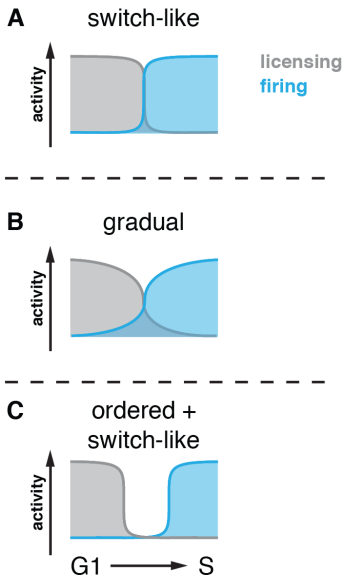

Figure 57 – Different models for transitions between replication phases. At the G1-S-transition cells finish origin licensing and commence origin firing. The transition between these two replication phases can in principle occur either (A) switch-like or (B) gradually. Furthermore, transitions can also be ordered if different regulators target licensing and firing factors with a temporal offset (C). Note the differences in potential overlap between licensing and firing phases depending on the type of transition as indicated by the shaded areas.

Based on the pivotal role of CDK phosphorylation in the regulation of replication factors, we first established a system to monitor these phosphorylation events during the cell cycle and elucidate the temporal regulation of replication phases in budding yeast (Figure 9 and Figure 10). This system revealed that activation and inactivation of replication factors occurs in a highly ordered manner, particularly during M phase. Cells first inactivate firing factors before they allow the re-activation of licensing factors and therefore separate these two processes with an intermittent gap phase. Such a temporal separation should in principle also be in place at the G1/S-transition, where licensing factors are inactivated first by G1-CDK and firing factors will only be activated later by S-CDK (Figure 7 and Figure 8). These gap phases ensure genomic stability by providing robustness to the regulation of replication. In the following, we therefore discuss how such gap phases can be generated on the molecular level (key mechanisms are highlighted in Figure 58).

1.1. Cyclin specificity and kinases in replication control

The regulation of DNA replication is tightly linked to the cyclin-dependent kinase CDK in budding yeast. CDK associates with its different regulatory cyclins at specific times during the cell cycle and gaps between cell cycle-regulated processes will therefore be explained by the intrinsic specificity of different cyclin-CDK complexes. Previous studies have characterized that cyclins can confer substrate specificity to CDK [170,242-244]. Indeed, this aspect of CDK regulation affects replication factors at the transition from G1 to S phase. It has been shown that G1-CDK (Cdc28 with Cln1/2 in budding yeast) can already phosphorylate and thereby inactivate the licensing factor Cdc6 as well as the Mcm2-7 complex [65,68,245]. An interaction between ORC and G1-CDK has also been reported, however it remains unclear if G1-CDK indeed phosphorylates ORC [246]. Yet, G1-CDK does not target the firing factors Sld2 and Sld3. These proteins require the

accumulation of S-CDK activity (Cdc28 with Clb5/6 in budding yeast) to become activated [30-32,72]. Thus, different cyclin-CDK complexes could order the inactivation and activation of replication factors at the G1/S-transition. Intriguingly, our phosphorylation shift-based experimental system was also able to recapitulate parts of this regulation in cycling cells (Figure 7 and Figure 8).

Interestingly, it is only S-CDK and not M-CDK that phosphorylates Sld2 and Sld3 efficiently. Cells lacking S phase cyclins Clb5 and Clb6 only achieve to phosphorylate about 50% of the Sld2 and Sld3 molecules at steady-state and also lose the phosphorylated species of these two proteins quickly if arrested in M phase (Figure 8 and data not shown). These data therefore emphasize the importance of cyclins for targeting the right CDK substrates at the right time and suggest that potent mechanisms counteract the CDK-phosphorylation of Sld2 and Sld3. Since licensing factors such as Orc6 or Cdc6 are targets of M-CDK (Cdc28 with Clb1/2 in budding yeast) [61,71,170], which is also present at later stages of M phase, cyclin specificity may thus also contribute to the generation of the gap in M phase.

It has been shown that multi-site modifications can in general introduce thresholds at transitions between two states [247-250]. Indeed, proteins involved in DNA replication are often phosphorylated at multiple sites [31,32,63,72,80,131,132,251] and, therefore, multi-site phosphorylation could also contribute to the generation of gap phases in the DNA replication program. Mathematical modelling of replication control at the G1/S-transition suggested that the requirement for multi-site phosphorylation of Sld2 and Sld3 for triggering origin firing could indeed sufficiently separate licensing and firing and thereby prevent over-replication [252]. However, it remains to be determined if modification of a protein on multiple sites or removal of these modifications also contributes in the same way to the separation of licensing and firing in M phase. Multisite phosphorylation of firing factors could for example facilitate an interaction with phosphatases or E3 ubiquitin ligases (see below) and thereby enable inactivation of origin firing in M phase prior to re-activation of origin licensing. Taken together, kinases are key regulators of DNA replication that enable robust control of replication through gap phases via their specificity and via multi-site modification of proteins.

1.2. Phosphatase-substrate interactions in replication control

Analogously to the regulation of the activity of replication factors by kinases, the removal of modifications by phosphatases is equally suited to generate gap phases. Studying phosphatases has been difficult due to the few experimental tools available and also in part due to the less specific interactions with substrates as compared to kinases. However, the mitotic phosphatase Cdc14 has previously been shown to target replication factors [93,94] and our data further extend this view (Figure 28). We observed that firing factors are more rapidly dephosphorylated compared to licensing factors. Interestingly, Cdc14 has been found to dephosphorylate its targets

in a specific order due to differential catalytic efficiency [187]. Consistent with our data, phosphorylated Orc6 has been found to be among the late targets of Cdc14 and therefore the gap phase in M phase could rely on the order of dephosphorylation imposed by the catalytic efficiency of Cdc14 towards its substrates. It is interesting to note in this context that such different efficiencies could in principle also be linked to multi-site modification of the substrates as discussed above, which may also serve to attract phosphatases. Furthermore, Cdc14 preferentially targets phospho-serines and binds to short peptide motifs on its substrates [188,253]. Therefore, these data suggest that the specific order for dephosphorylation could be encoded in the amino acid sequence of Cdc14's substrates. While being an important pathway to reverse CDK phosphorylation of substrates during the cell cycle in general, our experiments also clearly show that additional phosphatases must be involved in the regulation of replication proteins. In particular, dephosphorylation of firing factors is only marginally slower in a *cdc14-3* mutant thus suggesting that other phosphatases target these proteins very efficiently.

While Cdc14 is the predominant phosphatase for mitotic exit in budding yeast, protein phosphatase 1 (PP1) and protein phosphatase 2A (PP2A) are central regulators of mitosis in other organisms [254] and therefore constitute promising candidates to regulate replication factors also in budding yeast. Similar to Cdc14, PP2A in complex with its regulatory subunit Cdc55 has been implicated in ordering cell cycle phosphorylation events by preferentially dephosphorylating phospho-threonine residues [255]. Interestingly, origin firing critically requires phosphorylation of Sld2's threonine 84 and Sld3's threonine 600 by CDK [31,32,72]. While the contributions of individual phosphorylation sites on licensing factors has not been characterized in sufficient detail, many serine residues are in pivotal positions, e.g. at the nuclear import/export-switch for the Mcm2-7 complex [67]. It is thus tempting to speculate that PP2A-Cdc55 is involved in separating licensing from firing at the G1/S-transition by preferentially counteracting phosphorylation on critical threonine residues on firing factors. Even though the temporal resolution of our experiments is limited, our data do however not indicate that cells would enter S phase more quickly in the absence of Cdc55 (Figure 33). When studying cells in M phase, we also did not detect any effect on the gap between firing and licensing in *cdc55Δ* mutants (Figure 32). Even though redundancy with other phosphatases cannot be excluded, we conclude from these experiments that PP2A-Cdc55 does not play a major role in ordering replication phases and dephosphorylating firing factors prior to licensing factors in M phase.

Recently, it has been reported that PP1 in association with its targeting subunit Rif1 counteracts DDK-phosphorylation of the Mcm2-7 complex in G1 phase [83-85]. Even though this regulatory mechanism is mainly affecting the timing of origin firing locally, it might still contribute to the overall robustness of DNA replication control by helping to establish a general threshold for DDK activity. Despite the role of PP1-Rif1 in G1, it has not been assessed if PP1 also targets

replication proteins in other cell cycle phases. Our data provide a first evidence that PP1 in general is required for properly dephosphorylating replication factors in M phase (Figure 29). However, cells lacking *RIF1* still dephosphorylate firing factors rapidly in M phase (Figure 30 and Figure 31). Thus, PP1 probably engages with a different targeting subunit for this regulatory role and it will be crucial to identify this targeting subunit to obtain deeper insights into DNA replication control by phosphatase PP1.

In summary, either by shaping thresholds via efficiently counteracting kinases or by intrinsically dephosphorylating substrates with a different timing, phosphatases contribute to generating gap phases in the replication program. Unfortunately, our experimental tools to study phosphatases are more limited compared to the ones available to study kinases, so more work in this area will be needed to thoroughly address the contributions of phosphatases.

1.3. Degradation in DNA replication control

A specific order of events during the cell cycle can also be achieved by degradation of key proteins of interest. Central cell cycle regulators such as the CDK inhibitor Sic1 are for example targeted for degradation with an exquisite timing [249,256] and regulation of replication proteins by degradation is also a common theme.

In budding yeast, the most prominent example is licensing factor Cdc6. Multiple pathways target Cdc6 for degradation in G1-arrested cells and in S phase [68,213]. Rapid degradation of Cdc6 in late G1 phase is induced by G1-CDK and it is conceivable that Cdc6 is inactivated by this mechanism before cells begin to fire origins. Therefore, degradation of Cdc6 could generate a gap between licensing and firing at the G1/S-transition.

In M phase, the anaphase-promoting complex APC targets its substrates for degradation following a specific order [257,258]. Among the early substrates are the regulatory DDK subunit Dbf4 as well as S phase cyclin Clb5, which are both facilitating origin firing. Only at a later stage, the APC targets the major M phase cyclin Clb2, which facilitates the inhibition of origin licensing by several mechanisms. Thereby, the APC contributes to the temporal separation of firing and licensing during M phase.

Our study has identified a rapid and phosphorylation-mediated pathway that targets active Sld2 for degradation. This pathway is mediated by the ubiquitin ligases Dma1 and Dma2, which recognize a specific phosphorylation pattern on Sld2 (Figure 19, Figure 21, Figure 22, and Figure 23). As this phosphorylation-dependent degron is activated even prior to the APC, it ensures that firing and licensing are temporally separated by a gap phase at the transition in M phase. Intriguingly, rapid Sld2 degradation mediated by the same degron region also prevents aberrant DNA replication between meiotic divisions [259]. A related degron uses phosphorylation by CDK,

DDK and Mck1 but not Cdc5 to target the cohesion-establishing acetyltransferase Eco1 for degradation via SCF-Cdc4 precisely at the end of S phase [260-262]. Overall, these findings suggest that protein degradation is an effective mechanism to separate DNA replication phases.

Work in higher eukaryotes also suggests that degradation by the same ubiquitin-ligase could be used to order events during DNA replication: In human cells, the ubiquitin ligase Crl4-Cdt2 interacts with the replication factor PCNA and targets its substrates for degradation with different kinetics: Cdt1 is degraded first, while the G1/S- and S-CDK inhibitor p21 is only targeted later [263]. Even though the interpretation of these data is complicated by Crl4-Cdt2's requirement for DNA-bound PCNA and thus active replication, these data strongly suggest that origin licensing is stopped before S-CDK is fully activated and thus again indicate the presence of a gap phase. Despite these insights into the regulation of replication at the G1/S-transition in vertebrates, it remains unclear how firing factors are regulated during M phase in higher eukaryotes owing to our limited understanding of the control of origin firing in other organisms besides budding yeast. While it is likely that the substrate preferences of the APC resemble those in budding yeast and that regulation of DDK and cyclin levels plays a role, the critical regulators of origin firing first need to be identified in these organisms.

In summary, gap phases in the regulation of DNA replication are implemented at various levels. Protein degradation appears to be efficiently used to terminate a replication phase before the subsequent phase is about to start. In addition, endowing kinases and phosphatases with differential affinities towards their substrates ensures that the transitions between replication phases follow a precise order. Our data on the regulation of Sld2 suggest that proper regulation by kinases and phosphatases can still compensate for perturbed degradation (Figure 24 and Figure 25). A careful analysis of the interdependencies between these layers of regulation will be required to understand the roles of the regulatory gap phases within the replication program.

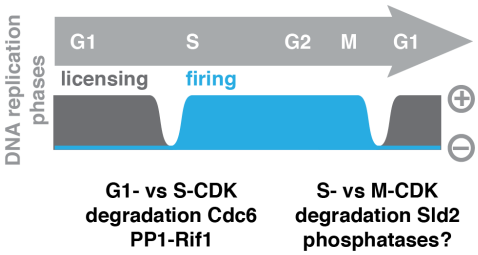

Figure 58 – Mechanisms contributing to the temporal separation of replication phases.
Origin licensing and origin firing are tightly coupled to different cell cycle phases. The specificity of CDK in complex with different cyclins as well as degradation of key replication factors such as Cdc6 or Sld2 generate such temporal separation. In addition, the phosphorylation states of replication factors and thus their activities are likely to be influenced by protein phosphatases.

2. Robust control by synergizing mechanisms

DNA replication initiates from many origins in order to facilitate a timely duplication of the genome. During a budding yeast S phase, replication initiates from approximately 400 origins and regulation at each of these origins needs to occur with a high accuracy to avoid over-replication [5,264]. Simple calculations can demonstrate how efficient this control needs to be [5]: Assuming a 99% efficient block to over-replication on the level of a single origin, this would mean that in budding yeast only 1.8% (= $(0.99)^{400}$) of S phases would occur without any over-replication. The problem would be even exacerbated when looking at human cells, which use approximately 50000 origins in S phase: Here, the ratio of S phases without any over-replication would be $(0.99)^{50000} = 6 \times 10^{-219}$. To ascertain that more than 99% of the S phases occur without any over-replication, the block to over-replication needs to achieve at least a 99.999% efficiency in budding yeast or 99.99999% efficiency in human cells [5]. This calculation highlights that the problem exponentially increases with genome size and that an even more robust control is required to replicate a larger genome. Obviously, achieving such a robust control with just one mechanism would be very difficult. However, combining multiple regulatory mechanisms can increase the efficiency and allows to synergistically block over-replication [63,139,140,149]. Multiple molecular mechanisms to regulate replication factors at the G1/S-transition have been described, comprising phosphorylation to block enzymatic activity, interactions with inhibitors, and degradation of key proteins. Furthermore, a specific licensing inhibitor called geminin is present in metazoans and constitutes an additional pathway to control replication. Yet, molecular mechanisms regulating firing factors were so far limited to activating and inhibiting phosphorylation.

Our study revealed a new regulatory mechanism affecting the firing factor Sld2. When cells enter M phase, Sld2 is targeted for degradation by a complex phosphorylation-dependent degron. At least four different kinases are required to generate a complex phosphorylation pattern on Sld2 that is recognized by the E3 ubiquitin ligases Dma1 and Dma2, which facilitate degradation of Sld2 with a precise timing. This molecular mechanism provides an additional pathway next to dephosphorylation to control the activity of firing factor Sld2 during M phase. Whether firing factors are also regulated through interactions with inhibitors is currently not known. However, the availability of multiple pathways to regulate firing factors suggests that these pathways synergize to robustly control Sld2 and thereby origin firing. Indeed, the stable *SLD2* mutants that were generated in the course of this study specifically perturbed the regulation of Sld2 in M phase but cells were still viable. Similar to mutations in pathways that regulate licensing factors [139,140], multiple mutations will likely need to be combined to affect viability indicating that these pathways can functionally backup each other. In this regard, it will be interesting to

disentangle the different contributions of these pathways and their relative importance. Our stable *SLD2* mutant will be a helpful tool in this endeavor.

Interestingly, it has also been shown that even though the same set of molecular mechanisms to regulate licensing factors is used in all model organisms, their specific targets differ even within the same genus [265]. Furthermore, regulatory mechanisms can be transplanted between licensing factors and thereby still allow robust replication control [265]. These data indicate that the precise target of a regulatory mechanism is probably less important than having such a mechanism available at all. In this regard, it will be interesting to see if rapid degradation of firing factors in M phase occurs also in other model organisms. Even though we are only beginning to understand how origin firing is regulated in model organisms apart from budding yeast, homologs of the critical CDK-regulated firing factors Dpb11, Sld2 and Sld3 are present in many eukaryotes and also interact with each other [266]. It is thus tempting to speculate that the complex *per se* could be regulated by the rapid degradation of one of the interacting partners.

In addition to molecular mechanisms directly affecting replication factors, replication control could also be exerted by controlling the accessibility of chromatin, which is the ultimate substrate of the replication factors. While the ORC complex binds to origins of replication throughout the cell cycle in budding yeast cells [267], higher eukaryotes dissociate ORC or some of its subunits from chromatin [268]. Intriguingly, a recent study in human cells has shown, that chromatin condensation mediated by methylation of lysine 20 on histone H4 can impose a threshold to restrict origin licensing during mitosis [269]. These data draw attention to the regulation of chromatin as another potent way to introduce a temporal control on DNA replication.

3. Differences between sporadic and overt over-replication

It has been a long-standing interest in the replication field to study the consequences of over-replication, i.e. repeated initiation from a subset of origins within the same cell cycle. In particular, over-replication caused in M phase by relieving licensing factors from CDK control has been studied in great detail in budding yeast [63,139,140]. Multiple characteristics and consequences of overt over-replication have been revealed by using this system [141,143-146]. Yet, overt over-replication is highly toxic and requires the deregulation of several controls at the same time.

As discussed before, the functional overlap between the molecular mechanisms controlling DNA replication provides a buffer in case one of the regulatory mechanisms is abrogated or fails. However, such a situation could give rise to sporadic over-replication as the probability for uncontrolled replication at a specific origin would be increased. As this lower amount might not be sufficient to activate the DNA damage checkpoint, this genomic instability might be a contributing factor during tumorigenesis where the control of the G1/S-transition is often affected [162-166].

In budding yeast, several systems are available to induce sporadic over-replication by partially deregulating either licensing factors [139,140,143] or firing factors [149,270]. Importantly, our stable *sld2* mutants provide the first tool to study the effect of deregulating replication specifically at transitions between licensing and firing.

Despite the availability of the experimental tools to study sporadic over-replication, there is a lack of sensitive methods to detect such rare events. Sporadic over-replication gives rise to intrinsically stochastic events that can occur throughout the genome. Physical assays such as the analysis of whole chromosomes by pulsed-field gel electrophoresis or Southern blots are not sensitive enough to resolve these events. The sensitivity of modern next-generation sequencing techniques would in principle be sufficient but so far genetic signatures that are unique to over-replication have not been characterized. Therefore, it will be a key challenge for the field to develop new methodology to sensitively detect over-replication and thereby facilitate the study of sporadic over-replication.

4. Characteristics and consequences of over-replication in G1

To advance the understanding of over-replication, we have established an experimental setup to induce and sensitively measure over-replication in G1 phase by flow cytometry and next-generation sequencing (Figure 35 and Figure 36). The utilization of EdU facilitates the quantification of our results as DNA synthesis can easily be compared to "normal" replication in S phase and allow us to obtain deeper mechanistic insights.

Consistent with previous studies [32,149], over-replication due to origin firing in G1 is highly toxic to the cells and leads to the accumulation of DNA damage. It has been speculated that origin firing might occur preferentially on specific chromosomes due to a high frequency of survivors that carried whole chromosome duplications [149]. Yet, our sequencing data demonstrate that all chromosomes are equally affected by origin firing in G1 phase on a population level (Figure 36 A). An under-representation of origins close to telomeres as well as an over-representation of origins close to centromeres is visible in our dataset and highlights that our system primarily recapitulates regular S phase replication timing [37,41,83-86].

Furthermore, we were able to demonstrate that replisomes assembled in G1 are highly similar to those assembled in S phase by using affinity purification combined with mass spectrometry [207]. Considering the central role of CDK phosphorylation in replication control, the replisomes that we recovered from G1 and S phase cells were remarkably similar. Interestingly, we observed one notable difference in the replisome composition: The cohesin complex associated with replisomes only in S and not G1 phase. Since cohesion between sister chromatids is normally established during DNA replication [209], this difference might provide an explanation for the observed slow progression through M phase (Figure 47) and genomic instability resulting from over-replication.

Despite the similar protein composition, replication in G1 phase appears to be less efficient than replication in S phase. While cells replicate their DNA within 20 min during a normal S phase, origin firing in G1 phase needs to be induced for at least 240 min to achieve the same amount of DNA synthesis. This difference could be explained in two different ways: Either DNA replication initiation occurs from fewer origins or replisomes progress slower in G1 phase. Indeed, our comparison of replisomes by mass spectrometry indicates that there are about four times more replisomes present in the S phase samples compared to our G1 phase replication setup (Figure 37). Since all origins can in principle contribute to replication in G1 phase (Figure 36), these data collectively demonstrate that replication initiation in G1 phase is less efficient than in S phase. Yet, there remains a discrepancy between the ten-times faster DNA synthesis in S phase but only four-times more replisomes. Therefore, it also seems plausible that replisomes in G1 phase progress with reduced speed. We hypothesized that other factors such as e.g. the cellular concentration of dNTPs could be limiting (Figure 41). However, upregulation of ribonucleotide reductase did not accelerate DNA synthesis in G1 phase. Another interesting hypothesis is that post-translational modifications such as CDK phosphorylation might be required to achieve full replication speed. Indeed, it has been shown that CDK phosphorylates DNA polymerases [271,272] and might thereby influence replication speed. Since the optimized *in vitro* replication reaction accurately reproduce the speed and efficiency of DNA replication *in vivo* [52-54], the contributions of CDK phosphorylation on different replisome components to overall replisome speed could be determined using this biochemical system. Similarly, DNA fiber analysis could yield detailed insights into the initiation pattern and replication fork speed *in vivo* after origin firing in G1 phase. Even though it remains to be determined why origin firing in G1 phase is less efficient, this experimental system allows us to efficiently induce over-replication and study its consequences.

Budding yeast cells do not detect over-replicated DNA in G1 phase. In line with a previous study [149], we observed hyperphosphorylation of Rad53 as a proxy for activation of the DNA damage checkpoint only later in the cell cycle after bulk replication was finished (Figure 42). Yet, our data also indicate, that a limited amount of DNA damage is already generated in G1 phase (Figure 38). In the course of our study, we thus aimed to elucidate where the delayed activation of the DNA damage checkpoint stems from.

5. No DNA damage checkpoint activation in G1

The DNA damage checkpoint monitors the integrity of DNA and arrests the cell cycle to facilitate adequate repair and prevent aggravation of the DNA damage. Previous studies have suggested that the DNA damage checkpoint distinguishes between different types and amounts of DNA damage [273-276]. In particular, resection of DNA double-strand breaks is strongly reduced in G1 phase cells [275,277] and therefore limits the amount of exposed single-stranded DNA.

Intriguingly, it has recently been shown that the DNA damage checkpoint comprises two distinct signaling circuits [235]: Local signaling as mediated by the γH2A modification is hardly influenced by the amount of exposed single-stranded DNA whereas global signaling via hyper-phosphorylated Rad53 quantitatively responds to this hallmark of DNA damage. Considering these findings, the low levels of γH2A signal that we detected in G1-arrested cells were probably not sufficient to trigger a robust checkpoint response (Figure 38). Notably, the γH2A signal only increases dramatically once cells commence S phase and replicate DNA (Figure 48 and Figure 49) indicating that it is not just the lack of DNA end resection in G1 phase cells but additional replication during S phase that leads to the increased γH2A signal, which indicates DNA damage.

Interestingly, when we hyper-sensitized checkpoint signaling by introducing a genetic fusion of *DDC1* and *RAD9*, we observed that these cells activate the DNA damage checkpoint in response to over-replication in G1 phase as read out by Rad53 hyper-phosphorylation (Figure 54). Yet, hyper-sensitized checkpoint signaling also led to a strong reduction of γH2A, most likely by inhibiting further origin firing and thus reducing the over-replication load. When these cells were released from the G1 arrest, hyper-phosphorylated Rad53 appeared to impose a block on origin firing and thereby slowed down overall DNA synthesis. Interestingly, hyper-sensitized checkpoint signaling also helped to largely avoid an increase of γH2A levels during S phase suggesting that these cells might be able to handle over-replicated DNA better (Figure 55 and Figure 56).

It remains to be determined if hyper-sensitized checkpoint signaling is beneficial for the cells with regards to over-replication. In the survival assays that we have performed (Figure 46), over-replication was equally toxic in wild-type and checkpoint-deficient cells. Yet, cells expressing *DDC1-RAD9*-fusion showed decreased levels of γH2A thus raising the possibility that the hyper-sensitized checkpoint signaling might render these cells less susceptible to over-replication by blocking it already at an early stage. Furthermore, there seems to be a dose-dependency between the toxicity of over-replication and the amount of copied DNA during the G1 arrest as judged by our results with a *mrc1Δ* mutant (compare Figure 43 and Figure 46). Cells lacking *MRC1* have been shown to replicate DNA less efficiently, but it is currently unclear if this is due to reduced origin firing or slower progression of replisomes. Since Rad53 activation in G1 phase via the *DDC1-RAD9-fusion* seems to inhibit origin firing (Figure 55), it appears from this perspective likely that survival of these cells could be increased even though they have to overcome a hyper-activated DNA damage checkpoint in order to proliferate.

6. Checkpoint activation after S phase

Despite the presence of minor DNA damage signals in over-replicating G1 phase cells, the DNA damage checkpoint is only activated and stops further cell cycle progression once cells have progressed through S phase. Interestingly, we observed that this checkpoint activation prevents cells from fully committing to mitosis (Figure 51). The active checkpoint most likely led to a transcriptional downregulation of mitotic genes [278]. Moreover, our data demonstrated that during S phase cells replicated their genomes further (Figure 45) but thereby generated additional DNA damage (Figure 48 and Figure 49) that ultimately triggered the activation of the DNA damage checkpoint. The lack of phosphorylation of Mms4 argues against a role of structure-specific nucleases in the generation of the DNA damage and highlights an interesting difference to the over-replication system in M phase-arrested cells [63]. In this system, replication forks would be exposed to active Mus81-Mms4, which could potentially cleave them and thereby generate DNA damage [224,227,279,280].

A similar timing of delayed checkpoint activation has been observed in other contexts as well. Cells lacking both topoisomerases Top1 and Top2 accumulate aberrant replication intermediates that result in hyper-phosphorylation of Rad53 [281]. In this case, the exonuclease Exo1 processes persistent replication forks and affects checkpoint activation. We considered that our over-replication system might give rise to replication forks that persist until M phase and could be processed similarly. However, unlike the *top1 top2* mutant, activation of the DNA damage checkpoint was not influenced by deletion of *EXO1* (data not shown) or even deletion of *EXO1* and *SGS1*, which results in a pronounced defect in DNA end resection.

Delayed activation of the DNA damage checkpoint in M phase was also observed after a transient arrest in S phase in cells expressing a mutant of the nuclease/helicase Dna2 [282,283]. In this scenario, replication forks are thought to undergo transitions during the arrest, which would normally be counteracted by Dna2. Interestingly, the DNA damage checkpoint arrests these cells in M phase. This arrest can eventually be overcome by the activation of the structure-specific endonuclease Yen1. However, origin firing in G1 phase seems to differ in several ways. Most prominently, deletion of the DNA damage checkpoint mediator *RAD9* has no beneficial effect on cellular survival (Figure 46) and mutation of various helicases and nucleases did not affect the timing of the activation of the DNA damage checkpoint (data not shown).

Overall, these studies demonstrate that diverse cellular scenarios could result in activation of the DNA damage checkpoint in M phase. It thus remains a critical question which DNA structures trigger its activation in response to over-replication and how the delayed timing is achieved. Our data on a mitotic CDK mutant (Figure 50) and on topoisomerase 1-deficient cells provide first hints into this direction.

7. Working model for DNA damage generation and checkpoint activation

Our data on over-replication in G1 phase can be integrated into one collective model (Figure 59). Whole chromosome duplications are tolerated as they can be recovered as survivors after a pulse of over-replication [149]. Thus, gene dosage or aneuploidy are probably not the major causes for cell death. In fact, a full round of replication in M phase is tolerated by cells without affecting their viability [147]. If over-replication generates partially replicated chromosomes, these replication structures could be converted to highly entangled structures containing recombination intermediates that might not be able to be resolved. However, our data argue against this model since blocking replication in S phase suppresses the generation of DNA damage and activation of the DNA damage checkpoint (Figure 48 and Figure 49).

The strong dependency on replication in S phase rather supports the following explanation for the generation of DNA damage: Over-replication in G1 could leave single-strand nicks or stretches of single-stranded DNA behind, which could give rise to double-strand breaks once a second replication forks in S phase encounters them [157,284]. Such nicks could for example stem from the mis-incorporation of ribonucleotides, which would be counteracted by topoisomerase 1 [230-234]. Deletion of *TOP1* would therefore suppress the generation of nicks and result in a reduced burden of DNA damage. Indeed, we observed decreased activation of the DNA damage checkpoint in response to over-replication in G1 (Figure 53). Consistent with this, head-to-tail collisions of replication forks traveling in the same direction could lead to fork breakage as previously shown in *Xenopus laevis* [156,285]. In principle, such collisions could already happen during over-replication in G1 phase, but might be relatively rare due to the slow speed and/or lower numbers of replisomes in G1 and thus escape detection, at least during the course of our experiments. Ultimately, such broken over-replication forks would give rise to single-ended double-strand breaks. Utilizing highly sensitive sequencing-based methods combined with analysis of full-length chromosomes by pulsed-filed gel electrophoresis will allow us to define the precise nature of these aberrant structures.

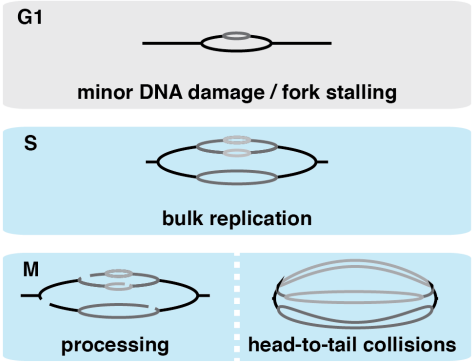

Figure 59 – Model for the cell cycle-specific response to DNA over-replication.
Over-replication in G1 directly triggers only minor DNA damage and bulk DNA replication in S phase occurs apparently unaffected. Yet, once cells enter mitosis, the DNA damage checkpoint is activated. This might either be due to processing of remaining terminally stalled replication forks or due to head-to-tail collisions of replication forks chasing previously initiated forks. A key challenge will be to reveal how the DNA damage is generated and how it triggers this very specific timing of DNA damage checkpoint activation is achieved.

Materials and Methods

If not stated otherwise explicitly, common chemicals and reagents were purchased from the following companies (in alphabetical order): BD Lifesciences, Bio-Rad, Cayman Chemicals, Greiner, Merck-Millipore, Roche, Roth, Serva, Sigma-Aldrich, Thermo Fisher Scientific, VWR.

1. Microbiology methods

All media were prepared using ultrapure water and were sterilized by autoclaving prior to use. Stock solutions of amino acids and sugars as well as small-scale preparations of buffers were sterilized by filtration.

E. coli media and buffers

LB medium (plates)	1%	tryptone	
	0.5%	yeast extract	
	1%	sodium chloride	
	(1.5%	agar)	
	for selection:	100 mg/ml	ampicillin
		30 µg/ml	kanamycin
		34 µg/ml	chloramphenicol
Inoue transformation buffer	10 mM	PIPES pH 6.7	
	250 mM	potassium chloride	
	55 mM	manganese chloride	
	15 mM	calcium chloride	

E. coli strains used in this study

strain	genotype	reference
XL-1 blue	*recA1 endA1 gyrA96 thi-1 supE44 relA1 hsdR17 lac [F´ proAB lacIqZΔM15 Tn10 (Tet^r)]*	Stratagene
BL-21 *pRIL*	*E. coli B F– ompT hsdS(rB– mB–) dcm+ Tet^r gal λ(DE3) endA Hte [argU ileY leuW Cam^r]*	Agilent Technologies
Stellar	*recA1 endA1 gyrA96 thi-1 supE44 relA1 phoA F– Φ80d lacZΔM15 Δ(lacZYA-argF) U169 Δ(mrr - hsdRMS - mcrBC) ΔmcrA λ–*	Clontech

***E. coli* plasmids used in this study**

plasmid	description	reference
pFZ025	pGEX-4T-1 *SLD2$^{1-150}$*	270
pFZ046	pGEX-4T-1 *SLD2$^{1-150}$ S128A*	270
pFZ047	pGEX-4T-1 *SLD2$^{1-150}$ S138A*	270
pFZ048	pGEX-4T-1 *SLD2$^{1-150}$ S128A S138A (2SA)*	270
pFZ051	pGEX-4T-1 *SLD2$^{1-150}$ T122A T143A (2TA)*	270
pKR245	pGEX-4T-1 *DMA1*	270
pKR314	pGEX-4T-1 *DMA1$^{FHA\ (1-298)}$*	270
pLG01	pET28a *DMA1$^{FHA(1-298)}$*	270

Cultivation and storage of *E. coli* cells

For short-term storage, *E. coli* cells were cultivated on agar plates and stored at 4 °C. For long-term storage, overnight cultures were supplemented with 15% glycerol (v/v) and kept at -80 °C. Overnight cultures or plates with *E. coli* cells were grown at 37 °C in LB medium or on LB plates supplemented with appropriate antibiotics. Cultures volumes of 5 ml were typically used for the preparation of plasmid DNA. For protein expression, *E. coli* cells where grown at lower temperatures such as 18 °C or 25 °C.

Preparation of chemically competent *E. coli* cells

Chemically competent *E. coli* cells were prepared according to the Inoue protocol [286]. Briefly, cells were grown at 18 °C to an OD_{600} of 0.55 and cooled down to 4 °C before washing and resuspending them in Inoue Transformation buffer supplemented with 7.5% DMSO and snap-freezing aliquots.

Transformation of *E. coli* cells

Chemically competent *E. coli* cells (50 µl) were thawed on ice and incubated with 2 µl of a cloning reaction for 15 min at 4 °C. Cells were then heat-shocked for 45 sec at 42 °C, supplemented with LB medium without antibiotics and left to recover for 30 min at 37 °C before plating them out on plates containing the appropriate selection.

S. cerevisiae media and buffers

YP medium (plates)	1%	yeast extract
	2%	bacto-peptone
	2%	glucose / galactose / raffinose
	(2 %	agar)
	for selection:	200 mg/l geneticin G418
		500 mg/l hygromycin B
		100 mg/l nourseothricin
SC medium (plates)	0.67%	yeast nitrogen base
	0.133%	master mix -8
	2%	glucose / galactose / raffinose
	as required	*Ade (22.5 mg/l), Leu (175 mg/l), His, Lys, Met, Arg, Ura, Trp (87.5 mg/l)*
	(2%	agar)
master mix -8	25 g	Ala, Asn, Asp, Cys, Gln, Glu, Gly, Ile, Phe, Pro, Ser, Thr, Tyr, Val
	25 g	myo-inositol
	2.5 g	para-aminobenzoic acid
SORB buffer	100 mM	lithium acetate
	10 mM	Tris-HCl, pH 8.0
	1 mM	EDTA pH 8.0
	1 M	sorbitol
PEG buffer	100 mM	lithium acetate
	10 mM	Tris-HCl, pH 8.0
	1 mM	EDTA pH 8.0
	40% (w/v)	PEG-3350
sporulation plates	0.2%	yeast extract
	1.2%	potassium acetate
	0.08%	glucose
	1.6%	agar
	1000 mg/l	Phe
	400 mg/l	Ade, Ura
	200 mg/l	His, Leu, Lys, Trp, Met, Arg
	80 mg/l	Tyr
zymolyase solution	0.5 mg/ml	zymolyase
	0.9 M	sorbitol
	100 mM	EDTA pH 8.0
	100 mM	Tris-HCl pH 8.0
	50 mM	dithiothreitol
FACS buffer	70%	ethanol
	50 mM	Tris-HCl pH 8.0
RNaseA buffer	50 mM	Tris-HCl pH 8.0
	0.38 mg/ml	RNase A
	0.38 mM	magnesium chloride

proteinase K buffer	50 mM	Tris-HCl pH 8.0
	1 mg/ml	proteinase K
	5%	glycerol
	2.5 mM	calcium chloride
SYTOX buffer	50 mM	Tris-HCl pH 8.0
	5 µM	SYTOX green

S. cerevisiae strains used in this study

strain	genotype	reference
W303a	*MATa ade2-1 ura3-1 his3-11,15 trp1-1 leu2-3,112 can1-100*	287
RH448	*MATa leu2 his4 lys2 ura3 bar1*	Jentsch lab
RC757	*MATα his6 met1 can1 cyh2 sst2-1*	Jentsch lab
L40	*MATα his3Δ200 trp1-901 leu2-3112 ade2 LYS2::(4 lexA$_{op}$-HIS3) URA3::(8 lexA$_{op}$-*lacZ) GAL4	Invitrogen
YKR554	W303a *SLD3-9myc::HIS3MX6 MCM3-3FLAG::hph-NT1*	270
YKR633	W303a *SLD3-9myc::HIS3MX6 MCM3-3FLAG::hph-NT1 cdc28-as1*	270
YKR575	W303a *SLD3-9myc::HIS3MX6 MCM3-3FLAG::hph-NT1 ura3::pGAL-SIC1ΔNT::URA3*	270
YKR617	W303a *SLD3-9myc::HIS3MX6 MCM3-3FLAG::hph-NT1 ura3::pGAL-SIC1ΔNT::URA3 clb5Δ::kanMX4 clb6Δ::nat-NT2*	270
YKR494	W303a *cdc14-3 cdc28-as1*	270
YKR503	W303a *sld2Δ::hph-NT1 SLD2(LEU2)*	270
YKR514	W303a *sld2Δ::hph-NT1 sld2$^{Δ100-150}$(LEU2)*	270
YKR516	W303a *sld2Δ::hph-NT1 sld2$^{Δ120-150}$(LEU2)*	270
YKR112	W303a *cdc28-as1*	270
JD2042	W303a *bob1-1::HIS3*	270
YKR102	W303a *bob1-1::HIS3 cdc7Δ::nat-NT2*	270
YKR090	W303a *mck1Δ::hph-NT1*	270
YKR162	W303a *pGALL-CDC5::kanMX4*	270
YFZ019	W303a *pep4Δ::LEU2 his3::MCK1-3FLAG-pGAL1-10-GAL4::HIS3*	270
YFZ020	W303a *pep4Δ::LEU2 his3::CDC5-3FLAG-pGAL1-10-GAL4::HIS3*	270
YFZ021	W303a *pep4Δ::hph-NT1 LEU2::GAL-DBF4-3FLAG::KanMx CDC7-myc::TRP1 HIS3::pGAL-GAL4*	270
YKR624	W303a *dma1Δ::TRP1*	270
YKR625	W303a *dma2Δ::TRP1*	270
YKR626	W303a *dma1Δ::TRP1 dma2Δ::HIS3MX6*	270

strain	genotype	reference
YKR640	L40 *dma1Δ::nat-NT2 dma2Δ::hph-NT1*	270
YKR685	W303a *CAN1::URA3 sld2Δ::hph-NT1 leu2::SLD2::LEU2*	270
YKR686	W303a *CAN1::URA3 sld2Δ::hph-NT1 leu2::sld2-2SA::LEU2*	270
YKR687	W303a *CAN1::URA3 sld2Δ::hph-NT1 leu2::sld2-2TA::LEU2*	270
YKR688	W303a *CAN1::URA3 sld2Δ::hph-NT1 leu2::sld2-4A::LEU2*	270
YKR689	W303a *CAN1::URA3 sld2Δ::hph-NT1 leu2::sld2-6A::LEU2*	270
YKR690	W303a *CAN1::URA3 SLD3-DPB11ΔN-fusion::kanMX4 sld2Δ::hph-NT1 leu2::SLD2::LEU2*	270
YKR691	W303a *CAN1::URA3 SLD3-DPB11ΔN-fusion::kanMX4 sld2Δ::hph-NT1 leu2::sld2-2SA::LEU2*	270
YKR692	W303a *CAN1::URA3 SLD3-DPB11ΔN-fusion::kanMX4 sld2Δ::hph-NT1 leu2::sld2-2TA::LEU2*	270
YKR693	W303a *CAN1::URA3 SLD3-DPB11ΔN-fusion::kanMX4 sld2Δ::hph-NT1 leu2::sld2-4A::LEU2*	270
YKR694	W303a *CAN1::URA3 SLD3-DPB11ΔN-fusion::kanMX4 sld2Δ::hph-NT1 leu2::sld2-6A::LEU2*	270
YKR396	W303a *sld2Δ::hph-NT1 leu2::sld2-2SA::LEU2*	270
YKR603	W303a *sld2Δ::hph-NT1 leu2::sld2-2TA::LEU2*	270
YKR607	W303a *sld2Δ::hph-NT1 leu2::sld2-4A::LEU2*	270
YKR612	W303a *sld2Δ::hph-NT1 leu2::sld2-6A::LEU2*	270
YKR787	W303a *ura3::pGAL-CDC5::URA3*	270
YKR897	W303a *CAN1::URA3 sml1Δ::HIS3MX6 mec1Δ::nat-NT2*	270
YKR847	W303a *CAN1::URA3 sml1Δ::HIS3MX6 mec1Δ::nat-NT2 sld2Δ::hph-NT1 leu2::sld2-6A::LEU2*	270
YKR872	W303a *CAN1::URA3 sld2Δ::hph-NT1 leu2::SLD2::LEU2 trp1::pGAL-DBF4::TRP1*	270
YKR873	W303a *CAN1::URA3 sld2Δ::hph-NT1 leu2::sld2-6A::LEU2 trp1::pGAL-DBF4::TRP1*	270
YKR809	W303a *CAN1::URA3 sld2Δ::hph-NT1 leu2::SLD2::LEU2 cdc6ΔNT::nat-NT2*	270
YKR810	W303a *CAN1::URA3 sld2Δ::hph-NT1 leu2::sld2-6A::LEU2 cdc6ΔNT::nat-NT2*	270
YKR510	W303a *cdc28-as1 SLD3-9myc::HIS3MX6*	this study
YKR1054	W303a *cdc28-as1 SLD3-9myc::HIS3MX6 glc7::LEU2 trp1::GLC7::TRP1*	this study
YKR1055	W303a *cdc28-as1 SLD3-9myc::HIS3MX6 glc7::LEU2 trp1::glc7-10::TRP1*	this study

strain	genotype	reference
YKR1056	W303a *cdc28-as1 SLD3-9myc::HIS3MX6 glc7::LEU2 trp1::glc7-12::TRP1*	this study
YKR898	W303a *cdc28-as1 SLD3-9myc::HIS3MX6 sld2-6A::hph-NT1*	this study
YKR916	W303a *cdc28-as1 SLD3-9myc::HIS3MX6 sld2-6A::hph-NT1 rif1Δ::nat-NT2*	this study
YKR309	W303a *SLD3-9myc::HIS3MX6*	this study
YKR967	W303a *SLD3-9myc::HIS3MX6 rif1Δ::nat-NT2*	this study
YKR901	W303a *cdc28-as1 SLD3-9myc::HIS3MX6 cdc55Δ::nat-NT2*	this study
YKR902	W303a *cdc28-as1 SLD3-9myc::HIS3MX6 sld2-6A::hph-NT1 cdc55Δ::nat-NT2*	this study
YKR607	W303a *leu2::sld2-4A::LEU2 sld2Δ::hph-NT1*	this study
YKR672	W303a *leu2::sld2-4A::LEU2 sld2Δ::hph-NT1 rts1Δ::HIS3MX6*	this study
YKR675	W303a *leu2::sld2-4A::LEU2 sld2Δ::hph-NT1 cdc55Δ::HIS3MX6*	this study
E3087	*MATa ade2-1 trp1-1 can1-100 leu2-3,112 his3-11,15 GAL psi+ RAD5+ ura3::URA3/pGPD-TK(5x) AUR1c::pADH-hENT1*	[205]
YKR1444	E3087 *leu2::SLD2-pGAL-DPB11::LEU2*	this study
YKR1445	E3087 *leu2::sld2-T84D-pGAL-DPB11::LEU2*	this study
YKR1447	E3087 *leu2::sld2-T84D-pGAL-DPB11::LEU2 his3::pGAL-DBF4::HIS3*	this study
YKR1500	E3087 *bar1Δ::nat-NT2*	this study
YKR1501	E3087 *leu2::SLD2-pGAL-DPB11::LEU2 bar1Δ::nat-NT2*	this study
YKR1502	E3087 *leu2::sld2-T84D-pGAL-DPB11::LEU2 bar1Δ::nat-NT2*	this study
YKR1503	E3087 *leu2::sld2-T84D-pGAL-DPB11::LEU2 his3::pGAL-DBF4::HIS3 bar1Δ::nat-NT2*	this study
YKR1546	E3087 *pep4Δ::kanMX4*	this study
YKR1558	E3087 *pep4Δ::kanMX4 PSF2-yeGFP::hph-NT1*	this study
YKR1553	E3087 *leu2::sld2-T84D-pGAL-DPB11::LEU2 his3::pGAL-DBF4::HIS3 bar1Δ::nat-NT2 pep4Δ::kanMX4*	this study
YKR1557	E3087 *leu2::sld2-T84D-pGAL-DPB11::LEU2 his3::pGAL-DBF4::HIS3 bar1Δ::nat-NT2 pep4Δ::kanMX4 PSF2-yeGFP::hph-NT1*	this study
YKR1603	E3087 *leu2::sld2-T84D-pGAL-DPB11::LEU2 bar1Δ::nat-NT2 his3::pGAL-dbf4-mut.D-box (R10A L13A R62A L65A)::HIS3*	this study
YKR1516	E3087 *bar1Δ::nat-NT2 his3::CDC6-pGAL-DBF4::HIS3*	this study
YKR1517	E3087 *bar1Δ::nat-NT2 leu2::sld2-T84D-pGAL-DPB11::LEU2 his3::CDC6-pGAL-DBF4::HIS3*	this study
YKR1625	E3087 *bar1Δ::nat-NT2 his3::RNR1-pGAL::HIS3*	this study

strain	genotype	reference
YKR1626	E3087 *bar1Δ::nat-NT2 his3::RNR1-pGAL::HIS3 leu2::sld2-T84D-pGAL-DPB11::LEU2*	this study
YKR1614	E3087 *bar1Δ::nat-NT2 his3::RNR1-pGAL-DBF4::HIS3 leu2::sld2-T84D-pGAL-DPB11::LEU2*	this study
YKR1209	W303a *leu2::pGAL-DPB11-VN::LEU2 ura3::pGAL-SLD2::URA3*	this study
YKR1210	W303a *leu2::pGAL-DPB11-VN::LEU2 ura3::pGAL-sld2-T84D::URA3*	this study
YKR1371	W303a *leu2::pGAL-DPB11-VN::LEU2 ura3::pGAL-sld2-T84D::URA3 his3::pGAL-DBF4::HIS3*	this study
YKR1256	W303a *leu2::pGAL-DPB11-VN::LEU2 ura3::pGAL-SLD2::URA3 mrc1Δ::hph-NT1*	this study
YKR1257	W303a *leu2::pGAL-DPB11-VN::LEU2 ura3::pGAL-sld2-T84D::URA3 mrc1Δ::hph-NT1*	this study
YKR1258	W303a *leu2::pGAL-DPB11-VN::LEU2 ura3::pGAL-SLD2::URA3 rad9Δ::hph-NT1*	this study
YKR1259	W303a *leu2::pGAL-DPB11-VN::LEU2 ura3::pGAL-sld2-T84D::URA3 rad9Δ::hph-NT1*	this study
YKR1396	W303a *leu2::pGAL-DPB11-VN::LEU2 ura3::pGAL-SLD2::URA3 csm3Δ::nat-NT2*	this study
YKR1397	W303a *leu2::pGAL-DPB11-VN::LEU2 ura3::pGAL-sld2-T84D::URA3 csm3Δ::nat-NT2*	this study
YKR1398	W303a *leu2::pGAL-DPB11-VN::LEU2 ura3::pGAL-SLD2::URA3 tof1Δ::nat-NT2*	this study
YKR1399	W303a *leu2::pGAL-DPB11-VN::LEU2 ura3::pGAL-sld2-T84D::URA3 tof1Δ::nat-NT2*	this study
YKR1438	W303a *RAD5+ leu2::pGAL-DPB11-VN::LEU2 ura3::pGAL-SLD2::URA3*	this study
YKR1455	W303a *RAD5+ leu2::pGAL-DPB11-VN::LEU2 ura3::pGAL-sld2-T84D::URA3 his3::pGAL-DBF4::HIS3*	this study
YKR1485	W303a *leu2::pGAL-DPB11-VN::LEU2 ura3::pGAL-SLD2::URA3 trp1::pTDH3-TIR1-9myc::TRP1 cdc45-AID(internal loop)::nat-NT2*	this study
YKR1486	W303a *leu2::pGAL-DPB11-VN::LEU2 ura3::pGAL-sld2-T84D::URA3 trp1::pTDH3-TIR1-9myc::TRP1 cdc45-AID(internal loop)::nat-NT2*	this study
YKR1487	W303a *leu2::pGAL-DPB11-VN::LEU2 ura3::pGAL-sld2-T84D::URA3 his3::pGAL-DBF4::HIS3 trp1::pTDH3-TIR1-9myc::TRP1 cdc45-AID(internal loop)::nat-NT2*	this study
YKR1526	E3087 *trp1::pGPD-TIR1-3myc::TRP1 sld3-3aid*::hph-NT1*	this study
YKR1527	E3087 *trp1::pGPD-TIR1-3myc::TRP1 sld3-3aid*::hph-NT1 leu2::SLD2-pGAL-DPB11::LEU2*	this study
YKR1528	E3087 *trp1::pGPD-TIR1-3myc::TRP1 sld3-3aid*::hph-NT1 leu2::sld2-T84D-pGAL-DPB11::LEU2*	this study

strain	genotype	reference
YKR1529	E3087 *trp1::pGPD-TIR1-3myc::TRP1 sld3-3aid*::hph-NT1 leu2::sld2-T84D-pGAL-DPB11::LEU2 his3::pGAL-DBF4::HIS3*	this study
YKR1476	E3087 *leu2::SLD2-pGAL-DPB11::LEU2 clb2Δ::nat-NT2*	this study
YKR1477	E3087 *leu2::sld2-T84D-pGAL-DPB11::LEU2 clb2Δ::nat-NT2*	this study
YKR1478	E3087 *leu2::sld2-T84D-pGAL-DPB11::LEU2 his3::pGAL-DBF4::HIS3 clb2Δ::nat-NT2*	this study
YKR1616	E3087 *MMS4-3FLAG::nat-NT2*	this study
YKR1617	E3087 *leu2::SLD2-pGAL-DPB11::LEU2 MMS4-3FLAG::nat-NT2*	this study
YKR1618	E3087 *leu2::sld2-T84D-pGAL-DPB11::LEU2 MMS4-3FLAG::nat-NT2*	this study
YKR1619	E3087 *leu2::sld2-T84D-pGAL-DPB11::LEU2 his3::pGAL-DBF4::HIS3 MMS4-3FLAG::nat-NT2*	this study
YKR1473	E3087 *leu2::SLD2-pGAL-DPB11::LEU2 dia2Δ::nat-NT2*	this study
YKR1474	E3087 *leu2::sld2-T84D-pGAL-DPB11::LEU2 dia2Δ::nat-NT2*	this study
YKR1475	E3087 *leu2::sld2-T84D-pGAL-DPB11::LEU2 his3::pGAL-DBF4::HIS3 dia2Δ::nat-NT2*	this study
YKR1324	E3087 *leu2::pGAL-DPB11-VN::LEU2 ura3::pGAL-SLD2::URA3 top1Δ::nat-NT2*	this study
YKR1325	E3087 *leu2::pGAL-DPB11-VN::LEU2 ura3::pGAL-sld2-T84D::URA3 top1Δ::nat-NT2*	this study
YKR1538	E3087 *trp1::DDC1-RAD9-3FLAG::TRP1*	this study
YKR1540	E3087 *leu2::sld2-T84D-pGAL-DPB11::LEU2 trp1::DDC1-RAD9-3FLAG::TRP1*	this study
YKR1541	E3087 *leu2::sld2-T84D-pGAL-DPB11::LEU2 his3::pGAL-DBF4::HIS3 trp1::DDC1-RAD9-3FLAG::TRP1*	this study
YKR1564	E3087 *trp1::DDC1-RAD9-3FLAG::TRP1 bar1Δ::nat-NT2*	this study
YKR1566	E3087 *leu2::sld2-T84D-pGAL-DPB11::LEU2 trp1::DDC1-RAD9-3FLAG::TRP1 bar1Δ::nat-NT2*	this study
YKR1567	E3087 *leu2::sld2-T84D-pGAL-DPB11::LEU2 his3::pGAL-DBF4::HIS3 trp1::DDC1-RAD9-3FLAG::TRP1 bar1Δ::nat-NT2*	this study

***S. cerevisiae* plasmids used in this study**

plasmid	description	reference
YCplac33	empty vector	288
pKR032	YCplac111 *pSLD2-SLD2*	270
pKR169	YCplac111 *pSLD2-SLD2$^{\Delta 100-150}$*	270
pKR170	YCplac111 *pSLD2-SLD2$^{\Delta 120-150}$*	270
pKR001	pRS406 *cdc28-as1* (F88G, lacks ATG)	270
pFZ029	pRS303 *MCK1-3FLAG pGAL1-10 GAL4*	270
pFZ030	pRS303 *CDC5-3FLAG pGAL1-10 GAL4*	270
pKR202	pACT2 *DPB11 (GAL4-AD-DPB11)*	270
pKR261	pACT2 *DMA1 (GAL4-AD-DPB11)*	270
pKR265	pACT2 *DMA1^{RING*} (C345S H350A)*	270
pKR290	pACT2 *DMA1$^{RING* +FHA1*}$ (S220A H223L C345S H350A)*	270
pKR291	pACT2 *DMA1$^{RING* +FHA2*}$ (G192E C345S H350A)*	270
pKR204	pBTM116 *SLD2 (lexA-BD-SLD2)*	270
pKR276	pBTM116 *sld2-2SA (S128A S138A)*	270
pKR277	pBTM116 *sld2-2TA (T122A T143A)*	270
pKR278	pBTM116 *sld2-4A (T122A S128A S138A T143A)*	270
pKR279	pBTM116 *sld2-6A (T122A S124A S128A S137A S138A T143A)*	270
pKR016	YIplac128 *pSLD2-SLD2*	270
pKR064	YIplac128 *pSLD2-sld2-2SA (S128A S138A)*	270
pKR226	YIplac128 *pSLD2-sld2-2TA (T122A T143A)*	270
pKR228	YIplac128 *pSLD2-sld2-4A (T122A S128A S138A T143A)*	270
pKR231	YIplac128 *pSLD2-sld2-6A (T122A S124A S128A S137A S138A T143A)*	270
pKR087	YIplac211 *CAN1*	270
pKR004	YIplac204 *pGAL-DBF4*	this study
pKR005	YIplac211 *pGAL-SLD2*	this study
pKR006	YIplac211 *pGAL-sld2-T84D*	this study
pKR520	pRS303 *pGAL-DBF4*	this study
pKR547	pRS303 *CDC6-pGAL-DBF4*	this study
pKR562	pRS303 *RNR1-pGAL-DBF4*	this study

plasmid	description	reference
pKR531	pRS303 *pGAL-dbf4-RL10,13AA RL62,65AA (D-box)*	this study
pKR497	YIplac128 *pGAL-DPB11-VN*	this study
pKR534	YIplac128 *SLD2-pGAL-DPB11*	this study
pKR535	YIplac128 *sld2-T84D-pGAL-DPB11*	this study
pKR563	pRS303 *RNR1-pGAL*	this study
pKR551	pFA6a-hph-NT1 *3aid**	this study
pKR537	YIplac204 *cdc45-AID(internal loop)*	this study
pKR548	pRS304 *pGPD-OsTIR1-3myc*	this study
pKR561	YIplac204 *DDC1-RAD9-3FLAG*	this study

Cultivation and storage of *S. cerevisiae* cells

For short-term storage, *S. cerevisiae* cells were cultivated on agar plates and stored at 4 °C. For long-term storage, overnight cultures were supplemented with 15% glycerol (v/v) and kept at -80 °C. Routinely, plates and liquid cultures were grown at 30 °C. Strains harboring temperature-sensitive alleles (*cdc14-3*, *glc7-10*, *glc7-12*) were grown at 25 °C (permissive temperature) and shifted to 37 °C (restrictive temperature) typically for two hours. Experiments were only performed in logarithmically growing cells (OD_{600} 0.5 - 1.0).

Genetic modification of *S. cerevisiae* cells

Standard yeast techniques were applied to introduce genetic modifications into *S. cerevisiae* cells. Integrative plasmids were linearized prior to transformation and single integration of plasmids were confirmed by PCR. Gene deletions and tags were introduce using a PCR-based protocol [289].

Drugs used with *S. cerevisiae* cells

Cell cycle arrests were induced when cultures reached OD_{600} 0.6 by adding 5 µg/ml mating pheromone α-factor (G1 phase arrest), 200 mM hydroxyurea (early S phase arrest), or 5 µg/ml nocodazole (M phase arrest) for about 90 min at 30 °C. Arrests were also confirmed using a microscope. The CDK-allele *cdc28-as1* was inhibited by treating cells with 3 µM 1NM-PP1 [168]. To deplete cells of a protein coupled to an auxin-inducible degron (AID), 3 mM indole-3-acetic acid (IAA) were added to the medium [219-221]. DNA synthesis was assessed by adding 100 µM EdU to the medium [205]. Finally, protein translation was inhibited by adding 500 µg/ml cycloheximide (CHX) to the growing *S. cerevisiae* cultures.

Preparation of competent *S. cerevisiae* cells

Cells were grown in YPD to OD_{600} 0.6, washed first with sterile water, then with SORB buffer and were then resuspended in SORB buffer supplemented with 1 mg/ml denatured herring sperm DNA. Aliquots (100 µl) of the competent cells were frozen and stored at -80 °C.

Transformation of *S. cerevisiae* cells

One aliquot of competent cells was incubated with 10 µl precipitated PCR product or linearized plasmid and six volumes of PEG buffer for 30 min at room temperature. Subsequently, DMSO was added to a final concentration of 10% and the cells were heat-shocked for 15 min at 42 °C. Depending on the needs for selection, cells were either plated out directly (auxotrophy markers) or were left to recover in YPD for three hours (antibiotic markers), before they were plated out. Single transformed colonies were picked and streaked on selective plates two to three days after the transformation.

Mating, sporulation and tetrad dissection

Cells of opposite mating types were mixed, spotted on YPD plates and incubated at 30 °C for at least three hours. Subsequently, zygotes were selected based on their characteristic shape using the micromanipulator of the tetrad microscope (Singer MSM 300 system) and grown at 30 °C.

Diploid cells were streaked on sporulation plates and incubated for at least three days at 30 °C (or at a lower temperature if required). Material from the sporulation plate was resuspended in water and 10 µl of this resuspension were digested with an equal volume of zymolyase solution for 10 min at room temperature. The digested tetrads were subsequently spread on YPD plates and subjected to tetrad dissection (Singer MSM 300 system).

Cell cycle analysis by flow cytometry

About 10^7 cells were harvested by centrifugation, resuspended in FACS buffer for fixation, and stored at 4 °C for at least one hour. Afterwards cells were digested with RNAseA buffer overnight at 37 °C and with proteinase K buffer for 30 min at 50 °C. Afterwards, cells were resuspended in 50 mM Tris-HCl pH 8.0 and sonicated. Sonicated cells were diluted 1:20 with SYTOX buffer and measured on a MACSquant analyzer flow cytometer (Miltenyi Biotec). Data was analyzed and plotted using FlowJo v.10.5.3 (FlowJo LLC).

Measuring DNA synthesis by EdU incorporation / click chemistry reaction

EdU-incorporating Cells were incubated with 100 µM EdU for the intended amount of time and afterwards processed as samples for cell cycle analysis by flow cytometry. The samples were afterwards incubated in PBS supplemented with 1% BSA for one hour and then split. One half was subjected to a click chemistry reaction with disulfo-Cy5-picolyl-azide (Jena Bioscience) for one hour, whereas the other half was kept as a control. A click chemistry reaction for 10^7 cells (1 OD) comprised 36 µl PBS, 2 µl freshly prepare 1 M ascorbic acid, 2 µl 1 M $CuSO_4$ and 0.5 µl disulfo-Cy5-picolyl-azide. After the click chemistry reaction, the cells were washed twice with 10% ethanol in PBS before they were resuspended in PBS. Both the click chemistry reaction and the control sample were diluted 1:20 with SYTOX buffer and measured on a MACSquant analyzer flow cytometer (Miltenyi Biotec). Data was analyzed and plotted using FlowJo v.10.5.3 (FlowJo LLC).

Preparation of cells for isolation of EdU-biotin labeled DNA

Cells were grown in 100 ml YPD to OD_{600} 0.6 before starting the cell cycle arrest and induction of replication by either expression of firing factors or releasing cells to early S phase. EdU was added to the growth medium when replication was induced to label all newly synthesized DNA. Cells were harvested by centrifugation, fixed with FACS buffer protected from light for at least one hour at 4 °C, and then digested with 25 ml RNaseA buffer overnight at 37 °C. Next, cells were washed and digested with 10 ml proteinase K buffer for one hour at 50 °C and subsequently incubated with 25 ml PBS supplemented with 1% BSA for another hour at room temperature. The cells were afterwards subjected to an upscaled click chemistry reaction with biotin-picolyl-azide (Jena Bioscience) for one hour at room temperature and washed twice with 10% ethanol in PBS afterwards. Finally, the cells were stored in 10% ethanol in PBS protected from light at 4 °C until they were used for DNA preparation (see below).

Spotting assays

Pre-cultures were grown to stationary phase overnight. Starting at OD_{600} 0.5, dilution series (5 steps, 1:5) were prepared from these cultures and spotted on YPD plates.

Yeast two-hybrid analysis

Episomal plasmids for the expression of proteins of interest fused to a *GAL4*-transcriptional activator domain or a *lexA*-DNA binding domain were co-transformed into yeast two-hybrid strain L40 or YKR640 (L40 *dma1Δ dma2Δ*) and grown under selective pressure for both plasmids. Cells from the transformation plates were resuspended in PBS, adjusted to OD_{600} 0.5, spotted in 1:5 dilution series on control plates (SC-Leu-Trp) or plates lacking histidine (SC-Leu-Trp-His) and grown for two to three days at 30 °C.

Plasmid loss assay

Cells were transformed with the ARS/CEN plasmid YCplac33 and grown to saturation in selective SC-Ura medium. Fresh non-selective YPD medium was inoculated with 10^5 cells and grown to saturation (approximately 11 generations). Serial dilutions of this stationary culture were prepared and plate on YPD as well as SC-Ura plates. Colonies were counted after incubation for two days at 30 °C and the mean plasmid loss rate per generation was calculated from two or three independent experiments.

Gross chromosomal rearrangement assay

Rates of gross chromosomal rearrangements were determined following a protocol from the Kolodner lab [180]. Briefly, pre-cultures of *S. cerevisiae* cells harboring a *CAN1::URA3* reporter on chromosome V were grown in SC-Ura medium and plated out on YPD plates so that colonies could form from single cells. For each condition at least eight colonies were excised from the plates and used to inoculate larger cultures in YPD (typically 50 ml, *SD-fusion* strains 2 ml), which were grown to stationary phase. The number of viable cells in these cultures by plating a serial dilution (10^{-6}) on non-selective YPD plates. The total number of GCR events was determined by plating the remaining culture on SC-Arg plates that were supplemented with the drugs L-canavanine (50 mg/L) and 5'-fluoroorotic acid (1000 mg/L) to select against both *CAN1* and *URA3*. No more than 10^9 cells were spread on each plate and the plates were incubated at 30 °C for two days (YPD) and three to five days (selection). Afterwards, the clones were counted and GCR rates as well as confidence intervals were calculated by fluctuation analysis using the web tool FALCOR [290-292].

2. Molecular biology methods

Standard molecular biology protocols have been used throughout this study [293]. Oligonucleotides were purchased from Eurofins Genomics; restriction enzymes and dNTPs were purchased from New England Biolabs; Phusion and Pfu Turbo polymerases were either from Thermo Fisher Scientific or replaced with an optimized Pfu polymerase purified at the MPIB core facility.

Buffers and solutions

TE buffer	10 mM	Tris-HCl pH 8.0
	1 mM	EDTA pH 8.0
DNA loading buffer (5x)	0.5%	SDS
	0.25%	orange G
	25%	glycerol
	25 mM	EDTA pH 8.0
TAE buffer	40 mM	Tris pH 7.6
	20 mM	acetic acid
	1 mM	EDTA pH 8.0
breaking buffer	2%	Triton X-100
	1%	SDS
	100 mM	sodium chloride
	10 mM	Tris-HCl pH 8.0
	1 mM	EDTA pH 8.0
2x WB buffer (dilute with TE buffer)	10 mM	Tris-HCl pH 8.0
	10 mM	EDTA pH 8.0
	1 M	sodium chloride
	0.02%	NP-40
E buffer	10 mM	Tris-HCl pH 8.0
	10 mM	EDTA pH 8.0
	0.1%	SDS

Small scale preparation of plasmid DNA

Small cultures (typically 5 ml) of LB medium containing the appropriate antibiotic were inoculated with an *E. coli* colony and grown overnight at 37 °C. Plasmid DNA was isolated from these cells using the AccuPrep Plasmid Mini Extraction Kit (Bioneer) following the instructions of the manufacturer.

Ethanol precipitation of DNA

The DNA containing solution was mixed with 0.1 volumes 3 M sodium acetate pH 4.8 and 2.5 volumes absolute ethanol and incubated for at least 30 min at -20 °C. The precipitated DNA was pelleted by centrifugation, dried, and resuspended in an appropriate amount of TE buffer or water.

Restriction digests

The DNA sample (2 µg) was digested in a 30 µl reaction with 5 U restriction enzymes (New England Biolabs) according to the instructions of the manufacturer for one to two hours at 37 °C. Afterwards, digested DNA was analyzed by agarose gel electrophoresis.

Agarose gel electrophoresis

DNA samples were mixed with DNA loading buffer and routinely separated on 1% agarose gels containing ethidium bromide (0.5 µl / 10 ml gel) in TAE buffer. Bands were visualized using a UV-light gel documentation system.

Agarose gel extraction

Bands of interest were excised from agarose gels and purified using a gel extraction kit (Clontech) following the manufacturer's instructions.

Standard polymerase chain reaction (PCR)

The PCR programs CASTORP and Phusion were used for routine tasks such as amplification of cassettes for introducing tags or deletions into yeast cells as well as for the confirmation of these modifications.

standard PCR reaction

2 µl	template
3.2 µl	primer 1 (10 µM)
3.2 µl	primer 2 (10 µM)
1.75 µl	dNTPs (10 mM)
10 µl	HF-buffer
1 µl	DMSO
0.5 µl	Phusion polymerase
28.35 µl	water

PCR program CASTORP

(1) 95 °C for 4 min
(2) 95 °C for 1 min
(3) 45 °C for 35 sec
(4) 72 °C for 1:40 min
repeat steps (2)-(4) for 10 cycles
(5) 95 °C for 1 min
(6) 54 °C for 30 sec
(7) 72 °C for 1:40 min
repeat steps (5)-(7) for 20 cycles and
increase extension time by 20 sec each cycle
(8) hold at 4 °C

PCR program Phusion

(1) 98 °C for 30 sec
(2) 98 °C for 30 sec
(3) 58 °C for 30 sec
(4) 72 °C for 2 min
repeat steps (2) to (4) for 35 cycles
(5) 72 °C for 5 min
(6) hold at 4 °C

Site-directed mutagenesis

Two complementary mutagenic oligonucleotides were used to introduce the intended mutation(s) by PCR (reaction and program below). Afterwards, the PCR mix was digested with restriction enzyme DpnI (New England Biolabs) for one hour at 37 °C and subsequently transformed into competent *E. coli* cells.

mutagenesis PCR reaction	
0.5 µl	template (25 µg/ml)
0.63 µl	primer 1 (10 µM)
0.63 µl	primer 2 (10 µM)
0.63 µl	dNTPs (10 mM)
2.5 µl	10x Pfu buffer
0.5 µl	Pfu Turbo polymerase
19.6 µl	water

mutagenesis PCR program	
(1)	95 °C for 3 min
(2)	95 °C for 30 sec
(3)	55 °C for 60 sec
(4)	68 °C for 2 min / kb plasmid
repeat steps (2)-(4) for 20 cycles	
(5)	hold at 4 °C

Sanger sequencing of PCR products or purified plasmids

Samples that were prepared according to the instructions of the Mix2Seq kit were sent to Eurofins Genomics for sequencing. Sequences were subsequently analyzed using ApE v2.053c (Wayne Davis, http://jorgensen.biology.utah.edu/wayned/ape/).

Molecular cloning

Most vectors were cloned using the InFusion HD cloning kit (Clontech) according to the manual. Inserts were amplified from previously cloned plasmids or from genomic DNA of *S. cerevisiae* using standard PCR reactions. Vectors (5 µg) were digested with two restriction enzymes for at least three hours at 37 °C. Inserts and digested vectors were purified from agarose gel, then assembled into the correct product with the InFusion enzyme mix for 1 hour at 50 °C. This strategy allowed to introduce up to four inserts into a vector in one step.

Alternatively, 30 fmol inserts and 10 fmol vectors were ligated by T4 ligase (New England Biolabs) in a 60 min reaction at room temperature. Finally, the InFusion reaction or T4 ligation reaction was transformed into chemical competent *E. coli* cells.

Isolation of genomic DNA from *S. cerevisiae* cells

A stationary overnight culture (10 ml YPD) of *S. cerevisiae* cells was harvested by centrifugation, transferred to a microcentrifuge tube and resuspended in breaking buffer supplemented with glass beads and mixed with an equal volume of phenol/chloroform/isoamyl alcohol. Cells were lysed by vortexing at highest speed for 3 min. After addition of one volume TE buffer, the aqueous layer was transferred to a fresh tube and precipitated using ethanol. The precipitate was resuspended in TE buffer and incubated with 30 µg RNaseA for 5 min at 37 °C. Next the digested DNA was precipitated by addition of 0.1 volumes of 1 M ammonium acetate and 2.5 volumes

absolute ethanol. After centrifugation, the precipitated DNA pellet was dried and resuspended in 100 µl TE buffer.

Preparation of DNA for next-generation sequencing

After processing with RNaseA and proteinase K followed by introducing a biotin-tag to EdU via click chemistry (see above), cells were resuspended in breaking buffer and lysed with MM301 bead beaters (Retsch). DNA from this lysate was sheared to 300 bp fragments using a BioRuptor UCD-200 sonifier (Diagenode). Cell debris were removed by high-speed centrifugation and DNA from the supernatant was isolated by ethanol precipitation, resuspended in TE buffer. Labeling of the DNA with biotin was confirmed in dot blots using HRP-coupled streptavidin for detection and the size distribution of DNA fragments was analyzed by agarose gel electrophoresis.

DNA-immunoprecipitation via EdU-biotin

Equal amounts (approx. 700 ng) of sheared, EdU-biotin-labeled DNA were mixed 1:1 with 2x WB buffer supplemented with 1 mg/ml BSA and incubated with 25 µl of magnetic Dynabeads M-280 streptavidin (Thermo Fisher Scientific) for 30 min at room temperature. The beads were washed five times for 5 min with 1x WB buffer. Subsequently, the beads were eluted twice with 100 µl buffer EB for one hour at 55 °C. The eluates were pooled, purified by phenol/chloroform/isoamyl alcohol extraction and precipitated in the presence of 50 µg/ml GlycoBlue coprecipitant (Invitrogen) with sodium acetate and absolute ethanol. After drying, the pellet was resuspended in 20 µl TE buffer.

Analysis of DNA replication by next-generation sequencing

Previously published protocols [294,295] have been adapted to fit our experimental requirements. Sequencing libraries were prepared by the MPIB core-facility using the NEBNext Ultra II DNA library prep kit (New England Biolabs) and the libraries were subjected to paired-end sequencing with 75 bp read length on an Illumina NextSeq 500 sequencer. Approximately 9 million de-multiplexed sequencing reads were obtained per condition. Quality checks were performed with FastQC (Simon Andrews, https://www.bioinformatics.babraham.ac.uk/projects/fastqc/) and the reads were aligned to the budding yeast reference genome sacCer3 (RefSeq assembly GCF_000146045.2, hosted at NCBI, provided by SGD [296] using the Burrows-Wheeler aligner bwa [297]. Alignments were sorted and indexed using SAMtools [298]. The bamCoverage, bamCompare and bigwigCompare tools of the deepTools2 software suite [299] were used to analyze the coverage of genomic regions in 1000 bp bins and compare them between samples / normalize them to input controls. The resulting bigWig files visualized using the integrative genomics viewer IGV 2.5.2 [300,301] and are presented on a $\log_2$ scale. Origins of replications were used as annotated in OriDB [2].

3. Biochemistry methods

Buffers and solutions

HU buffer	8 M	urea
	5%	SDS
	200 mM	Tris-HCl pH 6.8
	1.5%	DTT
	traces	bromophenolblue
MOPS buffer	50 mM	MOPS
	50 mM	Tris base
	0.1%	SDS
	1 mM	EDTA pH 8.0
	adjust to pH 7.7	
MES buffer	50 mM	MES
	50 mM	Tris base
	0.1%	SDS
	1 mM	EDTA pH 8.0
TA buffer	50 mM	tricine
	50 mM	Tris base
	0.1%	SDS
	adjust to pH 8.24	
SDS buffer	25 mM	Tris base
	192 mM	glycine
	0.1%	SDS
transfer buffer	48 mM	Tris base
	39 mM	glycine
	0.0375%	SDS
	20%	methanol
superblotto	2.5%	skim milk powder in TBS
	0.5%	bovine serum albumin
	0.5%	NP-40
	0.1%	Tween-20
western wash buffer	0.2%	NP-40 in TBS
PBS	10 mM	phosphate buffer pH 7.4
	137 mM	sodium chloride
	2.7 mM	potassium chloride
lysis buffer	100 mM	HEPES-KOH pH 7.9
	50 mM	potassium acetate
	10 mM	magnesium acetate
	2 mM	EDTA pH 8.0
glycerol mix buffer	100 mM	HEPES-KOH pH 7.9
	300 mM	potassium acetate
	10 mM	magnesium acetate
	2 mM	EDTA pH 8.0
	50%	glycerol
	0.5%	NP-40

inhibitors	2 mM	sodium fluoride
	2 mM	β-glycerophosphate
	1 mM	DTT
	1 cOmplete protease inhibitor (Roche) tablet per 25 ml buffer	
IP wash buffer	100 mM	HEPES-KOH pH 7.9
	100 mM	potassium acetate
	10 mM	magnesium acetate
	2 mM	EDTA pH 8.0
	10%	glycerol
	(+ 0.1%	NP-40)
elution buffer I	2 M	urea
	50 mM	Tris-HCl pH 7.5
	2 mM	DTT
	20 µg/ml	trypsin
elution buffer II	2 M	urea
	50 mM	Tris-HCl pH 7.5
	10 mM	chloroacetamide
kinase buffer	100 mM	potassium acetate
	10 mM	HEPES-KOH pH 7.6
	50 mM	β-glycerophosphate
	10 mM	magnesium chloride
	5 mM	magnesium acetate
	2 mM	β-mercaptoethanol
2x Laemmli	160 mM	Tris-HCl pH 6.8
	20%	glycerol
	7%	SDS
	500 mM	β-mercaptoethanol
	traces	bromophenolblue
binding buffer A	200 mM	potassium acetate
	100 mM	HEPES-KOH pH 7.6
	0.02%	NP-40
	2 mM	β-mercaptoethanol
	10%	glycerol
binding buffer B	100 mM	potassium acetate
	100 mM	HEPES-KOH pH 7.6
	0.02%	NP-40
	2 mM	β-mercaptoethanol
	10%	glycerol
binding buffer C	500 mM	potassium acetate
	100 mM	HEPES-KOH pH 7.6
	0.02%	NP-40
	2 mM	β-mercaptoethanol
	10%	glycerol
FLA buffer	170 mM	sodium chloride
	50 mM	Tris-HCl pH 7.5
	10%	glycerol
	0.02%	NP-40
	2 mM	β-mercaptoethanol

MST buffer	170 mM	sodium chloride
	50 mM	Tris-HCl pH 7.5
	10%	glycerol
	0.02%	tween-20
	1%	BSA
	2 mM	β-mercaptoethanol

Denatured whole cell lysates by TCA precipitation

Approximately $2x10^7$ cells were harvested by centrifugation and snap-frozen in liquid nitrogen. Afterwards, cells were resuspended in 1 ml water, supplemented with 150 µl 1.85 M NaOH and 7.5% β-mercaptoethanol and incubated for 15 min at 4 °C. Subsequently, 150 µl 55% tri-chloroacetic acid (TCA) were added for 10 min at 4 °C, before collecting the pellet, resuspending it in 50 µl HU buffer, and heating it for 10 min at 65 °C.

Gel electrophoresis

Protein samples were loaded on NuPAGE 12% or 4-12% Bis-Tris acrylamide gels (Invitrogen) and run for one hour at 200 V with MOPS buffer or MES buffer, according to the proteins that needed to be separated. To resolve phosphorylated isoforms of Orc6 and Rad53, standard 10% acrylamide gels were poured and run with SDS buffer. To resolve phosphorylated isoforms of Sld3 and Mcm3, 6% acrylamide supplemented with PhosTag ligand AAL-107 (Wako Chemicals) were prepared and handled following the instructions of the manufacturer.

Western blot techniques

After gel electrophoresis, proteins were transferred to nitrocellulose membrane using a tank blot system and methanol-containing transfer buffer. The transfer was carried out at 4 °C with 90 V for 1:30 hours. After transfer, primary antibodies were diluted in Superblotto and added to the membranes for incubation overnight at 4 °C. After washing once for 5 min with western wash buffer, secondary antibodies (diluted 1:3000 in superblotto) were added for 90 min at room temperature. For detection of the immune-blots, Pierce ECL western blotting substrate (Thermo Fisher Scientific) was added following the manufacturer's instructions and chemiluminescence was detected using a LAS-300 CCD camera system (Fujifilm).

Intensities of bands in blots were measured using the Fiji-distribution of ImageJ [302,303]. Data from cycloheximide chase experiments were fitted with an exponential function. For determining the timepoint where 50% of a specific replication protein was phosphorylated, a logistic function was fitted to the data points using Origin Pro 8.0 (OriginLab).

Antibodies used in this study

antibody	target protein	host organism	reference
JD147	Rad53	rabbit	John Diffley
sc-6733	Cdc5	goat	Santa Cruz
sc-9071	Clb2	rabbit	Santa Cruz
F1804	FLAG-tag	mouse	Sigma-Aldrich
PZ45	Sld2	rabbit	Philip Zegerman
SB49	Orc6	mouse	Bruce Stillman
4A6	myc-tag	mouse	Millipore
9H8/5	Cdc6	mouse	Abcam
22C5D8	Pgk1	mouse	Invitrogen
sc-459	GST	rabbit	Santa Cruz
sc-1663	Gal4-AD	mouse	Santa Cruz
sc-5705	Dbf4	goat	Santa Cruz
06-719	lexA-BD	rabbit	EMD Millipore
sc-9996 (B-2)	GFP	mouse	Santa Cruz
ab15083	γH2A	rabbit	Abcam
ab104232	Rad53	rabbit	Abcam
ab653	Pol30	rabbit	Stefan Jentsch
a0050	Cdc45	rabbit	Pfander lab
M214-3	miniAID-tag	mouse	MBL / Biozol
F7425	FLAG-tag	rabbit	Sigma-Aldrich

Microscale thermophoresis

The N-terminus of (phosphorylated) Sld2-peptides was labeled with 5-/6-carboxyfluorescein (mixed isomers). Increasing concentrations of ^{HIS}Dma1^{FHA} were incubated with 20 nM of labeled peptides in MST-buffer for one hour at 4 °C and measured on a Monolith NT.115 (NanoTemper Technologies) using the blue filter set, 20% MST power, 40% LED power, pre-/post-MST period of 5 sec, MST acquisition time of 30 sec, standard treated capillaries at room temperature. Data were analyzed using Affinity Analysis (MST) v2.0.2 (NanoTemper Technologies) and plotted using non-linear fitting with a one-site binding model.

Fluorescence anisotropy measurements

The N-terminus of (phosphorylated) Sld2-peptides was labeled with 5-/6-carboxyfluorescein (mixed isomers). Increasing concentrations of ^{HIS}Dma1^{FHA} were incubated with 10 nM of labeled peptides in FLA-buffer for one hour at 4 °C. On a Genios Pro (Tecan) and using an excitation wavelength of 485 nm, ten reads were measured for each titration point in triplicates with an integration time of 40 µs at 535 nm (emission). The BIOEQS software [306] was used to analyze polarization data by non-linear regression fitting with a one-site binding model.

Protein purification

Detailed purification strategies for the proteins used in this study have been published as supplemental material to our paper [270]. Briefly summarized, GST-tagged proteins Sld2$^{1-150}$, Dma1 and Dma1^{FHA} were affinity-purified from *E. coli* extracts via glutathione Sepharose 4 FF (GE Healthcare) and subsequent anion exchange chromatography on a MonoQ 5/50 GL column (GE Healthcare). HIS-tagged Dma1^{FHA} was purified via NiNTA agarose beads (Qiagen), subjected to size exclusion chromatography on a HiLoad 16/600 Superdex 200 pg column (GE Healthcare) and subsequently to cation exchange chromatography on a MonoS 5/50 GL column (GE Healthcare). The kinases Mck1, Cdc5 and DDK were overexpressed in and purified from *S. cerevisiae* extracts via FLAG tag strategy. Mck1 and Cdc5 were affinity-purified using FLAG-M2 agarose beads (Sigma-Aldrich) and afterwards subjected to anion exchange chromatography on a MonoQ 5/50 GL column. DDK was also affinity-purified using FLAG-M2 beads. While being bound to the beads, DDK was additionally treated with lambda-phosphatase to remove inhibitory phosphorylation and subjected to size exclusion chromatography on a Superdex 200 GL 10/300 column (GE healthcare) before anion exchange chromatography.

In vitro kinase assays using purified ^{GST}Sld2$^{1-150}$

Kinase assays were performed as described previously [304,305]. GST and GST-coupled Sld2 (20 pmol) were bound to glutathione affinity beads (GE healthcare, Themo Fisher Scientific) in kinase buffer together with 10 pmol kinase and 5 µg BSA. Reactions were started by adding 1 mM ATP + 5 µCi γ[^{32}P]-ATP (PerkinElmer) and incubated for 30 min at 30 °C. Reactions were stopped by adding 2x Laemmli buffer and boiling for 10 min. Proteins were separated by gel electrophoresis and analyzed by staining with Coomassie Brilliant Blue and by detecting an autoradiogram with a Typhoon FLA 9500 imager (GE healthcare).

For sequential phosphorylation assays, reactions were performed as described but omitting γ[^{32}P]-ATP. After incubation for 30 min at 30 °C, beads were recovered and washed with binding buffer A and binding buffer B to remove contaminants before starting the second kinase reaction as described above.

In vitro kinase assays using (phosphorylated) peptides

Dynabeads M-280 streptavidin (Thermo Fisher Scientific) were equilibrated in binding buffer C and incubated with a saturating dose of desthio-biotinylated peptides. Unbound peptides were removed by washing twice with binding buffer C, followed by washing once with binding buffer B. Kinase assays were performed with these beads as described above.

Peptide pulldowns

A saturating amount of desthio-biotinylated peptides was coupled to Dynabeads M-280 streptavidin (Sigma) in binding buffer C. Beads were washed twice with binding buffer C, before 1 µg GST together with 1 µg ^{GST}Dma1 or 1 µg ^{GST}Dma1^{FHA} in binding buffer C were added for one hour. After washing four times, beads were eluted by boiling in Laemmli buffers. Peptide pulldowns with ^{GST}Dma1^{FHA} were performed with binding buffer A instead of binding buffer C.

Immuno-precipitation of replisomes

Cells were grown under the conditions of interest and killed by the addition of 0.1% NaN_3. Subsequently, the culture was harvested by centrifugation and first washed with 10 mM HEPES-KOH pH 7.9 before washing with lysis buffer and resuspending the pellet in three ml of lysis buffer including protease inhibitors per grams of cell pellet. This resuspension was used to prepare yeast popcorn by snap-freezing it drop-by-drop in liquid nitrogen. The yeast popcorn was ground to fine powder using a cryogenic mill (SPEX SamplePrep system).

The yeast powder was thawed and supplemented with 0.25 volumes glycerol mix buffer to obtain an extract with 10% glycerol, 100 mM potassium acetate and 0.1% NP-40. After incubation with 800 U/ml SmDNase (MPIB core facility) for 30 min at 4 °C, the extract was cleared by centrifugation. The protein concentration was measured using a standard Bradford assay and, after adjusting the concentrations, the extracts were used directly for immunoprecipitation.

Agarose GFP-trap beads (Chromotek) were equilibrated with IP wash buffer including NP-40 and then incubated with 30 mg of total protein for two hours at 4 °C. Per sample, 20 µl of the GFP-trap slurry were used. After this incubation, the beads were washed three times with IP wash buffer including NP-40 and two times with IP wash buffer lacking NP-40. With the last wash step, the beads were transferred to a new microcentrifuge tube and eluted in two steps using elution buffer I for 30 min at 37 °C and elution buffer II for 5 min at 37 °C. The eluates were pooled and handed over to our collaborator Michael Wierer in the laboratory of Matthias Mann for measurement and analysis using MaxQuant and Perseus software [307-309].

References

1. Luo, H. & Gao, F. DoriC 10.0: an updated database of replication origins in prokaryotic genomes including chromosomes and plasmids. *Nucleic Acids Research* **47,** D74–D77 (2018).
2. Siow, C. C., Nieduszynska, S. R., Muller, C. A. & Nieduszynski, C. A. OriDB, the DNA replication origin database updated and extended. *Nucleic Acids Research* **40,** D682–D686 (2011).
3. Bell, S. D. in *DNA Replication* (eds. Masai, H. & Foiani, M.) **1042,** 99–115 (Springer Singapore, 2018).
4. Marks, A. B., Fu, H. & Aladjem, M. I. in *DNA Replication* (eds. Masai, H. & Foiani, M.) **1042,** 43–59 (Springer Singapore, 2018).
5. Diffley, J. F. Quality control in the initiation of eukaryotic DNA replication. *Philosophical Transactions of the Royal Society B: Biological Sciences* **366,** 3545–3553 (2011).
6. Alver, R. C., Chadha, G. S. & Blow, J. J. The contribution of dormant origins to genome stability: From cell biology to human genetics. *DNA Repair* **19,** 182–189 (2014).
7. Bell, S. P. & Labib, K. Chromosome Duplication in Saccharomyces cerevisiae. *Genetics* **203,** 1027–1067 (2016).
8. Bell, S. P. & Stillman, B. ATP-dependent recognition of eukaryotic origins of DNA replication by a multiprotein complex. *Nature* **357,** 128–134 (1992).
9. Diffley, J. F. & Cocker, J. H. Protein-DNA interactions at a yeast replication origin. *Nature* **357,** 169–172 (1992).
10. Rowles, A., Tada, S. & Blow, J. J. Changes in association of the Xenopus origin recognition complex with chromatin on licensing of replication origins. *Journal of Cell Science* **112 (Pt 12),** 2011–2018 (1999).
11. Natale, D. A., Li, C. J., Sun, W. H. & DePamphilis, M. L. Selective instability of Orc1 protein accounts for the absence of functional origin recognition complexes during the M-G(1) transition in mammals. *EMBO J.* **19,** 2728–2738 (2000).
12. Okuno, Y., McNairn, A. J., Elzen, den, N., Pines, J. & Gilbert, D. M. Stability, chromatin association and functional activity of mammalian pre-replication complex proteins during the cell cycle. *EMBO J.* **20,** 4263–4277 (2001).
13. Li, C. J. & DePamphilis, M. L. Mammalian Orc1 Protein Is Selectively Released from Chromatin and Ubiquitinated during the S-to-M Transition in the Cell Division Cycle. *Mol. Cell. Biol.* **22,** 105–116 (2002).
14. Sun, J. *et al.* Cryo-EM structure of a helicase loading intermediate containing ORC-Cdc6-Cdt1-MCM2-7 bound to DNA. *Nat. Struct. Mol. Biol.* **20,** 944–951 (2013).
15. Yuan, Z. *et al.* Structural basis of Mcm2-7 replicative helicase loading by ORC-Cdc6 and Cdt1. *Nat. Struct. Mol. Biol.* **24,** 316–324 (2017).
16. Ticau, S., Friedman, L. J., Ivica, N. A., Gelles, J. & Bell, S. P. Single-molecule studies of origin licensing reveal mechanisms ensuring bidirectional helicase loading. *Cell* **161,** 513–525 (2015).
17. Evrin, C. *et al.* A double-hexameric MCM2-7 complex is loaded onto origin DNA during licensing of eukaryotic DNA replication. *Proc. Natl. Acad. Sci. U.S.A.* **106,** 20240–20245 (2009).
18. Remus, D. *et al.* Concerted loading of Mcm2-7 double hexamers around DNA during DNA replication origin licensing. *Cell* **139,** 719–730 (2009).
19. Coster, G. & Diffley, J. F. X. Bidirectional eukaryotic DNA replication is established by quasi-symmetrical helicase loading. *Science* **357,** 314–318 (2017).
20. On, K. F. *et al.* Prereplicative complexes assembled in vitro support origin-dependent and independent DNA replication. *EMBO J.* **33,** 605–620 (2014).
21. Gros, J., Devbhandari, S. & Remus, D. Origin plasticity during budding yeast DNA replication in vitro. *EMBO J.* **33,** 621–636 (2014).

22. Walter, J. & Newport, J. Initiation of eukaryotic DNA replication: origin unwinding and sequential chromatin association of Cdc45, RPA, and DNA polymerase alpha. *Mol. Cell* **5,** 617–627 (2000).
23. Tercero, J. A., Labib, K. & Diffley, J. F. DNA synthesis at individual replication forks requires the essential initiation factor Cdc45p. *EMBO J.* **19,** 2082–2093 (2000).
24. Aparicio, O. M., Weinstein, D. M. & Bell, S. P. Components and dynamics of DNA replication complexes in S. cerevisiae: redistribution of MCM proteins and Cdc45p during S phase. *Cell* **91,** 59–69 (1997).
25. Aparicio, O. M., Stout, A. M. & Bell, S. P. Differential assembly of Cdc45p and DNA polymerases at early and late origins of DNA replication. *Proc. Natl. Acad. Sci. U.S.A.* **96,** 9130–9135 (1999).
26. Takayama, Y. *et al.* GINS, a novel multiprotein complex required for chromosomal DNA replication in budding yeast. *Genes Dev.* **17,** 1153–1165 (2003).
27. Pacek, M., Tutter, A. V., Kubota, Y., Takisawa, H. & Walter, J. C. Localization of MCM2-7, Cdc45, and GINS to the Site of DNA Unwinding during Eukaryotic DNA Replication. *Mol. Cell* **21,** 581–587 (2006).
28. Gambus, A. *et al.* GINS maintains association of Cdc45 with MCM in replisome progression complexes at eukaryotic DNA replication forks. *Nat. Cell Biol.* **8,** 358–366 (2006).
29. Moyer, S. E., Lewis, P. W. & Botchan, M. R. Isolation of the Cdc45/Mcm2–7/GINS (CMG) complex, a candidate for the eukaryotic DNA replication fork helicase. *Proc. Natl. Acad. Sci. U.S.A.* **103,** 10236–10241 (2006).
30. Masumoto, H., Muramatsu, S., Kamimura, Y. & Araki, H. S-Cdk-dependent phosphorylation of Sld2 essential for chromosomal DNA replication in budding yeast. *Nature* **415,** 651–655 (2002).
31. Zegerman, P. & Diffley, J. F. X. Phosphorylation of Sld2 and Sld3 by cyclin-dependent kinases promotes DNA replication in budding yeast. *Nature* **445,** 281–285 (2007).
32. Tanaka, S. *et al.* CDK-dependent phosphorylation of Sld2 and Sld3 initiates DNA replication in budding yeast. *Nature* **445,** 328–332 (2007).
33. Yardimci, H., Loveland, A. B., Habuchi, S., van Oijen, A. M. & Walter, J. C. Uncoupling of Sister Replisomes during Eukaryotic DNA Replication. *Mol. Cell* **40,** 834–840 (2010).
34. Fu, Y. V. *et al.* Selective Bypass of a Lagging Strand Roadblock by the Eukaryotic Replicative DNA Helicase. *Cell* **146,** 931–941 (2011).
35. Raghuraman, M. K. *et al.* Replication dynamics of the yeast genome. *Science* **294,** 115–121 (2001).
36. Yabuki, N., Terashima, H. & Kitada, K. Mapping of early firing origins on a replication profile of budding yeast. *Genes Cells* **7,** 781–789 (2002).
37. Mantiero, D., Mackenzie, A., Donaldson, A. & Zegerman, P. Limiting replication initiation factors execute the temporal programme of origin firing in budding yeast. *EMBO J.* **30,** 4805–4814 (2011).
38. Tanaka, S., Nakato, R., Katou, Y., Shirahige, K. & Araki, H. Origin Association of Sld3, Sld7,and Cdc45 Proteins Is a Key Stepfor Determination of Origin-Firing Timing. *Current Biology* **21,** 2055–2063 (2011).
39. Kamimura, Y., Tak, Y. S., Sugino, A. & Araki, H. Sld3, which interacts with Cdc45 (Sld4), functions for chromosomal DNA replication in Saccharomyces cerevisiae. *EMBO J.* **20,** 2097–2107 (2001).
40. Kanemaki, M. & Labib, K. Distinct roles for Sld3 and GINS during establishment and progression of eukaryotic DNA replication forks. *EMBO J.* **25,** 1753–1763 (2006).
41. Natsume, T. *et al.* Kinetochores coordinate pericentromeric cohesion and early DNA replication by Cdc7-Dbf4 kinase recruitment. *Mol. Cell* **50,** 661–674 (2013).
42. Fang, D. *et al.* Dbf4 recruitment by forkhead transcription factors defines an upstream rate-limiting step in determining origin firing timing. *Genes Dev.* **31,** 2405–2415 (2017).
43. Maric, M., Maculins, T., De Piccoli, G. & Labib, K. Cdc48 and a ubiquitin ligase drive disassembly of the CMG helicase at the end of DNA replication. *Science* **346,** 1253596 (2014).

44. Moreno, S. P., Bailey, R., Campion, N., Herron, S. & Gambus, A. Polyubiquitylation drives replisome disassembly at the termination of DNA replication. *Science* **346,** 477–481 (2014).
45. Dewar, J. M., Budzowska, M. & Walter, J. C. The mechanism of DNA replication termination in vertebrates. *Nature* **525,** 345–350 (2015).
46. Dewar, J. M., Low, E., Mann, M., Räschle, M. & Walter, J. C. CRL2Lrr1 promotes unloading of the vertebrate replisome from chromatin during replication termination. *Genes Dev.* **31,** 275–290 (2017).
47. Sonneville, R. *et al.* CUL-2LRR-1 and UBXN-3 drive replisome disassembly during DNA replication termination and mitosis. *Nat. Cell Biol.* **19,** 468–479 (2017).
48. Priego Moreno, S., Jones, R. M., Poovathumkadavil, D., Scaramuzza, S. & Gambus, A. Mitotic replisome disassembly depends on TRAIP ubiquitin ligase activity. *Life Sci. Alliance* **2,** e201900390–12 (2019).
49. Deng, L. *et al.* Mitotic CDK Promotes Replisome Disassembly, Fork Breakage, and Complex DNA Rearrangements. *Mol. Cell* **73,** 915–929.e6 (2019).
50. Heller, R. C. *et al.* Eukaryotic origin-dependent DNA replication in vitro reveals sequential action of DDK and S-CDK kinases. *Cell* **146,** 80–91 (2011).
51. Yeeles, J. T. P., Deegan, T. D., Janska, A., Early, A. & Diffley, J. F. X. Regulated eukaryotic DNA replication origin firing with purified proteins. *Nature* **519,** 431–435 (2015).
52. Kurat, C. F., Yeeles, J. T. P., Patel, H., Early, A. & Diffley, J. F. X. Chromatin Controls DNA Replication Origin Selection, Lagging-Strand Synthesis, and Replication Fork Rates. *Mol. Cell* **65,** 117–130 (2017).
53. Devbhandari, S., Jiang, J., Kumar, C., Whitehouse, I. & Remus, D. Chromatin Constrains the Initiation and Elongation of DNA Replication. *Mol. Cell* **65,** 131–141 (2017).
54. Yeeles, J. T. P., Janska, A., Early, A. & Diffley, J. F. X. How the Eukaryotic Replisome Achieves Rapid and Efficient DNA Replication. *Mol. Cell* **65,** 105–116 (2017).
55. Douglas, M. E., Ali, F. A., Costa, A. & Diffley, J. F. X. The mechanism of eukaryotic CMG helicase activation. *Nature* **555,** 265–268 (2018).
56. Taylor, M. R. G. & Yeeles, J. T. P. The Initial Response of a Eukaryotic Replisome to DNA Damage. *Mol. Cell* **70,** 1067–1080.e12 (2018).
57. Taylor, M. R. G. & Yeeles, J. T. P. Dynamics of Replication Fork Progression Following Helicase-Polymerase Uncoupling in Eukaryotes. *Journal of Molecular Biology* **431,** 2040–2049 (2019).
58. Deegan, T. D., Baxter, J., Ortiz Bazan, M. A., Yeeles, J. T. P. & Labib, K. P. M. Pif1-Family Helicases Support Fork Convergence during DNA Replication Termination in Eukaryotes. *Mol. Cell* **74,** 231–244.e9 (2019).
59. Duzdevich, D. *et al.* The Dynamics of Eukaryotic Replication Initiation: Origin Specificity, Licensing, and Firing at the Single- Molecule Level. *Mol. Cell* **58,** 483–494 (2015).
60. Ticau, S. *et al.* Mechanism and timing of Mcm2-7 ring closure during DNA replication origin licensing. *Nat. Struct. Mol. Biol.* **24,** 309–315 (2017).
61. Detweiler, C. S. & Li, J. J. Ectopic induction of Clb2 in early G1 phase is sufficient to block prereplicative complex formation in Saccharomyces cerevisiae. *Proc. Natl. Acad. Sci. U.S.A.* **95,** 2384–2389 (1998).
62. Wilmes, G. M. Interaction of the S-phase cyclin Clb5 with an 'RXL' docking sequence in the initiator protein Orc6 provides an origin-localized replication control switch. *Genes Dev.* **18,** 981–991 (2004).
63. Nguyen, V. Q., Co, C. & Li, J. J. Cyclin-dependent kinases prevent DNA re-replication through multiple mechanisms. *Nature* **411,** 1068–1073 (2001).
64. Chen, S. & Bell, S. P. CDK prevents Mcm2-7 helicase loading by inhibiting Cdt1 interaction with Orc6. *Genes Dev.* **25,** 363–372 (2011).
65. Labib, K., Diffley, J. F. & Kearsey, S. E. G1-phase and B-type cyclins exclude the DNA-replication factor Mcm4 from the nucleus. *Nat. Cell Biol.* **1,** 415–422 (1999).
66. Nguyen, V. Q., Co, C., Irie, K. & Li, J. J. Clb/Cdc28 kinases promote nuclear export of the replication initiator proteins Mcm2-7. *Curr. Biol.* **10,** 195–205 (2000).

67. Liku, M. E., Nguyen, V. Q., Rosales, A. W., Irie, K. & Li, J. J. CDK phosphorylation of a novel NLS-NES module distributed between two subunits of the Mcm2-7 complex prevents chromosomal rereplication. *Mol. Biol. Cell* **16,** 5026–5039 (2005).
68. Drury, L. S., Perkins, G. & Diffley, J. F. The cyclin-dependent kinase Cdc28p regulates distinct modes of Cdc6p proteolysis during the budding yeast cell cycle. *Current Biology* **10,** 231–240 (2000).
69. Perkins, G., Drury, L. S. & Diffley, J. F. Separate SCF(CDC4) recognition elements target Cdc6 for proteolysis in S phase and mitosis. *EMBO J.* **20,** 4836–4845 (2001).
70. Honey, S. & Futcher, B. Roles of the CDK phosphorylation sites of yeast Cdc6 in chromatin binding and rereplication. *Mol. Biol. Cell* **18,** 1324–1336 (2007).
71. Mimura, S., Seki, T., Tanaka, S. & Diffley, J. F. X. Phosphorylation-dependent binding of mitotic cyclins to Cdc6 contributes to DNA replication control. *Nature* **431,** 1118–1123 (2004).
72. Tak, Y.-S., Tanaka, Y., Endo, S., Kamimura, Y. & Araki, H. A CDK-catalysed regulatory phosphorylation for formation of the DNA replication complex Sld2-Dpb11. *EMBO J.* **25,** 1987–1996 (2006).
73. Boos, D. *et al.* Regulation of DNA Replication through Sld3-Dpb11 Interaction Is Conserved from Yeast to Humans. *Current Biology* **21,** 1152–1157 (2011).
74. Kumagai, A., Shevchenko, A., Shevchenko, A. & Dunphy, W. G. Direct regulation of Treslin by cyclin-dependent kinase is essential for the onset of DNA replication. *J. Cell Biol.* **193,** 995–1007 (2011).
75. Gaggioli, V. *et al.* CDK phosphorylation of SLD-2 is required for replication initiation and germline development in C. elegans. *The Journal of Cell Biology* **204,** 507–522 (2014).
76. Bousset, K. & Diffley, J. F. The Cdc7 protein kinase is required for origin firing during S phase. *Genes Dev.* **12,** 480–490 (1998).
77. Donaldson, A. D., Fangman, W. L. & Brewer, B. J. Cdc7 is required throughout the yeast S phase to activate replication origins. *Genes Dev.* **12,** 491–501 (1998).
78. Oshiro, G., Owens, J. C., Shellman, Y., Sclafani, R. A. & Li, J. J. Cell cycle control of Cdc7p kinase activity through regulation of Dbf4p stability. *Mol. Cell. Biol.* **19,** 4888–4896 (1999).
79. Hardy, C. F., Dryga, O., Seematter, S., Pahl, P. M. & Sclafani, R. A. mcm5/cdc46-bob1 bypasses the requirement for the S phase activator Cdc7p. *Proc. Natl. Acad. Sci. U.S.A.* **94,** 3151–3155 (1997).
80. Randell, J. C. W. *et al.* Mec1 Is One of Multiple Kinases that Prime the Mcm2-7 Helicase for Phosphorylation by Cdc7. *Mol. Cell* **40,** 353–363 (2010).
81. Sheu, Y.-J. & Stillman, B. The Dbf4-Cdc7 kinase promotes S phase by alleviating an inhibitory activity in Mcm4. *Nature* **463,** 113–117 (2010).
82. Deegan, T. D., Yeeles, J. T. & Diffley, J. F. Phosphopeptide binding by Sld3 links Dbf4-dependent kinase to MCM replicative helicase activation. *EMBO J.* **35,** e201593552–973 (2016).
83. Hiraga, S.-I. *et al.* Rif1 controls DNA replication by directing Protein Phosphatase 1 to reverse Cdc7-mediated phosphorylation of the MCM complex. *Genes Dev.* **28,** 372–383 (2014).
84. Davé, A., Cooley, C., Garg, M. & Bianchi, A. Protein phosphatase 1 recruitment by Rif1 regulates DNA replication origin firing by counteracting DDK activity. *Cell Rep* **7,** 53–61 (2014).
85. Mattarocci, S. *et al.* Rif1 Controls DNA Replication Timing in Yeast through the PP1 Phosphatase Glc7. *Cell Rep* **7,** 62–69 (2014).
86. Peace, J. M., Ter-Zakarian, A. & Aparicio, O. M. Rif1 Regulates Initiation Timing of Late Replication Origins throughout the S. cerevisiae Genome. *PLoS ONE* **9,** e98501–9 (2014).
87. Hafner, L. *et al.* Rif1 Binding and Control of Chromosome-Internal DNA Replication Origins Is Limited by Telomere Sequestration. *Cell Rep* **23,** 983–992 (2018).
88. Alver, R. C., Chadha, G. S., Gillespie, P. J. & Blow, J. J. Reversal of DDK-Mediated MCM Phosphorylation by Rif1-PP1 Regulates Replication Initiation and Replisome Stability Independently of ATR/Chk1. *Cell Rep* **18,** 2508–2520 (2017).

89. Hiraga, S.-I. *et al.* Human RIF1 and protein phosphatase 1 stimulate DNA replication origin licensing but suppress origin activation. *EMBO Rep.* **18,** 403–419 (2017).
90. Wei, L. & Zhao, X. A new MCM modification cycle regulates DNA replication initiation. *Nat. Struct. Mol. Biol.* **23,** 209–216 (2016).
91. Visintin, R. *et al.* The phosphatase Cdc14 triggers mitotic exit by reversal of Cdk-dependent phosphorylation. *Mol. Cell* **2,** 709–718 (1998).
92. Visintin, R., Hwang, E. S. & Amon, A. Cfi1 prevents premature exit from mitosis by anchoring Cdc14 phosphatase in the nucleolus. *Nature* **398,** 818–823 (1999).
93. Bloom, J. & Cross, F. R. Novel role for Cdc14 sequestration: Cdc14 dephosphorylates factors that promote DNA replication. *Mol. Cell. Biol.* **27,** 842–853 (2007).
94. Zhai, Y., Yung, P. Y. K., Huo, L. & Liang, C. Cdc14p resets the competency of replication licensing by dephosphorylating multiple initiation proteins during mitotic exit in budding yeast. *Journal of Cell Science* **123,** 3933–3943 (2010).
95. Costanzo, M. *et al.* The genetic landscape of a cell. *Science* **327,** 425–431 (2010).
96. Wallis, A. B. A. & Nieduszynski, C. A. Investigating the role of Rts1 in DNA replication initiation. *Wellcome Open Res* **3,** 23–15 (2018).
97. Archambault, V., Ikui, A. E., Drapkin, B. J. & Cross, F. R. Disruption of mechanisms that prevent rereplication triggers a DNA damage response. *Mol. Cell. Biol.* **25,** 6707–6721 (2005).
98. McGarry, T. J. & Kirschner, M. W. Geminin, an inhibitor of DNA replication, is degraded during mitosis. *Cell* **93,** 1043–1053 (1998).
99. Wohlschlegel, J. A. *et al.* Inhibition of eukaryotic DNA replication by geminin binding to Cdt1. *Science* **290,** 2309–2312 (2000).
100. Tada, S., Li, A., Maiorano, D., Méchali, M. & Blow, J. J. Repression of origin assembly in metaphase depends on inhibition of RLF-B/Cdt1 by geminin. *Nat. Cell Biol.* **3,** 107–113 (2001).
101. Arias, E. E. & Walter, J. C. Replication-dependent destruction of Cdt1 limits DNA replication to a single round per cell cycle in Xenopus egg extracts. *Genes Dev.* **19,** 114–126 (2005).
102. Jin, J., Arias, E. E., Chen, J., Harper, J. W. & Walter, J. C. A Family of Diverse Cul4-Ddb1-Interacting Proteins Includes Cdt2, which Is Required for S Phase Destruction of the Replication Factor Cdt1. *Mol. Cell* **23,** 709–721 (2006).
103. Hu, J. An Evolutionarily Conserved Function of Proliferating Cell Nuclear Antigen for Cdt1 Degradation by the Cul4-Ddb1 Ubiquitin Ligase in Response to DNA Damage. *Journal of Biological Chemistry* **281,** 3753–3756 (2006).
104. Ralph, E., Boye, E. & Kearsey, S. E. DNA damage induces Cdt1 proteolysis in fission yeast through a pathway dependent on Cdt2 and Ddb1. *EMBO Rep.* **7,** 1134–1139 (2006).
105. Arias, E. E. & Walter, J. C. PCNA functions as a molecular platform to trigger Cdt1 destruction and prevent re-replication. *Nat. Cell Biol.* **8,** 84–90 (2005).
106. Senga, T. *et al.* PCNA is a cofactor for Cdt1 degradation by CUL4/DDB1-mediated N-terminal ubiquitination. *Journal of Biological Chemistry* **281,** 6246–6252 (2006).
107. Higa, L. A. *et al.* L2DTL/CDT2 Interacts with the CUL4/DDB1 Complex and PCNA and Regulates CDT1 Proteolysis in Response to DNA Damage. *cc* **5,** 1675–1680 (2006).
108. Finn, K., Lowndes, N. F. & Grenon, M. Eukaryotic DNA damage checkpoint activation in response to double-strand breaks. *Cell. Mol. Life Sci.* **69,** 1447–1473 (2012).
109. Gerald, J. N. F., Benjamin, J. M. & Kron, S. J. Robust G1 checkpoint arrest in budding yeast: dependence on DNA damage signaling and repair. *Journal of Cell Science* **115,** 1749–1757 (2002).
110. Siede, W., Friedberg, A. S., Dianova, I. & Friedberg, E. C. Characterization of G1 checkpoint control in the yeast Saccharomyces cerevisiae following exposure to DNA-damaging agents. *Genetics* **138,** 271–281 (1994).
111. Siede, W., Allen, J. B., Elledge, S. J. & Friedberg, E. C. The Saccharomyces cerevisiae MEC1 gene, which encodes a homolog of the human ATM gene product, is required for G1 arrest following radiation treatment. *J. Bacteriol.* **178,** 5841–5843 (1996).

112. Galanti, L. & Pfander, B. Right time, right place—DNA damage and DNA replication checkpoints collectively safeguard S phase. *EMBO J.* **37,** e100681–3 (2018).
113. Bacal, J. *et al.* Mrc1 and Rad9 cooperate to regulate initiation and elongation of DNA replication in response to DNA damage. *EMBO J.* **37,** e99319–18 (2018).
114. García Rodríguez, N., Morawska, M., Wong, R. P., Daigaku, Y. & Ulrich, H. D. Spatial separation between replisome- and template-induced replication stress signaling. *EMBO J.* **37,** e98369 (2018).
115. Iyer, D. & Rhind, N. The Intra-S Checkpoint Responses to DNA Damage. *Genes* **8,** 74–25 (2017).
116. Ciardo, D., Goldar, A. & Marheineke, K. On the Interplay of the DNA Replication Program and the Intra-S Phase Checkpoint Pathway. *Genes* **10,** 94–24 (2019).
117. Weinert, T. A. & Hartwell, L. H. The RAD9 gene controls the cell cycle response to DNA damage in Saccharomyces cerevisiae. *Science* **241,** 317–322 (1988).
118. Downs, J. A., Lowndes, N. F. & Jackson, S. P. A role for Saccharomyces cerevisiae histone H2A in DNA repair. *Nature* **408,** 1001–1004 (2000).
119. Shroff, R. *et al.* Distribution and Dynamics of Chromatin Modification Induced by a Defined DNA Double-Strand Break. *Current Biology* **14,** 1703–1711 (2004).
120. Alcasabas, A. A. *et al.* Mrc1 transduces signals of DNA replication stress to activate Rad53. *Nat. Cell Biol.* **3,** 958–965 (2001).
121. Tanaka, K. & Russell, P. Mrc1 channels the DNA replication arrest signal to checkpoint kinase Cds1. *Nat. Cell Biol.* **3,** 966–972 (2001).
122. Sun, Z., Hsiao, J., Fay, D. S. & Stern, D. F. Rad53 FHA domain associated with phosphorylated Rad9 in the DNA damage checkpoint. *Science* **281,** 272–274 (1998).
123. Vialard, J. E., Gilbert, C. S., Green, C. M. & Lowndes, N. F. The budding yeast Rad9 checkpoint protein is subjected to Mec1/Tel1-dependent hyperphosphorylation and interacts with Rad53 after DNA damage. *EMBO J.* **17,** 5679–5688 (1998).
124. Emili, A. MEC1-dependent phosphorylation of Rad9p in response to DNA damage. *Mol. Cell* **2,** 183–189 (1998).
125. Pellicioli, A. *et al.* Activation of Rad53 kinase in response to DNA damage and its effect in modulating phosphorylation of the lagging strand DNA polymerase. *EMBO J.* **18,** 6561–6572 (1999).
126. Gilbert, C. S., Green, C. M. & Lowndes, N. F. Budding yeast Rad9 is an ATP-dependent Rad53 activating machine. *Mol. Cell* **8,** 129–136 (2001).
127. Ma, J.-L., Lee, S.-J., Duong, J. K. & Stern, D. F. Activation of the checkpoint kinase Rad53 by the phosphatidyl inositol kinase-like kinase Mec1. *Journal of Biological Chemistry* **281,** 3954–3963 (2006).
128. Shirahige, K. *et al.* Regulation of DNA-replication origins during cell-cycle progression. *Nature* **395,** 618–621 (1998).
129. Santocanale, C. & Diffley, J. F. A Mec1- and Rad53-dependent checkpoint controls late-firing origins of DNA replication. *Nature* **395,** 615–618 (1998).
130. Larner, J. M. *et al.* Radiation down-regulates replication origin activity throughout the S phase in mammalian cells. *Nucleic Acids Research* **27,** 803–809 (1999).
131. Zegerman, P. & Diffley, J. F. X. Checkpoint-dependent inhibition of DNA replication initiation by Sld3 and Dbf4 phosphorylation. *Nature* **467,** 474–478 (2010).
132. Lopez-Mosqueda, J. *et al.* Damage-induced phosphorylation of Sld3 is important to block late origin firing. *Nature* **467,** 479–483 (2010).
133. Duncker, B. P., Shimada, K., Tsai-Pflugfelder, M., Pasero, P. & Gasser, S. M. An N-terminal domain of Dbf4p mediates interaction with both origin recognition complex (ORC) and Rad53p and can deregulate late origin firing. *Proc. Natl. Acad. Sci. U.S.A.* **99,** 16087–16092 (2002).
134. Chen, Y.-C. *et al.* DNA replication checkpoint signaling depends on a Rad53-Dbf4 N-terminal interaction in Saccharomyces cerevisiae. *Genetics* **194,** 389–401 (2013).
135. Matthews, L. A. *et al.* A Novel Non-canonical Forkhead-associated (FHA) Domain-binding Interface Mediates the Interaction between Rad53 and Dbf4 Proteins. *Journal of Biological Chemistry* **289,** 2589–2599 (2014).

136. Can, G., Kauerhof, A. C., Macak, D. & Zegerman, P. Helicase Subunit Cdc45 Targets the Checkpoint Kinase Rad53 to Both Replication Initiation and Elongation Complexes after Fork Stalling. *Mol. Cell* **73,** 562–573.e3 (2019).
137. De Piccoli, G. *et al.* Replisome stability at defective DNA replication forks is independent of S phase checkpoint kinases. *Mol. Cell* **45,** 696–704 (2012).
138. Dungrawala, H. & Cortez, D. Purification of proteins on newly synthesized DNA using iPOND. *Methods Mol. Biol.* **1228,** 123–131 (2015).
139. Green, B. M., Morreale, R. J., Ozaydin, B., Derisi, J. L. & Li, J. J. Genome-wide mapping of DNA synthesis in Saccharomyces cerevisiae reveals that mechanisms preventing reinitiation of DNA replication are not redundant. *Mol. Biol. Cell* **17,** 2401–2414 (2006).
140. Tanny, R. E., MacAlpine, D. M., Blitzblau, H. G. & Bell, S. P. Genome-wide analysis of re-replication reveals inhibitory controls that target multiple stages of replication initiation. *Mol. Biol. Cell* **17,** 2415–2423 (2006).
141. Richardson, C. D. & Li, J. J. Regulatory Mechanisms That Prevent Re-initiation of DNA Replication Can Be Locally Modulated at Origins by Nearby Sequence Elements. *PLoS Genet.* **10,** e1004358–19 (2014).
142. Green, B. M. & Li, J. J. Loss of rereplication control in Saccharomyces cerevisiae results in extensive DNA damage. *Mol. Biol. Cell* **16,** 421–432 (2005).
143. Green, B. M., Finn, K. J. & Li, J. J. Loss of DNA replication control is a potent inducer of gene amplification. *Science* **329,** 943–946 (2010).
144. Finn, K. J. & Li, J. J. Single-Stranded Annealing Induced by Re-Initiation of Replication Origins Provides a Novel and Efficient Mechanism for Generating Copy Number Expansion via Non-Allelic Homologous Recombination. *PLoS Genet.* **9,** e1003192–15 (2013).
145. Hanlon, S. L. & Li, J. J. Re-replication of a Centromere Induces Chromosomal Instability and Aneuploidy. *PLoS Genet.* **11,** e1005039–30 (2015).
146. Bui, D. T. & Li, J. J. DNA Re-replication Is Susceptible to Nucleotide Level Mutagenesis. *Genetics* genetics.302194.2019–92 (2019). doi:10.1534/genetics.119.302194
147. Dahmann, C., Diffley, J. F. & Nasmyth, K. A. S-phase-promoting cyclin-dependent kinases prevent re-replication by inhibiting the transition of replication origins to a pre-replicative state. *Current Biology* **5,** 1257–1269 (1995).
148. Noton, E. & Diffley, J. F. CDK inactivation is the only essential function of the APC/C and the mitotic exit network proteins for origin resetting during mitosis. *Mol. Cell* **5,** 85–95 (2000).
149. Tanaka, S. & Araki, H. Multiple regulatory mechanisms to inhibit untimely initiation of DNA replication are important for stable genome maintenance. *PLoS Genet.* **7,** e1002136 (2011).
150. Pozo, P. N. & Cook, J. G. Regulation and Function of Cdt1; A Key Factor in Cell Proliferation and Genome Stability. *Genes* **8,** (2016).
151. Li, A. & Blow, J. J. Cdt1 downregulation by proteolysis and geminin inhibition prevents DNA re-replication in Xenopus. *EMBO J.* **24,** 395–404 (2005).
152. Maiorano, D., Krasinska, L., Lutzmann, M. & Méchali, M. Recombinant Cdt1 Induces Rereplication of G2 Nuclei in Xenopus Egg Extracts. *Current Biology* **15,** 146–153 (2005).
153. Melixetian, M. *et al.* Loss of Geminin induces rereplication in the presence of functional p53. *J. Cell Biol.* **165,** 473–482 (2004).
154. Zhu, W., Chen, Y. & Dutta, A. Rereplication by Depletion of Geminin Is Seen Regardless of p53 Status and Activates a G2/M Checkpoint. *Mol. Cell. Biol.* **24,** 7140–7150 (2004).
155. Machida, Y. J. & Dutta, A. The APC/C inhibitor, Emi1, is essential for prevention of rereplication. *Genes Dev.* **21,** 184–194 (2007).
156. Davidson, I. F., Li, A. & Blow, J. J. Deregulated replication licensing causes DNA fragmentation consistent with head-to-tail fork collision. *Mol. Cell* **24,** 433–443 (2006).
157. Neelsen, K. J. *et al.* Deregulated origin licensing leads to chromosomal breaks by rereplication of a gapped DNA template. *Genes Dev.* **27,** 2537–2542 (2013).

158. Nordman, J. & Orr-Weaver, T. L. Regulation of DNA replication during development. *Development* **139,** 455–464 (2012).
159. Alexander, J. L., Barrasa, M. I. & Orr-Weaver, T. L. Replication Fork Progression during Re-replication Requires the DNA Damage Checkpoint and Double- Strand Break Repair. *Current Biology* **25,** 1654–1660 (2015).
160. Alexander, J. L., Beagan, K., Orr-Weaver, T. L. & McVey, M. Multiple mechanisms contribute to double-strand break repair at rereplication forks in Drosophila follicle cells. *Proc. Natl. Acad. Sci. U.S.A.* **113,** 13809–13814 (2016).
161. Alexander, J. L. & Orr-Weaver, T. L. Replication fork instability and the consequences of fork collisions from rereplication. *Genes Dev.* **30,** 2241–2252 (2016).
162. Halazonetis, T. D., Gorgoulis, V. G. & Bartek, J. An oncogene-induced DNA damage model for cancer development. *Science* **319,** 1352–1355 (2008).
163. Macheret, M. & Halazonetis, T. D. DNA Replication Stress as a Hallmark of Cancer. *Annu. Rev. Pathol. Mech. Dis.* **10,** 425–448 (2015).
164. Petropoulos, M., Tsaniras, S. C., Taraviras, S. & Lygerou, Z. Replication Licensing Aberrations, Replication Stress, and Genomic Instability. *Trends Biochem. Sci.* 1–13 (2019). doi:10.1016/j.tibs.2019.03.011
165. Sherr, C. J. & McCormick, F. The RB and p53 pathways in cancer. *Cancer Cell* **2,** 103–112 (2002).
166. Meloche, S. & Pouysségur, J. The ERK1/2 mitogen-activated protein kinase pathway as a master regulator of the G1- to S-phase transition. *Oncogene* **26,** 3227–3239 (2007).
167. Nguyen, V. Q. & Li, J. J. Cyclin-dependent kinases prevent DNA re-replication through multiple mechanisms. *Nature* **411,** 1068–1073 (2001).
168. Bishop, A. C. *et al.* A chemical switch for inhibitor-sensitive alleles of any protein kinase. *Nature* **407,** 395–401 (2000).
169. Wilmes, G. M. *et al.* Interaction of the S-phase cyclin Clb5 with an'RXL'docking sequence in the initiator protein Orc6 provides an origin-localized replication control switch. *Genes Dev.* **18,** 981–991 (2004).
170. Loog, M. & Morgan, D. O. Cyclin specificity in the phosphorylation of cyclin-dependent kinase substrates. *Nature* **434,** 104–108 (2005).
171. Desdouets, C. *et al.* Evidence for a Cdc6p-independent mitotic resetting event involving DNA polymerase alpha. *EMBO J.* **17,** 4139–4146 (1998).
172. Chang, F. & Herskowitz, I. Identification of a gene necessary for cell cycle arrest by a negative growth factor of yeast: FAR1 is an inhibitor of a G1 cyclin, CLN2. *Cell* **63,** 999–1011 (1990).
173. Peter, M., Gartner, A., Horecka, J., Ammerer, G. & Herskowitz, I. FAR1 links the signal transduction pathway to the cell cycle machinery in yeast. *Cell* **73,** 747–760 (1993).
174. Tyers, M. & Futcher, B. Far1 and Fus3 link the mating pheromone signal transduction pathway to three G1-phase Cdc28 kinase complexes. *Mol. Cell. Biol.* **13,** 5659–5669 (1993).
175. Botchkarev, V. V. & Haber, J. E. Functions and regulation of the Polo-like kinase Cdc5 in the absence and presence of DNA damage. *Current Genetics* **105,** 1–10 (2017).
176. Durocher, D., Henckel, J., Fersht, A. R. & Jackson, S. P. The FHA domain is a modular phosphopeptide recognition motif. *Mol. Cell* **4,** 387–394 (1999).
177. Durocher, D. *et al.* The molecular basis of FHA domain:phosphopeptide binding specificity and implications for phospho-dependent signaling mechanisms. *Mol. Cell* **6,** 1169–1182 (2000).
178. Lee, H. *et al.* Diphosphothreonine-specific interaction between an SQ/TQ cluster and an FHA domain in the Rad53-Dun1 kinase cascade. *Mol. Cell* **30,** 767–778 (2008).
179. Pennell, S. *et al.* Structural and functional analysis of phosphothreonine-dependent FHA domain interactions. *Structure* **18,** 1587–1595 (2010).
180. Putnam, C. D. & Kolodner, R. D. Determination of gross chromosomal rearrangement rates. *Cold Spring Harb Protoc* **2010,** pdb.prot5492 (2010).

181. Schmidt, K. H., Pennaneach, V. & Putnam, C. D. Analysis of Gross-Chromosomal Rearrangements in Saccharomyces cerevisiae. *Methods in …* (2006). doi:10.1016/S0076-6879(05)09027-0
182. Chen, C. & Kolodner, R. D. Gross chromosomal rearrangements in Saccharomyces cerevisiae replication and recombination defective mutants. *Nat. Genet.* **23,** 81–85 (1999).
183. Drury, L. S., Perkins, G. & Diffley, J. F. The Cdc4/34/53 pathway targets Cdc6p for proteolysis in budding yeast. *EMBO J.* **16,** 5966–5976 (1997).
184. De Wulf, P., Montani, F. & Visintin, R. Protein phosphatases take the mitotic stage. *Curr. Opin. Cell Biol.* **21,** 806–815 (2009).
185. Wurzenberger, C. & Gerlich, D. W. Phosphatases: providing safe passage through mitotic exit. *Nat Rev Mol Cell Biol* **12,** 469–482 (2011).
186. Jaspersen, S. L., Charles, J. F., Tinker-Kulberg, R. L. & Morgan, D. O. A late mitotic regulatory network controlling cyclin destruction in Saccharomyces cerevisiae. *Mol. Biol. Cell* **9,** 2803–2817 (1998).
187. Bouchoux, C. & Uhlmann, F. A Quantitative Model for Ordered Cdk Substrate Dephosphorylation during Mitotic Exit. *Cell* **147,** 803–814 (2011).
188. Bremmer, S. C. *et al.* Cdc14 phosphatases preferentially dephosphorylate a subset of cyclin-dependent kinase (Cdk) sites containing phosphoserine. *J. Biol. Chem.* **287,** 1662–1669 (2012).
189. MacKelvie, S. H., Andrews, P. D. & Stark, M. J. The Saccharomyces cerevisiae gene SDS22 encodes a potential regulator of the mitotic function of yeast type 1 protein phosphatase. *Mol. Cell. Biol.* **15,** 3777–3785 (1995).
190. Sassoon, I. *et al.* Regulation of Saccharomyces cerevisiae kinetochores by the type 1 phosphatase Glc7p. *Genes Dev.* **13,** 545–555 (1999).
191. Andrews, P. D. & Stark, M. J. Type 1 protein phosphatase is required for maintenance of cell wall integrity, morphogenesis and cell cycle progression in Saccharomyces cerevisiae. *Journal of Cell Science* **113 (Pt 3),** 507–520 (2000).
192. Pinsky, B. A., Kotwaliwale, C. V., Tatsutani, S. Y., Breed, C. A. & Biggins, S. Glc7/protein phosphatase 1 regulatory subunits can oppose the Ipl1/aurora protein kinase by redistributing Glc7. *Mol. Cell. Biol.* **26,** 2648–2660 (2006).
193. Costanzo, M. *et al.* A global genetic interaction network maps a wiring diagram of cellular function. *Science* **353,** aaf1420–aaf1420 (2016).
194. Queralt, E., Lehane, C., Novák, B. & Uhlmann, F. Downregulation of PP2A(Cdc55) phosphatase by separase initiates mitotic exit in budding yeast. *Cell* **125,** 719–732 (2006).
195. Wang, Y. & Ng, T.-Y. Phosphatase 2A negatively regulates mitotic exit in Saccharomyces cerevisiae. *Mol. Biol. Cell* **17,** 80–89 (2006).
196. Yellman, C. M. & Burke, D. J. The role of Cdc55 in the spindle checkpoint is through regulation of mitotic exit in Saccharomyces cerevisiae. *Mol. Biol. Cell* **17,** 658–666 (2006).
197. Jackson, A. L., Pahl, P. M., Harrison, K., Rosamond, J. & Sclafani, R. A. Cell cycle regulation of the yeast Cdc7 protein kinase by association with the Dbf4 protein. *Mol. Cell. Biol.* **13,** 2899–2908 (1993).
198. Salic, A. & Mitchison, T. J. A chemical method for fast and sensitive detection of DNA synthesis in vivo. *Proc. Natl. Acad. Sci. U.S.A.* **105,** 2415–2420 (2008).
199. McNeil, J. B. & Friesen, J. D. Expression of the Herpes simplex virus thymidine kinase gene in Saccharomyces cerevisiae. *Mol. Gen. Genet.* **184,** 386–393 (1981).
200. Lengronne, A., Pasero, P., Bensimon, A. & Schwob, E. Monitoring S phase progression globally and locally using BrdU incorporation in TK(+) yeast strains. *Nucleic Acids Research* **29,** 1433–1442 (2001).
201. Vernis, L., Piskur, J. & Diffley, J. F. X. Reconstitution of an efficient thymidine salvage pathway in Saccharomyces cerevisiae. *Nucleic Acids Research* **31,** e120 (2003).

202. Hodson, J. A., Bailis, J. M. & Forsburg, S. L. Efficient labeling of fission yeast Schizosaccharomyces pombe with thymidine and BUdR. *Nucleic Acids Research* **31,** e134 (2003).
203. Sivakumar, S., Porter-Goff, M., Patel, P. K., Benoit, K. & Rhind, N. In vivo labeling of fission yeast DNA with thymidine and thymidine analogs. *Methods* **33,** 213–219 (2004).
204. Schwob, E. *et al.* Use of DNA combing for studying DNA replication in vivo in yeast and mammalian cells. *Methods Mol. Biol.* **521,** 673–687 (2009).
205. Talarek, N., Petit, J., Gueydon, E. & Schwob, E. EdU Incorporation for FACS and Microscopy Analysis of DNA Replication in Budding Yeast. *Methods Mol. Biol.* **1300,** 105–112 (2015).
206. Viggiani, C. J. & Aparicio, O. M. New vectors for simplified construction of BrdU-Incorporating strains ofSaccharomyces cerevisiae. *Yeast* **23,** 1045–1051 (2006).
207. Gambus, A. *et al.* GINS maintains association of Cdc45 with MCM in replisome progression complexes at eukaryotic DNA replication forks. *Nat. Cell Biol.* **8,** 358–366 (2006).
208. Michaelis, C., Ciosk, R. & Nasmyth, K. Cohesins: chromosomal proteins that prevent premature separation of sister chromatids. *Cell* **91,** 35–45 (1997).
209. Uhlmann, F. & Nasmyth, K. Cohesion between sister chromatids must be established during DNA replication. *Current Biology* **8,** 1095–1101 (1998).
210. Cheng, L., Collyer, T. & Hardy, C. F. Cell cycle regulation of DNA replication initiator factor Dbf4p. *Mol. Cell. Biol.* **19,** 4270–4278 (1999).
211. Weinreich, M. & Stillman, B. Cdc7p-Dbf4p kinase binds to chromatin during S phase and is regulated by both the APC and the RAD53 checkpoint pathway. *EMBO J.* **18,** 5334–5346 (1999).
212. Ferreira, M. F., Santocanale, C., Drury, L. S. & Diffley, J. F. Dbf4p, an essential S phase-promoting factor, is targeted for degradation by the anaphase-promoting complex. *Mol. Cell. Biol.* **20,** 242–248 (2000).
213. Kim, D.-H., Zhang, W. & Koepp, D. M. The Hect domain E3 ligase Tom1 and the F-box protein Dia2 control Cdc6 degradation in G1 phase. *J. Biol. Chem.* **287,** 44212–44220 (2012).
214. Elledge, S. J. & Davis, R. W. Two genes differentially regulated in the cell cycle and by DNA-damaging agents encode alternative regulatory subunits of ribonucleotide reductase. *Genes Dev.* **4,** 740–751 (1990).
215. Guarino, E., Salguero, I. & Kearsey, S. E. Cellular regulation of ribonucleotide reductase in eukaryotes. *Seminars in Cell and Developmental Biology* **30,** 97–103 (2014).
216. Pfander, B., Moldovan, G.-L., Sacher, M., Hoege, C. & Jentsch, S. SUMO-modified PCNA recruits Srs2 to prevent recombination during S phase. *Nature* **436,** 428–433 (2005).
217. Papouli, E. *et al.* Crosstalk between SUMO and ubiquitin on PCNA is mediated by recruitment of the helicase Srs2p. *Mol. Cell* **19,** 123–133 (2005).
218. Hoege, C., Pfander, B., Moldovan, G.-L., Pyrowolakis, G. & Jentsch, S. RAD6-dependent DNA repair is linked to modification of PCNA by ubiquitin and SUMO. *Nature* **419,** 135–141 (2002).
219. Nishimura, K., Fukagawa, T., Takisawa, H., Kakimoto, T. & Kanemaki, M. An auxin-based degron system for the rapid depletion of proteins in nonplant cells. *Nat. Methods* **6,** 917–922 (2009).
220. Morawska, M. & Ulrich, H. D. An expanded tool kit for the auxin-inducible degron system in budding yeast. *Yeast* **30,** 341–351 (2013).
221. Tanaka, S., Miyazawa-Onami, M., Iida, T. & Araki, H. iAID: an improved auxin-inducible degron system for the construction of a 'tight' conditional mutant in the budding yeast Saccharomyces cerevisiae. *Yeast* **32,** 567–581 (2015).
222. Matos, J., Blanco, M. G., Maslen, S., Skehel, J. M. & West, S. C. Regulatory control of the resolution of DNA recombination intermediates during meiosis and mitosis. *Cell* **147,** 158–172 (2011).

223. Gallo-Fernández, M., Saugar, I., Ortiz Bazan, M. A., Vázquez, M. V. & Tercero, J. A. Cell cycle-dependent regulation of the nuclease activity of Mus81-Eme1/Mms4. *Nucleic Acids Research* **40,** 8325–8335 (2012).
224. Matos, J., Blanco, M. G. & West, S. C. Cell-cycle kinases coordinate the resolution of recombination intermediates with chromosome segregation. *Cell Rep* **4,** 76–86 (2013).
225. Blanco, M. G., Matos, J. & West, S. C. Dual Control of Yen1 Nuclease Activity and Cellular Localization by Cdk and Cdc14 Prevents Genome Instability. *Mol. Cell* **54,** 94–106 (2014).
226. Eissler, C. L. *et al.* The Cdk/Cdc14 Module Controls Activation of the Yen1 Holliday Junction Resolvaseto Promote Genome Stability. *Mol. Cell* **54,** 80–93 (2014).
227. Szakal, B. & Branzei, D. Premature Cdk1/Cdc5/Mus81 pathway activation induces aberrant replication and deleterious crossover. *EMBO J.* **32,** 1155–1167 (2013).
228. Tuduri, S. *et al.* Topoisomerase I suppresses genomic instability by preventing interference between replication and transcription. *Nat. Cell Biol.* **11,** 1315–1324 (2009).
229. Ray Chaudhuri, A. *et al.* Topoisomerase I poisoning results in PARP-mediated replication fork reversal. *Nat. Struct. Mol. Biol.* **19,** 417–423 (2012).
230. Kim, N. *et al.* Mutagenic processing of ribonucleotides in DNA by yeast topoisomerase I. *Science* **332,** 1561–1564 (2011).
231. Williams, J. S. *et al.* Topoisomerase 1-mediated removal of ribonucleotides from nascent leading-strand DNA. *Mol. Cell* **49,** 1010–1015 (2013).
232. Williams, J. S. *et al.* Evidence that processing of ribonucleotides in DNA by topoisomerase 1 is leading-strand specific. *Nat. Struct. Mol. Biol.* **22,** 291–297 (2015).
233. Cho, J.-E. *et al.* Parallel analysis of ribonucleotide-dependent deletions produced by yeast Top1 in vitro and in vivo. *Nucleic Acids Research* **44,** 7714–7721 (2016).
234. Huang, S.-Y. N., Williams, J. S., Arana, M. E., Kunkel, T. A. & Pommier, Y. Topoisomerase I-mediated cleavage at unrepaired ribonucleotides generates DNA double-strand breaks. *EMBO J.* **36,** 361–373 (2017).
235. Bantele, S. C. S., Lisby, M. & Pfander, B. Quantitative sensing and signalling of single-stranded DNA during the DNA damage response. *Nat Commun* **10,** 944 (2019).
236. Liu, Y. *et al.* TOPBP1Dpb11 plays a conserved role in homologous recombination DNA repair through the coordinated recruitment of 53BP1Rad9. *The Journal of Cell Biology* **216,** 623–639 (2017).
237. di Cicco, G., Bantele, S. C. S., Reußwig, K.-U. & Pfander, B. A cell cycle-independent mode of the Rad9-Dpb11 interaction is induced by DNA damage. *Sci Rep* **7,** 11650 (2017).
238. Arias, E. E. & Walter, J. C. Strength in numbers: preventing rereplication via multiple mechanisms in eukaryotic cells. *Genes Dev.* **21,** 497–518 (2007).
239. Tyson, J. J. & Novak, B. Regulation of the eukaryotic cell cycle: molecular antagonism, hysteresis, and irreversible transitions. *J. Theor. Biol.* **210,** 249–263 (2001).
240. Chen, K. C. *et al.* Integrative analysis of cell cycle control in budding yeast. *Mol. Biol. Cell* **15,** 3841–3862 (2004).
241. Santos, S. D. M. & Ferrell, J. E. Systems biology: On the cell cycle and its switches. *Nature* **454,** 288–289 (2008).
242. Bhaduri, S. & Pryciak, P. M. Cyclin-specific docking motifs promote phosphorylation of yeast signaling proteins by G1/S Cdk complexes. *Curr. Biol.* **21,** 1615–1623 (2011).
243. Kõivomägi, M. *et al.* Dynamics of Cdk1 Substrate Specificity during the Cell Cycle. *Mol. Cell* **42,** 610–623 (2011).
244. Ord, M., Venta, R., Möll, K., Valk, E. & Loog, M. Cyclin-Specific Docking Mechanisms Reveal the Complexity of M-CDK Function in the Cell Cycle. *Mol. Cell* (2019). doi:10.1016/j.molcel.2019.04.026
245. Tanaka, S. & Diffley, J. F. X. Deregulated G1-cyclin expression induces genomic instability by preventing efficient pre-RC formation. *Genes Dev.* **16,** 2639–2649 (2002).
246. Weinreich, M., Liang, C., Chen, H. H. & Stillman, B. Binding of cyclin-dependent kinases to ORC and Cdc6p regulates the chromosome replication cycle. *Proc. Natl. Acad. Sci. U.S.A.* **98,** 11211–11217 (2001).

247. Nash, P. *et al.* Multisite phosphorylation of a CDK inhibitor sets a threshold for the onset of DNA replication. *Nature* **414,** 514–521 (2001).
248. Varedi K, S. M., Ventura, A. C., Merajver, S. D. & Lin, X. N. Multisite Phosphorylation Provides an Effective and Flexible Mechanism for Switch-Like Protein Degradation. *PLoS ONE* **5,** e14029 (2010).
249. Kõivomägi, M. *et al.* Cascades of multisite phosphorylation control Sic1 destruction at the onset of S phase. *Nature* **480,** 128–131 (2011).
250. Tang, X. *et al.* Composite low affinity interactions dictate recognition of the cyclin-dependent kinase inhibitor Sic1 by the SCFCdc4 ubiquitin ligase. *Proc. Natl. Acad. Sci. U.S.A.* **109,** 3287–3292 (2012).
251. Sheu, Y.-J. & Stillman, B. Cdc7-Dbf4 phosphorylates MCM proteins via a docking site-mediated mechanism to promote S phase progression. *Mol. Cell* **24,** 101–113 (2006).
252. Brümmer, A., Salazar, C., Zinzalla, V., Alberghina, L. & Höfer, T. Mathematical modelling of DNA replication reveals a trade-off between coherence of origin activation and robustness against rereplication. *PLoS Comput. Biol.* **6,** e1000783 (2010).
253. Kataria, M. *et al.* A PxL motif promotes timely cell cycle substrate dephosphorylation by the Cdc14 phosphatase. *Nat. Struct. Mol. Biol.* **25,** 1093–1102 (2018).
254. Grallert, A. *et al.* A PP1-PP2A phosphatase relay controls mitotic progression. *Nature* **517,** 94–98 (2015).
255. Godfrey, M. *et al.* PP2ACdc55 Phosphatase Imposes Ordered Cell-Cycle Phosphorylation by Opposing Threonine Phosphorylation. *Mol. Cell* **65,** 393–402.e3 (2017).
256. Venta, R., Valk, E., Kõivomägi, M. & Loog, M. Double-negative feedback between S-phase cyclin-CDK and CKI generates abruptness in the G1/S switch. *Front Physiol* **3,** 459 (2012).
257. Lu, D. *et al.* Multiple mechanisms determine the order of APC/C substrate degradation in mitosis. *The Journal of Cell Biology* **207,** 23–39 (2014).
258. Kamenz, J., Mihaljev, T., Kubis, A., Legewie, S. & Hauf, S. Robust Ordering of Anaphase Events by Adaptive Thresholds and Competing Degradation Pathways. *Mol. Cell* **60,** 446–459 (2015).
259. Phizicky, D. V., Berchowitz, L. E. & Bell, S. P. Multiple kinases inhibit origin licensing and helicase activation to ensure reductive cell division during meiosis. *Elife* **7,** e33309 (2018).
260. Lyons, N. A. & Morgan, D. O. Cdk1-dependent destruction of Eco1 prevents cohesion establishment after S phase. *Mol. Cell* **42,** 378–389 (2011).
261. Lyons, N. A., Fonslow, B. R., Diedrich, J. K., Yates, J. R. & Morgan, D. O. Sequential primed kinases create a damage-responsive phosphodegron on Eco1. *Nat. Struct. Mol. Biol.* **20,** 194–201 (2013).
262. Seoane, A. I. & Morgan, D. O. Firing of Replication Origins Frees Dbf4-Cdc7 to Target Eco1 for Destruction. *Curr. Biol.* **27,** 2849–2855.e2 (2017).
263. Coleman, K. E. *et al.* Sequential replication-coupled destruction at G1/S ensures genome stability. *Genes Dev.* **29,** 1734–1746 (2015).
264. Diffley, J. F. X. The many faces of redundancy in DNA replication control. *Cold Spring Harb. Symp. Quant. Biol.* **75,** 135–142 (2010).
265. Drury, L. S. & Diffley, J. F. X. Factors affecting the diversity of DNA replication licensing control in eukaryotes. *Curr. Biol.* **19,** 530–535 (2009).
266. Reußwig, K. U., Boos, D. & Pfander, B. Roles of Sld2, Sld3, and Dpb11 in Replication Initiation. *The Initiation of DNA Replication in …* (2016). doi:10.1007/978-3-319-24696-3_15
267. Diffley, J. F., Cocker, J. H., Dowell, S. J. & Rowley, A. Two steps in the assembly of complexes at yeast replication origins in vivo. *Cell* **78,** 303–316 (1994).
268. DePamphilis, M. L. Cell cycle dependent regulation of the origin recognition complex. *cc* **4,** 70–79 (2005).
269. Shoaib, M. *et al.* Histone H4K20 methylation mediated chromatin compaction threshold ensures genome integrity by limiting DNA replication licensing. *Nat Commun* **9,** 3704 (2018).

270. Reußwig, K.-U., Zimmermann, F., Galanti, L. & Pfander, B. Robust Replication Control Is Generated by Temporal Gaps between Licensing and Firing Phases and Depends on Degradation of Firing Factor Sld2. *Cell Rep* **17,** 556–569 (2016).
271. Schub, O. *et al.* Multiple phosphorylation sites of DNA polymerase alpha-primase cooperate to regulate the initiation of DNA replication in vitro. *Journal of Biological Chemistry* **276,** 38076–38083 (2001).
272. Kesti, T., McDonald, W. H., Yates, J. R. & Wittenberg, C. Cell cycle-dependent phosphorylation of the DNA polymerase epsilon subunit, Dpb2, by the Cdc28 cyclin-dependent protein kinase. *Journal of Biological Chemistry* **279,** 14245–14255 (2004).
273. Lisby, M., Barlow, J. H., Burgess, R. C. & Rothstein, R. Choreography of the DNA damage response: spatiotemporal relationships among checkpoint and repair proteins. *Cell* **118,** 699–713 (2004).
274. Barlow, J. H., Lisby, M. & Rothstein, R. Differential regulation of the cellular response to DNA double-strand breaks in G1. *Mol. Cell* **30,** 73–85 (2008).
275. Zierhut, C. & Diffley, J. F. X. Break dosage, cell cycle stage and DNA replication influence DNA double strand break response. *EMBO J.* **27,** 1875–1885 (2008).
276. Janke, R. *et al.* A truncated DNA-damage-signaling response is activated after DSB formation in the G1 phase of Saccharomyces cerevisiae. *Nucleic Acids Research* **38,** 2302–2313 (2010).
277. Aylon, Y., Liefshitz, B. & Kupiec, M. The CDK regulates repair of double-strand breaks by homologous recombination during the cell cycle. *EMBO J.* **23,** 4868–4875 (2004).
278. Edenberg, E. R., Vashisht, A., Benanti, J. A., Wohlschlegel, J. & Toczyski, D. P. Rad53 downregulates mitotic gene transcription by inhibiting the transcriptional activator Ndd1. *Mol. Cell. Biol.* **34,** 725–738 (2014).
279. Gritenaite, D. *et al.* A cell cycle-regulated Slx4-Dpb11 complex promotes the resolution of DNA repair intermediates linked to stalled replication. *Genes Dev.* **28,** 1604–1619 (2014).
280. Princz, L. N. *et al.* Dbf4-dependent kinase and the Rtt107 scaffold promote Mus81-Mms4 resolvase activation during mitosis. *EMBO J.* **36,** 664–678 (2017).
281. Bermejo, R. *et al.* Top1- and Top2-mediated topological transitions at replication forks ensure fork progression and stability and prevent DNA damage checkpoint activation. *Genes Dev.* **21,** 1921–1936 (2007).
282. Ölmezer, G. *et al.* Replication intermediates that escape Dna2 activity are processed by Holliday junction resolvase Yen1. *Nat Commun* **7,** 13157 (2016).
283. Falquet, B. & Rass, U. A new role for Holliday junction resolvase Yen1 in processing DNA replication intermediates exposes Dna2 as an accessory replicative helicase. *Microb Cell* **4,** 32–34 (2017).
284. Cortés-Ledesma, F. & Aguilera, A. Double-strand breaks arising by replication through a nick are repaired by cohesin-dependent sister-chromatid exchange. *EMBO Rep.* **7,** 919–926 (2006).
285. Blow, J. J. & Gillespie, P. J. Replication licensing and cancer--a fatal entanglement? *Nat. Rev. Cancer* **8,** 799–806 (2008).
286. Inoue, H., Nojima, H. & Okayama, H. High efficiency transformation of Escherichia coli with plasmids. *Gene* **96,** 23–28 (1990).
287. Rothstein, R. J. One-step gene disruption in yeast. *Meth. Enzymol.* **101,** 202–211 (1983).
288. Gietz, R. D. & Sugino, A. New yeast-Escherichia coli shuttle vectors constructed with in vitro mutagenized yeast genes lacking six-base pair restriction sites. *Gene* **74,** 527–534 (1988).
289. Janke, C. *et al.* A versatile toolbox for PCR-based tagging of yeast genes: new fluorescent proteins, more markers and promoter substitution cassettes. *Yeast* **21,** 947–962 (2004).
290. Hall, B. M., Ma, C.-X., Liang, P. & Singh, K. K. Fluctuation analysis CalculatOR: a web tool for the determination of mutation rate using Luria-Delbruck fluctuation analysis. *Bioinformatics* **25,** 1564–1565 (2009).
291. Rosche, W. A. & Foster, P. L. Determining mutation rates in bacterial populations. *Methods* **20,** 4–17 (2000).

292. Foster, P. L. Methods for determining spontaneous mutation rates. *Meth. Enzymol.* **409,** 195–213 (2006).
293. Green, M. R. & Sambrook, J. *Molecular cloning*. (Cold Spring Harbor Laboratory Press, 2012).
294. Saayman, X., Ramos-Pérez, C. & Brown, G. W. DNA Replication Profiling Using Deep Sequencing. *Methods Mol. Biol.* **1672,** 195–207 (2018).
295. Müller, C. A. *et al.* The dynamics of genome replication using deep sequencing. *Nucleic Acids Research* **42,** e3 (2014).
296. Cherry, J. M. *et al.* Saccharomyces Genome Database: the genomics resource of budding yeast. *Nucleic Acids Research* **40,** D700–5 (2012).
297. Li, H. & Durbin, R. Fast and accurate long-read alignment with Burrows-Wheeler transform. *Bioinformatics* **26,** 589–595 (2010).
298. Li, H. *et al.* The Sequence Alignment/Map format and SAMtools. *Bioinformatics* **25,** 2078–2079 (2009).
299. Ramírez, F. *et al.* deepTools2: a next generation web server for deep-sequencing data analysis. *Nucleic Acids Research* **44,** W160–5 (2016).
300. Robinson, J. T. *et al.* Integrative genomics viewer. *Nat. Biotechnol.* **29,** 24–26 (2011).
301. Thorvaldsdóttir, H., Robinson, J. T. & Mesirov, J. P. Integrative Genomics Viewer (IGV): high-performance genomics data visualization and exploration. *Brief. Bioinformatics* **14,** 178–192 (2013).
302. Schindelin, J. *et al.* Fiji: an open-source platform for biological-image analysis. *Nat. Methods* **9,** 676–682 (2012).
303. Schneider, C. A., Rasband, W. S. & Eliceiri, K. W. NIH Image to ImageJ: 25 years of image analysis. *Nat. Methods* **9,** 671–675 (2012).
304. Mordes, D. A., Nam, E. A. & Cortez, D. Dpb11 activates the Mec1-Ddc2 complex. *Proc. Natl. Acad. Sci. U.S.A.* **105,** 18730–18734 (2008).
305. Pfander, B. & Diffley, J. F. X. Dpb11 coordinates Mec1 kinase activation with cell cycle-regulated Rad9 recruitment. *EMBO J.* **30,** 4897–4907 (2011).
306. Royer, C. A. Improvements in the numerical analysis of thermodynamic data from biomolecular complexes. *Anal. Biochem.* **210,** 91–97 (1993).
307. Cox, J. & Mann, M. MaxQuant enables high peptide identification rates, individualized p.p.b.-range mass accuracies and proteome-wide protein quantification. *Nat. Biotechnol.* **26,** 1367–1372 (2008).
308. Cox, J. *et al.* Accurate proteome-wide label-free quantification by delayed normalization and maximal peptide ratio extraction, termed MaxLFQ. *Mol. Cell Proteomics* **13,** 2513–2526 (2014).
309. Tyanova, S. *et al.* The Perseus computational platform for comprehensive analysis of (prote)omics data. *Nat. Methods* **13,** 731–740 (2016).

Appendix

Abbreviations

A	adenine
AID	auxin-inducible degron
AP	affinity purification
APC	anaphase-promoting complex
ATP	adenosine 5'.triphosphate
BrdU	5-bromo-2'-deoxyuridine
BSA	bovine serum albumin
C	cytosine
CBB	Coomassie Brilliant Blue
CCD	charge-coupled device
CDK	cyclin-dependent kinase
Chr	chromosome
CHX	cycloheximide
CMG	Cdc45/Mcm2-7/GINS helicase
Cy5	cyanine-5
DDK	Dbf4-dependent kinase
DMSO	dimethyl sulfoxide
DNA	deoxyribonucleic acid
ds	double-stranded
DSB	double-strand break
DTT	dithiothreitol
E3	ubiquitin ligase
EDTA	ethylenediaminetetraacetic acid
EdU	5-ethinyl-2'-deoxyuridine
FEAR	fourteen early anaphase release
FHA	Forkhead-associated
FOA	5'-fluoroorotic acid
G	guanine
G1-CDK	Cdc28 in complex with Cln1/2
gal	galactose
GCR	gross-chromosomal rearrangement
GINS	Go-ichi-ni-san complex (Sld5-Psf1-Psf2-Psf3)
GST	glutathione S-transferase
HEPES	4-(2-hydroxyethyl)-1-piperazineethanesulfonic acid
HIS	hexahistidine
HRP	horseradish peroxidase
HU	hydroxyurea
IAA	indole-3-acetic acid

IP	immunoprecipitation
LB	lysogeny broth
log	logarithmic
M-CDK	Cdc28 in complex with Clb1/2
MEN	mitotic exit network
MES	2-(*N*-morpholino)ethanesulfonic acid
MOPS	3-(*N*-morpholino)propanesulfonic acid)
MS	mass spectrometry
mt	mitochondrial
NCBI	national center for biotechnology information
NGS	next-generation sequencing
NLS	nuclear localization signal
OD	optical density
ORC	origin recognition complex
PBS	phosphate-buffered saline
PCNA	proliferating cell nuclear antigen
PCR	polymerase chain reaction
PEG	polyethylene glycol
PP1	protein phosphatase 1
PP2A	protein phosphatase 2A
pre-RC	pre-replicative complex
raff	raffinose
RING	really interesting new gene
RNase A	ribonuclease A
RPA	replication protein A
RPC	replisome progression complex
S-CDK	Cdc28 in complex with Clb5/6
SC	synthetic complete
SD-fusion	*SLD3-DPB11ΔN*-fusion
SDS	sodium dodecyl sulfate
SGD	*Saccharomyces* genome database
ss	single-stranded
SUMO	small ubiquitin-like modifier
T	thymine
TBS	Tris-buffered saline
Tris	Tri(hydroxymethyl)aminomethane
WT	wild-type
YP	yeast extract/peptone
γH2A	Histone 2A phosphorylated on serine 129 (*S. cerevisiae*)

Amino acid abbreviations

amino acid	one-letter code	three-letter code
alanine	A	Ala
cysteine	C	Cys
aspartic acid	D	Asp
glutamic acid	E	Glu
phenylalanine	F	Phe
glycine	G	Gly
histidine	H	His
isoleucine	I	Ile
lysine	K	Lys
leucine	L	Leu
methionine	M	Met
asparagine	N	Asn
proline	P	Pro
glutamine	Q	Gln
arginine	R	Arg
serine	S	Ser
threonine	T	Thr
valine	V	Val
tryptophan	W	Trp
tyrosine	Y	Tyr

Prefixes and units

G	giga (10^9)	bp	base pair(s)	h	hour(s)
M	mega (10^6)	kb	kilobases	min	minute(s)
k	kilo (10^3)	Da	Dalton	sec	second(s)
m	milli (10^{-3})	°C	degrees Celsius	l	liter
µ	micro (10^{-6})	A	Ampère	g	gram
n	nano (10^{-9})	V	Volt		
p	pico (10^{-12})	M	molar		

Acknowledgements

First and foremost, I would like to express my deep gratitude to Dr. Boris Pfander. Thank you ever so much for nurturing my scientific curiosity and guiding as well as mentoring me through this exciting time of my life. I highly appreciated the scientific freedom you provided me with, your honest feedback, the inspiring scientific discussions, your trust and the many different ways I could learn from you, not only regarding science. Thanks for always being available and approachable, especially during busy times. Knowing that I can rely on you means a lot to me.

Furthermore, I am thankful to Prof. Dr. Heinrich Leonhardt, Prof. Dr. Peter Becker, Prof. Dr. Kirsten Jung, Prof. Dr. Robert Schneider, Prof. Dr. Angelika Böttger and Prof. Dr. Kai Papenfort for reviewing this PhD thesis and participating in my examination committee.

Many thanks to everyone from the former Molecular Cell Biology department and its junior research groups. It is hard to imagine a more inspiring and supporting research environment than the one Prof. Dr. Stefan Jentsch built here. I am grateful to him for letting me be a part of this vibrant community and for his generous support and advice. Moreover, I would like to thank Klara Schwander for all the administrative help and Massimo Bossi for the seemingly limitless supply from the media kitchen. Thank you also to all my new colleagues in the junior research group wing for providing such a pleasant and motivating atmosphere and to our lab manager Bianca for keeping everything running and in place.

Regarding the Max Planck Institute of Biochemistry, I would also like to acknowledge the outstanding scientific support by the core facilities, especially the NGS core facility headed by Dr. Marja Driessen and the proteomics core facility headed by Dr. Nagarjuna Nagaraj. Thank you to Dr. Michael Wierer for the collaboration on the analysis of replisomes by mass spectrometry.

I am very grateful to the Boehringer Ingelheim Fonds, particularly Dr. Claudia Walther, Dr. Anja Petersen and Sandra Schedler, for the truly outstanding support. This fellowship has enriched my PhD experience not only by providing funding and enabling conference participation, but also by supporting my personal development through insightful seminars and by introducing me to so many interesting people.

A big thank you to all members of the Pfander lab, past and present, for a great and welcoming atmosphere to work in. Thank you, Uschi, for all the support throughout the years. It feels like yesterday when I walked into the lab and Boris taught basic yeast techniques to the two of us. I cannot imagine the lab without you. Thank you, Dalia, for allowing me to break the gender bias in the lab and join your office. Thank you, Lissa, for countless barbecues and good electronic music. Thank you, Giulia, for entertaining discussions and the shared interest in basketball. Thank you, Fabian, for choosing to work with me for his Diploma thesis and the great collaboration.

Thank you, Martina, for constantly pushing the lab to practice volleyball and rewarding us with delicious cakes. Thank you, Leo, for providing maturity to the lab and being a great bench and office neighbor at the Pfander lab outpost. Also thank you to all the students, who became interested in replication control: Tom, Tobias, Peter, Ilektra and Lea – it has been my pleasure to work with you and most importantly also learn from you.

I am deeply grateful for having shared an outstanding time in the Pfander lab with a core group of wonderful people around me. Susi, thank you for all the small things that made the lab feel like home, for being bold in so many ways, for being the successful big sister in the lab to look up to, for fostering the ambitious and competitive spirit in the lab, and for sharing this intrinsic passion for science. I am glad we overlapped for such a long time in the lab. Julia, thank you for being as reliable and supportive as you are, for your creativity, for sharing the excitement about good food and seasonal beers, for all the organizational responsibilities that you took over, and for often being the voice of reason. Lorenzo, thank you for spicing up the lab with your many ideas and your originality, for your sometimes surprisingly strong opinions, for your never-ending interest and availability to discuss science, particularly late at night, and for joining me on the road to understand replication control.

I am thankful to my parents and my siblings for providing me with all the support and freedom I could have ever wished for. Thank you for understanding and accepting my peculiarities even though my work schedules sometimes caused you to worry.

Pursuing a PhD is a special time. Laura, I am incredibly grateful to have you by my side. Even though I enjoyed living in both Munich and Berlin, the prospect of starting the next chapter in our careers together in the same city is enticing. Your deep understanding of all the intricacies of the PhD journey has been invaluable throughout my PhD. Thank you not only for your love and perpetual support but also for giving me honest advice and challenging me. You continue to open my eyes for all the things that make life better.

CURRICULUM VITAE

Karl-Uwe Reußwig

HIGHER EDUCATION

08/2013 – present	**PhD in Biology** Department of Molecular Cell Biology DNA Replication and Genome Integrity Laboratory, Dr. Boris Pfander Max Planck Institute of Biochemistry, Martinsried, Germany
10/2007 – 07/2013	**Diploma in Biochemistry** Interfaculty Institute of Biochemistry Eberhard Karls University, Tuebingen, Germany

PUBLICATIONS

Reusswig KU, Pfander B (2019). Control of eukaryotic DNA replication initiation – mechanisms to ensure smooth transitions. *Genes*. 10(2): 99.

Di Cicco G, Bantele SCS, **Reusswig KU**, Pfander B (2017). A cell cycle-independent mode of the Rad9-Dpb11 interaction is induced by DNA damage. *Scientific Reports*. 7(1):11650.

Reusswig KU, Zimmermann F, Galanti L, Pfander B (2016). Robust replication control is generated by temporal gaps between licensing and firing phases and depends on degradation of firing factor Sld2. *Cell Reports.* 17(2):556-569.

Reusswig KU, Boos D, Pfander B (2016). Roles of Sld2, Sld3, and Dpb11 in Replication Initiation. In *The Initiation of DNA Replication in Eukaryotes* (pp. 297-318). Springer.

FELLOWSHIPS

08/2014 – 07/2016	PhD Fellowship, Boehringer Ingelheim Fonds
04/2008 – 07/2013	Undergraduate Fellowship, Friedrich Ebert Foundation

CONFERENCE PRESENTATIONS (ORAL)

2019	Inaugural Trieste Cell Cycle Meeting Jun 3-6, Trieste, Italy
2018	German Society for DNA Repair Sep 9-12, Karlsruhe, Germany
2015	Eukaryotic DNA Replication and Genome Maintenance Sep 1-5, Cold Spring Harbor, NY, USA